

# State of Wildfires 2023-24

## Authors:

Matthew W. Jones<sup>1,\*</sup>, Douglas I. Kelley<sup>2,\*</sup>, Chantelle A. Burton<sup>3,\*</sup>, Francesca Di Giuseppe<sup>4,\*</sup>, Maria Lucia F. Barbosa<sup>5,6</sup>, Esther Brambleby<sup>1</sup>, Andrew J. Hartley<sup>3</sup>, Anna Lombardi<sup>7</sup>, Guilherme Mataveli<sup>8,1</sup>, Joe R. McNorton<sup>4</sup>, Fiona R. Spuler<sup>9</sup>, Jakob B. Wessel<sup>10,11</sup>, John T. Abatzoglou<sup>12</sup>, Liana O. Anderson<sup>13</sup>, Niels Andela<sup>14</sup>, Sally Archibald<sup>15</sup>, Dolores Armenteras<sup>16</sup>, Eleanor Burke<sup>3</sup>, Rachel Carmenta<sup>17</sup>, Emilio Chuvieco<sup>18</sup>, Hamish Clarke<sup>19</sup>, Stefan H. Doerr<sup>20</sup>, Paulo M. Fernandes<sup>21</sup>, Louis Giglio<sup>22</sup>, Douglas S. Hamilton<sup>23</sup>, Stijn Hantson<sup>24</sup>, Sarah Harris<sup>25</sup>, Piyush Jain<sup>26</sup>, Crystal A. Kolden<sup>27</sup>, Tiina Kurvits<sup>28</sup>, Seppe Lampe<sup>29</sup>, Sarah Meier<sup>30</sup>, Stacey New<sup>3</sup>, Mark Parrington<sup>31</sup>, Morgane M. G. Perron<sup>32</sup>, Yuquan Qu<sup>33,34</sup>, Natasha S. Ribeiro<sup>35</sup>, Bambang H. Saharjo<sup>36</sup>, Jesus San-Miguel-Ayanz<sup>37</sup>, Jacquelyn K. Shuman<sup>38</sup>, Veerachai Tanpipat<sup>39</sup>, Guido R. van der Werf<sup>40</sup>, Sander Veraverbeke<sup>33,1</sup>, Gavriil Xanthopoulos<sup>41</sup>

## Institutions:

1. Tyndall Centre for Climate Change Research, School of Environmental Sciences, University of East Anglia, Norwich Research Park, Norwich, UK, NR4 7TJ
2. Hydro-climate risks, UK Centre for Ecology & Hydrology, Wallingford OX10 8BB, U.K.
3. Hadley Centre, Met Office, Fitzroy Road, Exeter, UK, EX1 3PB
4. Earth System Modelling Section, Forecast Department, European Centre for Medium-range Weather Forecast, Shinfield Park, Reading RG29AX, United Kingdom
5. Department of Remote Sensing, National Institute for Space Research, Avenida dos Astronautas, 1758. Jd. Granja - São José dos Campos - São Paulo, Brazil , 12227-010
6. Natural Sciences Center, Federal University of São Carlos, Rodovia Lauri Simões de Barros, km 12 - SP-189 - Aracaçu, Buri - São Paulo, Brazil, 18290-000
7. Climate Intelligence, Research Department, European Centre for Medium-range Weather Forecast, Shinfield Road, Reading, UK, RG29AX
8. Earth Observation and Geoinformatics Division, National Institute for Space Research, Avenida dos Astronautas, 1758. Jd. Granja - São José dos Campos - São Paulo, Brazil , 12227-010
9. Department of Meteorology, University of Reading, University of Reading, Earley Gate, Whiteknights Rd, Reading RG6 6ET
10. Department of Mathematics and Statistics, University of Exeter, Harrison Building, University of Exeter, North Park Road, Exeter, UK
11. The Alan Turing Institute, British Library, 96 Euston Road, London, UK
12. School of Engineering, University of California, Merced, 5200 N Lake Rd, Merced, CA, 95343, USA
13. Cemaden/MCTI, Estrada Doutor Altino Bondensan, 500 - Distrito de Eugênio de Melo, São José dos Campos - São Paulo, Brazil
14. BeZero Carbon, 25 Christopher Street, London, UK, EC2A 2BS
15. School of Animal Plant and Environmental Sciences, University of Witwatersrand Johannesburg, University Corner, Braamfontein, Johannesburg
16. Landscape Ecology and Ecosystem Modelling Group, Faculty of Sciences, Department of Biology, Universidad Nacional de Colombia, Cra. 30 # 45-03, Bogotá D.C., CP 111321, Colombia
17. Tyndall Centre for Climate Change Research, School of Global Development, University of East Anglia, Norwich Research Park, Norwich, UK, NR4 7TJ
18. Department of Geology, Geography and the Environment, Universidad de Alcalá, Colegios, 2 - 28801 Alcalá de Henares
19. FLARE Wildfire Research, School of Agriculture, Food and Ecosystem Sciences, University of Melbourne, Grattan St, Parkville, Australia, 3010
20. Centre for Wildfire Research, Swansea University , Singleton Park Swansea SA2 8PP Wales, UK
21. ForestWISE—Collaborative Laboratory for Integrated Forest & Fire Management, Centre for the Research and Technology of Agro-Environmental and Biological Sciences, Universidade de Trás-os-Montes e Alto Douro, Quinta de Prados, Vila Real, Portugal, 5000-801
22. Department of Geographical Sciences, University of Maryland, College Park, MD 20742
23. Marine, Earth and Atmospheric Science , North Carolina State University, Raleigh, North Carolina, USA, 27695
24. Program in Earth System Sciences, Faculty of Natural Sciences, Universidad del Rosario, Bogotá, Colombia
25. Fire Risk, Research and Community Preparedness, Country Fire Authority, Burwood East, Victoria, Australia

- 59 26. Northern Forestry Centre, Canadian Forest Service, Natural Resources Canada, 5320 122 St NW,  
60 Edmonton, AB T6H 3S5, Canada  
61 27. Wildfire Resilience Center, School of Engineering, University of California, Merced, 5200 N Lake Rd, Merced,  
62 CA, 95343, USA  
63 28. GRID-Arendal, P.O Box 183, N-4802, Arendal, NORWAY  
64 29. Department of Water and Climate, Vrije Universiteit Brussel, Pleinlaan 2, 1050 Brussel, Belgium  
65 30. Land, Environment, Economics and Policy Institute, Department of Economics, University of Exeter, Rennes  
66 Drive, Exeter, United Kingdom, EX4 4ST  
67 31. Atmospheric Composition Section, Research Department, European Centre for Medium-range Weather  
68 Forecast, Robert-Schuman-Platz 3, 53175 Bonn, Germany  
69 32. UMR 6539 CNRS/IRD/Ifremer/LEMAR, Institut Universitaire Européen de la Mer, University of Brest, F-29280  
70 Plouzané, France  
71 33. Department of Earth Sciences, Faculty of Science, Vrije Universiteit Amsterdam, De Boelelaan 1105, 1081  
72 HV Amsterdam, Netherlands  
73 34. Institute of Bio- and Geosciences: Agrosphere (IBG-3), Forschungszentrum Jülich, Wilhelm-Johnen-Straße,  
74 52428 Jülich, Germany  
75 35. Faculty of Agronomy and Forest Engineering, Eduardo Mondlane University, 3453 Avenida Julius Nyerere,  
76 Maputo, Mozambique  
77 36. Faculty of Forestry, Bogor Agricultural University, Kampus Ipb Darmaga, Bogor  
78 37. European Commission Joint Research Center, European Commission, Rue du Champ de Mars 21, 1050  
79 Brussels, Belgium  
80 38. NASA Ames Research Center, PO Box 1 Moffett Field, CA 94035-1000  
81 39. Upper ASEAN Wildland Fire Special Research Unit (WFSRU), Forestry Research Center, Faculty of Forestry,  
82 Kasetsart University, 5th Floor, 72nd Anniversary of Faculty Forestry Building  
83 40. Wageningen University, Droevendaalsesteeg 3, 6708PB Wageningen  
84 41. Forest Fire Laboratory, Institute of Mediterranean Forest Ecosystems, Hellenic Agricultural Organization  
85 (DIMITRA), Terma Alkmanos, Ilisia, 11528, Athens, Greece

86

87 ★ These authors contributed equally to this work.

88

89 Correspondence to:

90 [matthew.w.jones@uea.ac.uk](mailto:matthew.w.jones@uea.ac.uk)

91 [doukel@ceh.ac.uk](mailto:doukel@ceh.ac.uk)

92 [chantelle.burton@metoffice.gov.uk](mailto:chantelle.burton@metoffice.gov.uk)

93 [Francesca.DiGiuseppe@ecmwf.int](mailto:Francesca.DiGiuseppe@ecmwf.int)

94

95 **Key words:** Wildfire, Extreme Fire, Attribution, Climate Change

96

## 97 **Abstract**

98

99 Climate change contributes to the increased frequency and intensity of wildfires globally, with  
100 significant impacts on society and the environment. However, our understanding of the global  
101 distribution of extreme fires remains skewed, primarily influenced by media coverage and  
102 regionalised research efforts. This inaugural State of Wildfires report systematically analyses  
103 fire activity worldwide, identifying extreme events from the March 2023-February 2024 fire  
104 season. We assess the causes, predictability, and attribution of these events to climate  
105 change and land use, and forecast future risks under different climate scenarios. During the  
106 2023-24 fire season, 3.9 million km<sup>2</sup> burned globally, slightly below the average of previous  
107 seasons, but fire carbon (C) emissions were 16% above average, totalling 2.4 Pg C. Global  
108 fire C emissions were increased by record emissions in Canadian boreal forests (over 9 times  
109 the average) and reduced by low emissions from African savannahs. Notable events included  
110 record-breaking fire extent and emissions in Canada, the largest recorded wildfire in the  
111 European Union (Greece), drought-driven fires in western Amazonia and northern parts of  
112 South America, and deadly fires in Hawaii (100 deaths) and Chile (131 deaths). Over 232,000  
113 people were evacuated in Canada alone, highlighting the severity of human impact. Our  
114 analyses revealed that multiple drivers were needed to cause areas of extreme fire activity. In  
115 Canada and Greece a combination of high fire weather and an abundance of dry fuels

116 increased the probability of fires, whereas burned area anomalies were weaker in regions with  
117 lower fuel loads and higher direct suppression, particularly in Canada. The fire season in  
118 Canada was predictable three months in advance based on the fire weather index, whereas  
119 events in Greece and Amazonia had shorter predictability horizons. Attribution analyses  
120 indicated that the areas burned by fires in Canada, Greece and western Amazonia during the  
121 2023-24 fire season were up to 40.1%, 17.7%, and 50% higher due to climate change.  
122 Meanwhile, the probability of extreme fire seasons on these magnitudes has increased  
123 significantly due to anthropogenic climate change, with a 2.9-3.6-fold increase in likelihood of  
124 high fire weather in Canada and a 20.0-28.5-fold increase in Amazonia. By the end of the  
125 century, events of similar magnitude to 2023 in Canada are projected to occur 6.3-10.8 times  
126 more frequently under a medium-high emission scenario (SSP370). This report represents our  
127 first annual effort to catalogue extreme wildfire events, explain their occurrence, and predict  
128 future risks. By consolidating state-of-the-art wildfire science and delivering key insights  
129 relevant to policymakers, disaster management services, firefighting agencies, and land  
130 managers, we aim to enhance society's resilience to wildfires and promote advances in  
131 preparedness, mitigation, and adaptation.  
132

## 133 **Short Summary**

134  
135 This inaugural State of Wildfires report catalogues extreme fires of the 2023-24 fire season.  
136 For key events, we analyse their predictability and drivers and attribute them to climate change  
137 and land use. We provide a seasonal outlook and decadal projections. Key anomalies  
138 occurred in Canada, Greece, and western Amazonia, with other high-impact events  
139 catalogued worldwide. Climate change significantly increased the likelihood of extreme fires,  
140 and mitigation is required to lessen future risk.

## 141 **1 Introduction**

142

### 143 **1.1 Background**

144

145 The potential for wildfires is growing under climate change, with increases in the frequency  
146 and intensity of drought and periods of fire-favourable weather driving reductions in vegetation  
147 (fuel) moisture and priming landscapes to burn more regularly, severely, and intensely  
148 (Seneviratne et al., 2022; UNEP, 2022a; Jones et al., 2022; Abatzoglou et al., 2019;  
149 Cunningham et al., 2024a). Additionally, human activities and land use change can contribute  
150 to or exacerbate the risk of extremely large, fast-moving or intense fires, especially in tropical  
151 forests where people are the primary cause of ignition and forest degradation (Lapola et al.,  
152 2023). Recent years have been marked by a series of extreme wildfire events spanning the  
153 globe, with record levels of burned area (BA) occurring in the 2019-2020 Australian "Black  
154 Summer" bushfires (Abram et al., 2021) and a series of high-ranking wildfire seasons  
155 occurring in quick succession in the western US (2020 and 2021; Higuera & Abatzoglou,  
156 2020), Siberia (2020 and 2021; Zheng et al., 2023), Europe (2022; European Commission  
157 Joint Research Centre, 2023) and South America (2019, 2020; Kelley et al., 2021; Ferreira  
158 Barbosa et al., 2022; Silveira et al., 2020). The 2023-24 fire season was marked by  
159 unprecedented fire extent and emissions in Canada, deadly fast-moving fires in Hawaii and  
160 Chile, the largest individual wildfires on record in the European Union and Canada, and  
161 widespread fires in northwestern South America including parts of Amazonia such as Brazil,  
162 Bolivia, Colombia, and Venezuela (Mataveli et al., 2024; Kolden et al., 2024; European  
163 Commission EU Science Hub, 2023).  
164

165 The prominence of recent extreme wildfires and wildfire seasons notably contrasts with overall  
166 trends in the area burned by fires globally. Due mostly to a reduction in the global savannahs  
167 tied to landscape fragmentation and changing rainfall patterns, global BA has fallen since the

168 beginning of this century by around one-quarter (Andela et al., 2017; Jones et al., 2022; Chen  
169 et al., 2024). Critically, this decline in fire extent masks major shifts in the distribution of fires  
170 globally, with regions such as eastern Siberia and the western US and Canada experiencing  
171 a more than 40% increase in BA since 2000 (Jones et al., 2022; Zheng et al., 2021) and  
172 regions such as southeast Australia also showing significant increases over longer periods  
173 (Canadell et al., 2021). Likewise, there have been shifts in the global distribution of BA and  
174 fire carbon (C) emissions from non-forests to forests globally and from the tropics to the  
175 extratropics (Kelley et al., 2019). Hence, focussing on global aggregated BA extent underplays  
176 the scale and magnitude of changes in wildfire activity and impact on regional levels. An  
177 increase in forest and peatland burning is particularly concerning due to the rich ecosystem  
178 services that these regions provide, including C storage and biodiversity (UNEP, 2022b). The  
179 intensification of fire regimes in environments that are less fire-adapted is particularly  
180 important because these ecosystems are expected to be least resilient to such changes (Grau-  
181 Andrés et al., 2024).

182  
183 The extreme wildfire events of recent years have significantly impacted society and  
184 ecosystems across the globe (Cunningham et al., 2024a). Since 1990, wildfire disasters have  
185 directly killed or injured at least ~18,000 people, a conservative measure based on incomplete  
186 records and reporting biased to the global Northern countries (updated from Jones et al., 2022;  
187 Centre for Research on the Epidemiology of Disasters, 2024). In 2023, 232,000 people were  
188 evacuated due to wildfires in Canada alone (Jain et al., 2024; Kolden et al., 2024). Also since  
189 1990, fires are estimated to have caused on the order of 10 million premature deaths globally  
190 through degraded air quality (Johnston et al., 2012). Degraded air quality related to fires is  
191 experienced most strongly in the tropics (Pai et al., 2022) and often disproportionately affects  
192 traditional communities with poor public services or means of protection (Carmenta et al.,  
193 2021). Yet, images of North American cities blanketed in smoke during the 2023 fire season  
194 highlight the global nature of this problem.

195  
196 As anthropogenic emissions of CO<sub>2</sub> remain persistently high, the world's natural C sinks in  
197 forests, peatlands and other ecosystems are increasingly pivotal to moderating increases in  
198 atmospheric CO<sub>2</sub> concentration (Friedlingstein et al., 2023). Intact forests are often relied upon  
199 for delivering national plans for reaching Net Zero (Smith et al., 2023) and offering sites for  
200 nature based solutions (NBS). Yet, massive wildfire emissions from boreal forests and soils in  
201 Siberia and Canada across the years 2020, 2021, and 2023 amount to over 1 billion tonnes  
202 of C, a gross flux comparable in magnitude to annual CO<sub>2</sub> emissions from fossil fuel  
203 combustion in India, the EU27 or the USA (Friedlingstein et al., 2023; Zheng et al., 2023).  
204 While in a natural fire regime these gross emissions should be recuperated through post-fire  
205 recovery, the greater vegetation mortality and loss of ecosystem function associated with more  
206 widespread and severe fires can also contribute to shifts in local to regional terrestrial C  
207 budgets from sinks to sources (Zheng et al., 2021; Gatti et al., 2021; Nolan et al., 2021a;  
208 Phillips et al., 2022; Harrison et al., 2018; Cunningham et al., 2024b). Loss of vegetation during  
209 extreme fire seasons can also have wider lasting effects on ecosystems, for instance by  
210 reducing the habitat area available to endemic species (Ward et al., 2020).

211  
212 Extreme fires can moreover impact the livelihoods of various communities and landowners  
213 who depend on intact natural landscapes. For example, the lands and territories of traditional  
214 communities and Indigenous Peoples can be degraded and transformed by wildfires, raising  
215 climate justice issues (Garnett et al., 2018; Barlow et al., 2018; Lapola et al., 2023). Further,  
216 conflating the detrimental impacts of wildfires types has also stigmatised small-scale  
217 intergenerational fire use and led to prohibitive fire governance that affects local communities  
218 (Carmenta et al., 2021; Barlow et al., 2020).

219  
220 Mitigating and adapting to increases in wildfire potential are growing priorities of policymakers  
221 and require coordination with many other stakeholders. National and international disaster  
222 management centres are seeking to enhance predictive capacity, while fire management



223 agencies are expanding or re-allocating their resources to rapidly suppress fires to avoid them  
224 becoming too large, fast or intense. A number of international organisations such as the UN  
225 Environment Programme (UNEP, 2022a), the World Bank (2020, 2024), and the Organisation  
226 for Economic Co-operation and Development (OECD, 2023) and a range of other inter- or  
227 non- governmental organisations are producing reports that consolidate evidence on the  
228 changing risk of extreme fires and identify best practices for mitigating their impacts, including  
229 through land management and urban/rural planning. Many land managers are developing and  
230 implementing approaches such as fuel reduction, a process subject to permit systems issued  
231 by regional fire management agencies in some countries (Fernandes and Botelho, 2003;  
232 Stephens et al., 2012; Moreira et al., 2020; Chuvieco et al., 2023). Wildfire response agencies  
233 are exploring innovative approaches to detecting and responding to fires, and there is rising  
234 interest in the prospect of integrated fire management around the world (Food and Agriculture  
235 Organization of the United Nations, 2024). Operators of C market projects and forest carbon-  
236 conservation initiatives, such as REDD+ are particularly wary of the risks that wildfires present  
237 to the permanence of C offsets, which often feature as a key tool in national policies and  
238 international initiatives for achieving Net Zero emissions (Barlow et al., 2012; Smith et al.,  
239 2023).

240  
241 Amidst extreme wildfires and wildfire seasons, stakeholders increasingly turn to scientists for  
242 answers to pressing questions that naturally arise. How extreme was this fire event in a  
243 historical context? Is climate change to blame? Will we see more wildfires like this in the  
244 future? Did land management exacerbate or ameliorate the problem? Can we predict events  
245 like this in future to improve early warning? What is the role of climate policy in reducing risk  
246 of extreme wildfires in future?

247  
248 While observational, statistical, and modelling tools for assessing extreme wildfire drivers and  
249 predicting wildfire occurrence are advancing rapidly, their application to studying extreme  
250 wildfire seasons or events on timescales relevant to public and political interest remains  
251 limited. The State of Wildfires report represents a new initiative to routinely catalogue extreme  
252 wildfire events at annual frequency and explain their occurrence and relation to climate  
253 change. The report incorporates recent methodological advances in disentangling the drivers  
254 of selected extreme wildfire events to fuel dryness, fuel load, and weather, and ignition and  
255 suppression factors. By applying these methodological advances in conjunction with models  
256 of global change, we quantify the change in likelihood of the past year's events under climate  
257 and land use changes. Observable fire metrics (e.g. burned area) are the target variable of  
258 our causal inference and attribution work, which thereby advances on more common climate  
259 attribution studies that attribute change in fire-favourable meteorological conditions to climate  
260 change. Overall, this report capitalises on recent advances in the study of extreme fire events  
261 and seasons to provide timely information about shifting fire regimes and their causes. The  
262 findings of the report are relevant to policymakers, the media, and the wider public.

263

## 264 **1.2 Objectives of this Report**

265  
266 This inaugural edition of the State of Wildfires report aims to stimulate development of tools  
267 for understanding and predicting extreme fires and to deliver actionable information to policy  
268 and practice stakeholders and wider society. In this edition we:

- 269
- 270 1. Regionally identify extreme individual wildfires or extreme wildfire seasons of the  
271 period March 2003-February 2024, and place them in context of recent trends.
- 272 2. Shortlist a selective number of extremes (extreme individual wildfires or extreme  
273 wildfire seasons) with notable impacts on society or the environment, which we term  
274 the 'focal events' in this report.
- 275 3. Diagnose the contributions of fuel dryness, fuel load, ignitions and suppression to the  
276 occurrence of each focal event.

- 277 4. Assess the capacity of operational predictive systems to predict each focal event.
- 278 5. Attribute each focal event to anthropogenic factors including climate change and land
- 279 use.
- 280 6. Provide an outlook on the probability of extreme events in the coming fire season
- 281 (commencing March 2024).
- 282 7. Project future changes in the probability of each focal event under future climate
- 283 scenarios.

284  
285 Key methodologies used to achieve the above objectives are summarised as follows. To  
286 address objectives 1 and 2, we build a comprehensive dataset of fire metrics including BA,  
287 fire counts, fire C emissions, and individual fire properties (size and rate of growth) for  
288 consistent world regions and we quantitatively identify anomalies in these metrics during the  
289 past fire season (Giglio et al., 2018; van der Werf et al., 2017; Andela et al., 2019). To address  
290 objective 3 and 4, we leverage seasonal to sub-seasonal forecasts of fire weather from the  
291 European Centre for Medium-Range Weather Forecasts (ECMWF) and additionally employ  
292 two state-of-the-art fire models, *Controls on Fire* (ConFire) and *Probability of Fire* (PoF) (Kelley  
293 et al., 2019; McNorton et al., 2024) to pinpoint the causes of the extreme fire events of 2023-  
294 24. To address objective 5, we employ projections of fire weather from the Hadley Centre  
295 Large Ensemble to attribute change in the fire weather index (FWI) to climate change, and we  
296 drive ConFire (Kelley et al., 2019) with outputs from the Joint UK Land Environment Simulator  
297 Earth System model (JULES-ES; Mathison et al., 2023) to attribute extreme BA to climate and  
298 land use changes (Burton, Lampe, et al., 2023). To address objective 6, we consult predictions  
299 of the state of climate modes relevant to fire and present seasonal predictions of FWI from the  
300 ECMWF (Di Giuseppe et al., 2024). To address objective 7, we again pair ConFire (Kelley et  
301 al., 2019) with JULES-ES (Mathison et al., 2023) to project future changes in BA under several  
302 future climate and land use scenarios. comprehensive assessment of past and future extreme  
303 wildfire events.

304  
305 The State of Wildfires report will be an annually recurring report that can harness and adopt  
306 new methodologies brought forward by the scientific community between the annual iterations  
307 of the report. Over the coming years and decades, we aim to enhance the tools presented in  
308 this report for application in near-real time, thus enhancing our capacity to transfer key insights  
309 to decision-makers at the time they most need it.

## 310 **2 Extreme Wildfire Events of 2023-24**

311

### 312 **2.1 Methods**

313

314 We catalogued the extreme regional wildfire events or annual fire seasons in the period March  
315 2023-February 2024 based on a combination of anomalies in the distribution of several  
316 observable fire metrics from Earth observations (**Section 2.1.1**). In this work, the global fire  
317 season is defined as occurring in March-February windows oriented around the annual minima  
318 of global fire activity in boreal spring (see further details in **Section 2.1.1.2**).

319

320 Due to the diversity of environmental settings in which fires occur and the range of ecological,  
321 economic, or societal impacts caused, defining an extreme fire or an extreme fire season  
322 remains inherently challenging. To date, extreme fires have commonly been defined by their  
323 BA extent, by their feedback on the global climate, and by their socio-economic impact. While  
324 an extreme fire event or extreme fire season may be visible as a significant anomaly against  
325 historical Earth observations, the scientific community seeks to apply a more comprehensive  
326 definition of extreme fire, including its impacts on society and the environment. To catalogue  
327 extreme events that were not necessarily visible in Earth observations, regional expert panels  
328 were constructed and given responsibility for identifying extreme events of the past fire season  
329 (**Section 2.1.3**). The expert panel were given flexibility to identify and catalogue wildfire

330 characteristics or impacts that are considered regionally extreme but are not necessarily  
331 captured by Earth observations. Examples of extremes that can be captured by expert  
332 assessment (but not by Earth observations) include: suppression challenge; fatalities and  
333 structure loss; impacts on human health and wellbeing; impacts on agricultural and other  
334 economic sectors; impacts on biodiversity, and; impacts on diverse ecosystem services such  
335 as recreation, tourism or other cultural values. Hence, **Section 2.2** identifies a variety of  
336 impactful events displaying a broad range of characteristics and impacts that can occur across  
337 diverse fire regimes (e.g. Archibald et al., 2009; Cunningham et al. 2024b; Keeley, 2009).  
338

### 339 **2.1.1 Earth Observations of Fire**

#### 340 **2.1.1.1 Input Datasets**

341 We assembled observations of burned area (BA), synonymous with fire extent, for the period  
342 March 2002-February 2024 from the National Aeronautics and Space Administration (NASA)  
343 product MCD64A1 (collection 6.1). MCD64A1 provides daily BA observations at 500 m spatial  
344 resolution with global coverage and is based on retrievals from the Moderate Resolution  
345 Imaging Spectroradiometer (MODIS) sensors mounted to the Terra and Aqua satellites (Giglio  
346 et al., 2018, 2021).  
347  
348

349 We also produced a global record of individual fires for the period March 2002-February 2024  
350 by updating the Global Fire Atlas (Andela et al., 2019; Andela and Jones, 2023) through  
351 February 2024, driven by the 500m MODIS BA data. The Global Fire Atlas algorithm clusters  
352 burned cells into individual fires, tracks their daily progression, and logs attributes such as fire  
353 size and mean daily rate of growth. Our updates are provided at Andela and Jones (2024).  
354 The Global Fire Atlas is one of several products tracking daily fire progression and identifying  
355 individual fires at global scale based on moderate resolution satellite data (Andela et al., 2019;  
356 Laurent et al., 2018; Artés et al., 2019). The product uses the MODIS BA product and the  
357 smallest unit of disaggregation is 500m and the shortest timestep on which the expansion of  
358 a fire can be observed is daily. Given its resolution, Global Fire Atlas is expected to represent  
359 the dynamics of large fires better than small, fast-moving fires.  
360  
361

#### 362 **2.1.1.2 Uncertainties**

363 In addition, we gathered estimates of fire carbon (C) emissions for the period March 2023-  
364 February 2024 from two models driven by Earth observations of active fires or burned area:  
365 firstly, the Global Fire Assimilation System (GFAS) product, provided operationally by the  
366 Copernicus Atmospheric Services (CAMS) at 0.1 degree spatial resolution and daily temporal  
367 resolution (Kaiser et al., 2012; European Centre for Medium-Range Weather Forecasts,  
368 2024), and; secondly, the Global Fire Emissions Database (GFED; version 4.1s) product at  
369 0.25 degree spatial resolution and daily temporal resolution (van der Werf et al., 2017). GFAS  
370 is driven by the fire radiative power (FRP) retrievals in the MODIS active fire product  
371 MCD14A1 and biome-level relationships between FRP and biomass consumed based on  
372 GFED3 (Kaiser et al., 2012). For the 1997-2016 period, GFED4s is driven by MODIS BA data  
373 (MCD64A1 collection 5) supplemented with small fire BA based on MODIS active fire data,  
374 and a model for biomass productivity and fuel consumption (van der Werf et al., 2017). For  
375 the post-2016 period, emissions are based on active fire detections scaled to emissions using  
376 pixel-based scaling factors derived from the 2003-2016 overlapping period.  
377  
378

379 We note that the MODIS BA product data used in our analyses of anomalies in BA and  
380 individual fire properties (via the Global Fire Atlas) are known to be conservative due to the  
381 limitations to detecting small fires (e.g. agricultural fires) based on surface spectral changes  
382 at 500m resolution. Recent work has shown that including detections of small active fires  
383 increases global BA estimates by 93% (Chen et al., 2023). However, variability and trends in

384 regional BA totals using datasets that include small fires do not differ significantly from the  
385 variability and trends present in the MODIS BA product (Chen et al., 2023). Hence, inclusion  
386 or exclusion of small fires tends to generate biases in central estimates of BA in one direction  
387 or the other, in line with the sensitivity of different sensors to different fire types. Uncertainty  
388 in the detection of small fires is larger than in the case of fires detected in the MODIS BA  
389 product, due to limited validation (van der Werf et al., 2017). The MODIS BA product with  
390 resolution of 500 m is deemed highly suitable for addressing the research questions of this  
391 report, which focus on more impactful fires that tend to burn larger areas.

392  
393 Uncertainties in fire carbon emissions estimates from GFED4.1s are on the order of  $\pm 20\text{--}25\%$   
394 at 1 standard deviation for global totals (van der Werf et al., 2017; van der Werf et al., 2010).  
395 Uncertainties in GFED4.1s are made up of uncertainties in BA, the amount of biomass  
396 consumed per unit BA, and the carbon emitted per unit biomass burned. Revisions to BA input  
397 data, discussed above, have tended to influence GFED central estimates of fire C emissions  
398 to a greater degree than the uncertainties around central estimates (van der Werf et al., 2017;  
399 Chen et al., 2023). Uncertainties in fire carbon emissions estimates from GFAS are on the  
400 order of approximately  $\pm 25\%$  at 1 standard deviation for global totals. Uncertainties are  
401 introduced by missed active fire detections, either below the detection threshold of the MODIS  
402 instruments, or not observed during the limited diurnal coverage of Low Earth Orbiting  
403 satellites, assumptions made for biome classifications, coefficients used to convert observed  
404 thermal anomalies to consumed dry matter, and emission factors used to estimate emitted  
405 quantities of carbon and pyrogenic pollutants. Variation in C emissions estimates on the order  
406 of approximately 20-60% has been observed in studies comparing multiple emissions  
407 products (Wiedinmyer et al., 2023).

408

### 409 **2.1.1.3 Regional Burned Area, Carbon Emissions and Fire Count Totals**

410

411 We calculated regional totals of BA and C emissions based on a variety of regional layers  
412 defined in **Table 1**. The regional layers represent a range of biogeographical boundaries (e.g.  
413 biomes), geopolitical boundaries (e.g. countries), and values used in scientific reports (e.g. by  
414 the Intergovernmental Panel on Climate Change; IPCC). We calculated monthly totals of BA  
415 and fire C emissions for each region by aggregating monthly BA and daily C emissions data,  
416 summing the data from the input datasets both spatially and temporally as required. In the  
417 case of fire C emissions, we also calculated the mean estimate of fire C emissions from  
418 GFED4.1s and GFAS, regionally.

419

420 We adopt a March-February definition of the global fire season (e.g. the latest global fire  
421 season spans March 2023-February 2024). Due to an annual lull in the global fire calendar in  
422 the boreal spring months, fire season BA totals are least sensitive to the shifts in fire season  
423 cutoffs of 1-2 months if the fire season centres on spring (Boschetti and Roy, 2008). This  
424 makes the global fire season centred on spring a pragmatic option for the study of interannual  
425 variability or trends in fire extent (Boschetti and Roy, 2008). The period March-February is  
426 specifically oriented at the end of the austral fire season and before widespread fires have  
427 begun in the boreal extratropics. The regions where this global definition of the fire season is  
428 most problematic are: northern hemisphere South America, Southeast Asia, and Central  
429 America (Giglio et al., 2013).

430

431 In addition, we calculated totals of regional fire counts for each global fire season based on  
432 the number of individual fire ignition points present within each region, using ignition point  
433 vectors from the Global Fire Atlas. The resolution of the MODIS data supplied to the Global  
434 Fire Atlas algorithm is 500 m and hence fires that are smaller in scale are omitted. Regional  
435 or national systems may record greater fire counts due to the inclusion of smaller fires.

436

437 **Table 1:** Regional layers to which global Earth observations were disaggregated and used to  
 438 define regions with extreme wildfire seasons or extreme individual wildfire attributes. Regional  
 439 layers are available from Jones et al. (2024).

Layer	Short Form	Source	Notes
Biomes	NA	Olson et al. (2001)	
Continents	NA	ArcGIS Hub (2024)	
Continental Biomes	NA	See above	Spatial intersect of biomes and continents.
Countries	NA	EU Eurostat (2020)	
UC Davis Global Administrative Areas (GADM) Level 1	GADM-L1	UC Davis (2022)	First sub-national administrative level, such as states of the US or provinces of China. Version 4.1.
Intergovernmental Panel on Climate Change <i>Sixth Assessment Report (AR6) Working Group I (WGI) Reference Regions</i>	IPCC AR6 WGI Regions	Iturbide et al. (2020)	
Global C Project <i>Regional C Cycle Assessment and Processes (RECCAP2) Reference Regions</i>	RECCAP2 Regions	Ciais et al. (2022)	
Global Fire Emissions Database (GFED) Basis Regions	GFED4.1s Regions	van der Werf et al. (2006)	

440  
441

## 2.1.2 Identifying Extreme Fire Seasons and Events from Earth Observations

442  
443  
444  
445

### 2.1.2.1 Regions with Extreme Wildfire Seasons

446 Anomalies in BA, fire C emissions, and fire counts in the latest global fire season (March 2023-  
 447 February 2024) were calculated in several ways:

448

449 (i) as relative anomalies (expressed in %) from the annual mean during all previous March-  
 450 February periods since 2002 (2003 for fire C emissions);

451 (ii) as standardised anomalies (standard deviations) from the annual mean during all previous  
 452 March-February periods since 2002 (2003 for C emissions);

453 (iii) as a rank amongst all March-February periods since 2002 (2003 for fire C emissions),  
 454 March 2023-February 2024 inclusive.

455

456 In this report, anomalies in fire C emissions are reported based on the two-model mean  
 457 estimate from GFED4.1s and GFAS, however anomalies based on the GFED4.1s or GFAS  
 458 estimates individually are also available via Jones et al. (2024).

459

460 We identified regions in which the latest fire season was potentially classifiable as ‘extreme’  
 461 based on the rank of BA, C emissions and fire count amongst all fire seasons. For visualisation  
 462 purposes, we identified regions in which the latest fire season ranked in the top 5 of all annual  
 463 fire seasons on record (see **Section 2.2.1**). The BA data for the period March 2002-February  
 464 2024 includes 23 fire seasons, while the C emissions data for the period March 2003-February

465 2024 includes 21 fire seasons. Hence, a top-5 ranking translates approximately to a fire  
466 season in the upper quartile of those on record.

467

468 We further characterised the onset, peak, and cessation of anomalous monthly BA in March  
469 2023-February 2024. First, we identified the month of the event's peak as the maximum  
470 difference between monthly BA values in March 2023-February 2024 and the climatological  
471 mean monthly values from the prior March-February periods. Thereafter, the event's onset  
472 and cessation were defined as the bounds of consecutive months with above-average BA  
473 prior to and following the peak but limited to the March 2023-February 2024 period.

474

### 475 **2.1.2.2 Regions with Extreme Individual Wildfire Attributes**

476

477 We identified regions in which large or fast-moving fires occurred in the latest fire season  
478 based on records of individual fires from the Global Fire Atlas. For each region (**Table 1**) and  
479 year, we estimated the size of the largest fire, the daily rate of growth of the fire that spread  
480 most rapidly, the size of the 95th percentile fire, and the daily rate of growth of the 95th  
481 percentile fire. In the Global Fire Atlas, the daily rate of growth for any given fire is determined  
482 by calculating the average daily rate of growth at which the fire advanced across all its  
483 constituent cells. This method includes cells burned by the head, flank, and backfire and  
484 produces lower spread rates than if the calculation were based solely on the cells burned by  
485 the head fire.

486

487 Anomalies in each fire attribute were calculated using the same metrics as for BA (see *i-iii*  
488 above), and we identified regions in which the latest fire season featured fires with potentially  
489 extreme attributes based on the rank of BA and fire C emissions amongst all fire seasons.

490

### 491 **2.1.3 Identifying Extreme Fire Seasons and Events from Expert Consultation**

492

493 We assembled a panel of regional experts (two from each continent, **Table A1**), to contribute  
494 to the identification, description, and characterisation of extreme wildfire seasons or impactful  
495 events in the latest fire season. A key role of the expert panel was to catalogue regional events  
496 that significantly impacted society or the environment but which may not have been detected  
497 by Earth-observing satellites due to issues such as scale, short duration, timing of overpass,  
498 and cloud or canopy cover. This includes (but is not limited to) wildfires that impacted society  
499 by causing fatalities, evacuations, displacement (e.g. homelessness), direct structure or  
500 infrastructure loss or damage, degradation of air or water quality, loss of livelihood, cultural  
501 practice or other ways of life, and loss of economic productivity. This definition also includes  
502 (but is not limited to) wildfires that impact the environment via disturbance to vulnerable  
503 ecosystems, biodiverse areas, or ecosystem services such as C storage. This approach  
504 recognises that Earth observations do not provide a complete record of all impactful fires. We  
505 do not define ubiquitous quantitative thresholds of impact by any of the measures outlined  
506 above, but rather invite in-region experts to identify events that triggered impacts that were  
507 sufficient in magnitude to infiltrate public and political discourse. The sources of information  
508 available for cataloguing regional events include national/regional fire records, fire service  
509 reports, disaster management reports, news reports, and social media. A second key role of  
510 our expert panel was to describe and contextualise the impacts of the fire seasons highlighted  
511 as extreme by Earth observations or regional assessment (see **Section 2.2.3**).

512

513 The year in review by continent, produced by the expert panel, is presented in **Appendix A**.

514

### 515 **2.1.4 Context of Recent Extremes: Regional Trends in Burned Area**

516

517 To place recent extremes in the context of fire trends of the past two decades, we update our  
518 regional analyses of trends in annual BA from Jones et al. (2022). In contrast to Jones et al.

519 (2022), we present trends that align more closely with global fire seasons, spanning the period  
520 March 2002-February 2024 rather than trends over calendar years. We quantified trends using  
521 the Theil-Sen slope estimator, which is useful when data may contain outliers or be non-  
522 normally distributed making it less sensitive to outliers than a standard least squares  
523 regression slope. Changes were calculated by multiplying trends (unit year<sup>-1</sup>) by the number  
524 of fire seasons in the period of coverage for each variable (**Section 2.1.1.2**). Relative changes  
525 were calculated as the absolute changes divided by the mean annual BA during the period  
526 following Jones et al. (2022) and Andela et al. (2017). The significance of trends was evaluated  
527 using the Mann-Kendall test, with a confidence level set at 95%.

528  
529 In addition to reporting trends in *total* BA, we also present trends in *forest* BA as these regularly  
530 diverge from total BA trends (see **Section 2.2.2**). Forest BA is calculated as described in  
531 **Section 2.1.1** but after isolating burned cells in areas with tree cover exceeding 30% in  
532 NASA's annual MODIS MOD44B collection 6.0 Continuous Vegetation Field product (250 m)  
533 (DiMiceli et al., 2015). The 30% threshold is widely used amongst studies of forest cover  
534 change (e.g. Li et al., 2017; Cunningham et al., 2020; Sexton et al., 2016).

### 535 536 **2.1.5 Shortlisting of Focal Events**

537  
538 In later sections of this report, we conducted various analyses to understand the causes and  
539 predictability of a selection of extreme wildfire seasons or events during March 2023-February  
540 2024 (see **Sections 3-5**). We limited the number of analyses to three globally prominent focal  
541 events of the 2023-24 global fire season because the approaches used are not operational  
542 and time is required to train and optimise our models regionally.

543  
544 In discussion with our expert panel, we prioritised the three events studied in this report by  
545 weighing up the anomalies in Earth observations during the latest fire season as well as the  
546 impacts that these extremes had on people and the environment. The focal events are notable  
547 for their international significance, attracting attention from the media and policymakers both  
548 within and beyond their region.

## 549 550 **2.2 Results**

### 551 552 **2.2.1 Extreme Fire Seasons and Events of 2023-24**

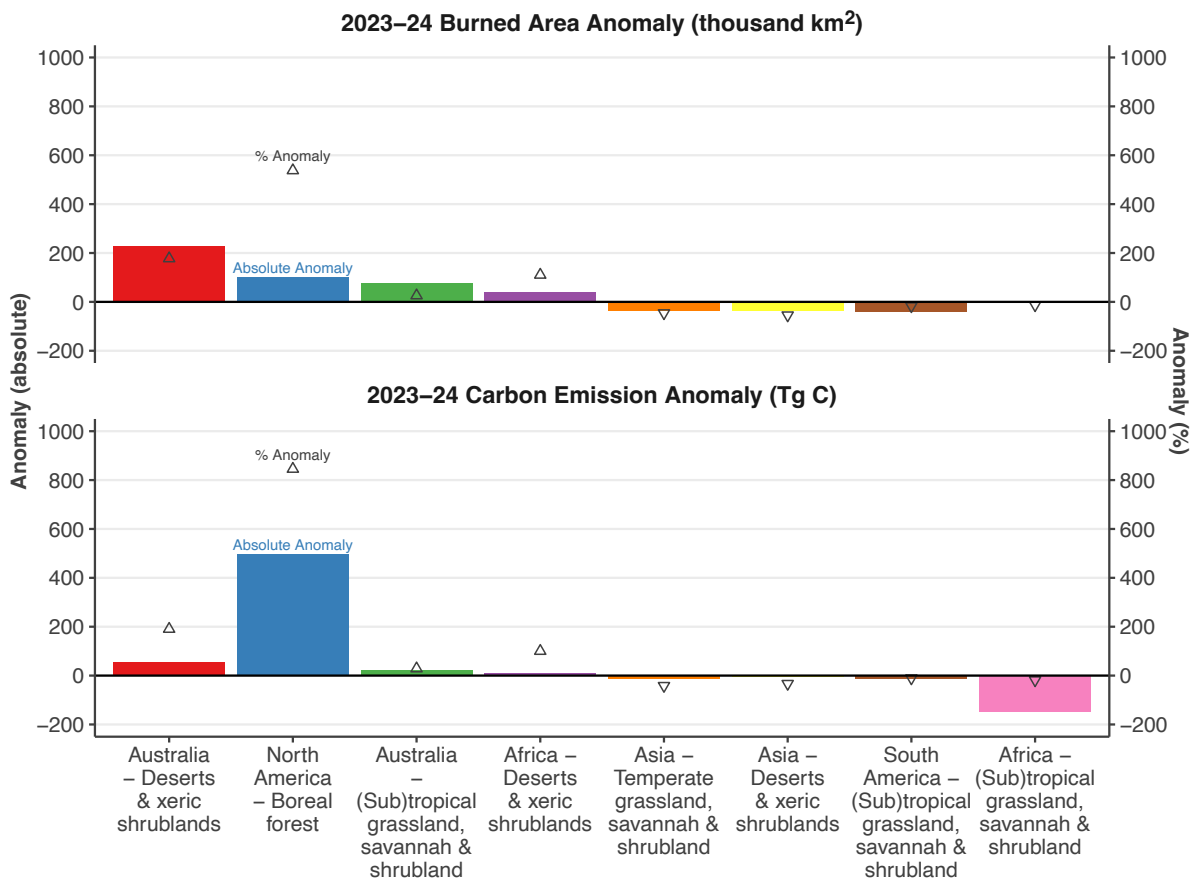
#### 553 554 **2.2.1.1 Extreme Fire Seasons from Earth Observations**

555  
556 According to the MODIS BA product, 3.9 million km<sup>2</sup> burned globally during the 2023-24 global  
557 fire season (March 2023-February 2024), slightly below the average of previous fire seasons  
558 (4.0 million km<sup>2</sup>) and overall ranking 12th of all fire seasons since 2002 (Jones et al., 2024).  
559 Despite this, fire C emissions were 16% above average at 2.4 Pg C during the 2023-24 global  
560 fire season, which ranks 7th amongst all fire seasons since 2003 (based on annual averages  
561 of GFED4.1s and GFAS estimates; see methods; Jones et al., 2024).

562  
563 Stark regional contrasts in the anomalies in BA, fire C emissions and individual fire properties  
564 are visible in the Earth observations on various regional scales (**Figure 1, Figure 2, Figure**  
565 **3**). **Figure 1** shows the strongest BA and fire C emissions anomalies of 2023-24 at continental  
566 biome scale versus previous fire seasons. BA was around 300 thousand km<sup>2</sup> (13%) below the  
567 average of previous fire seasons in the African grassland, savannah and shrubland biome,  
568 which is globally significant because the continental biome contributes 58% towards the global  
569 total BA in the average year up to February 2023 (Jones et al., 2024). BA was also around  
570 17% below average in the South American grassland, savannah and shrubland biome in 2023-  
571 24 and in Asian non-forest biomes. In contrast, BA was 26% above the average of fire seasons  
572 since 2002 in the Australian grassland, savannah and shrubland biome (**Figure 1, Figure 2**).

573 Collectively, these three biomes contributed 71% of total BA in the global total BA in the  
 574 average fire season between March 2002 and February 2023 and so departures from average  
 575 values are particularly impactful on global BA totals.  
 576

577 The North American boreal forests experienced a record-breaking fire season, with BA  
 578 reaching six times the average since 2002 and fire C emissions reaching over nine times the  
 579 average since 2003 (**Figure 1**; Jones et al., 2024). This strong regional signal primarily  
 580 explains the above-average global C emissions total of 2023-24, with the high rates of fire  
 581 emissions per unit area in boreal forests aggregating to override the reduced emissions totals  
 582 in African and South American savannahs. Record levels of fire C emissions were seen also  
 583 across the global pan-boreal forest biome, with fire C emissions surpassing the pan-boreal  
 584 record set in 2021 by more than 60%. This is despite a below-average fire season for BA and  
 585 fire C emissions in boreal Asia during 2023-24, in contrast to the 2021-22 fire season when  
 586 there was a synchronous peak in BA in both the Eurasian and North American boreal regions  
 587 (Zheng et al., 2021). According to the Global Fire Atlas, new records for individual fire size  
 588 and rate of spread were also set in the North American boreal forests during 2023-24, while  
 589 95th percentile fire size and rate of growth in 2023-24 were in the top 2 and 3 years on record  
 590 since 2002, respectively (Jones et al., 2024). Overall, the Canadian boreal forests contributed  
 591 24% towards total fire C emissions in the 2023-24 fire season, up from 3% in an average fire  
 592 season since 2003.  
 593



594 **Figure 1:** Anomalies in BA and C (C) emissions for selected continental biomes in the 2023-  
 595 24 global fire season (March 2023-February 2024), versus the average of prior fire seasons  
 596 since 2002. The selected regions all contribute at least 0.1% towards global mean annual BA  
 597 and experienced BA anomalies of over ±30,000 km<sup>2</sup> in the 2023-24 global fire season. Relative  
 598 changes (%) are also marked by triangular symbols and can be read on the same scale as  
 599 the absolute values.  
 600  
 601



602  
603 Anomalies in the African (sub-)tropical grasslands, savannahs and shrublands strongly drive  
604 inter-annual variability in global fire C emissions because this biome contributes on average  
605 40% towards total global fire C emissions (Jones et al., 2024). If fire C emissions from African  
606 (sub-)tropical grasslands, savannahs and shrublands had been around average fire season  
607 in 2023-24, then global fire C emissions would have been the greatest of any fire season on  
608 record since 2003.

609  
610 Elsewhere at the biome scale, BA extent was in the top three years on record in the South  
611 American broadleaf and mixed forests, the African xeric shrublands, and Australian xeric  
612 shrublands, and the Australian (sub-)tropical grasslands, savannahs and shrublands (**Figure**  
613 **1**). In contrast, BA or fire C emissions were the lowest on record in the European temperate  
614 broadleaf and mixed forests and Asian xeric shrublands, and in the bottom three years on  
615 record in the African savannahs, Asian montane grasslands and shrublands, and European  
616 tropical grasslands and shrublands.

617  
618 On national levels, the most prominent global anomaly of the 2023-24 fire season occurred in  
619 Canada where BA reached six times the average of previous fire seasons and fire C emissions  
620 reached nine times the average of previous fire seasons. Across the Canadian provinces and  
621 territories, the highest BA or fire C emissions on record were observed in Northwest  
622 Territories, British Columbia, Alberta, and Quebec while Yukon, New Brunswick, and Ontario  
623 also experienced high-ranking years (**Figure 2, Figure 3**). The positive BA anomalies in  
624 Canada were visible in the MODIS BA dataset from as early as April 2023 in most provinces  
625 and persisted throughout summer through to October and even through to December 2023  
626 and January 2024 in British Columbia and Alberta (**Figure S2**). Peak anomalies were  
627 observed in Eastern Canada in June 2023, arriving later in western Canada (August-  
628 September). Data on individual fire characteristics from the Global Fire Atlas further reveals  
629 new record fire counts in many Canadian provinces, and high-ranking anomalies in fire count  
630 and daily rate of growth across Canada, as well as new records for fire size and rate of spread  
631 in provinces of both eastern and western Canada (**Figure 4**; Jones et al., 2024). **Appendix A**  
632 discusses the unprecedented Canadian fire season of 2023-24 in greater detail, including its  
633 impacts and regional context.

634  
635 A second prominent regional feature of the 2023-24 global fire season, visible in Earth  
636 observations, is a cluster of administrative regions with positive BA and C emissions  
637 anomalies in the north and west of tropical South America (**Figure 2, Figure 3**). Bolivia,  
638 Guyana, Suriname and French Guiana, Honduras, Nicaragua and Belize all experienced a  
639 high-ranking fire season at national level in 2023-24. In addition, BA or fire emissions were  
640 ranked in the top three years in western parts of Amazonia including in Amazonas state of  
641 Brazil, the Loreto department of Peru, and the La Paz and Beni departments of Bolivia.  
642 Anomalies in the western Amazon spanned June 2023-January 2024, peaking in August-  
643 October 2023. In the north of South America, high-ranking fire seasons were seen in  
644 Venezuela, various subdivisions of Guyana, Suriname, and French Guiana, and in Amapá  
645 State in Brazil. The anomalies in northern South America spanned May 2023-February 2024,  
646 peaking in November 2023-February 2024 (**Figure S2**). The Global Fire Atlas data suggest  
647 that South American anomalies in BA during the 2023-24 fire season were principally driven  
648 by a large number of fires, whereas anomalies in fire size or rate of growth were uncommon  
649 in most of South America (**Figure 4**). **Appendix A** discusses the 2023-24 fire season of  
650 tropical South America and its impacts and regional context in greater detail.

651  
652 Several parts of South and Southeast Asia experienced high-ranking anomalies in BA or fire  
653 C emissions during the 2023-24 fire season, including various neighbouring administrative  
654 zones of Lao People's Democratic Republic (PDR), Thailand and Vietnam. The temporal peak  
655 of these anomalies was broadly in March-May 2023. Data on individual fire characteristics  
656 indicates that high-ranking fire counts, rather than anomalies in fire size, were the primary

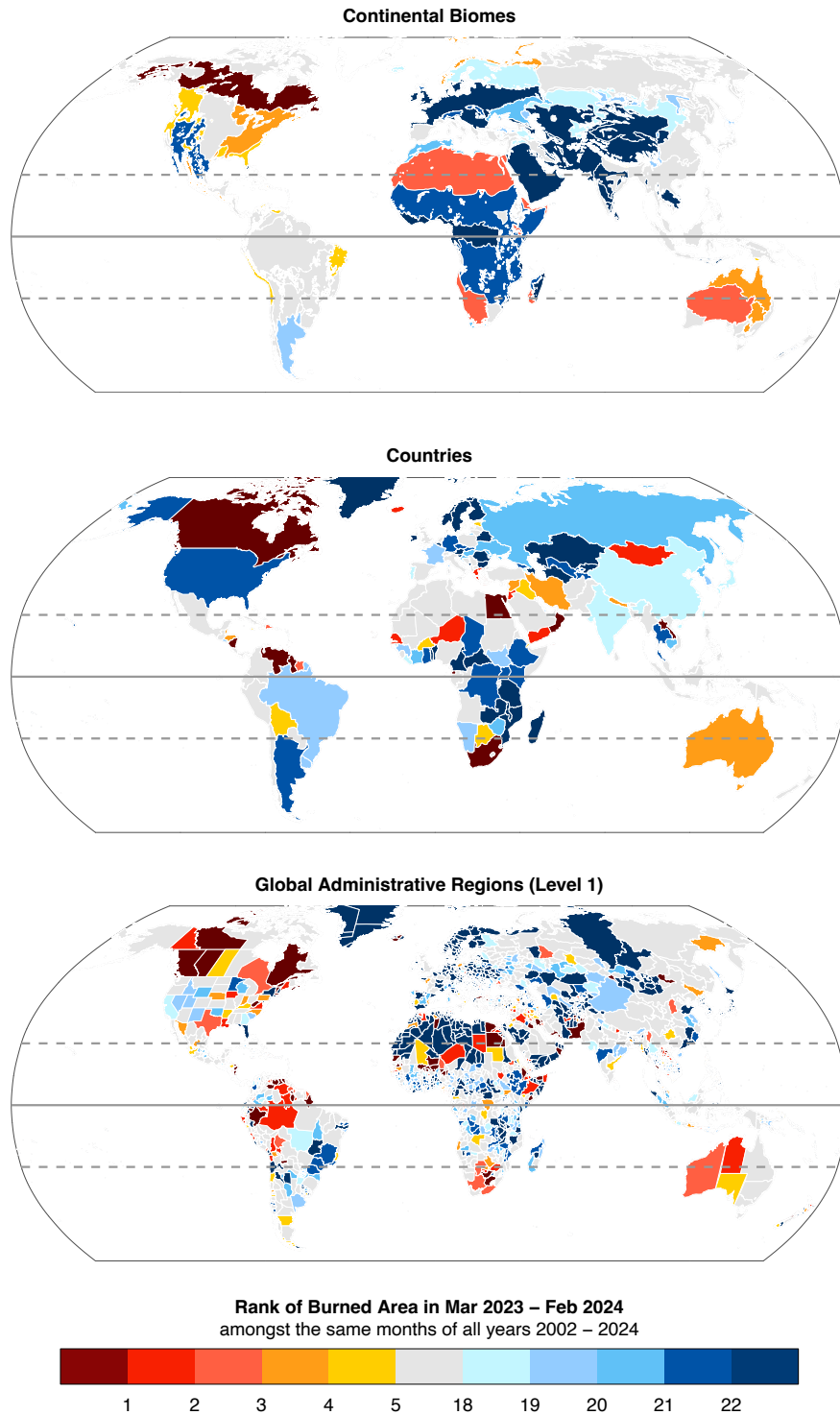
657 driver of the regional BA anomalies (**Figure 4**). **Appendix A** discusses these anomalies and  
658 their impacts in greater detail.

659

660 The anomalies observed in xeric biomes of Oceania are also apparent as high-ranking BA or  
661 C emissions in the 2023-24 fire season in western parts of Australia, particularly in Western  
662 Australia and the Northern Territory (**Figure 2, Figure 3**). Fires tended to affect more remote  
663 areas and so the impacts on society were muted in comparison to the Black Summer events  
664 affecting southeast Australia in 2019-20 (Abram et al., 2021); however, **Appendix A** discusses  
665 some notable exceptions.

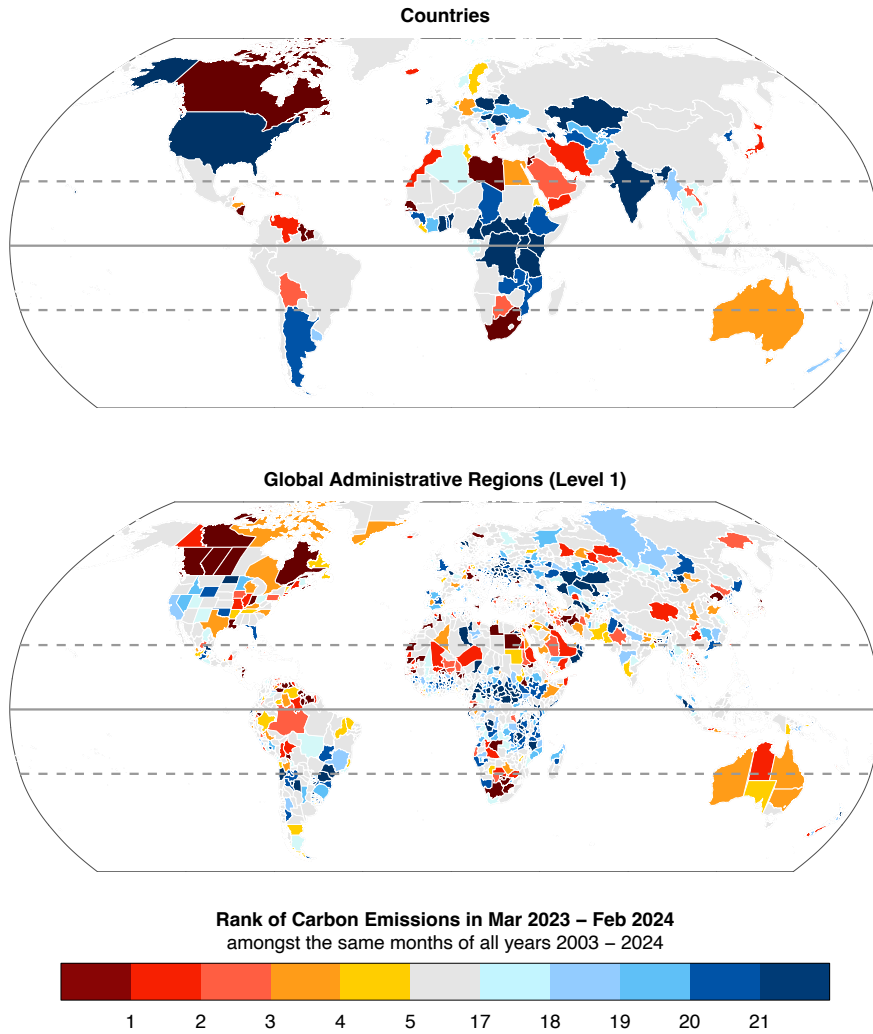
666

667 Other regional pockets of high-ranking BA anomalies or C emissions anomalies were  
668 observed in various dry zones of Africa and the Middle East, including the Sahel, Northern  
669 Africa and the Horn of Africa, Southern Africa (specifically South Africa and Botswana where  
670 three high rainfall years have resulted in grass fuel accumulation), parts of Iran, Iraq, parts of  
671 the Levant region, and parts of the Arabian Peninsula (**Figure 2, Figure 3**). Although various  
672 aspects of the fire season ranked highly in these regions, they are also fuel-limited with a  
673 generally a low baseline for BA and fire C emissions and the wildfire season. Nonetheless,  
674 regionally impactful wildfires were reported for Algeria, Tunisia and Morocco as well as coastal  
675 regions of South Africa and in Pakistan and are discussed further in **Appendix A** and  
676 **Appendix A**.



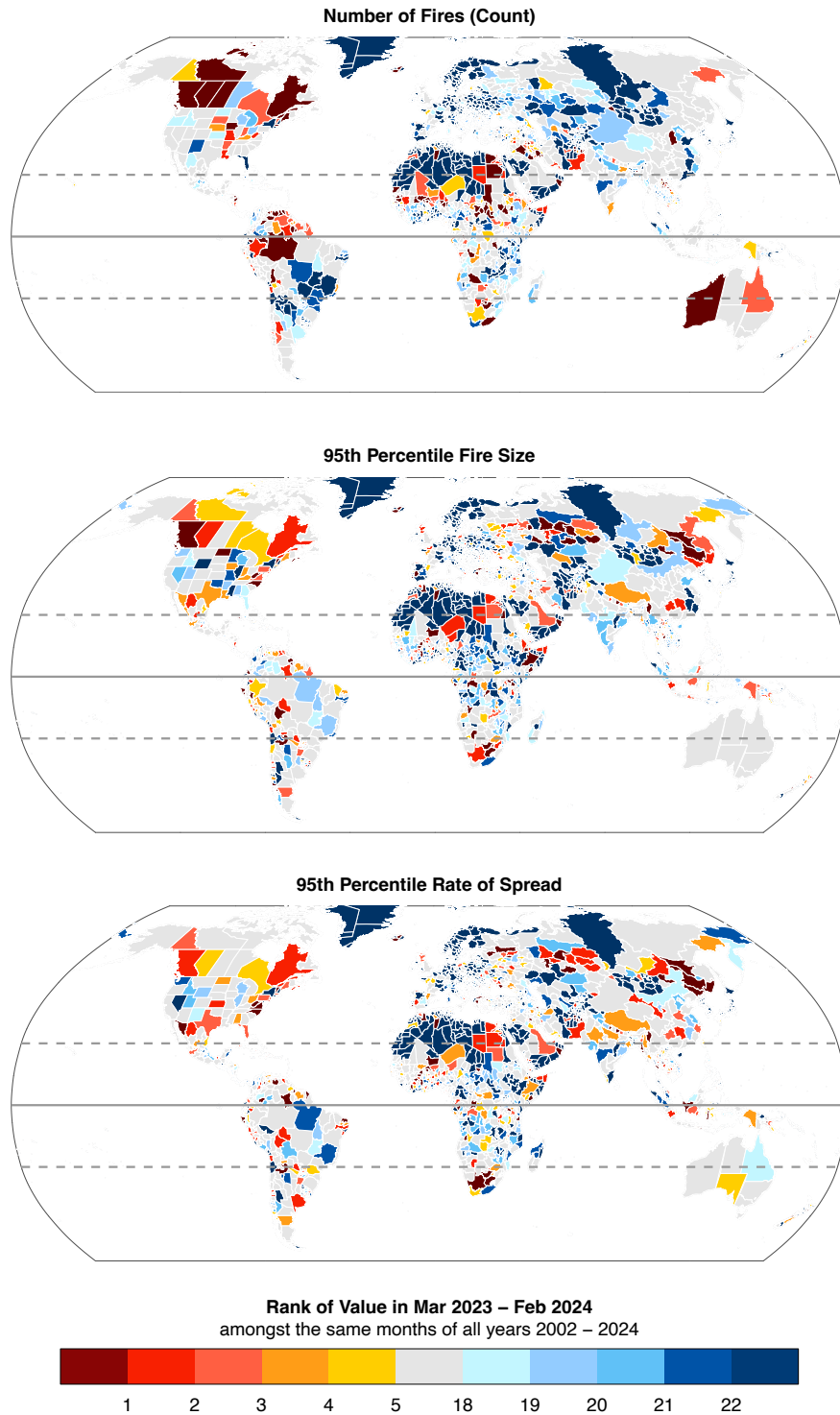
677  
678  
679  
680  
681  
682  
683

**Figure 2:** Ranks of BA during March 2023–February 2024 versus previous March–February periods ( $n = 23$  global fire seasons) for three regional layers: **(top panel)** continental biomes; **(middle panel)** countries, and; **(bottom panel)** states or provinces. Results for regions with high-ranking (top 5 years) or low-ranking (bottom 5 years) events are highlighted. The timing of BA anomalies is shown in **Supplementary Figure 2**.



684  
685  
686  
687  
688  
689  
690

**Figure 3:** Rank of fire C emissions during March 2023-February 2024 versus all March-January periods since 2003 ( $n = 21$  global fire seasons), at the scales of **(top panel)** countries and **(bottom panel)** level 1 administrative regions. We consider C emissions estimates from two products (GFAS and GFED), first calculating the mean emissions value from the two products, then ranking the values.



691  
692  
693  
694  
695  
696  
697  
698  
699  
700

**Figure 4:** Ranks of **(top panel)** fire count, **(middle panel)** 95th percentile fire size, and **(bottom panel)** 95th percentile daily rate of growth during March 2023-February 2024 versus all March-February periods since 2002, at the scale of states or provinces (GADM administrative level 1 regions).

### 2.2.1.2 *Extreme Individual Fires from Earth observations*

To support our analyses of anomalies in individual fire properties and provide insights into the limitations and uncertainties inherent in global-scale analysis of individual fires, we provide a

701 brief assessment of the skills with which the Global Fire Atlas represents some of the most  
702 impactful individual fires of 2023-24. The Global Fire Atlas represents some of the most  
703 impactful individual fire events in 2023-24 with varying skill (**Table 2; Figure S3, Figure S4,**  
704 **Figure S5**). For example, the Evros fire that occurred in the decentralised administration of  
705 Macedonia and Thrace, Greece, in late August was captured reasonably well. The Global Fire  
706 Atlas identifies two fires that ignited on 19th August and merged to form one contiguous  
707 burned unit with an area of approximately 900 km<sup>2</sup>. Alignment of the fire's timing, size and  
708 perimeter with high-resolution satellite imagery (**Figure S3**) and detailed reports  
709 (Xanthopoulos et al., 2024) suggest an overall reliable representation of this particular event  
710 by the Global Fire Atlas. The impacts of this fire are discussed in detail in **Appendix A**.

711  
712 A deadly fire near Valparaíso, Chile, is also captured with reasonable skill in the Global Fire  
713 Atlas (**Figure S4**). Around 90 km<sup>2</sup> was burned, with the fire skirting the city of Placilla de  
714 Peñuelas and encroaching upon Viña del Mar and Quilpué (**Appendix A**). The timing, extent  
715 and perimeter of the fire as recorded by the Global Fire Atlas compares well with those  
716 reported by other sources (**Table 2**).

717  
718 Among the largest fires to occur in Canada during 2023-24 happened near the La Grande  
719 Reservoir in Quebec, Canada. According to both the Global Fire Atlas and a separate NASA  
720 fire tracking product based on the Visible Infrared Imaging Radiometer Suite (VIIRS) sensor,  
721 the fire's extent was around 11 thousand km<sup>2</sup>, whereas the National BA Composite (NBAC;  
722 Skakun et al. 2022) shows a similar extent of 10 thousand km<sup>2</sup>. The timing of the fire also  
723 showed high correspondence across the products.

724  
725 The Lahaina wildfire in Maui, Hawaii, is an example of an event that was captured poorly by  
726 the GFA. Issues relating to the small scale of this fire relative to the resolution of the MODIS  
727 BA data are evident in **Figure S4**. As the MODIS BA algorithm is focussed on the detection of  
728 wildland fire, its effectiveness in tracking fires at the wildland-urban interface is limited. In this  
729 case, burned areas were not detected in cells in urban areas or at the wildland-urban interface,  
730 and hence the size of the fire was under-estimated significantly (**Table 2**). The timing of the  
731 fire on vegetation land adjacent Lahaina was compatible with reference reports.

732  
733 Another example of the challenges of defining individual fire extent and applying global  
734 algorithms to do so comes from Western Australia (**Figure S5**). Two fires recorded by the  
735 Department of Fire and Emergency Services, Western Australia (the Great Sandy Desert and  
736 Anna Plains fires) totalled 57 thousand km<sup>2</sup> in extent. In the Global Fire Atlas, the burned cells  
737 detected by MODIS were instead dissected into 53 separate fires with the largest unit burning  
738 560 km<sup>2</sup>. The date ranges were also rather different with the first record of fires logged in  
739 agency data one month later than in the Global Fire Atlas and the final record logged one  
740 month earlier.

741  
742

743  
744

**Table 2:** Representation of selected individual fire events in the MODIS BA product (Giglio et al., 2018) and Global Fire Atlas (Andela et al., 2019).

Event	Global Fire Atlas Fire Size (km <sup>2</sup> )	GFA Dates	Reported Area (km <sup>2</sup> ) (Reference)	Dates (Reference)	Reference	Comment
Alexandroupolis Wildfire, Evros, Greece	892	19/08/2023 to 30/08/2023	930	19/08/2023 to 31/08/2023	Xanthopoulos et al. (2024)	Good characterisation of the event, with two fires merging in the date range and ultimate fire size comparable to reference.
Fire near La Grande Reservoir, Quebec, Canada	10,725	29/05/2023 to 23/07/2023	11,400 (VIIRS) 9,694 (NBAC)	01/06/2023 to 23/07/2023	NASA Earth Observatory (2023; VIIRS); Jain et al. (2024; NBAC)	Reasonable characterisation of the fire's extent and timing.
Valparaíso Wildfire, Chile	91.54	31/01/2024 to 10/02/2024	85	02/02/2024 to 05/02/2024	NASA Earth Observatory (2024); Copernicus Emergency Management Service (2023a)	Good characterisation of the scale of the event and its perimeters at various wildland-urban interfaces, versus reference data.
Lahaina Wildfire, Maui, Hawaii	1.50	08/08/2023 to 12/08/2023	8.49	08/08/2023 to 09/08/2023	Fire Safety Research Institute (2024)	MODIS data has coarse spatial resolution relative to scale of event. Spread into urban areas not captured.
Western Australia (Great Sandy Desert and Anna Plains fires)	45,544	31/08/2023 to 28/11/2023	56,561	27/09/2023 to 01/11/2023	Department of Fire and Emergency Services, Western Australia (Shapefile for the Great Sandy Desert and Anna Plains fires; Agnes Kristina, pers. comm.)	Global Fire Atlas splits this event into 53 fires; we report their total combined area.  Largest individual fire area in Global Fire Atlas was 760 km <sup>2</sup> (ignited 06/09/2023).  Great Sandy Desert and Anna Plains fires merged on 25th October 2023.

745

## 2.2.2 Context of Recent Extremes: Regional Trends in Burned Area

746

747

748

749

750

751

752

753

754

755

756

757

The anomalies of 2023-24 occur against a backdrop of trends in BA this century that point towards shifts in fire regime. **Figure 5** shows significant trends in BA and forest BA across the fire seasons in the period March 2002-February 2024 derived from MODIS BA data. While many world regions are experiencing declines in total BA, increases in forest BA are far more prevalent than declines at the scale of continental biomes, countries, and administrative regions.

Northern hemisphere extratropical biomes in North America and Asia show a clear signal towards increased forest BA since 2002, which are also visible on national and provincial scales in Canada, the US and Russia and on provincial scales in various states of western

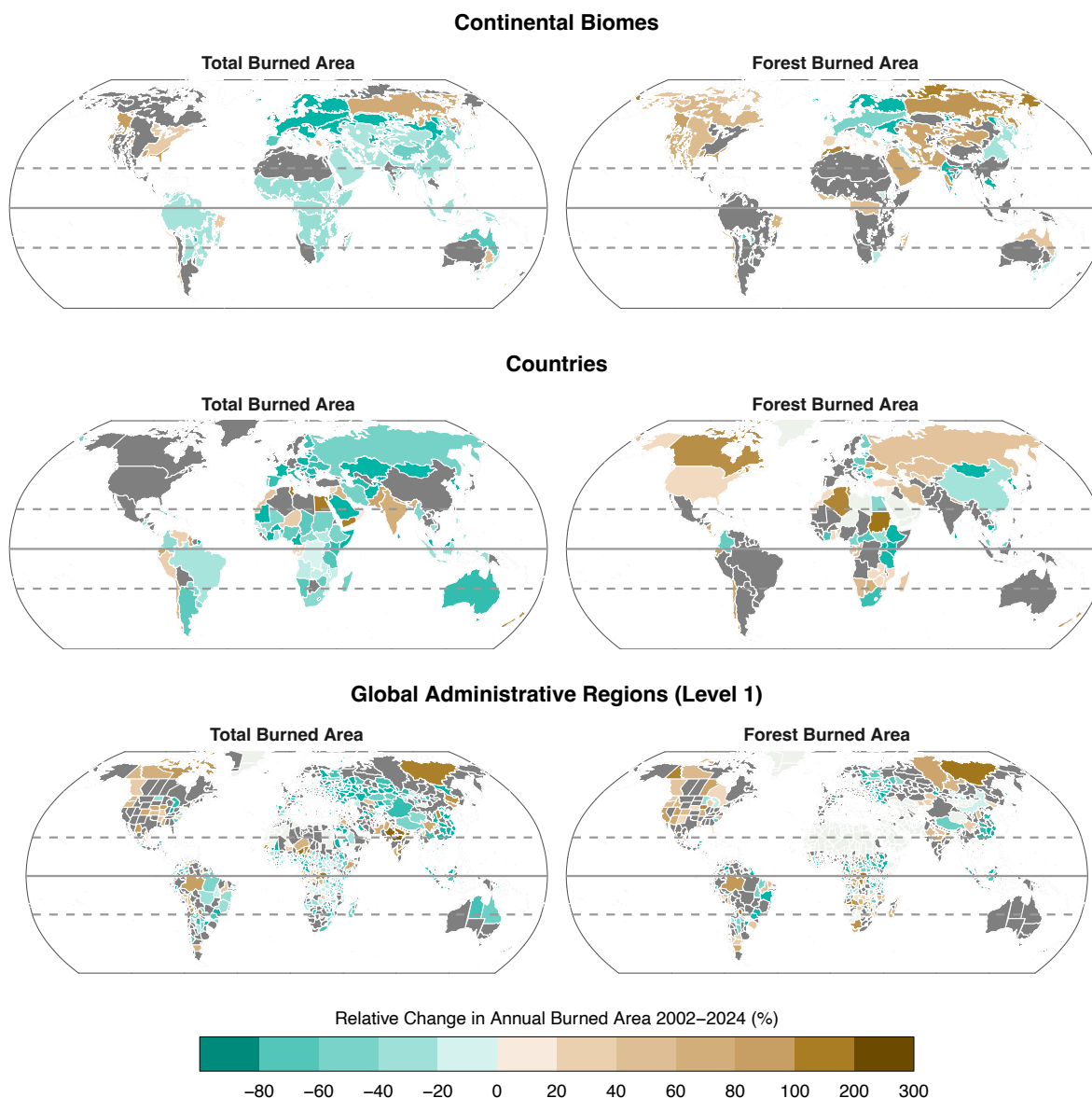
758 and eastern Canada, the western US, and Siberia. These trends occasionally propagate to  
759 trends in total BA, for example in western and northern Canada and in the Sakha Republic  
760 (eastern Siberia). The large 2023-24 anomalies in BA in Canada align with the doubling of  
761 forest BA in Canada across fire seasons since 2002 (a significant trend,  $p < 0.05$ ) and a 23%  
762 increase in total BA in Canada (marginally significant at  $p < 0.1$ ). Three Canadian provinces  
763 showed significant increases in both total and forest BA this century: British Columbia (+35-  
764 42%); Northwest Territories (+55-68%), and; Yukon (+60-135%). No Canadian provinces  
765 experienced a significant decline in forest BA or total BA. More widely, there was a 58%  
766 increase in forest BA in the North American boreal forest biome since 2002, and a 134%  
767 increase across the pan-boreal forest biome of North America and Eurasia. The succession  
768 of events affecting boreal forests in Canada in 2023, Siberia in 2020, and both North America  
769 and Asia during 2021 appear to be part of a continued trend towards rising fire extent in the  
770 high latitudes this century.

771  
772 Elsewhere in the southern hemisphere extratropics, significant rises in forest BA are seen in  
773 Chile since 2002 (+87%), including in the central regions of Araucanía, Bio bío, Maule, Ñuble,  
774 and Valparaíso ranging from 35 to 109%. Extreme fires in Valparaíso during 2023-24 and in  
775 Araucanía, Biobío and Ñuble in the 2022-23 fire season Maule, Nuble, Bio bío, Araucanía  
776 (**Appendix A**) are also consistent with a longer-term rise BA in central Chile (**Figure 5**).  
777 Increases in BA are not generally significant in fire-prone parts of the southern hemisphere  
778 extratropics, such as Africa or Australia.

779  
780 In the tropics, trends in total and forest BA show a variety of patterns. While total BA has  
781 reduced across much of the savannah-occupied regions of South America, Africa and northern  
782 Australia, trends in forest BA (>30% tree cover) are far more varied (**Figure 5**). Hence, fires  
783 in woody tropical vegetation show a less consistent global trend. In addition, exceptions to the  
784 general decline in total BA across the tropics are seen in the Brazilian state of Amazonas, the  
785 Congo basin, and across much of India (**Figure 5**). The trend in Amazonas, among the most  
786 pristine parts of Amazonia, contrasts with other states of Brazil such as Mato Grosso and  
787 Pará, where deforestation rates and deforestation-related fires have fallen since their peak  
788 during the early 2000s (Silva Junior, 2020). The anomalous fire activity and C emissions in  
789 Amazonas state during the 2023-24 fire season (but not other states of Brazil) thus appear to  
790 be consistent with the emerging pattern of increased fire in the region. Meanwhile, the 2023-  
791 24 anomalies in BA and other fire properties in the Bolivian, Peruvian, Colombian and  
792 Venezuelan parts of Amazonia (**Appendix A**) typically occurred against a backdrop of reduced  
793 BA or no significant trend in recent decades (**Figure 5**).

794  
795  
796  
797





798  
799  
800  
801  
802  
803  
804  
805  
806  
807  
808  
809  
810  
811  
812  
813  
814  
815  
816

**Figure 5:** Relative changes (%) in (left panels) total annual BA and (right panels) forest BA across March-February fire seasons during 2002-2024 for three regional layers: (top panels) continental biomes; (middle panels) countries, and; (bottom panels) level 1 administrative regions (e.g. states or provinces). Forest BA considers only areas with tree cover over 30% at the native (500 m) resolution of the BA observations. Relative changes are calculated as the trend in BA across fire seasons March 2002-February 2022 through March 2023-February 2024 multiplied by the number of years in the time series and divided by the mean annual BA during the period. Trends in BA are derived using the Theil-Sen slope estimator. Only significant trends in BA are shown (dark grey fill signifies no significant trend).

## 2.2.3 Focal Events of this Report

### 2.2.3.1 Canada

In this year's report, the extreme wildfire season in Canada is selected as one of our focal events. It emerges as a major event of global relevance for the following reasons (see section 2.2.1 and the results of the expert consultation presented in Appendix A):

- 817 ● **Record-Breaking Burned Area:** The North American boreal forests, particularly in  
818 Canada, experienced an unprecedented fire season. The BA reached six times the  
819 average since 2001.
- 820 ● **High C Emissions:** Fire C emissions in Canada were over nine times the average  
821 since 2003, contributing significantly to global C emission totals for the year. Canadian  
822 boreal forests contributed 24% towards the total above-average global fire C emissions  
823 in 2023-24, up from 3% in an average year.
- 824 ● **Early and Persistent Fires:** Positive BA anomalies were visible from April 2023  
825 (**Figure S9**) and persisted through to October, with some regions experiencing fires  
826 until January 2024. The fire season lasted nearly a month longer than normal, with the  
827 largest one-day BA total ever recorded in Canada occurring on 22nd September 2023.
- 828 ● **Regional Anomalies:** Peak fire anomalies were observed in Eastern Canada in June  
829 2023 and later in Western Canada (August-September), indicating widespread and  
830 prolonged fire activity across the country.
- 831 ● **Record Fire Size and Spread:** New records for individual fire size and rate of spread  
832 were set, with many provinces experiencing high-ranking anomalies in fire count and  
833 daily growth rates.
- 834 ● **Extensive Impact Across Provinces:** The highest BA or fire C emissions on record  
835 were observed in Northwest Territories, British Columbia, Alberta, and Quebec, with  
836 other provinces like Yukon, New Brunswick, and Ontario also experiencing significant  
837 fire activity.
- 838 ● **Air Quality Impact:** Smoke from these fires led to severe air quality issues, affecting  
839 major cities in North America, including New York, which experienced its worst air  
840 quality in half a century.
- 841 ● **Firefighting Challenges:** Canada was at its highest National Preparedness Level for  
842 an unprecedented 120 continuous days, indicating the significant resource sharing and  
843 international assistance required to manage the fires.
- 844 ● **Human and Economic Toll:** Over 232,000 people were evacuated across various  
845 regions, and despite the extreme fire activity, no civilian deaths were directly attributed  
846 to the fires, showcasing the effective, albeit strained, emergency response efforts.

847  
848 To assess the causes of specific regional BA anomalies, four anomalous BA regions/month  
849 combinations were chosen across Canada: Western Taiga Shield and Taiga Boreal Plains for  
850 May and June (includes Alberta and British Columbia Boreal plains, and the Mountain  
851 Cordillera); and Eastern Taiga Shield in Quebec for June and July. **Figure 6** maps the  
852 magnitude of anomalies in these regions and months. Though note the size and long period  
853 this protracted event means that even these regions/month do not capture all the anomalous  
854 BA over Canada in 2023 (**Figure S9**).

### 855 856 **2.2.3.2 Greece**

857  
858 In this year's report, the extreme wildfire season in Greece is selected as one of our focal  
859 events. It emerges as a major event of global relevance for the following reasons (see **Section**  
860 **2.2.1** and the results of expert consultation provided in **Appendix A**):

- 861 ● **Second-Highest BA on Record:** Greece experienced its second worst fire season in  
862 terms of total area burned, with 1,727 km<sup>2</sup> affected, despite recent efforts to strengthen  
863 firefighting mechanisms. The 2023 fire season was notably more severe than typical  
864 years, with the total BA significantly exceeding the country's historical averages and  
865 recent challenging fire seasons.
- 866 ● **Multiple Large Fires:** From mid-July to late August, Greece faced numerous large  
867 fires that overwhelmed firefighting capabilities. Key fires included those on the island  
868 of Rhodes, which burned 207 km<sup>2</sup>, and the massive Evros fire, which reached 938 km<sup>2</sup>.

- 870 ● **Evros Fire Disaster:** The Evros fire became the largest on record in recent European  
871 history, significantly impacting both forested and agricultural areas. It also led to the  
872 tragic deaths of 19 immigrants who were trapped by the flames.
- 873 ● **Urban and Infrastructural Impact:** Fires near populated areas necessitated large-  
874 scale evacuations, including 20,000 tourists on Rhodes and multiple settlements  
875 around Mount Parnis in Attica. The Evros fire also caused a powerful explosion at an  
876 Air Force base, resulting in damage to the town of Nea Aghialos.
- 877 ● **Significant Evacuations:** Numerous evacuations took place, highlighting the severity  
878 of the situation. These included evacuations in Alexandroupolis and its surrounding  
879 villages due to the Evros fire.
- 880 ● **Economic and Environmental Damage:** The fires caused extensive damage to  
881 properties, infrastructure, and natural reserves, with significant impacts on biodiversity  
882 and local economies.
- 883 ● **Firefighting Challenges:** The simultaneous spread of multiple fires stretched  
884 firefighting resources to their limits, with a notable focus on evacuations rather than  
885 fire suppression in some instances.

887 Abnormally high burned areas were reported around Alexandroupolis in August and extended  
888 further west across the administrative region of Macedonia and Thrace. Anomalies were also  
889 present in central Greece and around Athens in July and August (**Figure S10**). **Figure 6** maps  
890 the magnitude of the anomalies for August.

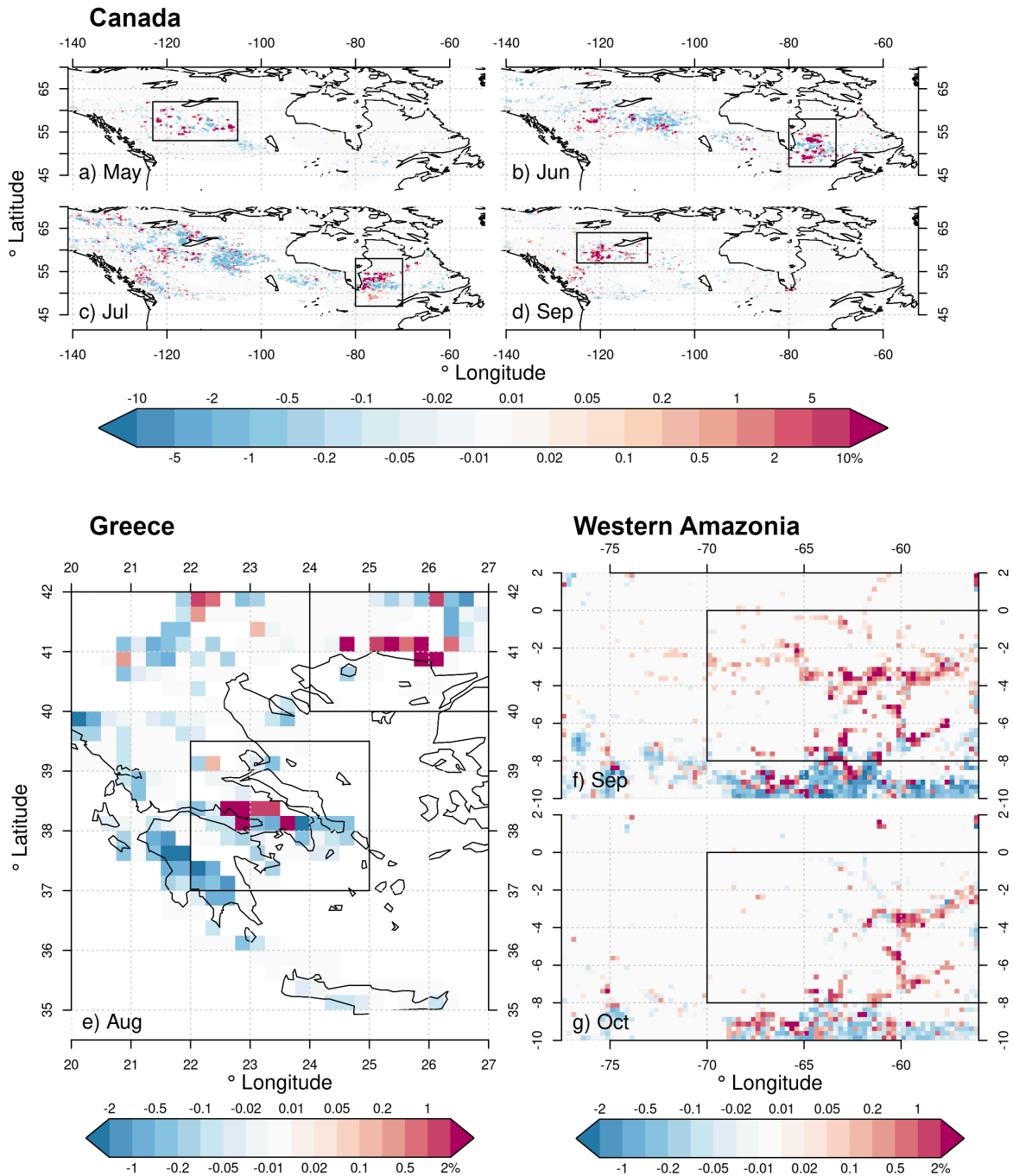
### 891 2.2.3.3 *Western Amazonia*

893 Our final focal event of 2023-24 is a box drawn in western Amazonia with bounding  
894 coordinates 2.25° N, -56.00° E, -9.75° S, -77.75° W. It includes Amazonas (Brazil), Loreto  
895 (Peru), and La Paz and Beni (Bolivia) where peak fire anomalies occurred simultaneously. It  
896 emerges as a major event of global relevance for the following reasons (see **section 2.2.1**  
897 and the results of expert consultation provided in **Appendix A**):

- 898 ● **Record-Setting Fire Activity:** The 2023 fire season in Western Amazonia saw  
899 unprecedented fire counts, with new records set across Amazonas state in Brazil,  
900 Loreto department in Peru, and La Paz and Beni departments in Bolivia.
- 901 ● **Severe Air Quality Degradation:** Smoke from widespread fires led to significantly  
902 degraded air quality across the region, impacting millions of people and posing serious  
903 public health risks.
- 904 ● **Broad Socio-Economic and Health Impacts:** The fires caused extensive socio-  
905 economic disruptions, including health issues from poor air quality, legal actions for  
906 inadequate fire prevention, and impacts on livelihoods, particularly for Indigenous and  
907 traditional communities.
- 908 ● **Widespread Environmental Degradation:** The fires contributed to significant C  
909 emissions and environmental degradation, affecting forest ecosystems and increasing  
910 the region's vulnerability to future climatic extremes. Western Amazonia has global  
911 significance due to its critical role in C storage and biodiversity and relatively low levels  
912 of disturbance.
- 913 ● **Impact on Indigenous and Traditional Communities:** Fires had potential to  
914 significantly disrupt the lives and livelihoods of Indigenous and traditional populations,  
915 exacerbating their vulnerabilities due to isolation and reduced access to resources.

916 Abnormally high burned areas were reported in Western Amazonia during September and  
917 October. **Figure 6** maps the magnitude of these anomalies. The most widespread BA  
918 anomalies emerged in August 2023 and extended through to November 2023 (**Figure S11**).

919  
920  
921



922  
923  
924  
925  
926  
927  
928  
929  
930  
931  
932

**Figure 6:** Spatially explicit anomalies in BA fraction (%) during key months for focal events in (a) Canada, (b) Greece and (c) Western Amazonia. Plotted data are the absolute change from the climatological mean BA fraction for the month (%), based on MODIS BA product aggregated to 0.25°. Red indicates higher BA in that month of 2023 vs the 2002-2022 climatological average for that month. Boxes indicate focus events for our analyses in this report. The top panels show anomalies in Canada for various months, the lower-left panel shows anomalies in Greece for August, and the lower-right panels show anomalies in Western Amazonia during September and August.

### 3 Diagnosing Drivers and Assessing Predictability

#### 3.1 Methods

##### 3.1.1 Predictability of Focal Extremes

We evaluated the time frame over which extreme events could have been forecasted using a common metric of fire danger, the Fire Weather Index (FWI). Developed by the Canadian Forest Service as part of the Canadian Forest Fire Danger Rating System (CFFDRS; van Wagner, 1987), the FWI comprises various components that consider the influence weather on fire danger, with 2m temperature, 10m wind speed, precipitation, and 2m relative humidity as prerequisite variables. The FWI combines three sub-indices, which are fuel moisture codes representing vegetation moisture state at different layers in the forest floor, as well as a spread index influenced by fuel moisture state and wind speed (van Wagner, 1987). A higher FWI indicates fire weather conditions more conducive to wildfires in environments with sufficient fuel load.

Owing to its original design for use in forest ecosystems, the FWI is especially useful for predicting the likelihood and severity of extreme events in ecosystems where weather is the primary limitation to fire (i.e. those mainly limited by moisture or temperature); its accuracy in forecasting BA in fuel-limited ecosystems is more limited (Carvalho et al., 2008; Bedia et al., 2015; Abatzoglou et al., 2018; Jones et al., 2022). Its applications encompass early warning systems, pre-suppression and suppression planning, prescribed burn planning and effectively alerting authorities and the public to abnormal fire danger conditions. FWI is extensively used in operational global information platforms such as the European Forest Fire Information System (EFFIS; <https://forest-fire.emergency.copernicus.eu/>, last access: 9 July 2024) and the Global Wildfire Information System (GWIS; <https://gwis.jrc.ec.europa.eu/>, last access: 9 July 2024), and the Canadian Wildland Fire Information System (CWFIS; <http://cwfis.cfs.nrcan.gc.ca/>, last access: 9 July 2024). The FWI is not the only index for fire danger, and other fire danger systems or sub-indices of this system may correlate more strongly with BA or fire behaviour metrics in some environments. Nonetheless, FWI is widely applied due to its good performance across a range of environments (Di Giuseppe, 2016; Jones et al., 2022) and so we adopt it in the current work.

In addition to well-established fire danger forecasts with lead times of a few days, skilful predictions of fire danger can be made on sub-seasonal to seasonal time scale (S2S) for Mediterranean Europe (Bedia et al., 2015), United States (Roads et al., 2010) and Asia (Spessa et al., 2015). Drought and fire weather conditions throughout the world have been found to correlate with large scale climate patterns such as the El Niño Southern Oscillation (ENSO) (Field et al., 2016; Chen et al., 2017), the Indian Ocean Dipole (Cai et al., 2009) for which current numerical weather prediction systems showcase a predictive skills. Other climate modes such as the Atlantic Multidecadal Oscillation and the Pacific Decadal Oscillation have been shown to influence fire-favourable weather conditions for some seasons and regions (Aragão et al., 2018; Turco et al., 2018) However, due to the larger uncertainties in their predictions, they are not considered here.

Following the concept of seamless prediction of fire weather on S2S timescales (Wetterhall et al., 2018; Di Giuseppe et al., 2020; Di Giuseppe et al., 2024; Dowdy, 2020), we collated FWI data from reanalyses and forecasts designed to operate on S2S lead times of 10 days to 7 months. Here, we take FWI estimates from the ERA5-Land reanalysis product (Muñoz-Sabater et al., 2021) as a proxy for observed FWI. Forecasts at different lead times are taken from the operational high-resolution ECMWF weather system, and seasonal predictions are sourced from ECMWF's seasonal forecasting system, ECMWF-SEAS5 (Johnson et al., 2019; Di Giuseppe et al., 2020; Di Giuseppe et al., 2024). A comparison between reanalysis and

987 forecast provides an indication of how weather forecast errors translate into FWI uncertainties  
988 (predictability). Additionally, the predictions are compared to recorded peaks in fire activity,  
989 both in terms of burned areas and active fires as observed by the MODIS satellites, to provide  
990 a qualitative assessment (skill) of the correlations between landscape flammability and actual  
991 fire events.

992  
993 The prediction systems utilised here vary in their spatial and temporal resolutions. Short to  
994 medium-range FWI forecasts (up to 10 days) are available daily at a resolution of 9 km with  
995 50 ensemble members, while the FWI seasonal forecast is available monthly at a resolution  
996 of approximately 25 km, however seasonal skill is limited to 1-2 months in normal conditions  
997 (Di Giuseppe et al., 2024). All prediction systems include a measure of uncertainties through  
998 the provision of ensemble simulation (**Figure S24, Figure S25, Figure S26**). Variance across  
999 the ensemble was previously estimated to be on the order of 10%-15% (Vitolo et al., 2020).

1000  
1001 Here, the predictive skill of the models is assessed qualitatively by visually examining the  
1002 extent to which extreme FWI (specifically the ensemble mean) was as a precursor of several  
1003 focal events, replicating the use of this indicator by fire agencies during the fire season. The  
1004 approach is designed to partially replicate the interpretation and application of the FWI by fire  
1005 management agencies. Most fire agencies would have local information on fuel conditions and  
1006 would thus be able to interpret FWI values in a more informed manner, reducing the  
1007 dependence of decisions on FWI anomalies alone. The FWI should not be evaluated using  
1008 traditional skill scores, as these would be dominated by false alarms. We maintain that the  
1009 FWI is an index representing flammability and, therefore, cannot be fairly validated against fire  
1010 activities.

### 1011 1012 **3.1.2 Identifying Key Drivers of Focal Events**

#### 1013 1014 **3.1.2.1 Modelling Systems**

1015  
1016 We used two modelling systems with similar fire predictors to diagnose the drivers of each  
1017 focal event. The models are the PoF model (McNorton et al., 2024) and the ConFire attribution  
1018 framework (Kelley et al., 2019; Kelley et al., 2021). The PoF model diagnoses the drivers of  
1019 active fire (AF) observations from the MODIS MCD14ML active fire product (collection 6.1; 1  
1020 km resolution; Giglio et al., 2016; NASA FIRMS, 2020) using Shapley values (Lundberg and  
1021 Lee, 2017), while ConFire diagnoses drivers of BA from the MODIS BA product (Giglio et al.,  
1022 2018; regridded to 0.5°). Fires flagged as low confidence in the AF product were not used.  
1023 Although AF and BA have been used widely in global and regional scientific studies, there are  
1024 substantial differences between the two branches of fire observation as reviewed extensively  
1025 elsewhere (Roy et al., 2008; Di Giuseppe et al., 2021; Chuvieco et al., 2019), and the strength  
1026 of the relationship between them can vary regionally (van der Werf et al., 2017; Hantson et  
1027 al., 2013). Our use of two observational fire products and two distinct model approaches  
1028 provides a way to account for inherent uncertainties in the observability of different fire events  
1029 and the uncertainties in the methodologies.

1030  
1031 Both modelling approaches use a number of individual predictors of AF or BA, which we refer  
1032 to as 'drivers'. The drivers are grouped into four main categories, which we refer to as the  
1033 controls. PoF and ConFire both include weather, fuel abundance, and fuel moisture as controls  
1034 on fire. In addition, PoF (but not ConFire) includes an "Other" category of controls and ConFire  
1035 (but not PoF) includes a "human" category of controls, as per **Table 3**. PoF drivers in "Other"  
1036 include ignition and suppression effects as well as the residual error between predicted and  
1037 observed fire activity. Grouping the set of drivers between the four identified controls —  
1038 weather, fuel moisture, fuel load, and human/other— is not always straightforward, as fuel  
1039 moisture and weather variables are strongly correlated, and fuel load is also related to weather  
1040 conditions. Hence, some drivers can be associated with more than one control (**Table 3**). The

1041 categorisation stems mostly from the way the driving datasets have been obtained and their  
1042 underlying resolutions. We have also considered the traditional approach of assessing fire  
1043 weather in isolation within most fire danger assessment metrics. We believe that grouping  
1044 these metrics under the umbrella term 'control weather' offers a concise way to reference the  
1045 drivers of the fire weather index (Matthews, 2009). Despite this, it is important to note that the  
1046 techniques employed ensure contribution from specific variables cannot be double-counted  
1047 between categories. Both ConFire and PoF are capable of disentangling the contributions of  
1048 individual drivers within the same control category (for example, the separate contributions of  
1049 dead or live vegetation) and quantifying these contributions (Kelley et al., 2019; McNorton et  
1050 al., 2024). However, we will focus our analysis on the impact of the controls.

1051  
1052

### 1053 **3.1.2.2 Drivers and Controls Used in Fire Event Analysis**

1054

1055 For our assessment of the contribution of weather and fuel moisture to the anomalous events  
1056 we take several predictors from ERA5-Land (9 km resolution; Muñoz-Sabater et al., 2021),  
1057 specifically variables that are known to correlate with AF or BA (Bistinas et al., 2014; Haas et  
1058 al., 2022). The drivers considered for each control are listed in **Table 3**. For the weather  
1059 component in isolation, we use 2m temperature, 2m dewpoint temperature, 10m wind speed  
1060 and daily total precipitation (note that these are the prerequisite variables used in the  
1061 formulation of the FWI; van Wagner, 1987). We use a fuel characteristic model to estimate the  
1062 fuel load and fuel moisture components following McNorton and Di Giuseppe (2024), with  
1063 model estimates of fuel moisture constrained by estimates of leaf area index (LAI) from the  
1064 ECMWF's Integrated Forecast System (IFS) and model estimates of fuel loads constrained  
1065 by aboveground biomass estimates from the ESA CCI (Santoro and Cartus, 2021) and net  
1066 ecosystem exchange estimates from the Copernicus Atmosphere Monitoring Service (CAMS;  
1067 Agustí-Panareda et al., 2019). Additional predictors regarding fuel load and state include  
1068 vegetation cover and type (**Table 3**). Proxies for ignition and suppression controls, placed  
1069 within the "Other" set of controls, are more challenging to establish. Currently, we use  
1070 population density, urban fraction, cropland fraction, pasture fraction, lightning, orography  
1071 (**Table 3**). For consistency all variables are interpolated to 9 km resolution. 'Others' not only  
1072 include factors related to ignitions but also the fraction of predictions missed by the models.  
1073 This is important because this category weights the importance of unaccounted-for factors.

1074

1075 Another important aspect is that models do not assume a specific direction for each factor's  
1076 influence on fire activity. Consequently, wetness can correlate with increased fire likelihood in  
1077 some locations and reduced fire likelihood in others. This aligns with established theory in our  
1078 field: in fuel-limited regions where grass and herbaceous fuels dominate, high rainfall  
1079 promotes fuel accumulation and increases fire extent. Conversely, in fuel-rich regions with  
1080 high tree cover, high rainfall increases fuel moisture and reduces fire extent. See "**Modelling  
1081 frameworks**" in the **Extended Methods Supplement** for a detailed description. See  
1082 "**Evaluation**" in the **Extended Methods Supplement** for detailed evaluation.

1083

1084



1085  
1086  
1087  
1088  
1089  
1090  
1091

**Table 3:** Drivers of fire and their parent control group included in the event fire analyses using ConFire and PoF. Drivers are individual variables, which serve as proxies for the influence of weather, fuel load, fuel moisture, or other controls on BA. \*\* The ‘Other’ category includes proxies for ignition and suppression controls plus the missed prediction. Note that for ConFire, explanatory variables can be associated with multiple controls (Kelley et al. 2019). Positive (+ive) or Negative (-ive) under “ConFire control” describes if a driver increases or decreases BA in ConFire.

Driver	POF control	ConFire controls	Frequency	Time Period	Source	Reference
2m Temperature	Weather	Weather +ive	Daily	Jan 2014-NRT	ERA5-Land	Muñoz-Sabater et al. 2021
2m Dewpoint Temperature	Weather	Weather -ive	Daily	Jan 2014-NRT	ERA5-Land	Muñoz-Sabater et al. 2021
10m Wind Speed+	Weather	Not used	Daily	Jan 2014-NRT	ERA5-Land	Muñoz-Sabater et al. 2021
Precipitation	Weather	Weather -ive	Daily	Jan 2014-NRT	ERA5-Land	Muñoz-Sabater et al. 2021
Live Leaf Fuel Load	Fuel Load	Not used	Daily	2014- 2020	Fuel Model	McNorton et al. 2024a
Live Wood Fuel Load	Fuel Load	Not used	Daily	2014- 2020	Fuel Model	McNorton et al. 2024a
Dead Foliage Fuel Load	Fuel Load	Not used	Daily	2014- 2020	Fuel Model	McNorton et al. 2024a
Dead Wood Fuel Load	Fuel Load	Not used	Daily	2014- 2020	Fuel Model	McNorton et al. 2024a
Mean & Max Vegetation Optical Depth (VOD) of the last 12 months	Not used	Fuel Load +ive	Monthly	2014-NRT	Satellite-Soil Moisture and Ocean Salinity (SMOS)	Wigneron et al 2021
Vegetation Optical Depth (VOD)	Moisture	Moisture -ive	Monthly	2014-NRT	Satellite (SMOS)	Wigneron et al 2021
Low Vegetation (LAI)	Fuel Load/Moisture	Not used	Monthly	2002-2020 climatology	Satellite (multi-sensor)	Boussetta et al., 2021
High Vegetation (LAI)	Fuel Load/Moisture	Not used	Monthly	2002-2020 climatology	Satellite (multi-sensor)	Boussetta et al., 2021
Live Fuel Moisture Content	Fuel Moisture	Fuel Moisture -ive	Daily	2014-NRT	Fuel Model	McNorton et al. 2024a
Dead Fuel Moisture Content	Fuel Moisture	Fuel Moisture -ive	Daily	2014-NRT	Fuel Model	McNorton et al. 2024a
Snow cover	Fuel Moisture	Snow -ive	Daily	2014-NRT	ERA5-Land	Muñoz-Sabater et al. 2021
Pasture	Not used	Ignitions +ive Suppression -ive	Annual	2014-2023	HYDE	Klein Goldewijk et al., 2011
Cropland	Not used	Ignitions +ive Suppression -ive	Annual	2014-2023	HYDE	Klein Goldewijk et al., 2011
Urban population	Not used	Ignitions +ive Suppression -ive	Annual	2014-2023	HYDE	Klein Goldewijk et al., 2011
Rural populations	Not used	Ignitions +ive Suppression -ive	Annual	2014-2023	HYDE	Klein Goldewijk et al., 2011
Lightning	Not used	Ignitions +ive	Monthly	2000- 2020 climatology	LIS/OTD	Cecil et al., 2014
Type of Vegetation	Other**	Not used	Fixed	Jan 2014-NRT	ECLand	Boussetta et al., 2021
Urban Fraction	Other**	Not used	Fixed	Jan 2014-NRT	ECLand	McNorton et al. 2023
Orography	Other**	Not used	Fixed	Jan 2014-NRT	ECLand	Boussetta et al., 2021

1092  
1093



### 3.1.2.3 Analysis of Fire Drivers

The PoF system uses gradient-boosted decision trees from the XGBoost library on detected AF (McNorton et al., 2024). The training iteratively adds decision trees to an ensemble of models to correct for errors made by previous iterations, resulting in a computationally efficient optimization (Chen and Guestrin, 2016). The system training uses a classifier approach which defines a positive hit as an AF detection within the grid cell on a given day. The driver attribution is performed using the SHapley Additive exPlanations (SHAP) method taken from the SHAP library (Lundberg and Lee, 2017). These are then combined to provide overall attribution to one of the four controls for AF predictions.

ConFire uses Bayesian Inference to assess fire behaviour uncertainty by evaluating control strengths' impact on BA. Instead of a single output, it produces a probability distribution based on data into a simplified fire model. Variables like weather and fuel moisture contribute simultaneously to the prediction of monthly BA. Monthly averages of daily values are aggregated using the Fogo Local Analisado pela Máxima Entropia (FLAME) system (Barbosa, 2024). Each control combines drivers using logistic functions. Bayesian inference optimises driver contributions and accounts for stochasticity, capturing fire unpredictability under similar conditions (Kelley et al., 2021). The mean logit-transformed BA distance with and without this term measures additional uncertainty. The model is trained and ran from 2014 to 2023 using driving datasets common across this period. Initially trained on 50% of BA, it is then applied predictively to the full dataset. A separate evaluation is conducted, training on data from 2014 to 2018 and testing against 2019 to 2023, following the protocol employed by Barbosa (2024). See **“Modelling frameworks”** and **“Evaluation”** in the **Extended Methods Supplement** for a detailed description.

For both models we include an estimate of uncertainty. ConFire is designed as an uncertainty quantification model, providing BA probabilities and their likelihoods for each region. Results in this report are based on 5-95% confidence intervals or likelihoods, supporting central (median) estimates. ConFire uses Bayesian inference to quantify how various factors impact fire occurrence, assuming that fuel increases BA, moisture decreases it, ignitions increase it, and suppression decreases it. The model trains on historical data to determine influence levels and accounts for uncertainties from fire stochasticity and unconsidered factors. Its probability distribution is a logit zero-inflated function, assessing changes in extreme fires even with small observed areas. ConFire manages uncertainties from unpredictable weather and vegetation responses. ConFire quantifies uncertainty estimates from different drivers by constraining them with observations and addresses structural uncertainties, such as missing explanatory variables and errors in mechanistic relationships. While it represents one relationship of control to BA, the probability distribution accounts for uncertainty across various potential relationships. Noise is considered, with the stochasticity of burned area accounted for both in areas with no fire and in the probability of different potential levels of burning where fire does occur. We test ConFire's uncertainty quantification using Bayesian inference evaluation techniques. However, ConFire does not account for some uncertainties, such as potential changes in feedbacks between fire and vegetation when transitioning to a new fire regime out of sample. The model assumes the accuracy of one bias-corrected model for fuel load (JULES-ES), neglecting uncertainty from Dynamic Global Vegetation Models (DGVM). While BA anomalies are used to reduce observational bias, any disagreements in bias across space or time are not included in ConFire's training.

Meanwhile, PoF outputs are provided in terms of probabilities calculated using ensemble predictions from weather forecasts each to generate a set of binary classifiers. The probabilities are therefore based on a wide parameter space, taking into account uncertainties in both the input parameters and the stochasticity of the classification algorithm itself.

1148 **3.2 Results**

1149

1150 **3.2.1 Predictability of Focal Events using Fire Weather Forecasts**

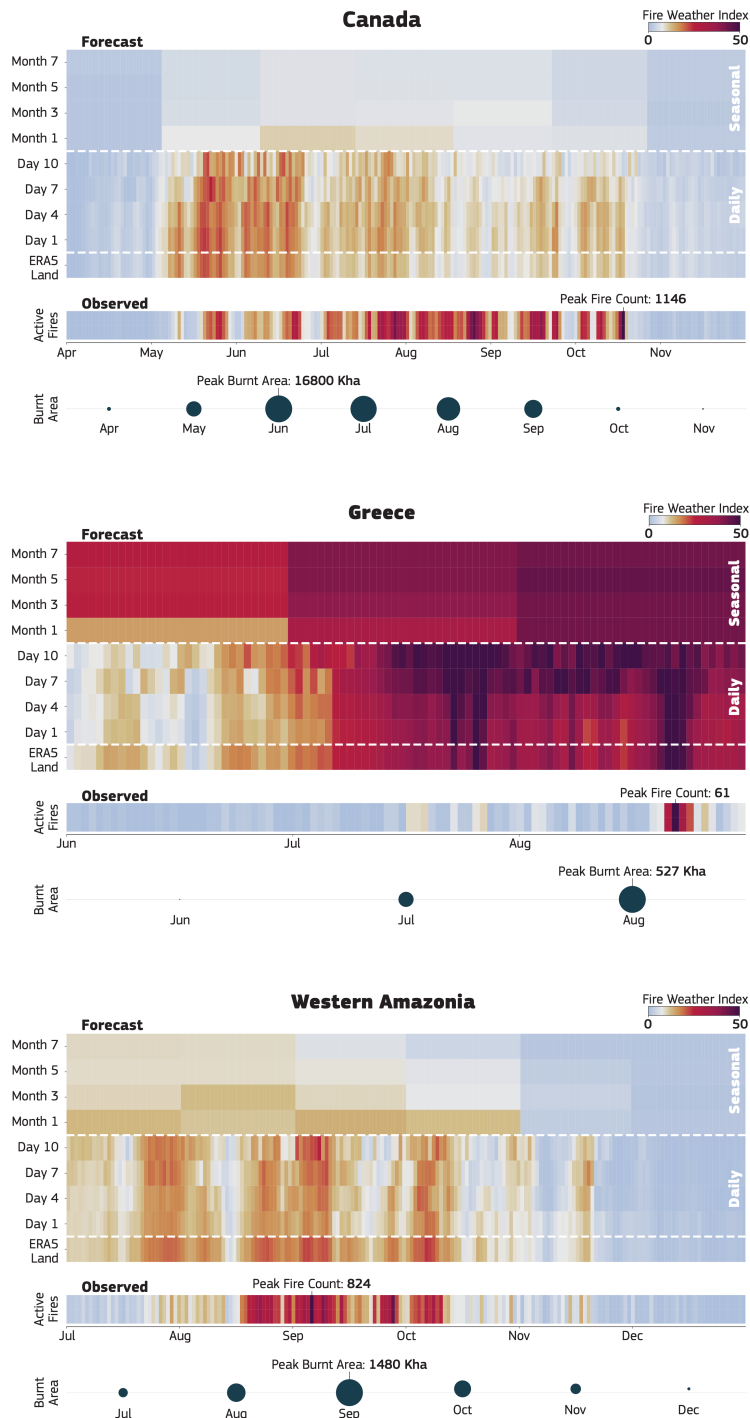
1151

1152 **3.2.1.1 Canada**

1153

1154 The early establishment of fire weather conditions as well as the late cessation of the fire  
1155 season are well captured in the FWI reanalysis in Canada (**Figure 7**). The FWI also captures  
1156 the intermittent pattern of fire danger and its correlation to actual fire activity. However, at the  
1157 seasonal time scale, the signal is weakened, and there were no prior indications that the  
1158 upcoming season would have been as extreme as it was with respect to fire activity (**Figure**  
1159 **7**). For most part of 2023 Canada was in drought. The weather-limited nature of the Canadian  
1160 fire season means that the FWI modelling framework serves as an essential indicator of  
1161 anomalous conditions, acting as a prerequisite for the intensity and spread of fires. It provides  
1162 valuable insights into the sequence and extent of extreme fire weather days during such  
1163 events. Notably, in this region, peaks of fire activity correspond to peaks of landscape  
1164 flammability, and there is a good correlation between observed fire activity and predicted fire  
1165 danger.

## Fire Activity & Prediction 2023



1166  
1167  
1168  
1169  
1170  
1171  
1172  
1173  
1174

**Figure 7:** Chicklet plots displaying seamless FWI predictions over time from various forecasting systems of the ECMWF (see Methods). The x-axis corresponds to specific dates throughout the year, while the y-axis denotes either observations or the time leading up to the date when a forecast was generated. The vertical colour coherence allows for quick identification of the time windows of predictability associated to the observed fire activity both provided in terms of number of detected active in a day fires and total burned areas in a month (circles).

1175 **3.2.1.2 Greece**

1176

1177 The establishment of fire-prone conditions in the Mediterranean, particularly in Greece, is part  
1178 of the region's seasonal weather cycle (**Figure 7**). In 2023, this pattern persisted, and extreme  
1179 landscape flammability could be forecasted well in advance. In arid and semi-arid regions fire  
1180 occurrence is driven not solely by weather but also by fuel availability and its intermittent short-  
1181 term drying. In these regions the FWI often reaches extreme levels for much of the summer.  
1182 However, fires do not always occur even when the FWI is extreme, as ignition and early  
1183 suppression play a crucial role. The anomalous fire extent in Alexandroupolis, including the  
1184 large Evros fire, highlights the limitations of relying solely on fire weather indices in these  
1185 areas. There were no discernible indications in the FWI records that the particular day was  
1186 more extreme than the days before or afterwards, emphasising the need for a more holistic  
1187 approach to fire risk assessment in regions where fuel is a limiting factor or live fuel moisture  
1188 plays a crucial role in the extent of the fires (Di Giuseppe, 2023).

1189

1190 **3.2.1.3 Western Amazonia**

1191

1192 The correlation between FWI and fire activity in the western Amazonia region at the shorter  
1193 lead times is generally poor, primarily due to the strong dependency on either lightning or  
1194 human ignitions (Kelley et al., 2021). In 2023, this pattern persisted (**Figure 7**), with the onset  
1195 of fire weather following the seasonal pattern well ahead of the time where fires were triggered.  
1196 Seasonal predictions indicated high fire danger during the summer period probably driven by  
1197 El Niño conditions.

1198

1199 **3.2.2 Identifying Key Drivers of Focal Events**

1200

1201 Weather, fuel moisture, fuel abundance, and ignitions are the four primary controls identified  
1202 as influencing the occurrence and intensity of the focal fire events. Anomalies in individual  
1203 drivers of these controls, such as temperature or soil moisture, are calculated by comparing  
1204 regional daily 2023 averages with the average for 2003-2022. Dead fuel, with its lower  
1205 moisture content and higher combustibility, often plays a significant role in determining fire  
1206 ignition. During extreme events, it is the dry live fuel that burns, contributing to the overall  
1207 severity and intensity of the fire.

1208

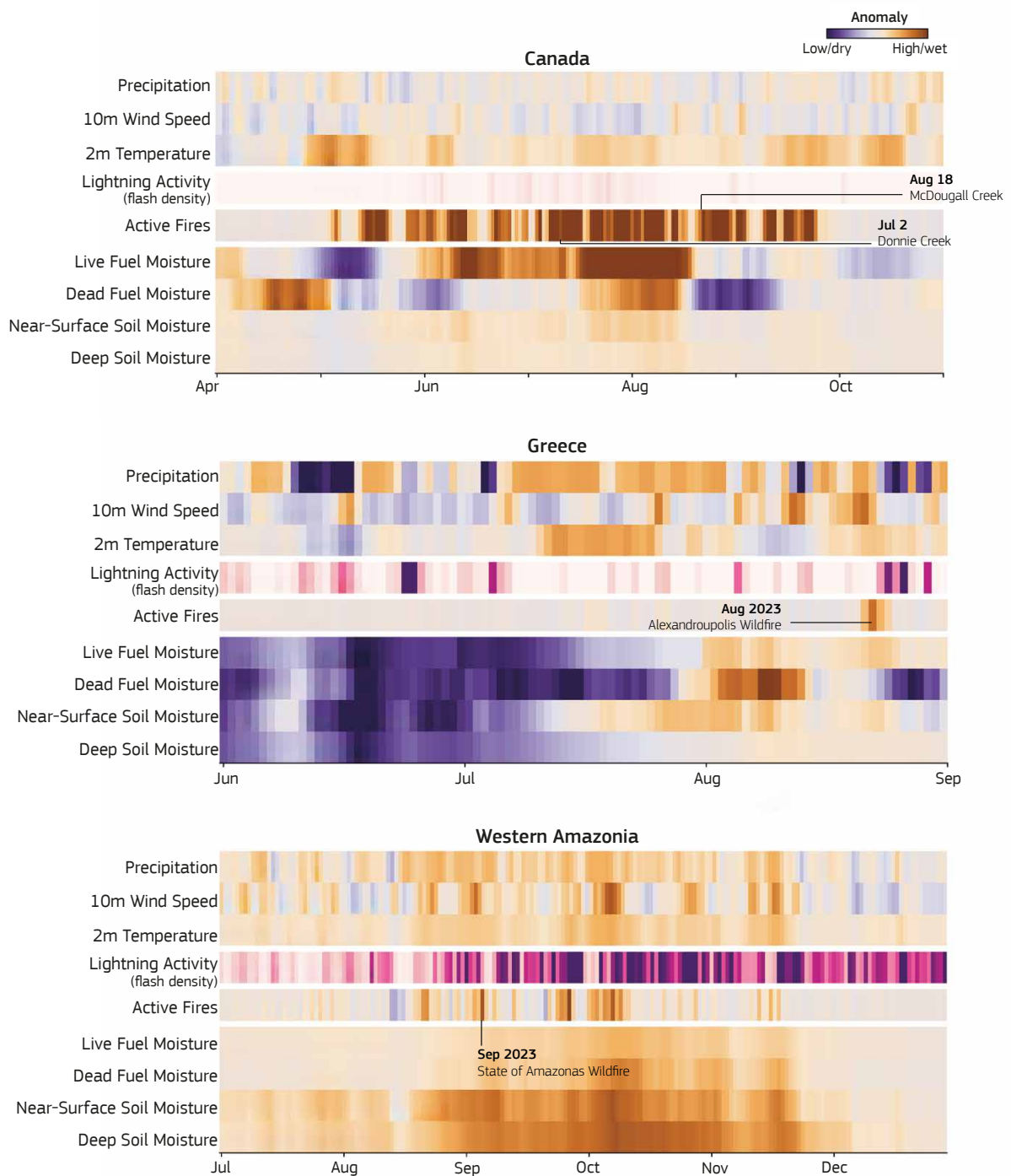
1209 Analysing the time series of key drivers contextualises the conditions under which events  
1210 occurred (see **Figure 8**). However, leveraging the PoF and ConFire models allows for a  
1211 statistical causality attribution of the four controls for observed fire occurrence (see **Figure 9**).  
1212 These models will provide control attribution even if no fire event is recorded, with a low  
1213 probability across all controls indicating an accurate prediction. High fire probability without  
1214 recorded fire activity could indicate successful suppression or fire-prevention policies.  
1215 Unaccounted human influence is categorised under "other," encompassing variables not  
1216 forecasted by the models. This analysis enhances our understanding of fire activity controls  
1217 and helps identify missing information that degrades the quality of the prediction.

1218

1219

1220

## Fire drivers in 2023



1221  
1222  
1223  
1224  
1225  
1226  
1227  
1228

**Figure 8:** Anomaly driver stripes for the three focal events. The drivers are selected to contextualise the conditions under which the examined events took place. All values are expressed as anomalies compared to the 2003-2021 climatology with the exception of lightning activity which is expressed as absolute flash density.

1229 **3.2.3 Drivers of Active Fire Extremes**

1230

1231 **3.2.3.1 Canada**

1232

1233 Persistent fire-favourable weather conditions played a crucial role in controlling the extent of  
1234 active fires in Canada during the summer of 2023. Dry weather contributed to extensive drying  
1235 of both live and dead vegetation, further exacerbating fire risk (**Figure 8, 13**). Most of the  
1236 explainability of the Canada event comes from anomalous weather conditions. Increased  
1237 lightning activity often coincides with or precedes significant fire periods, indicating lightning  
1238 as a key source of ignitions in the region given the contribution of the cloud-to-ground flashes  
1239 to the total predicted lightning activity. This is in agreement with the attribution of 59% of  
1240 wildfires and 93% of total BA to lightning ignition sources in Canada during 2023 (Jain et al.,  
1241 2024). Adverse weather conditions in mid-May in western Canada were identified as influential  
1242 factors in shaping fire events. However, multiple instances of intense burning events, notably  
1243 in mid-July, early August, and late September, fall into the 'Other' category, heavily  
1244 contributing to the total number of events for which there is no attribution among the controls.  
1245 The fact that clusters of events were not predicted suggests potential inadequacies in  
1246 accounting for some ignition sources or accurately representing fire propagation across these  
1247 landscapes.

1248

1249 **3.2.3.2 Greece**

1250

1251 The driver anomalies (**Figure 8**) and control attribution (**Figure 9**) did not suggest an  
1252 abnormally fire-prone year in Greece, failing to explain the large fire extent around the time of  
1253 the Evros fire near Alexandroupolis. An anomalously wet spring may have led to increased  
1254 foliage and subsequently quick drying of plant material. A sustained dry period in late July and  
1255 August further dried out new foliage, creating favourable conditions for fire activity, as  
1256 indicated by the anomalously dry live and dead fuel moisture content in August. Despite these  
1257 conditions, the unexpected extent and severity of fires around Alexandroupolis were not  
1258 predicted, highlighting the intrinsic difficulties in forecasting isolated extreme events even  
1259 when most predictors are included. Additionally, the high wind speeds at the time partially  
1260 contributed to the extensive BA during the fire.

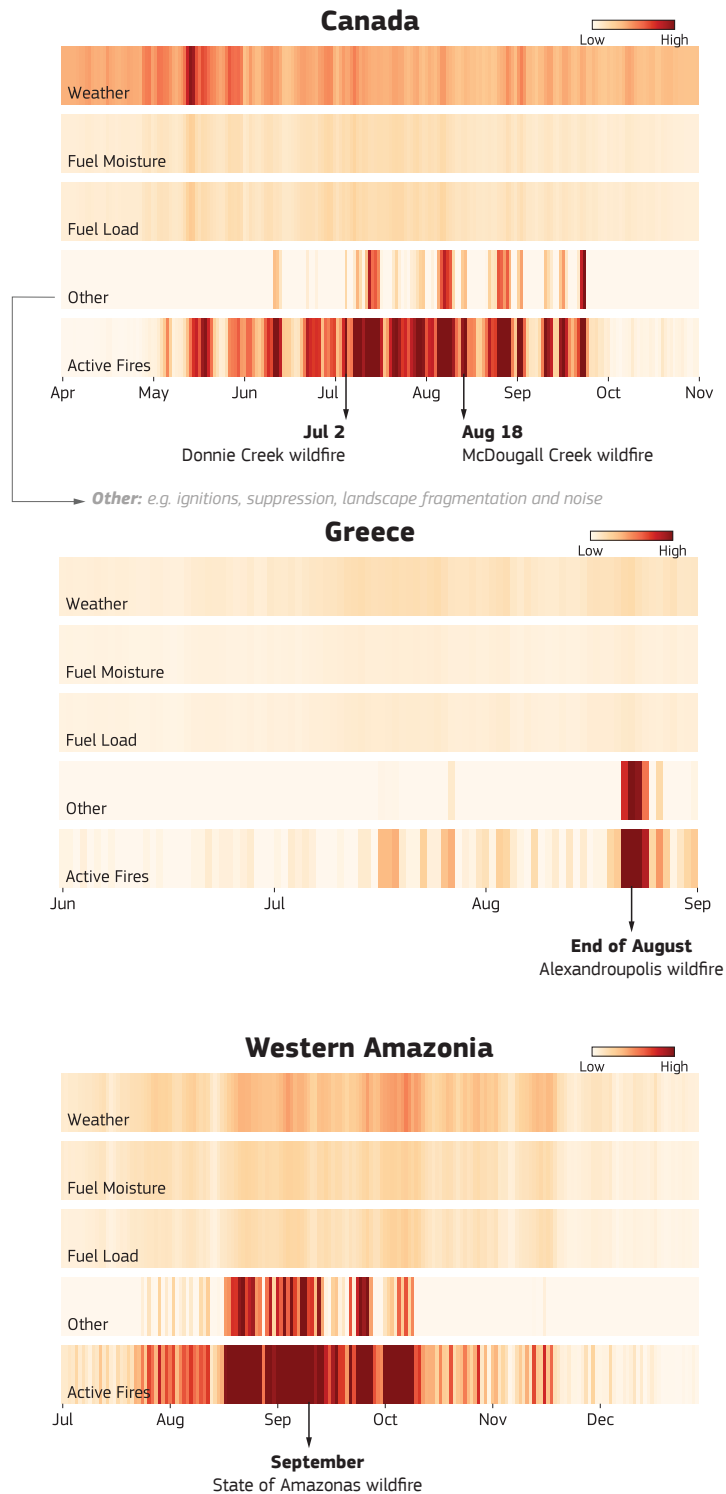
1261

1262 **3.2.3.3 Western Amazonia**

1263

1264 Prolonged drought conditions driven by a positive ENSO (Aragão et al., 2007; Jiménez-Muñoz  
1265 et al., 2016), stemming from anomalously low rainfall and high temperatures, created  
1266 favourable conditions for an active fire season in Western Amazonia (**Figure 8, Figure 9**).  
1267 These conditions had a significant impact on the typically wet ecosystem, affecting soil  
1268 moisture as well as live and dead fuel moisture. Despite weather conditions serving as a  
1269 persistent control for fire activity, several intense active fire periods in late August and  
1270 throughout September were not predicted, possibly due to unrepresented ignition sources.  
1271 Additionally, fire activity from September onwards was intensified by intense lightning activity,  
1272 characteristic of the region, which substantially contributed to ignitions.

## Fire controls 2023



1273  
1274  
1275  
1276  
1277  
1278  
1279

**Figure 9:** Contributions of different fire controls to daily active fire anomalies in our focal events. All values are scaled to the observed daily fire anomaly such that the sum of the 4 daily control values matches the total observed anomaly.

1280 **3.2.4 Drivers of Regional Burned Area Extremes**

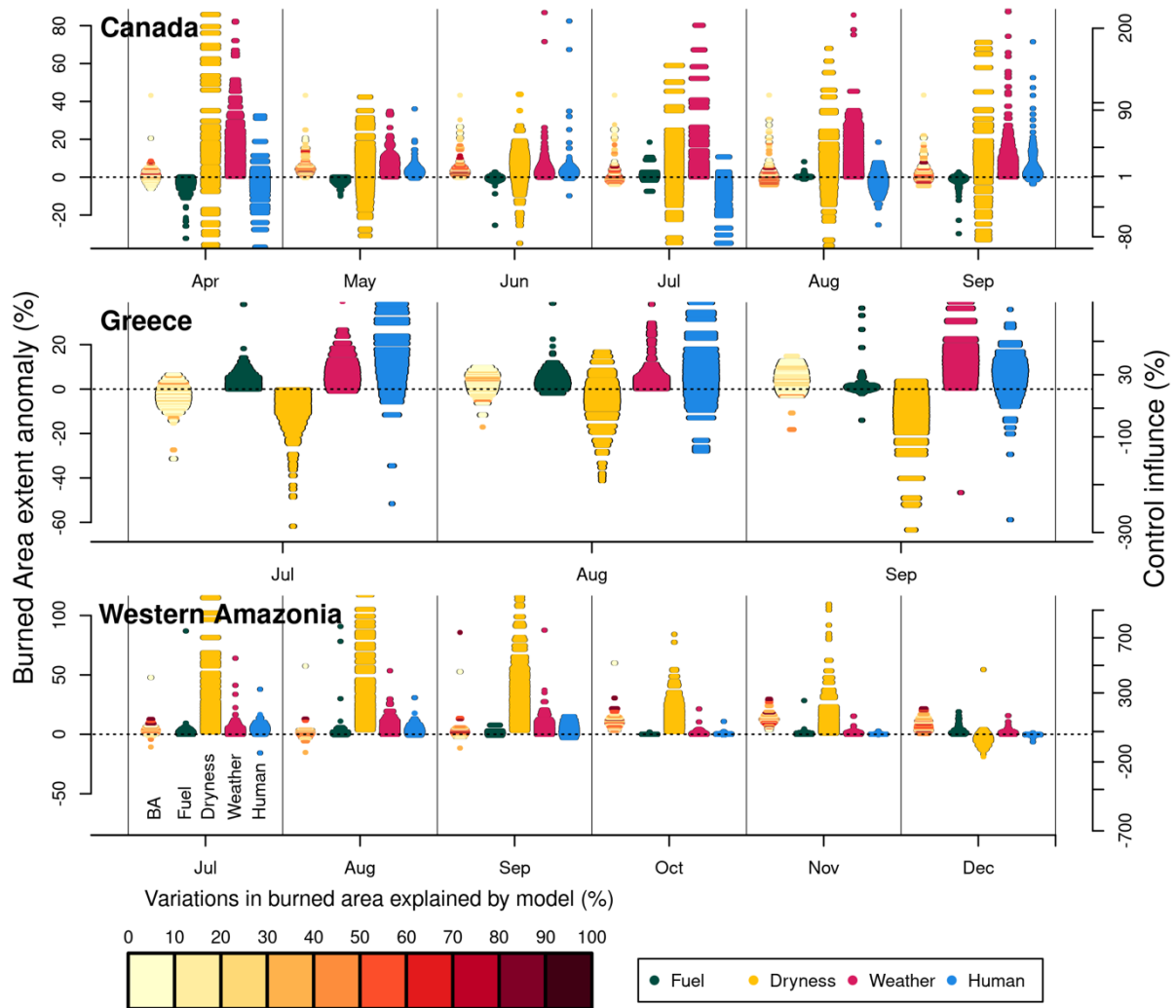
1281  
1282 **3.2.4.1 Canada**

1283  
1284 ConFire detected a significant anomaly in BA starting in late April, as seen in the observations  
1285 (**Figure S9**) with very high confidence between May (99.2% likelihood) and June 2023  
1286 (>99.9% likelihood; **Figure 10**). While less confident in a positive anomaly in September and  
1287 August (71% likelihood), ConFire detects the possibility of much higher burning in August and  
1288 September, corresponding with the increase in burning in the Western Shield (**Figure S9**).  
1289 **Figure 10** shows the controls that contribute to these anomalies. Our analysis indicates a  
1290 >99.9% likelihood that elevated fire weather conditions persisting throughout the 2023 fire  
1291 season, led to a notable increase in burning, explaining 19 [4.6-45]% of the BA anomaly in  
1292 May and 13 [1-110]% in June (median estimates, with 5th-95th percentile range in square  
1293 brackets). Anomalous weather conditions subsided in May through the early summer, though  
1294 by September showed an increased likelihood of contributing to the increase in BA anomaly  
1295 seen in the late fire season. Drier fuel conditions could have contributed significantly to the  
1296 increase in BA (up to 65% of the BA anomaly in May and 45% in June), though with low  
1297 confidence (60.5% in May and 61.3% in June), and wetter fuels exerting a suppressive effect  
1298 on fire spread was also possible, suggesting their potential role in mitigating fire severity. A  
1299 small but confident suppressive effect (100% likelihood in May, 64.8% likelihood in June) from  
1300 fuel load was observed, reducing relative increases in BA by 1.4 [0.17-7.1]% in May. Direct  
1301 human-induced landscape changes exhibited a small impact on the extent of burned areas  
1302 (likelihood of 97.4% in May), explaining between 5.4 [1.2-22]% of the anomaly in BA in May  
1303 and 5.2 [0.6-24]% in June.

1304  
1305 **3.2.4.2 Greece**

1306  
1307 The analysis reveals an anomalously high BA, particularly from mid-August onwards, though  
1308 with a lower confidence level compared to the Canadian case (69.9% likelihood; **Figure 10**).  
1309 **Figure 10** shows the controls that contribute to these anomalies. Our findings demonstrate  
1310 with very high confidence the presence of anomalously high fire weather conditions during the  
1311 2023 fire season in Greece (98.3% in July, and >99.9% in August and September). In August,  
1312 these conditions explained 24 [4.3-140]% of the increased BA, increasing to 34 [5.6-170]% by  
1313 September. Assessing the impact of fuel moisture on BA, our analysis shows a wide range of  
1314 possibilities, with confidence ranging from a 21% increase to 180% decrease in relative BA  
1315 extent, which would have offset some of the increases from fire weather. This uncertainty  
1316 underscores the complexity of the interactions between fuel moisture and fire behaviour in  
1317 Greece. Although direct human-induced landscape changes exerted greater influence on BA  
1318 extent in Greece than in the other focal regions, this influence remained small compared with  
1319 weather factors. While the analysis indicates a slightly higher than normal fuel load with only  
1320 a low likelihood of having a substantial influence on increased levels of burning.





1322  
 1323 **Figure 10:** Influence of fuel load, fuel dryness, fire weather, and human controls on burned  
 1324 area (BA) anomalies in 2023. **(Top row)** The colour indicates the modelled BA anomalies as  
 1325 relative increases/decreases in BA extent (% relative to the climatology). **(Rows 2-4)** The %  
 1326 of the anomaly explained by each control. At each timestep, the gradient of colours along the  
 1327 y-axis represent the range of modelled outcomes: high diversity in the colours indicates high  
 1328 uncertainty, whereas a consistent colour (e.g., red for positive BA anomalies) indicates greater  
 1329 confidence in the projected direction and magnitude of change. Dotted black line indicated  
 1330 threshold between positive and negative anomaly. **(Bottom row)** Uncertainty measure  
 1331 representing potential variations around our simulated BA anomaly as a result of factors not  
 1332 considered by the modelling framework, as a fraction of land area. Lower numbers (lighter  
 1333 colours) indicate higher confidence in the BA anomaly in the top row.

1334 **3.2.4.3 Western Amazonia**

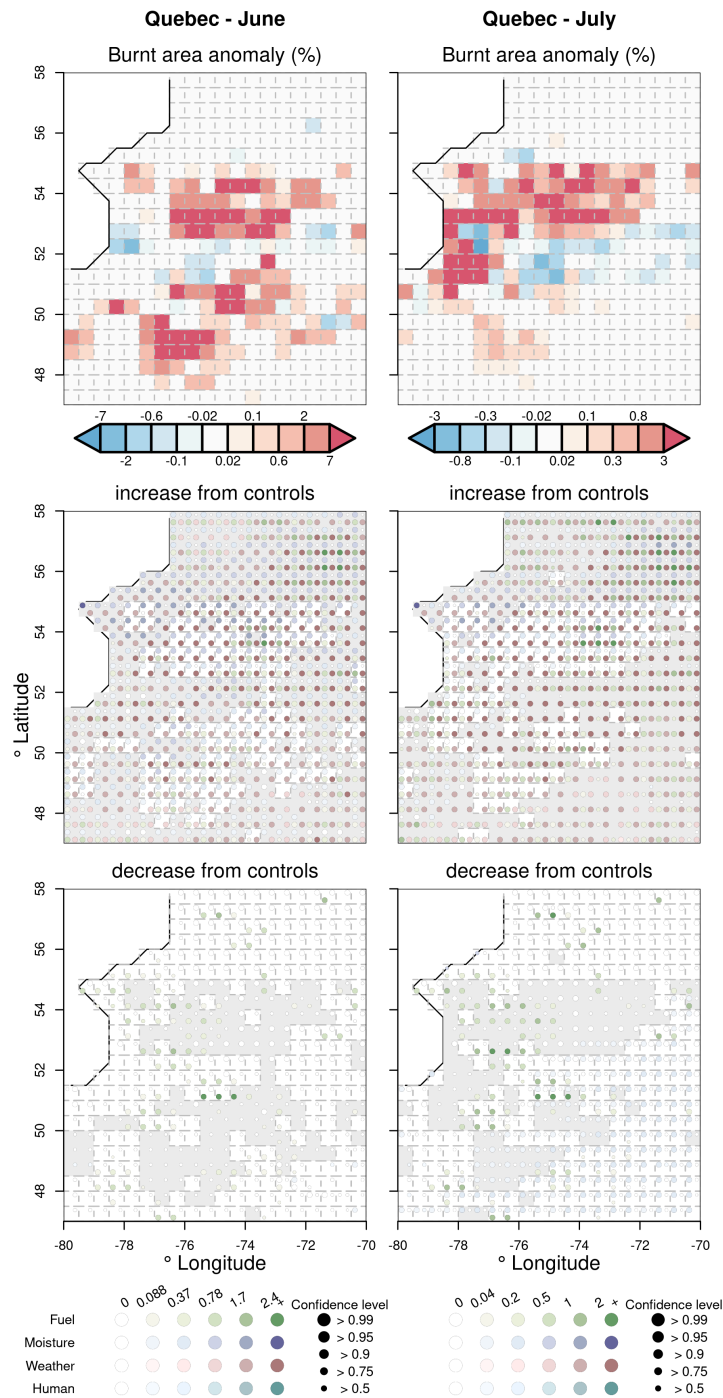
1335  
1336 Our analysis indicates a reasonably high confidence that the considered drivers contributed  
1337 to anomalous high burning during September (73.8% likelihood), October (94.9% likelihood)  
1338 and November (96.1% likelihood; **Figure 10**). **Figure 10** shows the controls that contribute to  
1339 these anomalies. The primary driver of the observed BA anomaly appears to be dry fuel  
1340 conditions, with a very high likelihood (99.7%) of drier-than-normal conditions persisting  
1341 through November. This led to a substantial increase in BA, explaining at least 57% of the  
1342 increase in BA. While fire weather conditions were also elevated (likelihood >99.9%), their  
1343 impact on BA was comparatively lower, resulting in at least 2% increase in BA during October  
1344 and November, though with a small probability of contributing much more. Direct human  
1345 influence was identified as a contributing factor, with a high likelihood (92.9% in September,  
1346 94.5% in October) of increasing burned area. However, the magnitude of this influence was  
1347 approximately one-tenth of that attributed to fuel dryness. There is little confidence in the  
1348 direction of the effect on BA anomaly, with potential influences ranging from a slight  
1349 suppressive effect (26.5% likelihood) to potentially explaining the majority of the increased BA  
1350 in September, to virtually no impact in October. This suggests that fuel dynamics played a  
1351 minor role in driving the observed fire activity. The analysis reveals a higher confidence in the  
1352 simulations indicating positive anomalies, indicating a robust signal in the attribution of drivers  
1353 to observed BA anomalies.

1354  
1355 **3.2.5 Spatial Variation in Drivers of Burned Area Extremes**

1356  
1357 **3.2.5.1 Canada**

1358  
1359 In Canada, most BA anomalies were linked to widespread high fire weather, with 95% of the  
1360 country being influenced by higher-than-normal fire weather (**Figure S12**). There was a  
1361 tendency for fuels to dry out, although this was not as widespread. Fuel load anomalies were  
1362 more scattered, but areas of low fuel anomaly did correspond to some boundaries in fire  
1363 extremes (**Figure 11, S12**). Increased human influence may have had some influence at  
1364 suppressing fires, but this is not significant, and in some places, the model indicates a small  
1365 possibility of increased fire from human activity. In the Eastern Shield, fire extremes in some  
1366 areas were driven by high fire weather and dry fuel, compounded with more vegetation cover  
1367 and hence higher-than-normal fuel load in some places (**Figure 11**). However, the borders of  
1368 extreme fires corresponded to a suppressive effect from decreased fuel load. In the Western  
1369 Shield, dry fuel and high fire weather drove fire incidents, with high fire weather dominating in  
1370 some areas. Increased suppression may have had some influence at suppressing fires, but  
1371 this is not significant, and in some places, the model indicates a small possibility of increased  
1372 fire from human activity.

1373  
1374 In June, there were high anomalous burned areas in Quebec's Eastern Shield, which were  
1375 divided into two major fire components with a slightly reduced BA in between (**Figure 11**).  
1376 Both components were associated with high fire weather, but in areas where high fire weather  
1377 occurred without the contribution of other controls, it tended not to cause high levels of burning.  
1378 The highest burned areas were mainly found in the northern component and were associated  
1379 with anomalously low levels of moisture and high fire weather. Some cells with the very highest  
1380 BA also showed anomalously high fuel load (**Figure 11**). In a region further north, around 56-  
1381 57 degrees north and 72-80 degrees west, there was high fuel load, dry conditions, and high  
1382 fire weather, but fire in the area was found to be highly fuel limited and largely insensitive to  
1383 even large changes in controls (Kelley et al. 2019). The southern component of high burning  
1384 corresponded with high fire weather and either fire fuel or high fuel load. Additionally, any  
1385 boundaries between higher and normal/lower levels of BA also saw lower than average fuel  
1386 loads, which may have inhibited fire spread (**Figure 11**).



1389  
1390

1391 **Figure 11:** Anomalies in controls during months and regions of high BA in Quebec. The top  
 1392 map of each region shows BA anomalies at 0.5 degrees for that month in 2023 versus the  
 1393 2014-2023 monthly average. The middle maps looks at anomalies in controls that would cause  
 1394 higher BA, with areas not greyed out representing regions with greater than monthly average  
 1395 BA in 2023. The bottom map shows drivers that would have led to lower than normal levels of  
 1396 burning, with areas not greyed out showing lower or non-change from monthly average BA in  
 1397 2023. Each grid cell has four points: green points show anomalies in fuel load, purple in fuel  
 1398 moisture, red in fire weather, and cyan in humans. This way, we can see if controls acted in  
 1399 unison to cause extreme levels of burning or prevent extreme fires from extending further. The

1400 shade of the point shows the most likely expected level of anomaly in that control, while the  
1401 size shows how confident we are in the direction of the anomaly.

1402  
1403

1404 In May, the Western Shield and Taiga/Boreal plains experienced higher-than-normal fire  
1405 weather across the region (**Figure S13**). The increased burned areas in the west were due to  
1406 extreme low fuel moisture and high fire weather, as well as higher fuel loads. In contrast, areas  
1407 to the south experienced high fire weather without the extreme burned areas. Additionally,  
1408 anomalies in fuel loads and burning levels became more evident in September, with some  
1409 areas displaying lower-than-average fuel and burning (**Figure S13**). These anomalies  
1410 persisted, with regions still experiencing high fire weather and variations in fuel moisture  
1411 levels. Furthermore, the eastern areas with higher fire weather also showed higher fuel loads,  
1412 while drier fuel moisture was observed in less extreme regions to the east. Additionally,  
1413 specific locations saw higher fire weather and above-average fuel moisture, while areas just  
1414 north of the extreme fires experienced wetter-than-normal fuel moisture (**Figure S13**).

1415

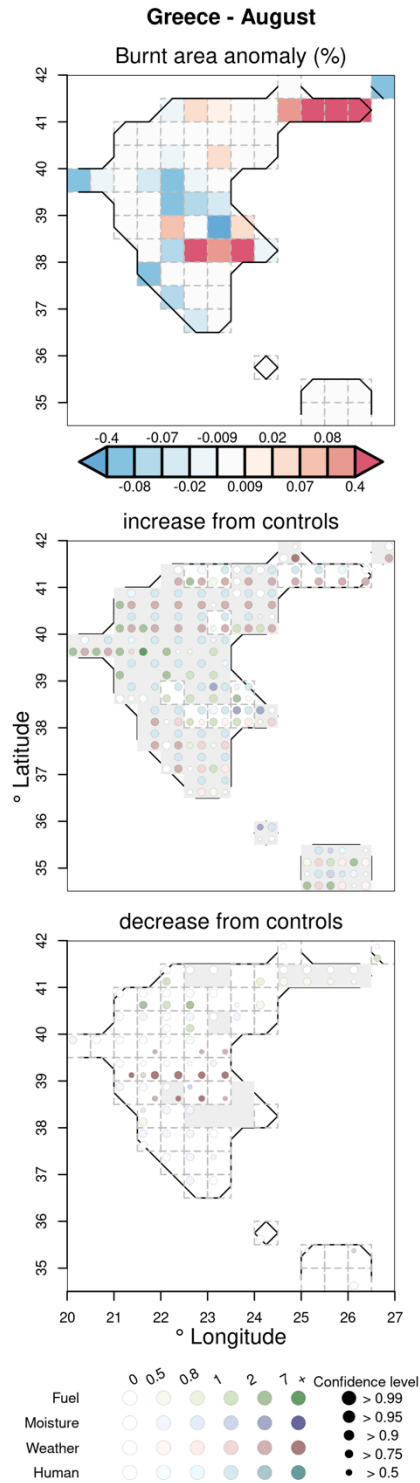
### 1416 3.2.5.2 Greece

1417

1418 Interestingly, most of Greece showed a tendency towards less suppression from people  
1419 (**Figure S12**). However, the dominant driver over most (73%) of Greece was high fire weather,  
1420 with some areas in central Greece showing notably low fire weather. These areas do not  
1421 correspond to a fire anomaly, though higher fuel loads were detected. Except for central  
1422 Greece, other areas of lower than average BA correspond to lower than average fuel loads  
1423 (**Figure 12**). There was no significant anomaly in fuel moisture across Greece, though the  
1424 northeastern fire extreme does correspond to a joint increase in fire weather and decrease in  
1425 fuel moisture. Extremes in Eastern Coastal Greece correspond to anomalies in fuel load, fuel  
1426 dryness, and heightened fire weather (**Figure 12**).

1427

1428 In August, Northern Greece experienced high fire weather and low fuel moisture, particularly  
1429 around Alexandroupolis in Macedonia and Thrace (**Figure 12**). The region extended further  
1430 east, experiencing extreme fires that reached into Central Macedonia. Unlike Canada, the  
1431 framework in North Greece did not show the same level of detail in the boundaries around  
1432 extreme levels of burning. However, the transition to less burning in the South of West  
1433 Macedonia did correspond to reduced fuel load. Areas around Athens and Central Greece  
1434 that saw unusually high levels of burning also experienced decreased fuel moisture and  
1435 increased fuel load (**Figure 12**). In contrast, areas in Southern Thessaly and Central Greece  
1436 that did not experience high burned areas saw lower than normal fire weather. In the  
1437 Peloponnese region, there was either high fire weather or reduced fuel moisture, but these  
1438 conditions rarely occurred together, which might explain the lack of increased BA throughout  
1439 the region. (**Figure 12**)



1440

1441 **Figure 12:** Same as Figure 11 but for Greece.

### 1442 **3.2.5.3 Western Amazonia**

1443

1444 High fire weather anomalies were almost universal across our Western Amazonia region  
 1445 (**Figure S12**). However, anomalies in other controls varied widely across the region, which  
 1446 appears to modulate the occurrence of areas with above average BA (**Figure S12, S14**). In  
 1447 September, the regions of high burning in the Western Amazon all exhibited higher than

1448 average fire weather, with the highest BA anomalies associated with the highest fire weathers.  
1449 The areas with the highest BA anomalies along the Amazon River were located around  
1450 Manaus and also showed lower than average fuel moisture and higher than average fuel load.  
1451 The very highest pixels exhibited the anomaly in increased fuel loads. In the southern and  
1452 central part of the region (65 to 62 west/7/8 south), near Porto Velho, BA anomalies were  
1453 associated with extremely high fire weather and higher fuel loads. The areas of highest burning  
1454 also showed an increase in human-driven burning. Further east (59 west, 7 south), the highest  
1455 fire weather and decreased fuel moisture occurred alongside higher burning. Areas of higher  
1456 BA in the north (63 west, 0 north) were associated with extreme fire weather, though offset by  
1457 below average fuel loads. This may explain why they were not as extreme as the fires around  
1458 Manaus, though the area is not generally considered fuel-limited (Kelley et al. 2019), and fuel  
1459 had little overall impact across the region **Figure 10**.  
1460

## 1461 **4 Attribution to Global Change Factors**

1462

### 1463 **4.1 Methods**

1464

1465 Many of the direct drivers and controls on fire events, outlined in the **Section 3** (e.g. weather,  
1466 fuel, moisture, ignition and suppression), are influenced by global change factors such as  
1467 climate and land-use change. Since the pre-industrial era, global mean temperature has  
1468 increased by between 1.1-1.3°C (Betts et al., 2023; Forster et al., 2024), with greater rates of  
1469 warming at higher latitudes, adding potential for fuel drying. Climate change has also resulted  
1470 in altered precipitation patterns, with total rainfall and dry season length increasing or  
1471 decreasing variably across regions (Polade et al., 2014; Swain et al., 2018; IPCC, 2023a).  
1472 Meanwhile, changes to fuel load and ignition rates are driven by climate change and  
1473 anthropogenic land-use, with varying effects regionally (Finney et al., 2018; Roms, 2019).  
1474 For example, in fuel-limited savannah biomes land-use change can drive more fragmented  
1475 fuel loads and a reduction in fire (or an increase in fire resulting from land abandonment),  
1476 whereas in forest ecosystems fragmentation provides more potential for ignition and leads to  
1477 increases in fire occurrence (Andela et al., 2017; Rosan et al., 2022).  
1478

#### 1479 **4.1.1 Overview of Attribution Approaches**

1480

1481 In this report, we apply various modelling techniques for each focal region to attribute (i)  
1482 regional changes in the probability of high fire weather to anthropogenic forcing (**Section**  
1483 **4.1.2**) and (ii) changes in monthly BA to total climate forcing, socio-economic change, and all  
1484 forcing (**Section 4.1.3**).  
1485

1486 The types of forcing considered vary across the attribution techniques applied, and so we  
1487 define here the terminology used throughout the paper when describing attribution results  
1488 (summarised in **Table 4**).  
1489

1490 Our attribution to *anthropogenic forcing* explicitly targets the changes driven by anthropogenic  
1491 greenhouse gas emissions and land-use change, following the IPCC WGI definition (Hegerl  
1492 et al., 2009; Mengel et al., 2021). We prescribe these emissions in a model to specifically  
1493 isolate human forcing from natural variability (**Section 4.1.2**).  
1494

1495 Our attribution to *total climate forcing* considers changes driven by climate change since the  
1496 pre-industrial period, including both anthropogenic forcing and natural variability in line with  
1497 the IPCC WGII and the Intersectoral Impacts Model Intercomparison Project 3a (ISIMIP3a)  
1498 definition of climate change impact attribution (IPCC, 2023b; IPCC 2023c; Mengel et al.,  
1499 2021). This involves comparing simulations driven with historical reanalysis to a detrended  
1500 counterfactual simulation with the historical warming signal removed (with both simulations

1501 including historical transient land-use change) and therefore only the impacts of climate  
 1502 change are attributed, not distinguishing between anthropogenic or natural causes (Mengel et  
 1503 al., 2021; Burton, Lampe et al., 2023).

1504  
 1505 Our attribution to *socio-economic factors* is applied via the same set of simulations as our  
 1506 attribution to *total climate forcing*. The role of socio-economic factors is isolated by comparing  
 1507 the early industrial period to the late industrial period in the counterfactual scenario, in which  
 1508 only land-use and population density are allowed to change (Burton, Lampe et al., 2023).

1509  
 1510 Finally, attribution to *all forcing* compares the early industrial period in the counterfactual  
 1511 scenario to the last industrial period in the factual scenario, which gives the net effect of all  
 1512 forcings combined. These are summarised in the **Table 4** below.

1513  
 1514  
 1515

**Table 4:** Summary of the attribution approaches used in this report.

Term	Definition	Experiments compared	Framework	Application
<b>Event attribution for fire weather</b>				
<b>Anthropogenic Forcing</b>	Change in fire weather driven by anthropogenic emissions from greenhouse gases, land-use change and aerosols. As per (Ciavarella et al., 2018; Li et al., 2021)	<b>ALL:</b> natural forcing plus human emissions <b>NAT:</b> Natural-only forcing from solar variability and volcanoes	HadGEM3-A attribution ensemble. 0.5 degree resolution	Fire weather (FWI)
<b>Impacts attribution for burned area</b>				
<b>Total climate forcing</b>	Changes in BA due to climate change, irrespective of the cause of warming. As per ISIMIP (Intersectoral Impacts Model Intercomparison Project) (Mengel et al., 2021 and Frieler et al., 2024)	<b>Factual (2003-2019):</b> present-day climate (driven by GSWP3-W5E5 reanalysis), CO <sub>2</sub> , land-use and population <b>Counterfactual (2003-2019):</b> De-trended historical climate (warming signal removed), CO <sub>2</sub> fixed at 1901 value, present-day land-use and population	ISIMIP3a impact attribution. 0.5 degree resolution	FireMIP ensemble and ConFire
<b>Socio-economic factors</b>	Changes in BA due to land-use and population change. As per (Burton, Lampe et al., 2023)	<b>Counterfactual (1901-1917):</b> Warming trend removed, fixed 1901 CO <sub>2</sub> , limited land use and population change <b>Counterfactual (2003-2019):</b> Warming trend removed, fixed 1901 CO <sub>2</sub> , present-day land use and population	ISIMIP3a impact attribution	FireMIP ensemble and ConFire
<b>All forcing</b>	Changes in BA due to climate, land-use and population change. As per (Burton, Lampe et al., 2023)	<b>Counterfactual (1901-1917):</b> Warming trend removed, fixed 1901 CO <sub>2</sub> , limited land use and population change <b>Factual (2003-2019):</b> Historical climate driven by reanalysis	ISIMIP3a impact attribution	FireMIP ensemble

1516 The tools described here enable us to assess the influence of climate and socio-economic  
 1517 forcing on fire with respect to 3 different target variables. We use the FWI to assess how the  
 1518 probability of high (90th percentile) fire danger has changed as a result of anthropogenic  
 1519 forcing. As climate change has a direct impact on fire weather, this approach enables us to  
 1520 isolate its effects without confounding factors of land-use change and ignitions, and reveals  
 1521 how a fire might develop once ignited.

1522 In a second branch of analyses, we attribute the change in BA to total climate forcing, socio-  
1523 economic factors, and all forcing, specifically targeting the observed month of peak burning in  
1524 the 2023-24 fire season for each focal event. We use ConFIRE to assess the change in  
1525 likelihood of a BA fraction (BA divided by the total area available to burn) that lies in the 90th  
1526 or 95th percentiles of observations from the 2023-24 fire season (percentile thresholds vary  
1527 regionally due to differing domain sizes).

1528 Separately, we attribute change in the monthly median BA in the present-day using  
1529 simulations from fire-enabled dynamic global vegetation models (DGVMs) contributing to the  
1530 Fire Model Intercomparison Project (FireMIP). Each of these methods is described in more  
1531 detail below.

1532 In each approach we include an explicit estimate of uncertainty. We use bootstrapping to give  
1533 uncertainty estimates for the FWI risk ratios. ConFire is designed as an uncertainty  
1534 quantification model (see **Section 3.2.4**), giving the likelihood of all possible burned areas for  
1535 each region based on a probabilistic analysis of past burn patterns and environmental conditions.  
1536 We combine the information from the FireMIP models in a weighted multi-model ensemble to  
1537 give uncertainty ranges across the models. Each result therefore presents a 5-95<sup>th</sup> percentile  
1538 probability estimate.

#### 1539 **4.1.2 Attributing Change in Likelihood of Fire Weather to Anthropogenic Forcing**

1540 We use an established approach to attribute change in probability of high (90th percentile) fire  
1541 weather conditions to anthropogenic forcing. The approach uses estimates of FWI, as used in  
1542 previous studies from the World Weather Attribution (Barnes et al., 2023), using outputs from  
1543 the HadGEM3-A large ensemble (Christidis et al., 2013; Ciavarella et al., 2018). It follows the  
1544 approach introduced by Stott et al. (2004) for attributing extreme weather events, and it has  
1545 been employed in other attribution studies targeting fire weather, such as Li et al. (2021).

1546 As outlined in **Section 3.1.1**, the FWI is used operationally and in research contexts to rate  
1547 fire danger based on meteorological conditions. Due to the availability of model output  
1548 variables we use maximum daily temperature at 1.5 m as a proxy for noon values, total daily  
1549 precipitation, mean daily relative humidity at 1.5 m, and mean daily wind speed at 10 m,  
1550 following Perry et al. (2022). We calculate the daily FWI for the month of 2023-24 peak BA  
1551 anomaly for each focus region, using the same month and region for validation over the  
1552 historical timeseries (1960-2013).

1553 We validate and bias-adjust the model estimates of high FWI for the period 1960-2013 by  
1554 comparing a 15-member HadGEM3-A ensemble with ERA5 reanalysis data (C3S, 2024)  
1555 representing “observed” FWI. The 0.25 degree resolution observed FWI from ERA5 was  
1556 coarsened by linear interpolation (calculated by extending the gradient of the closest two  
1557 points) to match the 0.5 degree model grid. We compare the timeseries of individual  
1558 components of the FWI (**Figure S40**), and the distribution of the modelled and observed FWI  
1559 (**Supplementary Figures S41-S43**), and apply a simple linear regression to find the bias  
1560 correction required for the 2023 model output. Before bias-adjustment, the modelled FWI is  
1561 generally higher than the observed FWI, and some regions (e.g. Greece) require a larger  
1562 correction than others. The correction adjusts the trend and absolute value while maintaining  
1563 variability, and the model successfully reproduces the observed distribution after applying the  
1564 correction in each region (see **Extended Methods and Evaluation Supplement**).

1565 For the events occurring in the 2023-24 fire season, we calculate the FWI from the HadGEM3-  
1566 A model simulations comprising 2 experiments of 525 members each, one driven by all  
1567 forcings including historical greenhouse gas emissions, aerosols, zonal-mean ozone  
1568 concentrations, land-use change and natural forcing (ALL), and a second counterfactual  
1569 simulation with natural-only forcing from solar variability and volcanic emissions, and 1850



1573 land-use (NAT) (**see Table 4**). By applying the bias-adjustment from the previous step, and  
1574 comparing the fire weather in the two simulations to the 2023 observed FWI from ERA5, we  
1575 calculate the change in probability of high (90th percentile) fire weather due to anthropogenic  
1576 forcing.

### 1577 **4.1.3 Attributing Change in Regional Burned Area to Total Climate Forcing, Socio-** 1578 **economic Factors and All Forcing**

1579

#### 1580 **4.1.3.1 Peaks in Burned Area during 2023-24**

1581

1582 We use the ConFire attribution framework to attribute anomalies in BA fraction in the month  
1583 of peak burning during the 2023-24 fire season to total climate forcing and socio-economic  
1584 factors using the the Inter-Sectoral Impact Model Intercomparison Project (ISIMIP) 3a  
1585 attribution protocol (**see Table 4**). For Canada and Western Amazonia, the attribution  
1586 approaches are applied to cells with BA fractions in the 95th percentile of the BA fraction  
1587 distribution during 2023-24. For Greece, the attribution approaches are applied to cells with  
1588 BA fractions in the 90th percentile of the BA fraction distribution during 2023-24, with the lower  
1589 percentile threshold selected due to the smaller domain size of Greece.

1590

1591 We trained ConFire on observed monthly BA from the MODIS BA product during 2003-2019  
1592 at 0.5° across the entire region. For model training, we drive ConFire with Global Soil Wetness  
1593 Project Phase 3 (GSWP3-W5E5) forcings provided at a 0.5° spatial resolution by ISIMIP3a  
1594 (**Table 5**). The land surface information (tree cover and non-tree vegetated cover) is derived  
1595 from the JULES-ES ISIMIP configuration (Mathison et al., 2023) driven by GSWP3-W5E5.  
1596 This model includes dynamic vegetation, i.e changing vegetation cover in response to climate  
1597 variables, growth, plant competition and mortality. So as not to double count the impact of fire,  
1598 we turn the interactive vegetation-fire model off. The bias in this land surface information is  
1599 adjusted to the MODIS Vegetation Continuous Fields collection 6.1 remote sensed data for  
1600 <60°N (DiMiceli et al., 2022) and collection 6 for >60°N (DiMiceli et al., 2015) using a trend-  
1601 preserving empirical quantile mapping bias adjustment method. This method significantly  
1602 reduces the model bias in the JULES-ES output for most regions and variables, ensuring  
1603 accurate means and distribution while preserving trends between historical and future periods  
1604 (**Figure S22**). **See “Data and Data Processing” in Extended Methods Supplement** for  
1605 details.

1606

1607 We ran ConFire in predictive mode on monthly timesteps with a structure similar to that used  
1608 in **Section 3.1.2**, again grouping specific drivers into controls (**Table 5**). However, specific  
1609 driving variables differed for this application: fuel load controls were represented by total  
1610 vegetation cover and tree cover; fuel moisture controls were represented by mean consecutive  
1611 dry days within each month, the fraction of dry days within the month, daily mean precipitation,  
1612 mean and maximum monthly temperature, mean and maximum Vapour Pressure Deficit  
1613 (VPD); ignition controls were represented by climatological lightning, pasture, crop and  
1614 population density; and suppression controls were represented by pasture, crop and  
1615 population density. ConFire’s Bayesian inference procedure proved useful because it allowed  
1616 us to discern individual driver contributions (Gelman et al., 2013; Kelley et al., 2023). These  
1617 modified ConFire simulations applied to all data in each of three experiments (see “simulation  
1618 framework”).

1619

1620 To determine the impact of total climate forcing and socioeconomic factors on the increased  
1621 BA during our focal events, we conducted a paired sampling of monthly BA in the target  
1622 months (**see Table 4**). As there is no climate influence in the Early Industrial simulation, we  
1623 first adjusted the target event (a monthly regional BA value) to that expected without climate  
1624 change. For this adjustment, we find the percentile of the observed BA in the factual and find  
1625 the BA at the same percentile in the counterfactual. We used paired samples to account for

1626 the uncertainty in the underlying mechanisms relating our drivers to BA, which would co-vary  
1627 between experiments as per Kelley et al. (2021). In total, we took 200 samples over the 17  
1628 years of each simulation, resulting in 3400 pairs.

1629  
1630 The likelihood was then simply determined by the number of ensemble members in the  
1631 factual scenario that predicted greater BA than the counterfactual for total climate forcing, or  
1632 the counterfactual predicting greater BA than the early industrial scenario for socioeconomic  
1633 factors. The relative increase in BA extent is the BA in factual over counterfactual (total  
1634 climate forcing) or counterfactual over early industrial (socioeconomic).

1635  
1636 As per **Section 3.1.2**, we evaluated the model following Barbosa (2024). We separately train  
1637 ConFire on 50% of the data between 2003-2011 and perform evaluation on years 2012-2019.  
1638 Further details of the model fitting and validation can be found in supplement **Extended**  
1639 **Methods and Evaluation Supplement**.

1640  
1641

1642  
1643  
1644  
1645  
1646

**Table 5:** Explanatory variables used for attributing extreme BA (**Section 4.1.3**) and multi-decadal outlook (**Section 5.1.2**). The explanatory variables are forcing data from the Inter-Sectoral Impact Model Intercomparison Project (ISIMIP) protocols ISIMIP3a and ISIMIP3b (Frieler et al., 2024). Positive (+ive) or negative (-ive) under “Controls” describes if a driver increases or decreases BA.

Variable	Controls	Construction	Source	Reference
Max. consecutive dry days	Moisture +ive	Monthly max of running count of days since rainfall > 0.1mm/m	Based on precipitation from ISIMIP3a/3b	Frieler et al. (2024)
No. dry days	Moisture +ive	fractional no. days of rainfall < 0.1mm/m	Based on precipitation from ISIMIP3a/3b	Frieler et al. (2024)
Maximum monthly temperature	Moisture +ive	maximum of maximum daily temperature within the month	Daily temperature approximated as ISIMIP3a/3b daily mean temperature + 0.5xdaily temperature range	Frieler et al. (2024)
Mean monthly temperature	Moisture +ive		ISIMIP3a/3b	Frieler et al. (2024)
Mean monthly Vapour Pressure Deficit (VPD)	Moisture +ive	mean of daily values constructed from specific humidity, surface pressure and max. temperature	ISIMIP3a/3b	Frieler et al. (2024); Barbosa (2024)
Maximum monthly VPD	Moisture +ive	max of daily values	ISIMIP3a/3b	Frieler et al. (2024); Barbosa (2024)
Tree Cover	Moisture -ive & Fuel +ive	JULES-ISIMIP annual mean tree cover bias-corrected to VCF vs JULES-ISIMIP3a factual interpolated to monthly from annual values	Joint UK Land Environment Simulator Earth System model (JULES-ES)-ISIMIP corrected to MODIS Vegetation Continuous Fields (VCF)	DiMiceli et al. (2017); Adzhar et al. (2022); Mathison et al. (2023)
Total vegetation cover	Fuel +ive	Tree cover plus non-tree vegetated cover simulated by JULES and bias-corrected as above	JULES-ES-ISIMIP corrected to MODIS VCF	DiMiceli et al. (2017); Adzhar et al. (2022); Mathison et al. (2023)
Lightning	Ignitions +ive	Climatology	LIS taken from ISIMIP3a	Kelley et al. (2014); Frieler et al. (2024)
Cropland	Ignitions +ive/ Suppression -ive	Interpolated from annual to monthly	ISIMIP3a/3b	Frieler et al. (2024))
Pasture	Ignitions +ive/ Suppression -ive	Interpolated from annual to monthly	ISIMIP3a/3b	Frieler et al. (2024)
Population Density	Ignitions +ive/ Suppression -ive	Interpolated from annual to monthly	ISIMIP3a/3b	Frieler et al. (2024)

1647  
1648  
1649

#### 4.1.3.2 Background Changes in Burned Area during 2003-2019

1650  
1651  
1652  
1653  
1654  
1655  
1656

Finally, we attribute changes in median monthly BA across all months in 2003-2019 to total climate forcing, socio-economic factors and all forcings, using the novel attribution method developed using state-of-the-art global fire models from the FireMIP (Burton, Lampe et al., 2023). This represents an assessment of how BA has changed during the 2003-2019 period versus counterfactual scenarios. Our method employs the same ISIMIP3a simulation framework outlined above with 7 fire-enabled DGVMs (see **Table S1**) for the period 1901-2019 for the factual and counterfactual experiments (see **Table 4** for descriptions). The

1657 ConFire was not used in this element of our attribution approaches; rather, the native fire  
1658 modelling scheme of each fire-enabled DGVM was employed. Model fire schemes are  
1659 described in Burton, Lampe et al. (2023).

1660 A weighted ensemble of the monthly outputs of BA, based on the regional performance of the  
1661 unweighted models against observational data from GFED5 and FireCCI, is used for the  
1662 analysis. Due to large differences in absolute values of BA between the GFED5 and FireCCI  
1663 observational datasets and across the models, the weightings in the ensemble are based on  
1664 model capability to capture relative anomalies present in the observational datasets on a  
1665 regional basis, and all changes are reported as relative anomalies. We focus on the change  
1666 in median monthly BA across all months in 2003-2019 because the fire models underpredict  
1667 the high tails of the distribution. The weighted models are randomly resampled to generate  
1668 uncertainty estimates for each region. The method and results are reported in full for all 43  
1669 IPCC AR6 regions in Burton, Lampe et al. (2023), and in the current report we select the IPCC  
1670 regions that align most closely with our focus regions defined in **Section 3.2**.  
1671

## 1672 **4.2 Results**

### 1673 **4.2.1 Change in the Likelihood of High Fire Weather in 2023-24**

#### 1674 **4.2.1.1 Canada**

1675  
1676 The fire weather conditions in Canada during June 2023 were 2.9-3.6 times more likely due  
1677 to anthropogenic forcing. Here we assess the 95th percentile of FWI over the country during  
1678 the month of peak anomaly in BA (June) in the ALL and NAT HadGEM3 simulations. More of  
1679 the ALL distribution lies above the observed 95th percentile of FWI from ERA5 compared to  
1680 the NAT distribution (**Figure 13**), and we therefore conclude that the probability of  
1681 experiencing the high fire weather observed during June 2023 is more likely in a climate forced  
1682 with anthropogenic emissions.  
1683  
1684  
1685

#### 1686 **4.2.1.2 Greece**

1687 The high fire weather conditions experienced during the peak anomaly in BA in August 2023  
1688 were 1.9-4.1 times more likely due to anthropogenic forcing (**Figure 13**). In this case the 95th  
1689 percentile of FWI is outside of the distribution so we instead assess the 90th percentile of FWI  
1690 over the country. This is likely a result of our linear inference of 2023 for the bias correction  
1691 based on the 1960-2013 period, where in fact 2023 was so anomalous that it doesn't fit this  
1692 trend. The 2023 event threshold here also lies at the very high end of simulated fire weather,  
1693 meaning it was very unusual in the model simulations. The result range here is also larger  
1694 than for Canada, meaning there is less certainty about how much human influence has  
1695 increased the probability, although it does highlight at least a 50% increase in likelihood of  
1696 high fire weather.  
1697  
1698

#### 1699 **4.2.1.3 Western Amazonia**

1700 High fire weather in western Amazonia during Sept-Oct 2023 was 20.0-28.5 times more likely  
1701 due to anthropogenic forcing (**Figure 13**). In this region there is a large shift in the ALL forcing  
1702 distribution compared to the NAT only forcing for the 95th percentile of FWI, and the high risk  
1703 ratio shows a strong anthropogenic signal in driving the meteorological conditions that led to  
1704 high fires over this period.  
1705  
1706

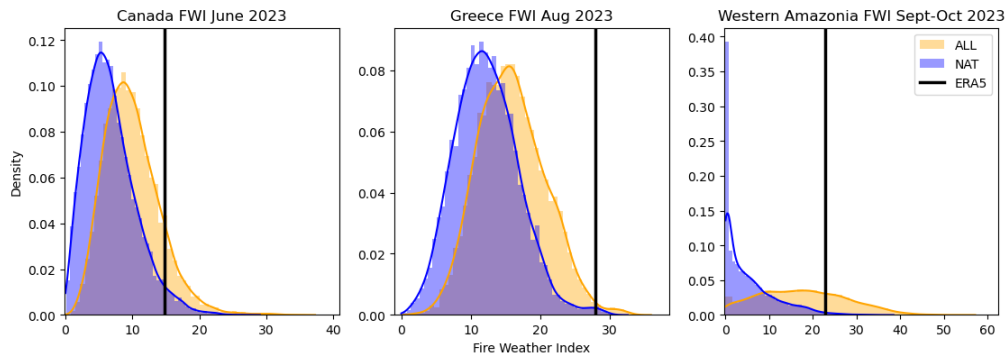


**Figure 13:** High FWI in 2023: **(left)** 95th percentile FWI in June over Canada, **(middle)** 90th percentile FWI in August over Greece and **(right)** 95th percentile FWI in September-October over western Amazonia, in the HadGEM3 ensemble of ALL (anthropogenic plus natural forcing, orange) and NAT (natural-only forcing, blue) bias-adjusted simulations, and ERA5 reanalysis (black line).

## 4.2.2 Change in the Likelihood of Peaks in Burned Area in 2023-24

### 4.2.2.1 Canada

We show that total climate forcing was virtually certain (99.9% confidence) to have led to greater BA in Canada during June 2023 (**Figure 14**). Our attribution results indicate that total climate forcing increased BA extent by 4.1 [2.3-7.8]% during the month of June across the period 2003-2019. Additionally, considering the anomalies in fire drivers during 2023, we estimate an additional 5.7 [1-30]% absolute increase in BA extent during June 2023, on top of the 2003-2019 period (**Figure 10**). The impact of socio-economic factors is less certain, with only a 64.8% likelihood of decreasing burning, affecting BA extent by between -22.5 and 6.6% during 2003-2019.

Overall, we estimate that BA in Canada in June 2023 was 10.1 [3.3-40.1]% greater due to total climate forcing in the 2003-2019 period combined with this year's anomaly in the climatic variables. As a caveat, we note that this is not a formal attribution of the 2023 anomaly because no counterfactual exists for the year, but rather an attribution of the change in BA in 2003-2019 with the additional influence of climate factors on BA in 2023 superimposed (this caveat also applies to the other focal regions). For Canada, the BA attribution targets cells in the 95th percentile of the BA fraction distribution.

1736 **4.2.2.2 Greece**

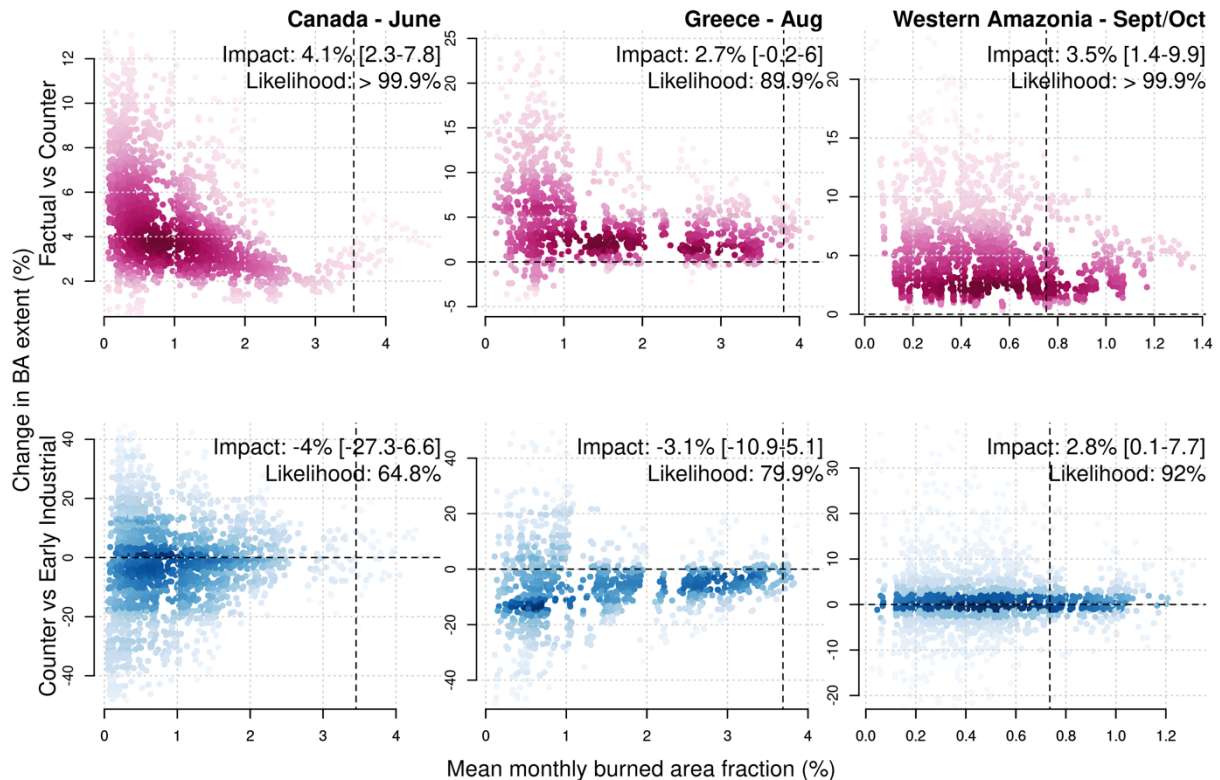
1737  
1738 Total climate forcing caused a change in the likelihood of high BA in Greece of 2.7 [-0.2 to  
1739 6.0]% in the period 2003-2019 in the cells with the greatest BA fraction (90th percentile), with  
1740 90% confidence (**Figure 14**). In this case we use the 90th percentile to represent high BA over  
1741 the region for the month of August, over 2003-2019. This increase is likely a conservative  
1742 figure given the additional warming since 2019, and estimating the additional burning that  
1743 might have been experienced during the anomalous conditions of 2023, we find an additional  
1744 change of 1.3 [-9.3-11]% (**Figure 10**). Socioeconomic factors likely (79.9%) caused a  
1745 decrease in burning, though could have caused an increase, affecting BA extent by -3.1 [-10.9  
1746 to 5.1]%.  
1747

1748 Overall we estimate that BA in Greece in August 2023 was increased by 4 [-9.5 to 17.7]% due  
1749 to total climate forcing in the 2003-2019 period combined with this year's anomaly in the  
1750 climatic variables. In the case of Greece, uncertainties around the influence of total climate  
1751 forcing and socioeconomic factors are greater because the smaller region size limits  
1752 information available for model optimization. For Greece, the BA attribution targets cells in the  
1753 90th percentile of the BA fraction distribution.  
1754

1755 **4.2.2.3 Western Amazonia**

1756  
1757 Over the period 2003-2019, total climate forcing was virtually certain to have caused an  
1758 increase in burned areas like the one experienced in western Amazonia in September and  
1759 October 2023 (>99.9% likelihood), with a likely range of increase in extent of 3.5 [1.4-9.9]%  
1760 (**Figure 14**). Here we assess the change in BA due to total climate forcing in the cells that  
1761 burn most regularly (95th percentile) of our defined region of western Amazonia over Sept and  
1762 Oct 2003-2019. Extending our analysis to the 2023 anomaly, we estimate that additional  
1763 burning could have been up to 7.4 [0.8-36.2]% on top of the 2003-2019 levels. Despite finding  
1764 little influence of humans specifically in 2023 compared to the previous 10 years in **Figure 10**,  
1765 since early-industrial, we show socioeconomic factors have had a large influence on the  
1766 occurrence of extreme levels of burning. Events similar to 2023 were very likely exacerbated  
1767 by socioeconomic conditions (92.0% likelihood) increasing BA by 2.9 [0.1-7.8]%.  
1768

1769 Overall we estimate that BA in western Amazonia in September-October 2023 was increased  
1770 by 11.1 [2.2-49.7]% due to total climate forcing in the 2003-2019 period combined with this  
1771 year's anomaly in the climatic variables. For western Amazonia, the BA attribution targets cells  
1772 in the 95th percentile of the BA fraction distribution.  
1773  
1774



1775  
1776  
1777  
1778  
1779  
1780  
1781  
1782  
1783  
1784  
1785  
1786  
1787  
1788  
1789

**Figure 14:** Estimated change in BA in selected months in the period 2003-2019 (e.g. seventeen Junes for Canada) as modelled by ConFire when driven by the ISIMIP3a reanalysis versus counterfactual scenarios. The panels shows the change in BA extent (%) due to (**top row**) total climate forcing versus a scenario without climate forcing and (**bottom row**) socioeconomic forcing versus a scenario without socioeconomic forcing. Results are shown for (**left**) Canada, (**middle**) Greece, and (**right**) Western Amazonia. Many points are plotted because each point represents a posterior estimate of change in BA for a month and there are 1,000 iterations of ConFire to explore the effect of uncertainty in input parameters and structural relationships between BA and input variables. Impact values are the central (median) and 5th-95th percentile range of the estimated values of change in BA (%). The likelihoods shown are the probability of the change being significant, measured as the % of the posterior estimates being above/below zero when the median is above/below zero.

1790  
1791  
1792

#### 4.2.3 Background Changes in Burned Area due to Total Climate Forcing, Socioeconomic Factors, and All Forcing

1793  
1794

##### 4.2.3.1 Canada

1795  
1796  
1797  
1798  
1799  
1800  
1801  
1802  
1803  
1804  
1805

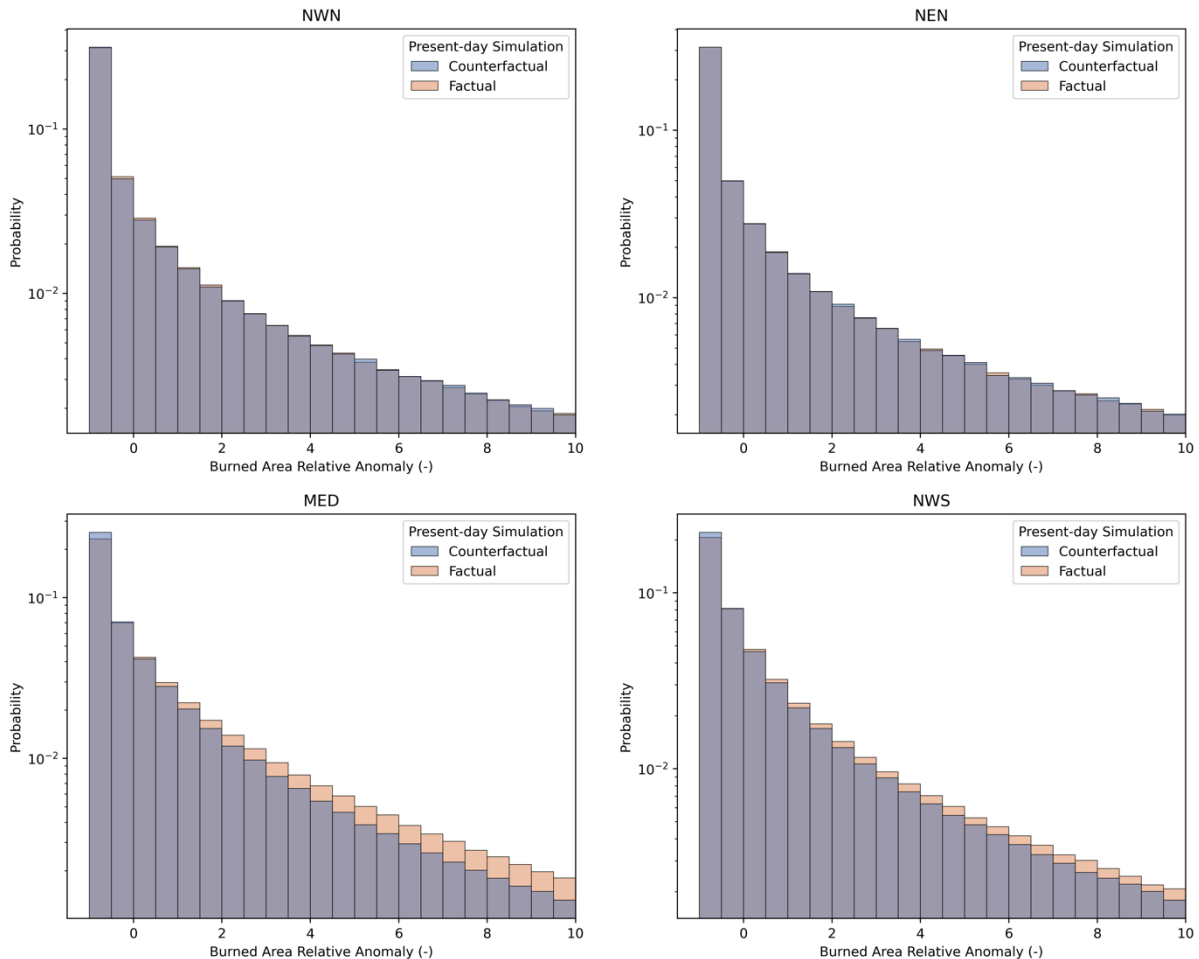
As reported in Burton, Lampe et al. (2023), we also show how background levels of fire extent, represented by the modelled median BA for months of interest, has changed overall in Canada due to total climate forcing (**Figure 15**), socioeconomic forcing (**Figure S15**), and all forcings (**Figure S16**). Using AR6 regions that best match our focus areas, we show that BA has increased by 1.9% [0.1, 3.6] in North West North America (NWN) due to total climate forcing, but reduced by -0.2% [-1.7, 1.3] in North East North America (NEN) (**Figure 15**). In these regions, socioeconomic forcing has dampened the effects of climate change, by reducing BA by -9.5% [-13.6, -6.3] in NWN, and -8.5% [-12.5, -5.7] in NEN (see Supplement). All forcings combined have led to an overall reduction in BA of -8.3% [-12.5, -4.9] in NWN and -8.7% [-12.8, -5.8] in NEN (**Figure S16**).

1806 **4.2.3.2 Greece**

1807  
 1808 Burton, Lampe et al. (2023) find a larger increase in median BA for months of interest due to  
 1809 total climate forcing in the Mediterranean region (MED), with an increase of 14.5% [11.5, 18.1]  
 1810 today compared to the counterfactual (**Figure 15**). This is particularly the case for the high  
 1811 burned areas, where the increase is larger compared to the lower end of the distribution.  
 1812 However, socioeconomic factors have largely offset this by reducing BA by -10.2% [-13.6, -  
 1813 6.6]. All forcings combined have led to an overall regional increase in BA of 0.5% [-3.5, 5.5]  
 1814 (see **Figure S16**).  
 1815

1816 **4.2.3.3 Western Amazonia**

1817  
 1818 As per Burton, Lampe et al. (2023), total climate forcing has increased median BA for months  
 1819 of interest by 11.5% [5.4, 18.4] in Northwest South America (NWS) today compared to the  
 1820 counterfactual (**Figure 15**). Again, this increase is mostly impacting the BA at the higher end  
 1821 of the distribution. This is mostly offset by socioeconomic factors (-9.0% [-18.9, 1.2]), although  
 1822 all forcings combined have still led to an overall increase in BA of 1.5% [-6.9, 10.5] in the  
 1823 region (see Supplement).  
 1824



1825  
 1826  
 1827 **Figure 15:** Change in median BA due to total climate forcing from FireMIP. Present day BA  
 1828 (2003-2019) for factual (historical forcing, orange) and counterfactual (detrended climate,  
 1829 blue), for AR6 regions. Panels show (**top left**) North West North America (NWN), (**top right**)  
 1830 North East North America NEN, (**bottom left**) Mediterranean (MED), and (**bottom right**) North  
 1831 West South America (NWS). Probability is shown on a log scale.  
 1832



## 1833 5 Seasonal and Multi-Decadal Outlook

1834

### 1835 5.1 Methods

1836

#### 1837 5.1.1 Seasonal Forecasts

1838

1839 Among the modes of variability in the climate system most relevant to wildfire activity globally  
1840 is the El Niño-Southern Oscillation (ENSO) (Mariani et al., 2016; Fuller and Murphy, 2006;  
1841 Cardil et al., 2023). Numerous studies have demonstrated that there is a predictable cascade  
1842 of fire across tropical continents during ENSO events, highlighting staggered responses of  
1843 wildfire to ENSO (Chen et al., 2017). The utility of using ENSO as a predictor of fire is  
1844 highlighted by its application in Indonesia, where severe fires during the 2015 El Niño led to  
1845 hazardous haze in Singapore and diplomatic tensions in the region, prompting better regional  
1846 cooperation and enforcement of anti-burning laws (Field et al., 2016; Forsyth, 2014; Carmenta  
1847 et al., 2021). Consequently, Indonesia now implements preemptive bans on agricultural  
1848 burning based solely on ENSO predictions, a measure that proved successful in 2023 when  
1849 no significant fire anomalies were recorded despite a strong positive ENSO event (Lin et al.,  
1850 2020; Sloan et al., 2022).

1851

1852 Another phenomenon demonstrably linked to global fire activity is the Indian Ocean Dipole  
1853 (IOD), which occurs in the Indian Ocean. There is ongoing debate regarding the direct  
1854 influence of the IOD on Australian fires, for example as the signal is often modulated by  
1855 changes in land management practices (Harris and Lucas, 2019). Other atmospheric modes  
1856 of variability in the Southern, Northern hemisphere and in the arctic regions can also have  
1857 influence on interannual BA patterns, and **Figure S1** shows the climate modes with strongest  
1858 influence on regional BA globally.

1859

1860 Outputs available from the Copernicus Climate Change Service (C3S) multi-model seasonal  
1861 prediction system are used to evaluate large-scale climate modes with the most proven links  
1862 to variation in fire activity: ENSO and IOD (CDS, 2018). As not all regions display similar  
1863 seasonal direct correlations between fire activity and ENSO, we also use seasonal outlooks  
1864 of the FWI from one of the models, ECMWF-SEAS5, to identify probabilities for the  
1865 establishment of anomalous landscape flammability in the next season. This is done using a  
1866 51-member forecast ensemble and a 24-year model climatological distribution (derived from  
1867 a 25-member ensemble re-forecast) covering the period 1993-2016. The probability of  
1868 exceedance is determined based on the proportion of forecast members meeting an  
1869 distributional threshold at any given geographical point. We consider the 75th percentile  
1870 threshold indicative of moderate anomalous conditions and the 95th percentile indicative of  
1871 extreme anomalous conditions.

1872

#### 1873 5.1.2 Decadal Projections of Burned Area

1874

1875 In order to project future changes in BA, we utilised the same modelling approach detailed in  
1876 **Section 4.1.3.1**, following a similar protocol to UNEP (2022a). We drive the ConFire model  
1877 with ISIMIP3a and bias-corrected JULES-ES data. For predictive mode, we used bias-  
1878 corrected global climate model (GCM) outputs from ISIMIP3b. While ISIMIP3a provides  
1879 reanalysis datasets to drive models for impact assessments, ISIMIP3b provides driving data  
1880 from 5 bias-corrected GCMs, including historical data up to 2014 and future scenarios from  
1881 2015-2100 under Shared Socioeconomic Pathway (SSP) scenarios SSP126, SSP370, and  
1882 SSP585. Each SSP represents future socio-economic pathways and includes GHG emissions  
1883 to drive the GCMs. The 5 GCMs used are: GFDL-ESM4 (Held et al., 2019), IPSL-CM6A-LR  
1884 (Boucher et al., 2020), MPI-ESM1-2-HR (Mauritsen et al., 2019), MRI-ESM2-0 (Yukimoto et

1885 al., 2019), and UKESM1-0-LL (Tang et al., 2019; Sellar et al., 2019). As part of ISIMIP3b, each  
1886 GCM is bias-corrected as described in Lange (2019).

1887 At present, future projections for land use and population density forcing were not available  
1888 for ISIMIP3b, so we only considered the influence of climate and vegetation fuel loads (related  
1889 to land cover) on fire, and not changes in ignitions or land use. We used JULES-ES land cover  
1890 outputs as per the previous section, but this time with JULES driven by each of the 5 different  
1891 bias-corrected GCMs and for the 3 different SSP scenarios instead of historical reanalysis.  
1892 The land cover output was then bias-corrected (using the same mapping procedure as  
1893 **Section 4.1.3.1**, based on biases between JULES-ES driven by reanalysis and VCF  
1894 observations) to maintain consistency with the GCM bias-correction procedures. We apply an  
1895 additional bias-correction to preserve the trend in vegetation cover from the historical period,  
1896 and to smooth the transition between the historical and future periods (see “**Data and Data**  
1897 **Processing**” in **Extended Methods Supplement** for details). The results in **Section 5.2.2**  
1898 are for the months June-August for Canada, July-September or Greece and August-October  
1899 for Western Amazonia, corresponding to those regions' fire seasons today.

1900 Our approach provides a probability distribution of future BA representing the uncertainty  
1901 range from cross-model (GCM) spread in the response of climate and vegetation to emissions  
1902 for each scenario and year in the period 2010-2100. Years 2010-2014 were consistently  
1903 adopted from the historical experiment.

1904 For Western Amazonia focal event, we additionally tested a 1-in-100 year event under 2010-  
1905 2020 climate, defined as the BA at the 99th percentile ConFires distribution. We also use the  
1906 1-in-100 definition at a grid cell level to determine spatial variations in the change in extreme  
1907 fire for each region. We then calculated decadal average likelihoods of the regions' event in  
1908 each decade up to 2100. Return times are 1/likelihood. The change in likelihood of an event  
1909 occurring on a given return time was calculated relative to the 2010-2020 baseline period.

1910 For the Canada focal event, we also calculated the integrated probability of an event with  
1911 similar magnitude to 2023 within the expected lifespan of a Canadian citizen. According to UN  
1912 population statistics, the average life expectancy of a Canadian citizen born today is 83 years  
1913 (United Nations Population Division, 2022). In order to cover the 7-year period after 2100, we  
1914 extrapolated the annual trend in probabilities. The integrated probability is calculated as one  
1915 minus the product of the annual probability of not seeing a fire event like 2023, for each year  
1916 between 2023 and 2106.

1917

## 1918 **5.2 Results**

1919

### 1920 **5.2.1 Seasonal Outlook for 2024**

1921

1922 The 2023–2024 El Niño event emerged as the fourth-most powerful on record, causing  
1923 widespread droughts, floods and other anomalous conditions worldwide. Officially declared by  
1924 the World Meteorological Organization (WMO) on July 4, 2023, its meteorological impacts  
1925 have unfolded between November 2023 and April 2024 (Joshi, 2023). Climate scientists have  
1926 found that the 2023–24 El Niño event, superimposed on climate change signal, has elevated  
1927 global temperatures beyond the records set during the 2016 El Niño event. Global mean  
1928 surface temperatures in 2023 were 1.31°C above pre-industrial levels of 1850-1900 (Forster  
1929 et al., 2024).

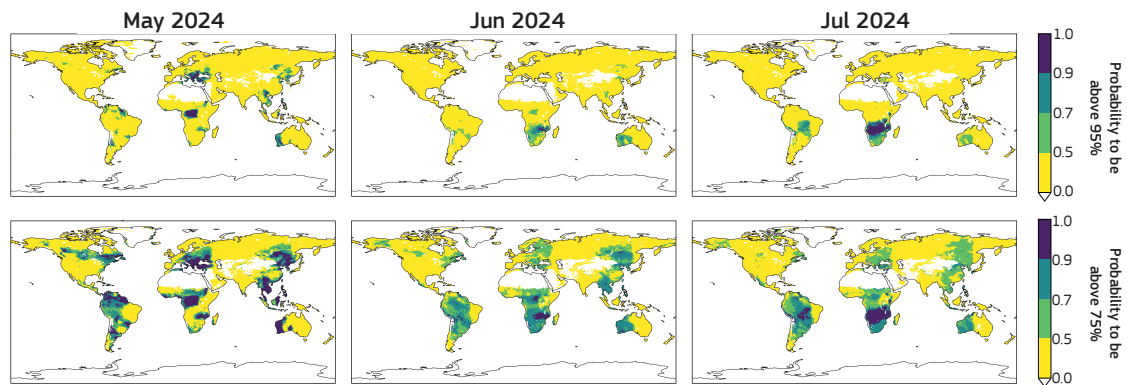
1930

1931 As of mid-June 2024, El Niño conditions have transitioned toward neutral conditions, which  
1932 are forecasted to persist during the boreal summer. The Indian Ocean Dipole (IOD) index is  
1933 currently positive, and forecasts indicate that it will remain in a positive state for the next  
1934 season. Connections are established between a positive IOD phase and fire risk in Indonesia

1935 and parts of Australia, though outcomes generally depend on interactions with the ENSO  
 1936 phase (Pan et al., 2018; Ren et al., 2024; Abram et al., 2021). Similarly, the positive phase of  
 1937 the IOD is linked with heightened fire risk in South America, particularly in the Amazon basin,  
 1938 where it can interact with other climate teleconnections to exacerbate droughts (Cardil et al.,  
 1939 2023; Dong et al., 2021).

1940  
 1941 **Figure 16** shows the predicted probabilities of the monthly average FWI exceeding moderate  
 1942 (75th percentile) or high (95th percentile) thresholds of the monthly climatology. Most areas in  
 1943 Southeast Asia and South America are predicted to experience a decrease in the likelihood of  
 1944 anomalous conditions over May, June and July 2024. Parts of Canada are predicted to reach  
 1945 moderate anomalous conditions once again in early summer, and this combined with  
 1946 overwintering fires could promote a second consecutive high fire season as has already been  
 1947 reported in the media (*BBC News*, 2024, *New York Times*, 2024). Predictions also suggest  
 1948 that the moderate FWI threshold will be exceeded in southeast, central, and western Brazil  
 1949 with the high threshold exceeded in southern and western parts. In parts of Africa, moderate  
 1950 FWI anomalies may be experienced throughout June-August.

1951



1952  
 1953 **Figure 16:** Probability for the monthly average FWI exceeding the **(top row)** 95th percentile  
 1954 threshold (anomalous conditions) and **(bottom row)** 75th percentile threshold (extremely  
 1955 anomalous conditions) of the monthly climatological distributions. The probability is calculated  
 1956 using the 51 ensemble member realisation from ECMWF’s long-range forecasting system,  
 1957 ECMWF-SEAS5 FWI, and comparing them with the 1991-2016 climatology (Copernicus  
 1958 Emergency Management Service, 2019).

1959

## 5.2.2 Future Changes in Likelihood of Extreme Fire Events

1960

### 5.2.2.1 Canada

1961

1962 The probability of Canada experiencing BA extent similar to June 2023 (specifically, for cells  
 1963 with BA fraction in the 95<sup>th</sup> percentile in that month) is estimated to be 0.15% in any given year  
 1964 under the climate conditions of 2010-2020, according to estimates made using reanalysis data  
 1965 (**Table 6; Figure 17**). Bias-correction did not fully resolve all discrepancies between the GCMs  
 1966 and reanalysis data, and the GCMs gave a range of likelihoods spanning 0.02 to 0.71% for  
 1967 any given year under the climate conditions of 2010-2020. We describe future changes as  
 1968 significant if the range across GCM projections for a future period does not overlap with the  
 1969 range given by the GCMs for 2010-2020.

1970

1971 By the 2040s, the likelihood of an event like 2023 increases significantly to 0.42% - 2.2%  
 1972 across scenarios, which is two to six times as likely as in the 2010s (**Table 6; Figure 17**).  
 1973 While the likelihood of an event like 2023 occurring in the 2040s is slightly higher in SSP585  
 1974  
 1975

1976 (0.6%-2.2%) than other scenarios (0.41%-1.6% for SSP126 and 0.5%-1.7% for SSP370),  
1977 differences between future scenarios are not significant at the mid-century point.  
1978

1979 The SSP126 scenario diverges significantly from SSP370 and SSP585 after 2070. Under  
1980 SSP126, the likelihood of an event like 2023 stabilises at 0.3-0.8% in the 2070s and remains  
1981 largely unchanged until the 2090s (**Figure 17**). In contrast, the likelihood of an event like 2023  
1982 continues to rise to 2.1-3.7% in the 2090s under SSP585 (**Table 6, Figure 17**). Under  
1983 SSP126, the probability of at least one event like 2023 recurring in any year (of any decade)  
1984 between 2024 and 2100 is estimated to be 18%-73%, compared with 59-87% under SSP585.  
1985 Hence the probability of an event like 2023 recurring by the 2090s is estimated to be twice  
1986 greater in SSP585 than in SSP126.  
1987

1988 Someone born in Canada in the current decade, with a life expectancy of 83 years (United  
1989 Nations Population Division, 2022), has a 65-90% probability of seeing a similar event in their  
1990 lifetimes under SSP585, compared with only an 12% likelihood of someone who reached 83  
1991 years old in the 2010s. Someone born in Canada today would also have a 42-80% probability  
1992 of seeing an event of similar magnitude *twice* under SSP585. Under SSP370, a citizen has a  
1993 48-84% probability of seeing a similar event once and 29-76% probability of seeing a similar  
1994 event twice. This reduces to 19-76% for one occurrence and 4-58% for two occurrences under  
1995 SSP126.  
1996

1997 These differences outlined above highlight the divergence in future likelihood of a 2023-like  
1998 event in Canada between high-mitigation (SSP126) and no-mitigation (SSP585) scenarios.  
1999 The divergence of likelihoods between the two scenarios is associated with increases in both  
2000 fuel load and fuel dryness (**Figure 17**).  
2001

2002 Future changes in probability of an event like 2030 under the SSP370 lie closer to those of  
2003 SSP585 than SSP126 (**Table 6; Figure 17**). For example, the probability of an event like 2023  
2004 occurring at least once by the 2090s is estimated to be between 48% and 84% under SSP370,  
2005 only slightly below the range projected under SSP585. This highlights that high-mitigation, low  
2006 emissions pathways are required to limit future increases in the potential for high-impact  
2007 events in Canada this century.  
2008

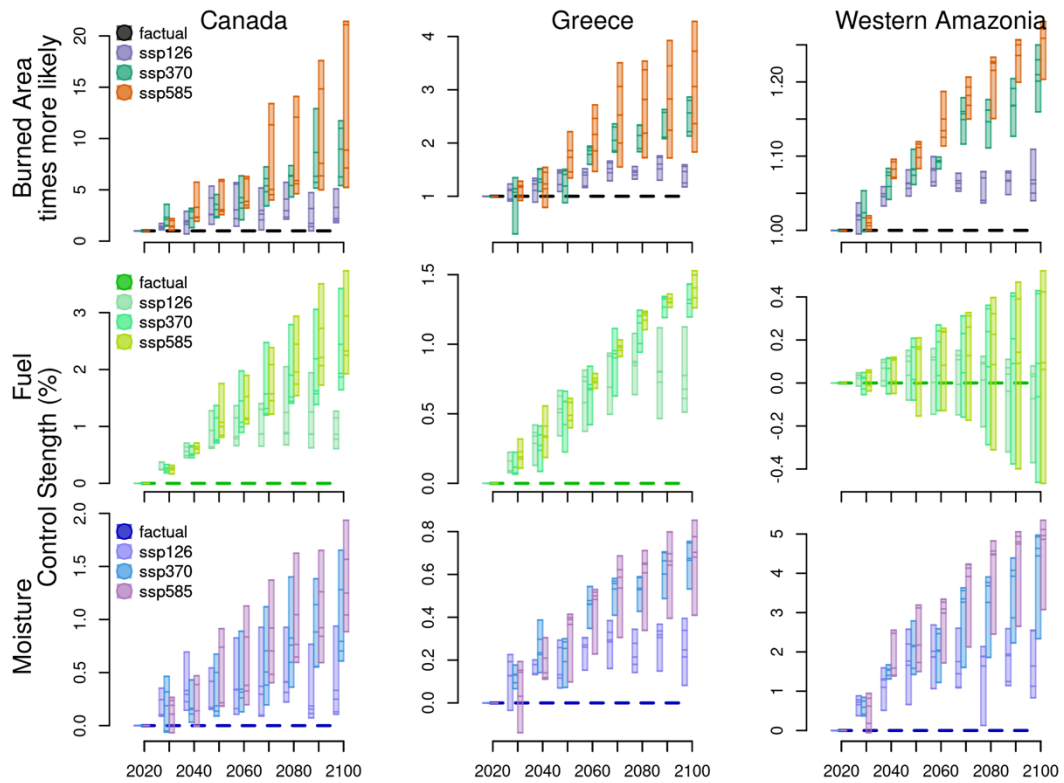
2009 **Figure 18** shows the spatial variability of changes in summer BA and 1-in-100 year BA events  
2010 in Canada. While some areas see increases in BA and fire extremes in all scenarios, the  
2011 greatest rates of change are projected in Southern Alberta and Saskatchewan and under  
2012 SSP585. These patterns emerge as early as 2030 (**Figure S17**). Meanwhile, the Yukon and  
2013 Northwest Territories are projected to see increased BA from 2040 in all scenarios, with 1-in-  
2014 100 year BA events becoming around twice as likely in parts of these provinces (**Figure S18**).  
2015 By the end of the century, a larger increase in BA is seen under SSP585 and SSP370 than in  
2016 SSP126, with 1-in-100 year BA events becoming up to 5 times more likely in parts of Yukon  
2017 and Northwest Territories. Uniquely under SSP585, factor-two increases in BA and 1-in-100  
2018 year BA events extend into British Columbia.

2019  
2020  
2021  
2022  
2023  
2024  
2025

**Table 6:** Summary of the likelihood of extreme events today using reanalysis ‘factual’ and today and into the future using bias-corrected GCMs for our three focal regions. ‘2023’ events focuses on the BA extreme identified in **Section 3.4.3**. 1-in-100 for Western Amazonia additionally looks at the likelihood of a 1-in-100 event under present day climate conditions, following the definition of extreme in (UNEP, 2022a). We also determine how much more frequent the events will be at two different time horizons based on each models likelihood in the future projections over likelihood during 2010-2020. Asterisks (\*) indicate non-significant changes from 2010-2020 values. Colours show linear increase of likelihood (red) and frequency (orange), where darker shade indicates higher values.

Region	Event	SSP	Represents	Likelihood (%/year)						How much more frequent (multiplier)			
				2010-2020		2040-2050		2090-2100		2040-2050		2090-2100	
				<i>min</i>	<i>max</i>	<i>min</i>	<i>max</i>	<i>min</i>	<i>max</i>	<i>min</i>	<i>max</i>	<i>min</i>	<i>max</i>
Canada	2023 (~1-in-700)	Factual	observed	0.15									
		SSP126	strong mitigation	0.1	0.61	0.42*	1.6*	0.22*	2*	2.6*	4.2*	2.2*	3.3*
		SSP370	middle of the road	0.12	0.54	0.5*	1.7*	1.3	3.4	3.1*	4.2*	6.3	10.8
		SSP585	no mitigation	0.1	0.71	0.6*	2.2*	2.1	3.7	3.1*	6*	5.2	21.1
Greece	2023 (~1-in-80)	Factual	observed	1.3									
		SSP126	strong mitigation	0.91	1.7	1.4*	1.8*	1.4*	1.9*	1.1*	1.5*	1.2*	1.6*
		SSP370	middle of the road	0.99	1.5	0.87*	2.2*	2.5	3.1	0.9*	1.5*	2.1	2.6
		SSP585	no mitigation	0.67	1.8	1.2*	2.4*	2.9	3.3	1.3*	1.7*	1.8	4.3
Western Amazonia	2023 (~1-in-6)	Factual	observed	16.6									
		SSP126	strong mitigation	15.1	16.6	15.8*	17.9*	15.9*	17.6*	1.1*	1.1*	1.1*	1.1*
		SSP370	middle of the road	15.2	16.3	16.2*	18.1*	17.7	20.4	1.1*	1.1*	1.2	1.3
		SSP585	no mitigation	15.1	16.5	16.4*	18.3*	18.2	21	1.1*	1.1*	1.2	1.3
	1-in-100	Factual	observed	1.5									
		SSP126	strong mitigation	0.82	1.5	1.2*	2.2*	1.2*	2*	1.4*	1.5*	1.3*	1.5*
		SSP370	middle of the road	0.81	1.5	1.3*	2.2*	2	3.1	1.5*	1.6*	2.2	2.4
		SSP585	no mitigation	0.8	1.5	1.4*	2.4*	2.3	3.3	1.6*	1.8*	2.2	2.9

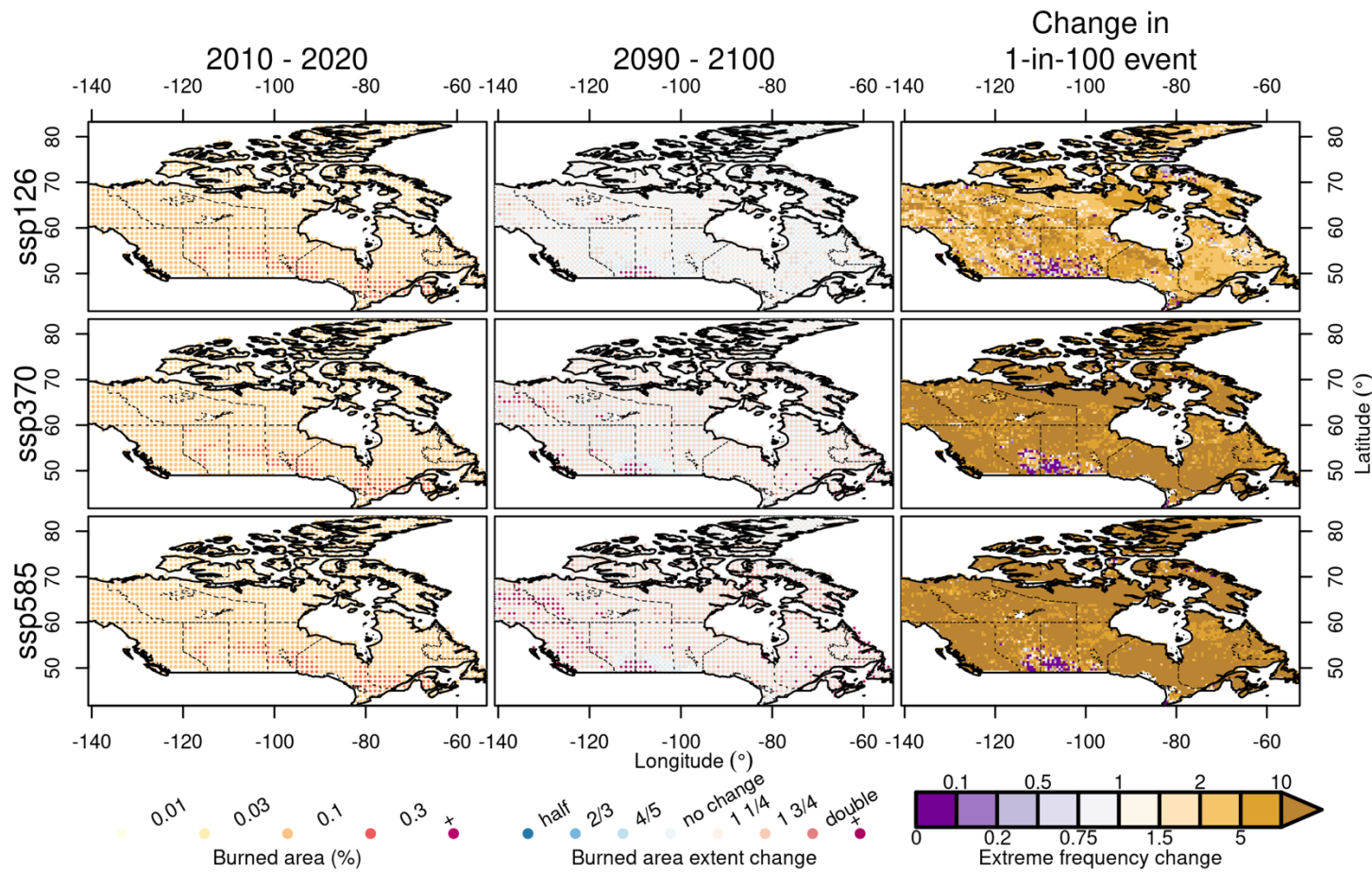
2026



2027  
2028  
2029  
2030  
2031  
2032

**Figure 17:** Future projections from ConFire of the change in likelihood of BA extent of the magnitude seen in 2023-2024, and the contribution of fuel and moisture controls towards those changes. Each set of bars shows changes for each decade relative to the 2010-2020, with each bar representing a different SSP scenario and the spread of bars indicating the variation across GCMs, with individual bars representing different GCMs.





2033  
2034  
2035  
2036  
2037  
2038  
2039

**Figure 18:** Projected changes in June-August BA over Canada by 2090-2100 under three SSP scenarios, with BA simulated by ConFire. **(Left)** Average June-August BA fraction (%) for 2010-2020. **(Middle)** Relative change in June-August BA extent projected for 2090-2100 period, expressed as a multiplier of 2010-2020 values. **(Right)** Increased (or decreased) frequency in the 2090-2100 period of a 1-in-100 year event defined for the period 2010-2020, expressed as a multiplier of 2010-2020 values. In the left column, the size of the dot in each grid cell indicates the likelihood (larger = higher likelihood) of a BA fraction (or being greater than the threshold indicated by the coloured dot (see legend at the base). Likewise, the size of the dot varies with likelihood that the BA fraction exceeds the threshold indicated by the coloured dot (see legend at the base). For example, a

2040 large pale orange dot in the left column indicates a high likelihood of the BA fraction exceeding 0.05%, whereas a small dark red dot indicates a small (but non-zero) likelihood  
2041 of the BA fraction exceeding 0.5%.



2042  
2043  
2044  
2045  
2046  
2047  
2048  
2049  
2050  
2051  
2052  
2053  
2054  
2055  
2056  
2057  
2058  
2059  
2060  
2061  
2062  
2063  
2064  
2065  
2066  
2067  
2068  
2069  
2070  
2071  
2072  
2073  
2074  
2075  
2076  
2077  
2078  
2079  
2080

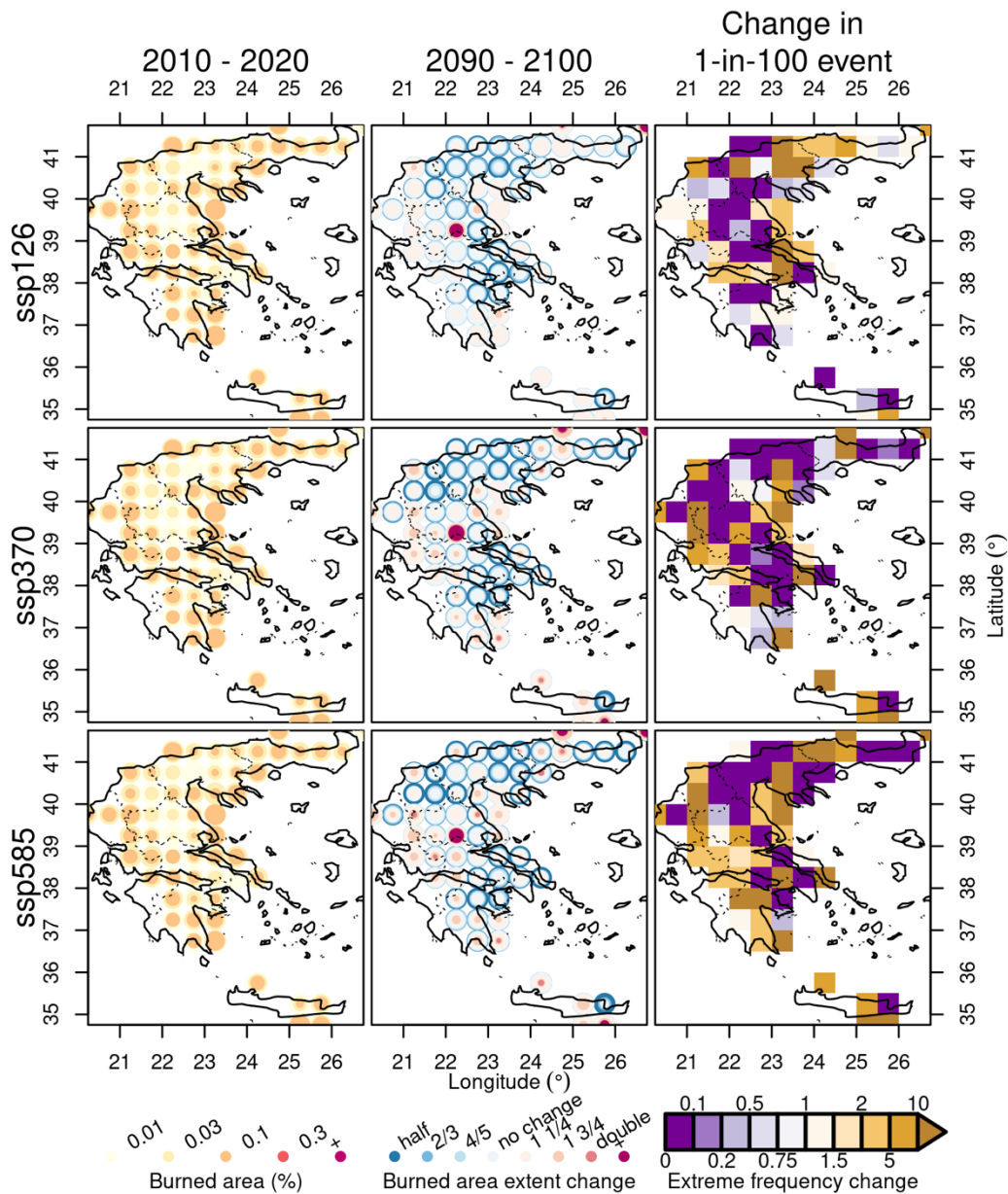
### 5.2.2.2 Greece

The probability of Greece experiencing BA extent similar to August 2023 (specifically, for cells with BA fraction in the 90<sup>th</sup> percentile in that month) is estimated to be 1.3% in any given year under the climate conditions of 2010-2020, according to estimates made using reanalysis data (**Table 6; Figure 17**). Bias-correction did not fully resolve all discrepancies between the GCMs and reanalysis data, and the GCMs gave a range of likelihoods spanning 0.7-1.8% for any given year under the climate conditions of 2010-2020.

In SSP126, no significant increase in likelihood of an event like 2023 is projected for any decade through 2100 (i.e., beyond the range of 0.7-1.8% for the 2010s). This is despite the likelihood of a 2023-like event in some decades being as high as 2.3 times more likely than in the 2010s under SSP126 (**Figure 17**). The lack of significance in these changes may in part reflect our strict definition of significance (i.e., no overlap with the range of the 2010s). When likelihoods vary considerably across models due to the incomplete resolution of biases, the thresholds for significance are high. The small number of observations available for model training in Greece due to its small domain size, which likely contributes to wider uncertainty bounds and higher biases than in the other, larger focal regions. Overall, Greece could see large increases in the occurrence of extreme BAs even under strong mitigation (SSP126), but uncertainties are large.

SSP350 and SSP585 show significant increases in the likelihood of an event like 2023 by the 2070s (relative to the 2010s), and also diverge significantly beyond SSP126 in the 2080s. SSP585 and SSP370 do not diverge from one another throughout this century and, in 2100, both scenarios give a likelihood of an event like 2023 of 2.5-3.3%. This range is equivalent to a 1.8-to-4.3-fold increase on the values of the 2010s, and an average return time of 31-39 years. The divergence of likelihoods between SSP126 and the two other scenarios (SSP350 and SSP585) is associated with increases in both fuel load and fuel dryness, with particularly striking differences in the latter across the scenarios (**Figure 17**).

There are some spatial patterns in the future trajectory of summer BA and the likelihood of future 1-in-100 year BA events in Greece by the 2090s (**Figure 19**). Interior parts of Greece tend to see a decline in BA, while coastal parts see an increase in BA and this pattern broadly holds for 1-in-100 year events. Across scenarios with increasingly low levels of climate change mitigation, there is an expansion to the portion of Greece's total area that experiences increased summer BA and increased frequency of 1-in-100 year events.



2081  
2082 **Figure 19:** Same as **Figure 18**, but for Greece and months July-September.

2083  
2084  
2085 **5.2.2.3 Western Amazonia**

2086  
2087 The probability of Western Amazonia experiencing BA extent similar to September-October  
2088 2023 (specifically, for cells with BA fraction in the 95<sup>th</sup> percentile in that month) is estimated  
2089 to be 16.58% in any given year under the climate conditions of 2010-2020, according to  
2090 estimates made using reanalysis data (**Table 6; Figure 17**). Bias-correction did not fully  
2091 resolve all discrepancies between the GCMs and reanalysis data, and the GCMs gave a range  
2092 of likelihoods spanning 15.1-16.6% for any given year under the climate conditions of 2010-  
2093 2020. As expected, these results suggest that the events observed in Amazonia in 2023 were  
2094 not as extreme as those in Canada and Greece, with returns times of around 6-7 years.

2095  
2096 We note that spatial patterns of fire are highly dependent on patterns of land use and human  
2097 ignition sources in Amazonia (e.g. **Figure S14**), and an important caveat is that the BA

2098 responses to future climate and land cover change, presented below, is likely to be highly  
2099 modulated by socioeconomic factors (Lapola et al., 2023; Kelley et al., 2021; Silveira et al.,  
2100 2020).

2101  
2102 Under the SSP585 scenario, the likelihood of an event like 2023 increases significantly in the  
2103 2090s to 18.2-21.0%, representing a factor 1.2-1.3 increase versus the 2010s. This increase  
2104 is primarily attributed to lower fuel moisture, in line with declines in fire weather in this region  
2105 (**Section 4.2.1**). On the other hand, in the SSP126 scenario representing strong climate  
2106 change mitigation, the likelihood of an event like 2023 does not change significantly at any  
2107 point this century (**Table 6**).

2108  
2109 The likelihood of an event like in 2023 increases substantially in the centre of the region by  
2110 the 2030s under SSP370 and SSP585 (**Figure S21**) and the affected area expands through  
2111 2100 (**Figure S22**). Southern regions with greater population and infrastructure densities see  
2112 lesser increases in likelihood. Perhaps more important for the region's fire-sensitive forests is  
2113 the projected increase in BA in SSP370 and SSP585 across forests in the north of the region,  
2114 which would be expected to impact on some of Earth's most remote and pristine forests by  
2115 the end of this century (**Figure S23**).

2116  
2117 The 2023 event in Amazonia had a relatively high return interval compared with other focal  
2118 regions. Hence we tested for change in likelihood of a rarer, 1-in-100 year event in western  
2119 Amazonia. Under SSP585, we found that the likelihood of a 1-in-100 year event increased  
2120 significantly by the end of the century, to 2.3-3.3% in the 2090s (representing a factor 2.2-2.9  
2121 increase in likelihood). The likelihood of a 1-in-100 year event also increased significantly  
2122 under SSP370 towards the end of this century, but under SSP126 no significant change  
2123 occurred this century.

2124  
2125 Our results show that SSPs associated with lesser climate change mitigation (SSP585 and  
2126 SSP370) promote more frequent extreme BA in western Amazonia, irrespective of change in  
2127 land use and human ignition factors with potential to strongly modulate the BA response to  
2128 climate. There is greater potential for compounding effects of human factors and climate-  
2129 driven increases in extreme BA likelihood under scenarios with no or low climate change  
2130 mitigation than in the case of scenarios with high climate mitigation (such as SSP126).

2131

## 2132 **6 Conclusions**

2133

### 2134 **6.1 Summary of the State of Wildfires in 2023-24**

2135

#### 2136 **6.1.1 Extreme Wildfire Events of 2023-24**

2137

2138 ● **Global:** A total of 3.9 million km<sup>2</sup> burned globally during the 2023-24 fire season,  
2139 slightly below the average of previous seasons (4.0 million km<sup>2</sup>) and ranking 13th since  
2140 2002. Despite the lower BA, fire C emissions were 16% above average, totaling 2.4  
2141 Pg C, ranking 7th highest since 2003. Global C emissions were pushed up by record  
2142 emissions in Canadian boreal forests and pulled down by below-average fire activity  
2143 in the African savannahs (significant because fires in the African savannahs make, on  
2144 average, the largest contribution of any continental biome to global mean annual BA  
2145 and emissions). If global savannah fire emissions had been in line with their average  
2146 in 2023-24, global fire C emissions would have been the highest on record.

2147

2148 ● **North America:** Record fire activity in Canada's boreal forests, with BA reaching six  
2149 times the average and fire C emissions over nine times the average and contributing  
2150 significantly towards global C emissions (24%, up from a mean value of 3% from prior

2151 fire seasons). Canada experienced extreme and widespread fires, with over 150,000  
2152 km<sup>2</sup> burned, prompting evacuations of 232,000 people. Eight firefighters lost their lives.  
2153 Fires in Canada led to a significant degradation of air quality, with populations living in  
2154 the US and Canada exposed to atmospheric concentrations of PM2.5 over daily  
2155 standards for periods of 2 weeks to multiple months. The United States saw generally  
2156 below-average fire activity, but the Lahaina wildfire in Maui, Hawaii, resulted in 100  
2157 civilian deaths, destroyed 2,000 homes, and displaced 10,000 people. Texas recorded  
2158 its largest ever single fire, which destroyed 130 homes and killed two civilians.

2159  
2160 ● **South America:** South America experienced somewhat below-average fire extent  
2161 overall, but notable exceptions included significant anomalies in the northwest of the  
2162 continent. In Brazil's Amazonas state, fire counts reached record highs amidst drought  
2163 conditions, severely impacting air quality in Manaus. In neighbouring parts of Bolivia,  
2164 Peru, Venezuela, and Guyana, also affected by regional drought, record or high-  
2165 ranking levels of fire counts, extent, and carbon emissions were observed. In Chile,  
2166 the Valparaíso wildfire in February 2024 killed 131 people and caused widespread  
2167 property destruction.

2168  
2169 ● **Europe:** Europe experienced low fire extent in 2023-24, however the Evros fire in  
2170 Greece set a new EU record for individual fire size (around 900 km<sup>2</sup>) and killed 19  
2171 people. Individual fires in Greece, Spain, Italy, Portugal, France, and Scotland led to a  
2172 range of impacts including large-scale evacuations, significant suppression costs,  
2173 disruption of water supplies, damage to infrastructure or agricultural lands, impacts on  
2174 tourism and local economies, destruction of properties (see **Appendix A**).

2175  
2176 ● **Oceania:** Above-average fire activity and extent were observed in the savannahs,  
2177 grasslands, and shrublands of western and northern Australia. Although less impactful  
2178 than the 2019-20 Black Summer fires due to their remoteness, wildfires near Perth  
2179 resulted in property destruction. The Tara and Mount Isa fires in Queensland destroyed  
2180 65 homes and claimed two lives. In Victoria, fires destroyed over 40 homes and injured  
2181 five firefighters. In New South Wales, forest fires caused widespread smoke-related  
2182 damages.

2183  
2184 ● **Asia:** Most parts of Asia saw low fire activity. Lao PDR, Thailand, and Vietnam  
2185 experienced high fire counts amidst reported heatwave conditions and a possible  
2186 uptick in agricultural fire use, leading to regional haze and air quality issues. In  
2187 Mongolia's Dornod Aimag province, wildfires burned large parts of the Daurian steppe  
2188 and firefighting was required to stop fires crossing the border into Russia.

2189  
2190 ● **Africa:** Africa experienced low fire extent in general during 2023-24, with BA 13%  
2191 below average in the African grassland, savannah, and shrubland biome. However,  
2192 extreme fires in Northern Africa, particularly Algeria and Tunisia, prompted significant  
2193 emergency responses including assistance from the EU. In Algeria, wildfires occurring  
2194 in temperatures around 50°C resulted in 34 deaths and over 1,500 evacuations, with  
2195 over 8,000 personnel deployed to combat the fires. Tunisia faced similar challenges  
2196 with strong winds exacerbating wildfires, leading to evacuations in the northwestern  
2197 region. In coastal South Africa, fires in the Western Cape caused structure damage  
2198 and evacuations.

## 2199

### 2200 **6.1.2 Diagnosing Drivers and Assessing Predictability**

2201  
2202 ● **In Canada, fire weather conditions were the primary drivers of the record-**  
2203 **breaking fire activity and extent during 2023.** However, there were notable  
2204 contributions from other drivers such as upticks in ignitions or human factors that were  
2205 not explicitly represented in our analyses. This highlights potential inadequacies in

2206 predicting some ignition sources or accurately representing fire propagation in current  
2207 forecasting systems.

2208

2209 ● **The exceptional nature of Evros fire in Alexandroupolis, Greece, could not have**  
2210 **been predicted using fire weather forecasts.** While there were discernible  
2211 indications in the Fire Weather Index (FWI) records that the days around the event  
2212 were more extreme than most days in the fire season, similar conditions were also  
2213 observed in other periods without resulting in the same catastrophic impacts. This  
2214 highlights the intrinsic difficulties in forecasting isolated extreme fire events and  
2215 underscores the need to advance early warning systems beyond fire weather to  
2216 consider fuel availability and ignition variability.

2217

2218 ● **The extreme fire season in western Amazonia was driven by prolonged drought**  
2219 **conditions linked to the strong El Niño.** Many fires developed, triggered by lightning  
2220 ignitions early in the season amidst high fire weather anomalies. Other than weather  
2221 conditions that acted as persistent controls for fire activity, several periods with high  
2222 active fire counts were not predicted in late August and throughout September likely  
2223 due to the result of unrepresented ignition sources.

2224

2225 ● **In all focal events, extreme burned areas were driven by anomalies in multiple**  
2226 **controls on fire. Weather, fuel moisture, and fuel abundance were all critical**  
2227 **factors.** The synchronous occurrence of anomalies in fire weather, high fuel load, and  
2228 low fuel moisture created the conditions leading to the anomalous burned areas  
2229 recorded in all three events. This underscores that no single bioclimatic factor can  
2230 explain the most severe fires. Instead, multiple contributing controls must coincide for  
2231 the most extreme events to arise. Factors such as ignitions, suppression, and landscape  
2232 fragmentation, related to human activities, likely played important roles in modulating the  
2233 Western Amazonian and Greece events.

2234

2235 ● **Fuel load is an important modulator of the relationship between fire extent and**  
2236 **fire weather.** Higher and/or drier fuel loads combined with high fire weather conditions  
2237 caused the unprecedented extent of burning in Canada and Western Amazonia. The  
2238 boundaries (extinction points) of extreme fires in Canada and Greece often  
2239 corresponded to areas with lower fuel loads, demonstrating that discontinuity in fuel  
2240 availability constrained fire spread.

2241

### 2242 6.1.3 Attribution to Global Change

2243

2244 ● **In Canada, anthropogenic forcing increased the chance of high fire weather in**  
2245 **2023. Total climate forcing led to higher BA, whereas socio-economic factors**  
2246 **may have decreased burning.** Anthropogenic forcing (resulting from greenhouse gas  
2247 emissions and land-use change) at least doubled the probability of experiencing high  
2248 fire weather in June 2023. It is virtually certain that total climate forcing (resulting from  
2249 climate change since the pre-industrial period) increased the BA in Canada by up to  
2250 40.1%. Socioeconomic factors related to land use, ignitions and suppression may have  
2251 reduced burning, though with low confidence.

2252

2253 ● **In Greece, anthropogenic forcing increased the chance of high fire weather in**  
2254 **2023. Total climate forcing led to higher BA, and socio-economic factors may**  
2255 **have increased or decreased BA.** Anthropogenic forcing increased the probability of  
2256 experiencing high fire weather in August 2023 by 1.9-4.1 times. It is likely that total  
2257 climate forcing increased the BA in Greece by up to 17.7%, whereas socio-economic  
2258 factors could have led to an increase or decrease. Climate change has increased

2259 average BA in the wider Mediterranean region, but this has been mainly offset by  
2260 socio-economic factors.

2261

2262

2263

2264

2265

2266

2267

2268

2269

2270

- **In western Amazonia, anthropogenic forcing has greatly increased the chance of high fire weather in 2023. It is virtually certain that total climate forcing led to higher BA, and very likely that socio-economic factors also contributed.** Anthropogenic forcing increased the probability of experiencing high fire weather by more than a factor of 20. It is virtually certain that total climate forcing increased BA in western Amazonia by up to 49.7%, and very likely that socio-economic factors exacerbated the increase. Climate change has increased today's average BA in the region, and all forcings have led to an overall increase in burning.

2271

#### 6.1.4 Seasonal and Multi-Decadal Outlook

2272

2273

2274

2275

2276

2277

2278

2279

2280

- **While the positive El Niño phase of ENSO is subsiding towards a neutral phase in 2024, the Indian Ocean Dipole is persisting in its positive phase, with potential to influence global fire patterns.** The 2023–2024 El Niño event emerged as the fourth-largest positive anomaly on record, however most simulations forecast a transition to ENSO-neutral conditions in 2024. Positive IOD phases are associated with elevated BA Amazonia, Indonesia, and parts of Australia though these tend to depend on interactions with ENSO.

2281

2282

2283

2284

2285

2286

- **Seasonal predictions of fire weather through August 2024 highlight moderate positive anomalies (75th percentile) in parts of Canada and much of South America including Amazonia,** as well as in central Africa, Southern Africa, southeast Europe, western Australia, southeast Asia, and northeast Asia. Extreme (95th percentile) anomalies are rare in the forecast through August 2024.

2287

2288

2289

2290

2291

2292

2293

2294

2295

2296

2297

2298

- **In Canada, future likelihood of events like in 2023 are increased by rising fuel load and dryness, with high mitigation pathways significantly reducing these risks.** The likelihood of extreme fire events similar to those in June 2023 is currently low (0.15% for any given year in the 2010s, or 1-in-700 years). The likelihood is expected to increase to 0.42-2.2% by the 2040s, and thereafter continue to increase under high emissions scenarios (SSP585) reaching 2.1-3.7% by the 2090s. The probability of experiencing such events at least once by the 2090s is estimated to be 59-87% under SSP585, compared to 18-73% under SSP126. Individuals born in Canada during the current decade have a 54-87% likelihood of witnessing an event on the scale of 2023 again in their lifetime under SSP370 (a scenario close to present day trajectories without additional mitigation efforts).

2299

2300

2301

2302

2303

2304

2305

2306

2307

2308

- **In Greece, high mitigation scenarios result in no significant change in the likelihood of an event like 2023 through 2100, whereas scenarios without mitigation lead to significant increases.** The current likelihood of extreme fire events like those in August 2023 is around 1.3% annually for any given year in the 2010s (or roughly 1-in-100 years). Under SSP126, there is no significant increase projected through 2100 whereas significant increases in likelihood (to up to 3.3%) are projected under SSP585 and SSP370 by the 2090s, implying more frequent extreme fire events. Coastal areas of Greece are expected to experience the greatest increases in risk, whereas interior regions may experience declines.

2309

2310

2311

2312

2313

- **In Western Amazonia, the effects of climate change on extreme fire likelihood in future scenarios is chiefly governed by fuel moisture effects, which are likely to be strongly modulated by local changes in land use and human ignition sources. The potential for compounding effects between fuel dryness and local stress factors is minimised in high-mitigation scenarios.** The current likelihood of extreme

2314 fire events like those in September-October 2023 is 16.6% (or roughly 1-in-6 years).  
2315 Under SSP585, the likelihood of such events increases significantly to 18.2-21.0% by  
2316 the 2090s. In addition, there is a significant rise in the probability of 1-in-100 year  
2317 events by the end of the century under SSP585 and SSP370. No significant rise in  
2318 probability of 1-in-6 or 1-in-100 events is seen under SSP126. Hence, while increased  
2319 fire risks related to climate change in the Amazon can be compounded by human  
2320 activities, this is least likely under SSP126. The impact of extreme fire events is  
2321 expected to be severe in pristine northern forests, emphasising the need for strong  
2322 climate change mitigation.

2323  
2324 ● **Overall, high-emissions scenarios (e.g. SSP585, SSP370) lead to significantly**  
2325 **increased likelihood of major events like those seen in the 2023-24 fire seasons**  
2326 **in future, highlighting the critical importance of strong climate change mitigation**  
2327 **efforts (e.g. SSP126) to reduce the future likelihood of extreme fire events.** Even  
2328 though SSP370 and SSP585 scenarios suggest significant increases in extreme  
2329 events, the confidence that strong mitigation (SSP126) can avoid significant portions  
2330 of increased risk is a major promising outcome of this work. Our findings emphasise  
2331 the importance of continued and enhanced mitigation efforts.  
2332

## 2333 **6.2 Roadmap for the State of Wildfires Report**

2334  
2335 The report successfully achieved its primary objectives, which included identifying and  
2336 contextualising extreme wildfires and wildfire seasons over the past year, selecting focal  
2337 events with significant societal and environmental impacts, and diagnosing the factors  
2338 contributing to these events. The report also assessed the predictive capabilities of existing  
2339 systems, highlighting their strengths and limitations, and attributed the occurrence of focal  
2340 events to anthropogenic factors, including climate change and land use. Additionally, it  
2341 provided an outlook for future wildfire probabilities, emphasising the limitations of current long-  
2342 term forecasting tools and the increasing likelihood of extreme fire events under future climate  
2343 scenarios, particularly highlighting the need for improved accuracy in regional projections.  
2344

2345 The fire science community is currently navigating several research frontiers to improve  
2346 prediction of extreme fires and understanding of their causes, with the view to enhance  
2347 preparedness, response, mitigation, and adaptation to wildfires in wider society. The field is  
2348 advancing its ability to observe individual fires, assess conditions leading to extreme fires, and  
2349 predict their occurrence on timescales ranging from hours to decades. Additionally, there is  
2350 increasing focus on monitoring and modelling the diverse impacts of extreme fires on society,  
2351 the environment, and the economy.  
2352

2353 As part of this inaugural edition of the State of Wildfires report, we present, in **Appendix B**, a  
2354 stocktake of current capabilities, challenges, and emerging opportunities in the observation  
2355 and modelling of extreme fires and their impacts. **Appendix B** is intended for the  
2356 interdisciplinary community of fire scientists and represents a contribution to agenda-setting  
2357 within this field of research. It will not be revised annually but may be revisited in future to  
2358 serve as a stocktake of progress in this field. Here, we briefly summarise the specific role that  
2359 the State of Wildfires report should serve as advances in the observation, prediction, and  
2360 modelling of extreme fires and their impacts come to fruition.  
2361

### 2362 **6.2.1 Definition**

2363  
2364 **The State of Wildfires Report will facilitate a community effort on a protocol for defining**  
2365 **extreme fire events or fire seasons.**  
2366



2367 This report emphasises important issues in the definition of extreme fires, a problem that  
2368 affects the definition of many terms used in fire science including ‘wildfire’ and ‘megafire’  
2369 (**Appendix B**; e.g. Shuman et al., 2022, Linley et al., 2022). Definition is complicated by the  
2370 impact of fires on society and the environment across many impact sectors, with the  
2371 magnitude of impact not necessarily correlating with observable fire traits such as BA  
2372 (**Appendix B**). In future years, regional experts would benefit from a protocol or guidelines  
2373 that can be used for categorising extreme fire events or seasons. To support future iterations  
2374 of the State of Wildfires report, we will coordinate workshops with broader sections of the fire  
2375 science community with the aim to produce guidance for future years. Central to this task is  
2376 the inclusion of communities from broad geographies so that any output respects fire impacts  
2377 that are considered to be regionally significant.  
2378

### 2379 **6.2.2 Observation**

#### 2380 **The State of Wildfires report will advocate for and utilise new harmonised fire** 2381 **observation products.**

2382  
2383  
2384 Consistent, long-term records of fire extent and properties are fundamental for studying  
2385 extremes, which cannot be characterised without reference to historical ranges (**Appendix B**).  
2386 The MODIS instrument has been crucial in tracking global fire progression and emissions over  
2387 two decades, but its continuity is threatened as the Terra satellite nears decommissioning,  
2388 necessitating harmonisation with newer datasets like VIIRS, Landsat, and Sentinel with  
2389 MODIS records for consistent fire observation.  
2390

2391 The State of Wildfires report further underscores the critical strategic need for a continuous  
2392 and harmonised dataset of fire observations beyond the MODIS era (**Appendix B**). To support  
2393 future iterations of the report, we will advocate for the provision of harmonised products within  
2394 the Earth observations communities. In addition, regional products often provide scope to  
2395 characterise the extremity of events over multi-decadal timescales and are now being provided  
2396 in globally harmonised formats compatible with global analyses such as ours. These regional  
2397 dataset should be utilised in future iterations of the State of Wildfires report.  
2398

#### 2399 **The State of Wildfires Report will stimulate progress on combining multiple fire** 2400 **observation streams to better identify and characterise extreme fire.**

2401  
2402 This report highlights the need to advance our capacity to observe fires that are impactful in  
2403 diverse ways (**Appendix B**). In particular, there is a growing need to move ‘beyond burned  
2404 area’ and towards a wider set of intensity, severity and behaviour metrics that often relate  
2405 more strongly to impacts on society and the environment than BA. The integration of individual  
2406 fire data from the Global Fire Atlas in this iteration of the State of Wildfires Report is one  
2407 example of including wider fire parameters such as size and rate of growth. Further  
2408 applications of the dataset or other individual fire atlases (e.g. Laurent et al., 2018; Artés et  
2409 al., 2019) could include assessing days with many synchronous large fires, which challenge  
2410 fire management (e.g., Abatzoglou et al., 2021), and identifying impactful fires by their  
2411 intersection with population centres (e.g., Modaresi Rad et al., 2023). Combining individual  
2412 fire behaviour data with fire radiative power and biomass combustion estimates might better  
2413 identify intense or severe fires with significant consequences for ecosystems and society (e.g.,  
2414 Nolan et al., 2021a).  
2415

2416 Overall, the State of Wildfires report must stimulate progress on moving ‘beyond burned area’  
2417 and combining diverse observational capacities to better identify and characterise extreme fire  
2418 events, and we intend to expand our use of such insights in future iterations. Likewise, the  
2419 report must be poised to adopt into its definition of extreme fires any emerging datasets that  
2420 quantify fire impacts on the various impact sectors outlined in **Appendix B**.  
2421



2422 **6.2.3 Prediction**

2423

2424 **The State of Wildfires report will advocate for the use of extended range forecast to**  
2425 **identify early onset of fire weather conditions.**

2426 Global fire danger monitoring systems currently use short to medium-range weather forecasts,  
2427 typically up to 10 days (**Appendix B**). However, state-of-the-art seasonal forecasting systems  
2428 can predict fire-conducive conditions up to one month in advance, and in some regions, up to  
2429 two months. Longer-term predictability is achievable in regions where fire activity corresponds  
2430 strongly with climate modes such as ENSO.

2431 By presenting an annual opportunity to take stock of current capabilities in forecasting horizons  
2432 for significant global fire events, the State of Wildfires report will continue to showcase and  
2433 advocate for advances in the forecasting window for extreme fire potential on subseasonal to  
2434 seasonal timescales.

2435 **The State of Wildfires report will stimulate progress on the use of AI and informatics**  
2436 **methods to aid the forecast of fire activity globally.**

2437 There is strong potential for data-driven applications, such as machine learning, to improve  
2438 predictions of extreme fire occurrence and move beyond traditional prediction systems based  
2439 on meteorological indices such as FWI (**Appendix B**). These methods can incorporate diverse  
2440 data inputs representing the influence of fuel loads, fuel moisture, ignition opportunities, and  
2441 suppression on fire likelihood, therefore improving upon indices that are mostly a function of  
2442 weather conditions. Tools used in this report, such as ConFire, are structured to harness new  
2443 data as they become available, including near-real-time data, improved fuel observations, and  
2444 detailed human/fire interaction data. ConFire is also being developed to optimise its  
2445 representation of extreme fire events by incorporating more flexible response curves into its  
2446 BA predictions (Barbosa 2024). The State of Wildfires report will showcase the benefits of  
2447 these emerging technologies in enhancing fire prediction and management.

2448 **6.2.4 Attribution**

2449

2450 **The State of Wildfires report will promote the enhancement of low-latency attribution**  
2451 **approaches.**

2452 Fire attribution techniques are relatively novel compared with more established approaches  
2453 for extremes such as heatwaves. Part of the challenge in attributing fire is that it is a complex  
2454 hazard comprising multiple compound risks across both meteorological and human drivers,  
2455 all of which must be represented in the driving data sets used by models (**Appendix B**). A  
2456 particular challenge that we faced in our current work was latency in the reanalysis datasets  
2457 used to drive our model for novel attribution of fire extent. Our working group will therefore  
2458 engage with the ISIMIP project to promote the creation of low-latency reanalysis products to  
2459 support responsive attribution assessment in future State of Wildfires reports, and in other  
2460 near real-time applications. An additional avenue for enhancement of future reports is to  
2461 include a greater number of climate models in the attribution work by widening the participation  
2462 of other groups working on attribution internationally.

2463 **The State of Wildfires report will support the expansion of attribution methods that**  
2464 **target a range of extreme fire metrics.**

2465 Extending attribution approaches to a broader range of extreme fire properties (e.g. aspects  
2466 of the fire size or fire behaviour distributions) is increasingly possible as observations of  
2467 individual fire characteristics and behaviour avail (**Appendix B**). Capacity to attribute  
2468 individual fire properties can be built by coupling the ConFire model with process-based

2469 models within attribution frameworks, allowing attribution of specific extreme fire  
2470 characteristics to climate change and other forms of global change.

2471

## 2472 **6.2.5 Projection**

2473

2474 **The State of Wildfires report will harness projections from multi-model ensembles.**

2475 In the coming years, FireMIP and ISIMIP will provide ensembles of model projections of future  
2476 BA for the first time (**Appendix B**). The State of Wildfires report will make use of these  
2477 simulations as soon as they are available, thus improving upon the single model (ConFire)  
2478 employed in the current edition and improving characterisation of uncertainty in the  
2479 projections.

2480 **The State of Wildfires report will support the expansion of projection methods to target**  
2481 **a range of extreme fire metrics.**

2482 An ambition for the State of Wildfires report is to provide projections of future fire properties  
2483 “beyond burned area”, such as the fire size and behaviour distribution (**Appendix B**). This  
2484 capacity can be built by combining the ConFire model with multiple process-based models  
2485 from FireMIP and ISIMIP. Advances in this area have particular societal relevance in resource  
2486 planning, as changes in fire behaviour (not only fire extent) are likely to factor into decision-  
2487 making around future suppression resource requirements.

2488  
2489  
2490  
2491  
2492  
2493  
2494  
2495

## 7 Appendix A: Year in Review by Continent

This appendix includes the review completed by an expert panel to supplement our quantitative analyses of extremes in the 2023-24 fire season (see **section 2.1**). Details of the assembled panel are provided in **Table A1**, below.

**Table A1:** Experts contributing to the identification of extreme events and characterisation of the global fire season during March 2023-February 2024.

Region	Expert	Country of Organisation / Nationality	Professional Background(s)	Others Consulted
Africa	Natasha Ribeiro	Mozambique	Research	Robert Ang'ila, Karatina University; Kebonyethata Dintwe, Botswana University; John Mendelsohn, Okavango Research Institute; Ronald Heath, Forestry South Africa; Helen De Klerk, Stellenbosch University
	Sally Archibald	South Africa	Research	
Asia	Bambang Saharjo	Indonesia	Research, Litigation	
	Veerachai Tanpipat	Thailand	Research, Fire Control and Management Instructor and Consultant	
Europe	Paulo Fernandes	Portugal	Research	Davide Ascoli, University of Turin, Italy; Hellenic Agricultural Organization "DIMITRA"; Institute of Mediterranean Forest Ecosystems; Niall MacLennan, Scottish Fire and Rescue Service
	Stefan Doerr	UK / Germany	Research	
	Gavriil Xanthopoulos	Greece	Research	
North America	Crystal Kolden	USA	Research, Firefighting	
	Jacquelyn Shuman	USA	Research	
	Piyush Jain	Canada	Research	
Oceania	Hamish Clarke	Australia	Research, Environmental Management	Grant Pearce, Fire and Emergency New Zealand; Simeon Telfer, South Africa Country Fire Service; Agnes Kristina, Department of Fire and Emergency Services; Russell Stephens Peacock, Queensland Fire and Emergency Services; Chris Collins, Tasmania Fire Service; David Field, NSW Rural Fire Service.
	Sarah Harris	Australia	Research, Emergency Management	
South America	Dolors Armenteras	Colombia	Research	The Chico Mendes Institute for Biodiversity Conservation (ICMBio), Brazil, Santarém Office
	Liana Anderson	Brazil	Research, Disaster risk reduction strategies	

2496  
2497

## 7.1 Africa

South Africa and Botswana experienced higher than average BA and fire size (**Figure 2, Figure 4**) in 2023-24, which some regional experts had expected following three consecutive years of above-average rainfall that increased grassy fuel loads in the fuel-limited savannas and grasslands. This has potentially been exacerbated by a lack of prescribed burning and active fire suppression in the privately held land and conservancies in the region, that likewise would have resulted in fuel build-up (*Atlas of Namibia*, 2021). The socio-economic impacts of these large fires were minimal (extensive grassland fires linked to high rain years are expected due to periodic 7-20 year wet-dry cycles in these ecosystems).

In East Africa, the area burned was extremely low in 2023-24. This was in line with the expectations of regional experts given the effects of a triple La Niña in this region, which causes droughts in East Africa (in contrast to southern Africa). This multi-year drought meant that there were limited grass fuels to burn and reduced the likelihood of spread of accidental ignitions in many of the East African rangelands. However, the extreme fire weather enabled fires to burn through upland forests, which are not normally flammable. This included a regionally significant fire in Aberdare Forest, Nyeri county, Kenya, which reportedly burned 160 km<sup>2</sup> on 17th of Feb 2023 (*Citizen Digital*, 2023).

The 2023 heatwave in North Africa exacerbated fire behaviour in the region (*Al Jazeera*, 2023a). Algeria recorded significant fires in the latter half of July, facilitated by high temperatures that reached upwards of 48°C (*Al Jazeera*, 2023b). Over 8,000 personnel, including firefighters and the military, were deployed to combat rapidly spreading fires across 15 provinces (*South African Broadcasting Corporation*, 2023a). These efforts were critical in managing fires that forced over 1,500 people from their homes (*euronews*, 2023). Despite these efforts, the wildfires claimed the lives of at least 34 individuals, including 10 soldiers (*Al Jazeera*, 2023b).

Neighbouring Tunisia also faced wildfire outbreaks, exacerbated by strong winds that carried fires across the national border from Algeria, leading to the closure of two border crossings (*Reuters*, 2023a). The Tunisian wildfires prompted evacuations in the north-western region of Tabarka, affecting at least 300 people and extending firefighting efforts to Bizerte, Siliana, and Beja (Sullivan and Tondo, *The Guardian*, 2023). Resources such as firefighting aircraft and personnel were sent from EU nations to help tackle the fires, despite the challenging conditions imposed by near-record temperatures of 49°C (Gauldie, *AirMed&Rescue*, 2024). In August, forest fires in mountainous regions of Morocco were also fanned by strong winds and facilitated by protracted hot spring and summer temperatures (Erraji, *Morocco World News*, 2023; Copernicus Climate Change Service, 2024a).

During December 2023-January 2024, the Western Cape of South Africa experienced wildfires related to prolonged hot and windy conditions, causing substantial damage and prompting widespread evacuations. In the Overstrand local municipality, which includes coastal towns like Pringle Bay and Betty's Bay, multiple fires necessitated evacuations and destroyed properties. The Hangklip area between Pringle Bay and Betty's Bay was particularly affected with the fires destroying properties in the Sea Farm private nature reserve. On January 29, a "code red" status was declared, indicating a serious threat to residential areas, and evacuations were advised for communities including Silversands and Seafarms (*Crisis24*, 2024; *AfricaNews*, 2024). A wildfire swept from Simonstown to Scarborough in Cape Town, necessitating large-scale evacuation (Hough, *IOL News*, 2023). This fire was challenging due to its rapid spread fueled by strong south-easterly winds and high temperatures. The firefighting efforts were supported by multiple helicopters and ground teams (*South African Broadcasting Corporation*, 2023a). The most extensive damage was reported from the Kluitjieskraal fire near Wolseley, where over 220 km<sup>2</sup> were burned, and more than 40 structures were destroyed. This fire also prompted evacuations and remained uncontained for

2553 several days due to its size and complex terrain that hindered ground access (*Crisis24, 2024*)  
2554 . Despite these extreme wildfires, the plantation forestry industry was not affected, with  
2555 relatively low losses due to fire.  
2556

## 2557 7.2 Asia

2558

2559 The 2023-24 fire season in Asia was generally not an extreme one, with much of central Asia  
2560 experiencing low BA. Siberia, which has seen several record-breaking fire seasons since 2020  
2561 resulting in globally significant fire emissions (Zheng et al., 2021), also experienced a  
2562 somewhat typical year for BA and fire C emissions. Likewise most provinces of China and  
2563 states of India experience a fairly typical fire season.  
2564

2565 Nonetheless, there were regional examples of high fire activity in the 2023-24 fire season. The  
2566 Dornod Aimag province of eastern Mongolia, near the borders with Russia and China,  
2567 experienced several extreme fires during April 2023 that are also visible as anomalies in the  
2568 global fire observations (**Figure 2, Figure 4**). Over 15% of the area of Dornod Aimag burned  
2569 in 2023-24 in contrast to the 23-year average of below 5%. The province includes the  
2570 Mongolian part of the Daurian steppe, notable for being one of the last remaining undisturbed  
2571 steppes in the world (UNESCO World Heritage Centre, 2017). Unusually dry and warm  
2572 conditions in eastern Mongolia during spring led to severe wildfires. A notable wildfire spread  
2573 into Dornod from neighbouring Sukhbaatar province, fanned by windy, dry conditions (*Borneo  
2574 Bulletin, 2023*). The National Emergency Management Agency mobilised over 250 individuals,  
2575 including firefighters and local residents, and helicopters were deployed to manage the fast-  
2576 spreading fires (*Borneo Bulletin, 2023*). The effects of these wildfires on herder and nomadic  
2577 populations and the Mongolian Red Cross has provided aid to 4,800 herder households  
2578 (International Federation of Red Cross and Red Crescent Societies, 2023).  
2579

2580 Although BA extent and fire counts were overall below the 2002-2023 average along the  
2581 southern border regions of Russia during 2023-24 (**Figure 2, Figure 4**), a number of disruptive  
2582 wildfires fanned by strong winds broke out during April and May and affected regions bordering  
2583 Kazakhstan, such as in the Tyumenskaya, Omskaya, and Amurskaya Oblasts, and Mongolia,  
2584 such as in Irkutsk and Krasny Yar where at least one fatality was recorded (*Le Monde, 2023*).  
2585 As well as detecting anomalies in fire size and rate of spread in these areas, the Global Fire  
2586 Atlas also identified regionally large and fast-moving wildfires in the Russia-China border zone  
2587 of Manchuria (**Figure 4**), however these were not widely reported on by media outlets or local  
2588 authorities.  
2589

2590 Lao People's Democratic Republic (PDR) experienced a notable fire season in 2023-24,  
2591 marked by record-setting BA at national level since 2002 in the MODIS BA data (**Figure 2;**  
2592 **Figure S6**). The fires were widespread, affecting various provinces from the south to the north,  
2593 including Attapu, Khammouan, Louangphabang, Xaignabouli, and Bokeo. In Attapeu, BA in  
2594 2023-24 was over twice the average of prior fire seasons since 2002. The fires in 2023-24  
2595 were generally small in scale but anomalously numerous, consistent with the widespread use  
2596 of slash-and-burn agricultural fires in these regions that have been problematic for regional air  
2597 quality in this region during recent years (Meadley, *Laotian Times, 2024*). The uptick in fire  
2598 counts in 2023-24 has been attributed in part to economic factors such as the high price of  
2599 cassava and demand for greater corn supplies to supply animal feed, which act as incentives  
2600 for farmers to clear forests for additional planting (Bhandari, *Radio Free Asia, 2024*). On top  
2601 of economic factors, a heatwave that spanned South and Southeast Asia in April 2023 was  
2602 reported to have been an enabling driver (Zachariah et al., 2023). The persistent smoke from  
2603 these fires worsened air quality significantly in southeast Asia, where efforts to manage  
2604 transboundary haze have been challenging during regional droughts, despite a new  
2605 transboundary agreement being signed in 2023 (Antara News, 2023). Differences in fire  
2606 management between Thailand and Lao PDR were evident during the 2023 event, with

2607 authorities intensifying patrols and seeking to control forest fires and agricultural burning for  
2608 improved air quality in Thailand (Meadley, *Laotian Times*, 2024). Conversely, deforestation  
2609 remains a critical issue in Lao PDR, with the Laotian government facing challenges in gaining  
2610 local community support for the prevention of agricultural expansion and logging.

2611  
2612 Earth observations data showed high-ranking BA anomalies and fires with large size and rate  
2613 of growth during 2023-24 in several regions of Pakistan, Iran, Iraq, and parts of the Levant  
2614 region (**Figure 4**), consistent with reports of extreme drought-driven wildfires in some of these  
2615 regions (*Reuters*, 2023b).

2616

### 2617 **7.3 Europe**

2618

2619 Overall, fires burned 8,400 km<sup>2</sup> in Europe from March 2023 to February 2024 according to the  
2620 European Forest Fire Information System (EFFIS, 2024), of which 64.5% were from July to  
2621 September and 18.1% were in March and April. Large fires (>5 km<sup>2</sup>) amounted to 53.4% of  
2622 the total BA, and those particularly large (>100 km<sup>2</sup>, n=5) accounted for 17.7% of the total  
2623 burned area. More than half (52.6%) of the BA corresponded to transitional woodland, with  
2624 forests, shrublands and grasslands, and agriculture respectively amounting to 19.1%, 13.2%,  
2625 and 14.4%. At least 44 people died as a direct result of wildfires (Copernicus Climate Change  
2626 Service, 2024; Centre for Research on the Epidemiology of Disasters, 2024).

2627

2628 Most countries in the Mediterranean Basin experienced mild to typical fire seasons in general,  
2629 with variable timing but affecting mostly non-forest (open) vegetation types (EFFIS, 2024). In  
2630 the Balkans, fire activity varied among countries, but was mostly very low by historical patterns  
2631 such as in Croatia, however, a major exception was Greece described in more detail below  
2632 (**Figure 2, Figure 4, Figure A1**). The other exceptions were North Macedonia, with a typical  
2633 fire year and Bulgaria, the worst year in a decade, with fire activity extending into October in  
2634 both countries; and Bosnia and Herzegovina, Serbia and Montenegro, where collectively ~270  
2635 km<sup>2</sup> burned in January-February 2024.

2636

2637 Greece's 2023 fire season was reviewed at length by Xanthopoulos et al. (2024). It was the  
2638 second worst on record regarding total area burned (1,727 km<sup>2</sup>), despite the recent efforts to  
2639 strengthen the firefighting mechanism of the country with more aerial resources and new  
2640 personnel, after another challenging fire season in 2021. The situation was kept under control  
2641 until mid-July, but in the period July 13-27, maximum temperature in many parts of the country  
2642 exceeded the average for the 2010-2019 period by as much as 10°C, according to the records  
2643 of the National Observatory of Athens. This resulted in multiple fire starts pushing the limits of  
2644 firefighting, which relies heavily on the aerial resources. The fires starting 18th of July on the  
2645 tourist island of Rhodes grew rapidly on the second day, finally burning 207 km<sup>2</sup> and stopping  
2646 at the sea. About 20,000 tourists had to be evacuated from hotels along the coast. While the  
2647 fire on Rhodes was still burning, three forest fires started on 3rd of July started near the city  
2648 of Aigio, in North Peloponnese, on the island of Corfu and near the town of Karystos in the  
2649 south of Evia island. On July 25th a Canadair CL-215 crashed near the village of Platanistos  
2650 while fighting this last fire. Then, on July 26th, the tail of a cold front that passed over Greece,  
2651 with the characteristic wind direction change that accompanies it, created further challenges,  
2652 as a number of fire starts in central Greece and Thessaly spread fast, burning mostly in light  
2653 fuels, challenged firefighters and threatened inhabited areas. The fast-spreading fire in  
2654 Thessaly entered an Air Force base and caused a powerful explosion resulting in damage to  
2655 the nearby town of Nea Aghialos. By the end of July, the BA across the country had reached  
2656 550 km<sup>2</sup>.

2657

2658 The next wave of multiple challenging fires in Greece began on 19th August. A lightning-  
2659 caused fire that started before dawn NE of Alexandroupolis in the prefecture of Evros received  
2660 limited attention at first and was destined to become the largest fire in recent European history.

2661 The fact that firefighting resources were focussed on evacuation of the villages in the path of  
2662 the fire, rather than fire suppression may have contributed to its eventual size. On the 21st of  
2663 August, a second fire started to the north of the first one, near the village of Dadia. Fanned by  
2664 a strong NE wind, it spread quickly and within a few hours it reached the rear of the first one.  
2665 On that day fire behaviour both in terms of spread and intensity was extreme (Athanasίου,  
2666 2024). Nineteen migrants were trapped by the flames and were found dead on the 22nd of  
2667 August. Another group was saved by the firefighters at the last moment. The authorities  
2668 emphasised safety and evacuated the hospital in the outskirts of Alexandroupolis.  
2669

2670 On Aug. 22, while the Evros fire was the focus of attention, a fire originating at more than one  
2671 point near the village of Phyli, south of mount Parnis in Attica, at the outskirts of Athens started  
2672 growing against the strong NE wind. Once more, many settlements were evacuated and  
2673 firefighting attention focused on protecting homes, as the fire moved slowly up the mountain  
2674 slopes finally burning 62 km<sup>2</sup> in three days. The Evros fire kept growing at various rates for  
2675 the next 15 days, finally reaching 938 km<sup>2</sup> and becoming the largest on record in recent history  
2676 in Europe. The simultaneous spread of the Evros fire, the fire in Attica and a number of smaller  
2677 fires, is likely to have increased the growth rate statistics (km day<sup>-1</sup>) for fires in the region  
2678 (**Figure 4** and **Figure A1**).  
2679

2680 The BA of the Evros fire included 258 km<sup>2</sup> of deciduous oak forest and 218 km<sup>2</sup> of oak forest  
2681 mixed with other species (Konstantinos Kaoukis, personal communication). The usually most  
2682 challenging forest types regarding fire behaviour, contributed less to burned area: 128 km<sup>2</sup>  
2683 forest and 152 km<sup>2</sup> of evergreen shrubs. The fire was mostly brought into control only when it  
2684 reached agricultural areas and barren lands. The final size of the Evros fire may not be solely  
2685 attributed to adverse meteorological conditions. One aggregating factor may have been the  
2686 recent shift in directing firefighting personnel more strongly from suppression towards  
2687 evacuation, another the emphasis on aerial firefighting resources (Xanthopoulos et al., 2024).  
2688 The latter was not effective once the extreme fire behaviour commenced (21st to 23rd of  
2689 August). Deep forest litter layers further hampered fire suppression in some areas, although  
2690 a group of local forest workers working with handtools, were credited by the local forest service  
2691 officers with control of a large part of the fire perimeter to the north, saving an estimated 100  
2692 ha of forest (Athanasίου, 2024).  
2693

2694 Italy was the second most affected country after Greece, with continuous fire activity from July  
2695 to October. More than 1,000 km<sup>2</sup> burned in the country, of which 69% were in Sicily (including  
2696 17 fires >10 km<sup>2</sup>), although the largest fire (31 km<sup>2</sup>) occurred in the nearby region of Calabria  
2697 (Istituto Superiore per la Protezione e la Ricerca Ambientale, 2023). A defining characteristic  
2698 of these large fires was the importance (42% overall) of agricultural land in the BA composition.  
2699 The outskirts of Palermo and the Madonie Natural Regional Park were impacted by multiple  
2700 wildfires in late September, causing one fatality and affecting wildland-urban interfaces, farms,  
2701 and tourism.  
2702

2703 Fire activity was insignificant in France, except for benign mountain burning (175 km<sup>2</sup>) in  
2704 March-April and then in January-February, mostly in the western Pyrenees. Like in France,  
2705 the north of Spain (Asturias-Cantabria) experienced unusual Spring burning activity,  
2706 amounting to 423 km<sup>2</sup> during late March and early April (Educación Forestal, 2023a). In  
2707 particular, the Foyedo wildfire (27th March 2023) was the largest on record for Asturias,  
2708 burning 101 km<sup>2</sup> across variable vegetation but with the predominance of conifer plantations,  
2709 mostly *Pinus pinaster*. It was a wind- and spot-driven fire but its soil and overstorey burn  
2710 severity were respectively low and mostly moderate, as slower-drying fuels were not available  
2711 to burn (Cátedra Cambio Climático de la Universidad de Oviedo, 2023).  
2712

2713 Only two other notable large wildfires occurred in 2023 in continental Spain, and again were  
2714 unusual in that they happened in spring rather than summer. The Villanueva de Viver wildfire  
2715 (23rd March 2023, Castellón and Teruel) burned around 50 km<sup>2</sup> and was driven by abnormal

2716 seasonally dry conditions, combined with a shift in wind direction. It mostly burned naturally-  
2717 regenerated continuous pine forest of *Pinus halepensis*. Canopy fire severity was  
2718 heterogeneous, with 39% of the wildfire area being classified as high to very high severity  
2719 (Mediterranean Center for Environmental Studies, 2023). The cost of fire suppression was  
2720 2M€ and 1,800 people were evacuated (*Las Provincias*, 2023).

2721  
2722 At over 100 km<sup>2</sup>, the Pinofranqueado wildfire (17th May 2023, Cáceres) was the largest fire in  
2723 the Iberian Peninsula in 2023 (Copernicus Emergency Management Service, 2023b). The BA  
2724 was 90% forest, mostly pine (*Pinus pinaster*, *Juntaex.es*, 2023). It was a wind-driven fire and  
2725 the Canadian FWI indexes indicate all fine fuel was available to burn and extreme fire  
2726 behaviour (FWI>50). The fire significantly impacted the nesting of protected bird species and  
2727 rainfall shortly after the wildfire caused important runoff, erosion, and disruption of water  
2728 supply to the local population (Armero, *Hoy*, 2023).

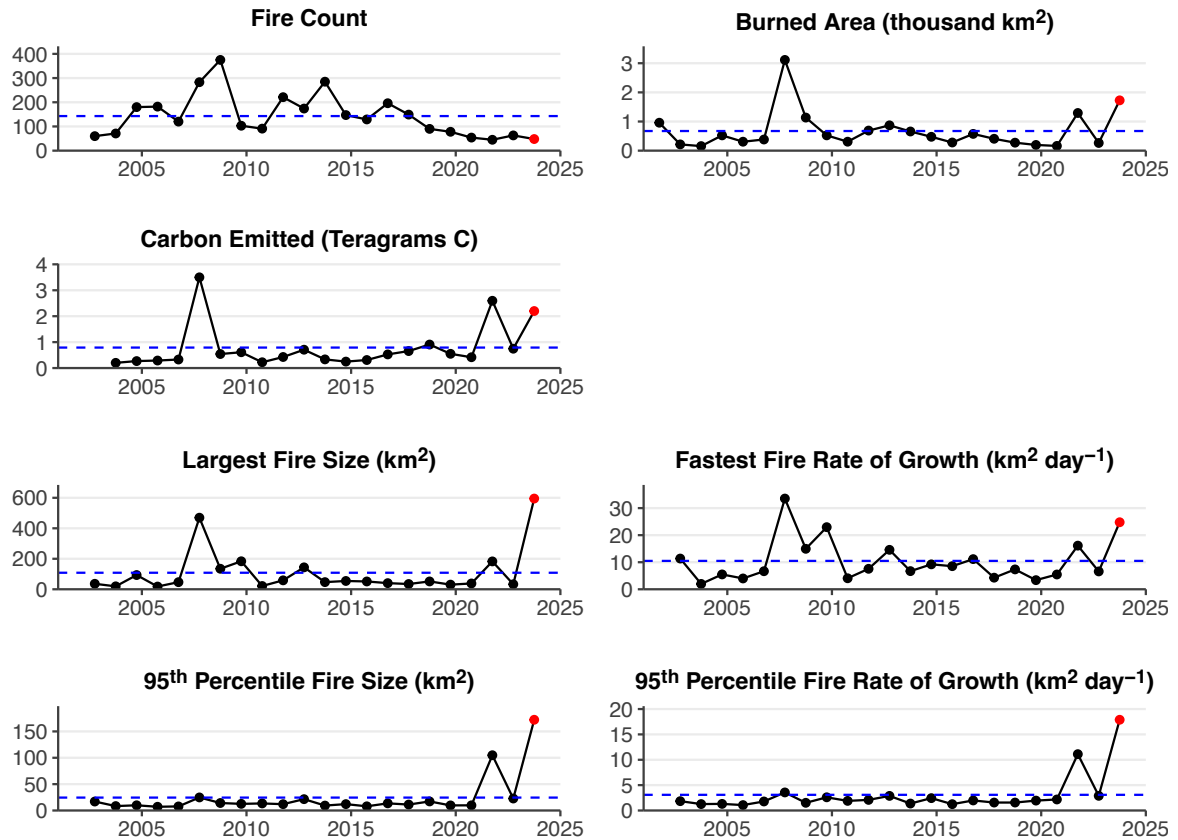
2729  
2730 The two other significant fires in Spain happened in the Canary Islands, the Puntagorda  
2731 wildfire (14th July 2023, La Palma, 32 km<sup>2</sup>) and the Arafo-Candelaria wildfire (15th August  
2732 2023, Tenerife, 123 km<sup>2</sup>; Copernicus Emergency Management Service, 2023c). The latter  
2733 spread for 9 days and 94% of its area was forest under conservation status, mostly of Canary  
2734 pine (*Pinus canariensis*). The fire was exacerbated by local topography and mostly low to  
2735 moderate severity (Educación Forestal, 2023b). Nonetheless, 26,000 people were evacuated,  
2736 364 farms and 246 buildings (none residential) were affected, smoke impacts were substantial  
2737 and damage was estimated at 80.4M€.

2738  
2739 Like in Spain, winter shrubland burning was relevant in continental Portugal (~50 km<sup>2</sup> in  
2740 February) but subsequent significant wildfire activity was restricted to two fires. The Sarzedas  
2741 (66 km<sup>2</sup> ha) and Baiona (75 km<sup>2</sup>) wildfires started on the 5th of August under extreme fire  
2742 weather (FWI>50), and burned mostly (~70%) forest, respectively of pine (*P. pinaster*) and  
2743 eucalypt (*Eucalyptus globulus*) stands (Direção Nacional de Gestão do Programa de Fogos  
2744 Rurais, 2023). Prevailing burn severity was moderate and damage to infrastructure and  
2745 emergency restoration amounted to 6.4 M€ cost for the Sarzedas fire and a forest value loss  
2746 of 1.4 M€ (Instituto da Conservação da Natureza e das Florestas, 2023). The major run of the  
2747 Baiona wildfire was on August 7, corresponding to 73% of the total BA, when it threatened  
2748 wildland-urban interfaces and damaged several buildings; one camping park and 20 small  
2749 villages were evacuated (*Economia Online*, 2023). Moderate to high burn severity classes  
2750 were dominant and costs were estimated at 2.7 M€ (tourism) and 7 M€ (houses), plus 1.4 M€  
2751 in forest values loss and 2.9 M€ for emergency stabilisation (*Rádio e Televisão de Portugal*,  
2752 2023; SIC Notícias, 2023). Finally, on 12th October, and under anomalously extreme fire  
2753 weather for the time of the year, the Ponta do Pargo wildfire burned 48 km<sup>2</sup> in Madeira island,  
2754 with an estimated agriculture-related cost of 3 M€ (*Rádio e Televisão de Portugal*, 2023).

2755  
2756 The year was also mild in other European countries where burned areas can be extensive,  
2757 namely Romania, Hungary, and Poland, which collectively summed only ~210 km<sup>2</sup> burned.  
2758 EFFIS recorded 2461 km<sup>2</sup> burned in Ukraine, the largest fire attaining 42 km<sup>2</sup>, but these figures  
2759 are far from those registered in recent years. In northern Europe, a notable fire occurred in  
2760 Scotland near Cannich, during the spring, the primary fire season in the humid Atlantic climate  
2761 of the UK (Belcher et al., 2021). It started on 19th of April and burned ~33 km<sup>2</sup> of mainly  
2762 moorland making it one of the largest fires in the UK in recent history (Sabljak, *The Herald*,  
2763 2023; personal communication Niall MacLennan, Scottish Fire and Rescue Service).

2764  
2765





2766  
2767  
2768  
2769  
2770  
2771  
2772

**Figure A1:** Summary of the 2023-2024 fire season in Greece. Time series of annual fire count, BA, C emissions, PM2.5 emissions, 95th percentile fire size, fastest daily rate of growth, and 95th percentile fire daily rate of growth. Black dots show annual values prior to the latest fire season, red dots the values during the latest fire season, and blue dashed lines the average values across all fire seasons.

2773  
2774

## 7.4 North America

2775  
2776  
2777  
2778  
2779  
2780  
2781  
2782  
2783  
2784

Wildfire across North America in 2023-2024 was characterised by record fire activity across Canada, lower than normal BA in the most flammable regions of the western US, near-average fire activity across Mexico, and several extreme events that resulted in disastrous impacts to human communities (Kolden et al., 2024). Over 150,000 km<sup>2</sup> burned in Canada in 2023 according to national statistics, over twice the previous record and over seven times the annual average (Jain et al. 2024). The US burned 10,900 km<sup>2</sup> in 2023, well below the long-term annual average (National Interagency Fire Center [NIFC], 2024a). Mexico has a relatively short national wildfire recording system, but March 2023-February 2024 saw among the highest area burned in the last decade (10,000 km<sup>2</sup>) and this has been associated with ongoing drought conditions (Comisión Nacional Forestal, 2024).

2785  
2786  
2787  
2788  
2789  
2790  
2791  
2792  
2793  
2794

The fire season began earlier than normal in Canada, which regional experts have linked to early snowmelt across much of the country and persistent drought conditions in the west. Abnormally high temperatures and lack of rainfall also saw forested regions of eastern Canada, including Quebec, transition rapidly to drought conditions at the end of May. British Columbia province recorded its first wildfire evacuation in mid-April, and in late May, over 16,000 people were evacuated from Halifax, the capital city of Nova Scotia, which saw its largest ever wildfire in 2023 (Jain et al. 2024). In June, two lightning outbreaks in Quebec initiated several hundred new fires in what would eventually become a record BA year for the province (4,300 km<sup>2</sup>) (Boulanger et al., 2024). While the majority of the Quebec fires were in

2795 remote regions, the smoke they generated was carried to several major cities in eastern North  
2796 America, including New York which experienced its worst air quality in half a century as the  
2797 observed daily mean PM<sub>2.5</sub> concentration rose to 148.3 µg m<sup>-3</sup>, over 4 times the recommended  
2798 daily limit (Wang et al. 2023). In total over 50 million people were exposed to high levels of  
2799 PM<sub>2.5</sub> for several days (Yu et al. 2024). This situation was further exacerbated in New York  
2800 City by several wildfires in the nearby New Jersey pine barrens, a fire-prone dry pine forest  
2801 that sees large fires during periods of drought.

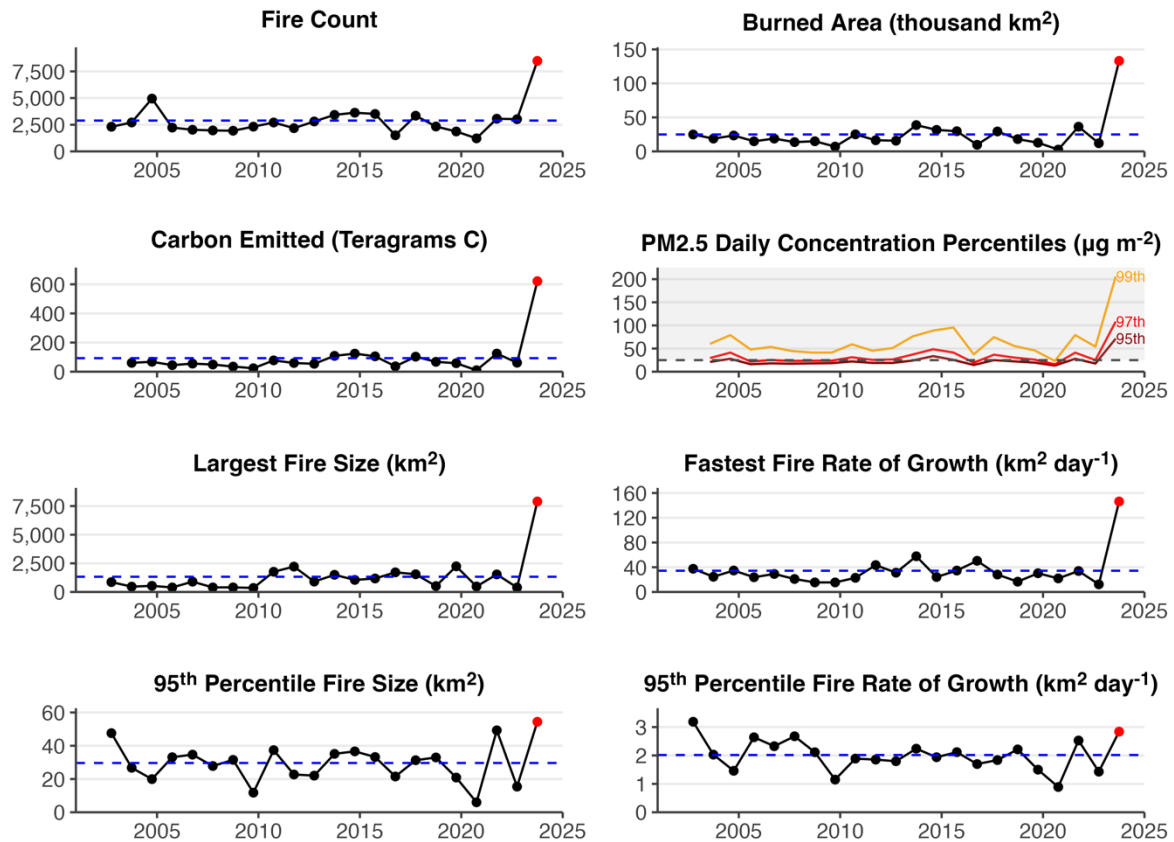
2802  
2803 The year started with low fire activity across the USA. In the high plains of the central US, an  
2804 outbreak of large wildfires occurred coincident with dry conditions and strong winds in March-  
2805 April 2023. One wind-driven wildfire started by power lines in Oklahoma destroyed several  
2806 dozen homes (Oklahoma Department of Emergency Management, 2023). Outside of the high  
2807 plains, dry conditions also elevated fire activity across the Southern, Eastern, and New  
2808 England regions of the USA. Mexico saw slightly above average fire activity during spring,  
2809 which is the peak period of the fire season as debris burning and field clearing activities provide  
2810 ignitions for predominantly shrubland and grassland wildfires.

2811  
2812 As summer arrived in Canada, the western and boreal provinces and territories saw extreme  
2813 and widespread fire activity, even as Quebec continued to burn. By the end of the year, record  
2814 area had burned in British Columbia (2,300 km<sup>2</sup>), Alberta (2,700 km<sup>2</sup>), and the Northwest  
2815 Territories (3,500 km<sup>2</sup>) accompanied evacuations of 232,000 people in numerous rural villages  
2816 and large cities such as Yellowknife, NT and Kelowna/West Kelowna, BC, where a wildfire  
2817 jumped the 2 km-wide Okanagan Lake (Jain et al., 2024; *CBC News*, 2023). The extreme  
2818 behaviour of these fires not only shrouded large swaths of North America in smoke, but also  
2819 generated an unprecedented 140 pyrocumulonimbus clouds (Jain et al. 2024). Eight  
2820 firefighters were killed during summer 2023 in Canada (Jain et al. 2024), but miraculously no  
2821 civilians died directly in the fires. Canada was at the highest National Preparedness Level 5  
2822 for an unprecedented 120 continuous days starting on May 11, indicative of the significant  
2823 resource sharing required by fire management; in all, over 5500 international personnel from  
2824 12 countries and the EU were deployed to Canada during the 2023 fire season (Canadian  
2825 Interagency Forest Fire Centre, 2023).

2826  
2827 In the US, a relatively low activity fire season became deadly in August owing to unusual  
2828 weather conditions facilitating extreme fire behaviour in multiple areas around the country. On  
2829 8<sup>th</sup> August, a pressure gradient-induced katabatic wind event fanned several small wildfires in  
2830 Hawaii, and 101 civilians died as the town of Lahaina on the island of Maui was consumed in  
2831 the worst wildfire disaster in the US in a century (Pyne, 2017). Over 2,000 homes were  
2832 destroyed and over 10,000 people were displaced as a result. Fires with extreme behaviour  
2833 killed five additional civilians in the US states of Washington (2 fatalities), Louisiana (2  
2834 fatalities) and California (C. Kolden, unpublished data). These extreme events stood in  
2835 contrast to overall low fire activity and were notable for where they occurred. Washington does  
2836 not typically see many extreme, wind-driven wildfires, and Louisiana is one of the wettest  
2837 states in the US. By the end of August, the US BA was only 40 percent of normal and the  
2838 lowest since at least 2000 (NIFC, 2023; National Oceanic and Atmospheric Administration  
2839 [NOAA], 2023).

2840  
2841 As North America transitioned to fall and then winter, Canada continued to burn nearly a month  
2842 longer than normal, with the last large fires not controlled until late October. On 22<sup>nd</sup>  
2843 September, remarkably late in the fire season, Canada saw its largest ever one-day total for  
2844 BA at approximately 4,400 km<sup>2</sup> (Jain et al., 2024). While many of the Canadian fires were fully  
2845 extinguished by winter, others simply smouldered into the deep peat layers, aided by a  
2846 warmer-than-normal winter with a reduced snowpack. At the end of February 2024,  
2847 spaceborne thermal sensors detected several dozen fires in northern Alberta and British

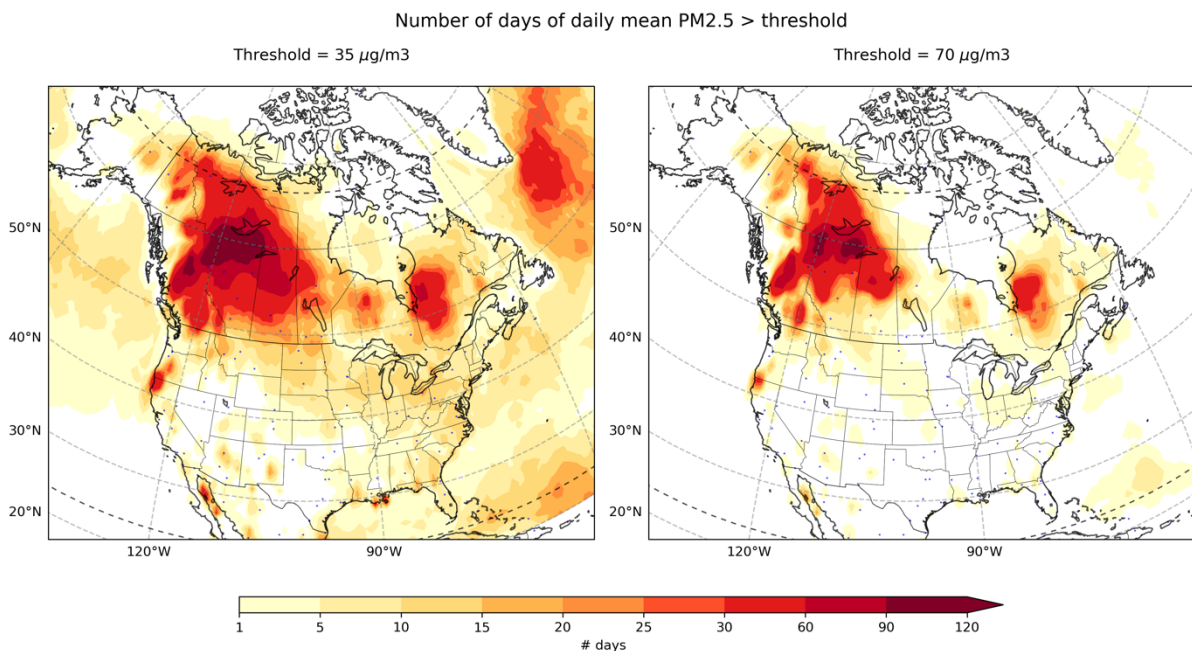
2848 Columbia that were overwintering fires, likely sustained by peat smouldering (Shingler, *CBC*  
 2849 *News*, 2024; Scholten et al., 2021).  
 2850



2851  
 2852 **Figure A2:** Summary of the 2023-2024 fire season in Canada. Time series of annual fire  
 2853 count, BA, C emissions, PM2.5 daily concentration percentiles (95th, 97th, and 99th), 95th  
 2854 percentile fire size, fastest daily rate of growth, and 95th percentile fire daily rate of growth.  
 2855 Black dots show annual values prior to the latest fire season, red dots the values during the  
 2856 latest fire season, and blue dashed lines the average values across all fire seasons. The  
 2857 PM2.5 daily concentration percentiles are based on area-weighted daily mean surface PM2.5  
 2858 concentrations within each year across Canada from the CAMS atmospheric reanalysis  
 2859 (Inness et al., 2019). The grey zone marks concentrations exceeding reference levels for 24-  
 2860 hour mean PM2.5 concentration in Canada (25 µg m<sup>-3</sup>) Canadian Environmental Protection  
 2861 Act Federal-Provincial Working Group on Air Quality, 1998).  
 2862  
 2863  
 2864

2865 US fire agencies recorded just over 10,900 km<sup>2</sup> burned in 2023, just over half of the 20-year  
 2866 mean of 29,000 km<sup>2</sup> (NIFC, 2024a). Notably, over half of the BA was associated with higher  
 2867 fire activity in the central plains grasslands and the southeastern US, while below normal fire  
 2868 activity characterised California and the western US throughout 2023 as the region exited a  
 2869 multi-year drought. However, the number of fires recorded was only slightly lower than  
 2870 average. This quiet pattern broke in February 2024, however, when drought conditions from  
 2871 the high plains region of the US down into north central Mexico coupled with strong winds to  
 2872 produce massive, fast moving wildfires across multiple states on both sides of the US-Mexico  
 2873 border. The US state of Texas recorded its largest ever single fire at over 4,000 km<sup>2</sup>  
 2874 (Smokehouse Creek fire) in late February and early March that destroyed 130 homes across  
 2875 the high plains region of the central US (NIFC, 2024b). Two civilians were killed by the flames

2876 in the relatively rural area dominated by ranching, over 10,000 head of cattle died, and  
2877 damages are estimated to be at least \$4.6 million (NOAA, 2024).  
2878  
2879



2880  
2881 **Figure A3:** Impact of Canadian wildfires visible in air quality metrics for North America. Panels  
2882 show the number of days in 2023 with mean PM2.5 concentration over a threshold of (**left**  
2883 **panel**) 35  $\mu\text{g m}^{-3}$  and (**right panel**) 70  $\mu\text{g m}^{-3}$ . Both the National Ambient Air Quality Standards  
2884 (NAAQS) in the USA and the Canadian Ambient Air Quality Standards (CAAQS) have  
2885 exposure targets of 35  $\mu\text{g}/\text{m}^3$  on average within a single day.

2886

2887 The impact of North American fires on air quality is significant with half of the PM2.5 in America  
2888 suggested to originate from fires (O'Dell et al. 2019). An exceptional fire season, such as seen  
2889 in Canada in 2023, therefore poses an elevated level of health risk. Canada's wildfires  
2890 produced levels of PM2.5 across the country that were well in excess of the last 20 years  
2891 (**Figure A2**). Additionally, long-range transport of pollution from Canada affected the Pacific  
2892 Northwest, northern Midwest, and many eastern states (**Figure A3**). According to the National  
2893 Ambient Air Quality Standards (NAAQS) in the USA, the threshold for PM2.5 exposure is not  
2894 to exceed 35  $\mu\text{g}/\text{m}^3$  on average within a single day. CAMS analysis suggests that people living  
2895 within over half of US states experienced up to 2 weeks of exposure at or above this level. In  
2896 Canada, the safe limit for PM2.5 exposure, as defined by the Canadian Ambient Air Quality  
2897 Standards (CAAQS), is also 35  $\mu\text{g}/\text{m}^3$  over a 24-hour period. However, the situation was worse  
2898 in Canada due to closer proximity to fires, with many territories along the border experiencing  
2899 up to a month of degraded air quality that exceeded national recommended exposure limits,  
2900 British Columbia possibly facing twice the number of days at up to 2 months, and the Northern  
2901 Territories potentially with 3 to 4 months of exposure.

2902 The scale of the impact becomes particularly evident when comparing the number of days at  
2903 double the exceedance level (70  $\mu\text{g}/\text{m}^3$ ) due to short-range versus long-range transport of  
2904 pollutants. In Canada, where the pollution sources were more localised, the number of days  
2905 above this higher level remains substantial, ranging from a week along the border to months  
2906 still at the fire epicentres. In contrast, the USA, affected primarily by long-range transport from  
2907 Canada, experienced approximately half the number of such high-pollution days. It is also  
2908 important to consider the context of interannual variability in fire occurrence. Last year the

2909 USA experienced its lowest number of fires in 2 decades (**Figure 4**), so most of the pollution  
2910 impacts came from Canada.

## 2911 7.5 Oceania

2912  
2913 As is commonly the case, there was a marked latitudinal difference in wildfire patterns in  
2914 Oceania in 2023-24. Fire activity was above average in the savannahs, grasslands and  
2915 shrublands of tropical, subtropical and arid northern Australia. In contrast, fire activity in the  
2916 southern states of Australia was generally below average, and well below the levels seen  
2917 during the high impacting 'Black Summer' fires of 2019-20. In New Zealand and the Pacific  
2918 Islands, fire activity was relatively low compared to the preceding two decades.

2919  
2920 Given the vast scale of savannah fires, 2023-24 ranked among the top five years in BA for  
2921 Australia as a whole since 2002 (Fisher, 2024; **Figure 2**). Fire in tropical and arid areas is  
2922 tightly linked to rainfall in the preceding season (Alvarado et al., 2020). The above average  
2923 fire seasons in the Northern Territory and northern Western Australia were driven to a large  
2924 extent by elevated fuel growth associated with the La Nina conditions of the previous three  
2925 years. These fires represented the vast majority of areas burned across the country in 2023-  
2926 24 (**Figure S7**).

2927  
2928 In the monsoonal north, savannah fires follow a strong seasonal pattern, with regular summer  
2929 rain predictably followed by fire in the dry winter and spring months. In arid regions further  
2930 south, fire remains tightly coupled to rain, but the seasonality is less pronounced. Anomalously  
2931 large fires began as early as May and June in Western Australia and the Northern Territory  
2932 respectively, continuing to as late as January.

2933  
2934 The year was also marked by a series of early season, high impact fires in populated areas of  
2935 southwestern Western Australia, southeast Queensland, NSW, Victoria and Tasmania. Hot,  
2936 dry, windy conditions, and extended dry periods, are a major driver of forest, woodland and  
2937 shrubland fires of the subtropical and temperate south of Australia (Collins et al., 2022). In  
2938 addition to 2023 being the eighth-warmest year on record, the three months from August to  
2939 October were the driest in over 100 years of records (Bureau of Meteorology, 2024).

2940  
2941 From October to January a string of fire events led to loss of life, property and a range of other  
2942 human and environmental impacts throughout the country's southeast and southwest. In some  
2943 cases, significant fire activity was observed in areas impacted by the 2019-20 fire season.  
2944 Despite these impacts, average rain in southern and eastern parts of Australia tempered fire  
2945 activity for the austral summer. In Queensland and NSW, large fires in remote areas pushed  
2946 the total BA in line with the long term mean, but this figure was well below average in Victoria,  
2947 the Australian Capital Territory and Tasmania.

2948  
2949 In the southwest of Australia, a volunteer firefighter was killed while responding to a fire near  
2950 Esperance. The Kings Park fire in October occurred in a popular tourist area containing  
2951 vulnerable flora and threatened Perth Children's Hospital. Perth was again affected by fires in  
2952 December, with several injured and five homes lost. A further two homes were lost in the  
2953 region in mid-January from fires that burned 60 km<sup>2</sup>. A similar sized fire burned through rugged  
2954 terrain in the Gammon Ranges 600 km north of Adelaide, threatening highly significant cultural  
2955 and ecological values.

2956  
2957 A large number of significant fires affected the eastern States of Australia in October. The  
2958 Tara and Mount Isa fires in Queensland burned well over 400 km<sup>2</sup> combined, destroying 65  
2959 homes and claiming the lives of two people. International and interstate support were deployed  
2960 from New Zealand and Victoria to respond to the fires. Further south in New South Wales,  
2961 significant fires included the Coolagolite Rd fire in Bega (over 70 km<sup>2</sup>, 2 houses destroyed),  
2962 the Willi Willi Rd fire in Kempsey (over 290 km<sup>2</sup>, 8 houses destroyed, one person killed) and

2963 large fires around Tenterfield (approximately 300 km<sup>2</sup>, four homes destroyed). In November  
2964 the Hudson Fire burned 228 km<sup>2</sup>, destroyed 4 properties and led to the death of a volunteer  
2965 fire fighter, who was killed by a falling tree while fighting the fire. In December the Duck Creek  
2966 Pilliga Forest fire burned 1,385 km<sup>2</sup> and initiated 3 documented fire-generated thunderstorms,  
2967 with smoke impacts extending 500 km away and reaching Sydney.  
2968

2969 In neighbouring Victoria the fire season was bookended by high impact events in October and  
2970 then in February and March. Fires in Gippsland during October totalled 120 km<sup>2</sup> and exhibited  
2971 some overnight fire runs that were regarded as unusual (Mills et al., 2022). An extended dry  
2972 period saw fires impacting towns in central and western parts of the state in late February and  
2973 early March. Over 40 homes were lost and five firefighters were injured fighting two fires that  
2974 originated in the Grampians National Park and burned 60 km<sup>2</sup>. Interactions with the  
2975 atmosphere and topography were suggested to explain extreme behaviour that was reported.  
2976 This fire was followed by another near Ballarat affecting grass, forest and a pine plantation.  
2977 Despite several extreme fire weather days and evacuation advice, a significant suppression  
2978 effort aided by interstate deployments minimised impacts. The fire burned over 200 km<sup>2</sup>.  
2979

2980 In the island state of Tasmania the fire season began early with the Coles Bay Bushfire burning  
2981 27 km<sup>2</sup> of both private land and national park in September and then fires on Flinders Island  
2982 in October. Other impactful fires that occurred during the season include the Dolphin Sands  
2983 fire on the east coast of Tasmania that destroyed two homes and burned 2.5 km<sup>2</sup> and the  
2984 multiple fires in the Brady lake area (Tasmania's central highlands) in February that destroyed  
2985 two homes and burned up to 100 km<sup>2</sup> and a fire in the Waterhouse Conservation areas that  
2986 required campers to evacuate.  
2987

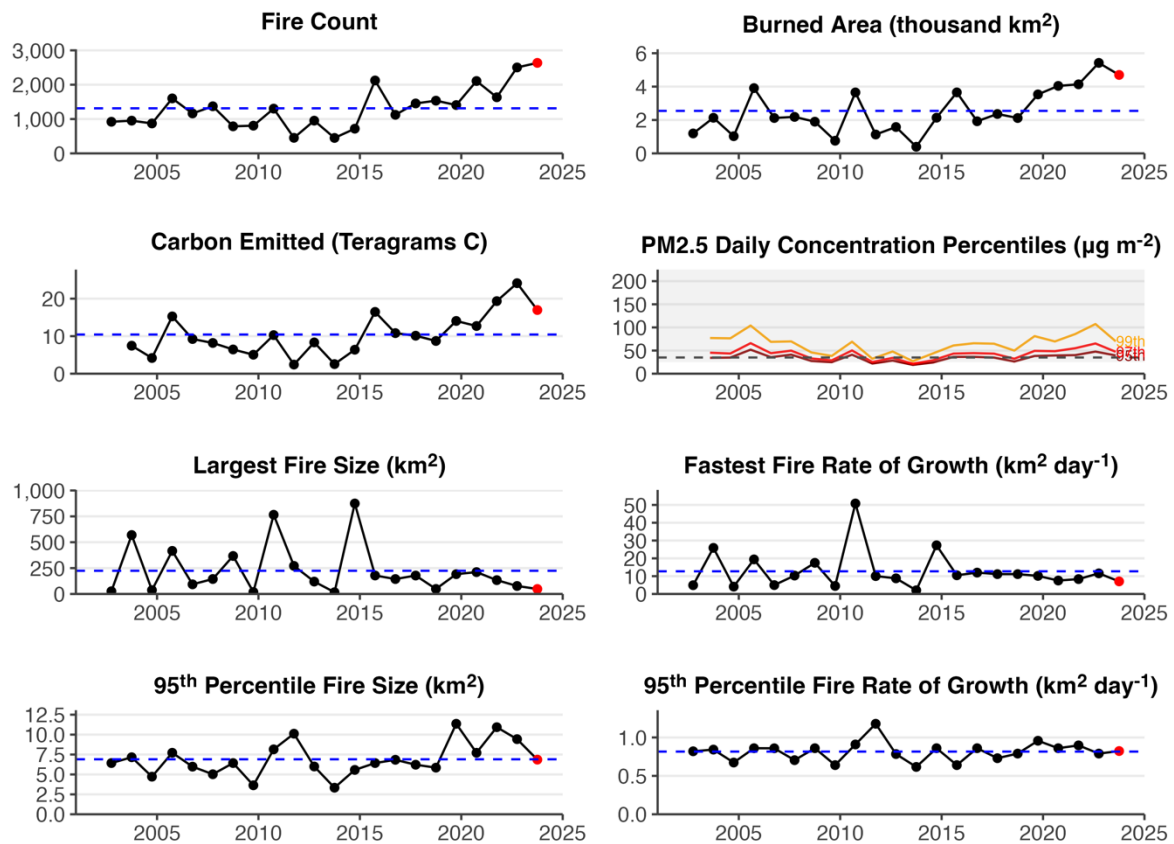
2988 New Zealand experienced a normal fire season after three well below average seasons prior  
2989 under La Nina conditions. The fire season began early with a relatively large fire in September  
2990 on the western side of Lake Pukaki in the central South Island in wilding pines. This fire totalled  
2991 29 km<sup>2</sup> and this was the third major wildfire event in recent years in this area at an earlier than  
2992 normal stage of the fire season, following the 2020 Pukaki (Aug.) and Ohau (Oct.) fires. New  
2993 Zealand then experienced a spate of fires around Canterbury, on the South Island between  
2994 late January and mid February 2024 with several houses burned and farmlands affected.  
2995

## 2996 7.6 South America

2997  
2998 The 2023-24 fire season in South America was characterised by a moderately below average  
2999 fire activity but with positive wildfire anomalies in specific regions, which were reportedly  
3000 exacerbated by extended periods of drought and heatwave across the continent (Clarke et al.,  
3001 2024; **Figure 2**, **Figure 3**, **Figure 4**). In the Brazilian State of Amazonas, which features the  
3002 largest extent of preserved old growth forests in Amazonia, June and October 2023 saw the  
3003 highest fire counts since records began in 1998 (National Institute for Space Research, 2024;  
3004 see also **Figure A4**). This continues a recent trend towards record-setting months for fire in  
3005 Amazonas state, with new maxima being set in 7 months of the year since 2019 (National  
3006 Institute for Space Research, 2024). Recent changes in deforestation and land use patterns  
3007 are contributing to elevated fire ignitions in the state, reportedly compounded in 2023 by a  
3008 historic drought and heatwave driven by El Niño (Espinoza et al., 2024, Clarke et al., 2024).  
3009 Due to emissions of wildfire smoke, many areas of Amazonas experienced poor air quality  
3010 from September to December 2023, including in the state capital, Manaus, where over 2  
3011 million people were exposed to the second-worst air quality in the world in October (Ministério  
3012 Público Federal, 2023). The event was so severe that, in November 2023, the Federal Public  
3013 Ministry opened a Civil Action case against the State of Amazonas, demanding evidence that  
3014 the State was investing in fire prevention and combat in line with the Plan for the Prevention  
3015 and Control of Deforestation and Fires (Estado do Amazonas, 2020). This procedure  
3016 evaluates whether Amazonas authorities are accountable for environmental damage causing



3017 severe air pollution, reflecting the Public Ministry's growing involvement at both federal and  
 3018 state levels in monitoring environmental degradation and seeking to make authority figures  
 3019 accountable (Ministério Público Federal, 2023).  
 3020  
 3021



3022  
 3023 **Figure A4:** Summary of the 2023-2024 fire season in the Brazilian state of Amazonas. Time  
 3024 series of annual fire count, BA, C emissions, PM2.5 emissions, 95th percentile fire size, fastest  
 3025 daily rate of growth, and 95th percentile fire daily rate of growth. Black dots show annual  
 3026 values prior to the latest fire season, red dots the values during the latest fire season, and blue  
 3027 dashed lines the average values across all fire seasons. The PM2.5 daily concentration  
 3028 percentiles are based on area-weighted daily mean surface PM2.5 concentrations within each  
 3029 year across Amazonas from the CAMS atmospheric reanalysis (Inness et al., 2019). The grey  
 3030 zone marks concentrations exceeding the reference level for 24-hour mean PM2.5  
 3031 concentration in Brazil's National Air Quality Guidelines ( $25 \mu\text{g}/\text{m}^3$ ; Siciliano et al., 2020).  
 3032  
 3033

3034 National fire monitoring systems in Brazil indicate that some areas of Amazonia experienced  
 3035 anomalies in BA at the sub-state level. For example, BA in the municipality of Santarém in the  
 3036 State of Pará rose from an average of  $70 \text{ km}^2$  in 2019 to 2022 to over  $1,000 \text{ km}^2$  in 2023, and  
 3037 has already exceeded  $250 \text{ km}^2$  in 2024 (MapBiomass Brasil, 2024). Similarly, in neighbouring  
 3038 Belterra municipality, BA extent was more than 3 times greater during the year 2023 than in  
 3039 2019-2022 (MapBiomass Brasil, 2024). In Floresta Nacional do Tapajós, one of the most  
 3040 studied forest sites in the Amazon which spans Satarém and Belterra, forest fires accounted  
 3041 for more than 60% of the burned areas (MapBiomass Brasil, 2024). 4 thousand people live in  
 3042 24 communities of traditional and Indigenous populations in the region and depend on  
 3043 protected forest resources for their cultural heritage, food security, economy and livelihood in  
 3044 Floresta Nacional do Tapajós and Reserva Extrativista Tapajós-Arapiuns (Instituto Chico  
 3045 Mendes de Conservação da Biodiversidade, 2019). Fires in 2023 compounded the challenges

3046 faced by these communities, who were already isolated by low river levels resulting from the  
3047 drought that severely reduced their mobility and fishing, impacting on food security and  
3048 enhancing socio-economic vulnerabilities.

3049  
3050 In Chile, the 2023-24 fire season was marked by a significant escalation in both the number  
3051 and size of wildfires, especially in the central and southern regions (**Figure 4**). Chile  
3052 experienced its second-highest BA in the past 20 years (>4,000 km<sup>2</sup>; Jones et al., 2024). The  
3053 peaks in BA at national scale were accompanied by peaks in the 95th percentile of fire size  
3054 and daily rate of growth in highly-populated regions such as Valparaíso (**Figure 2, Figure 4**),  
3055 indicating unusually large and fast-moving fires. These fires drew international attention due  
3056 to their deadly impacts on society. In February 2024, severe wildfires struck the Valparaíso  
3057 region in Chile, particularly affecting Viña del Mar and other surrounding areas (NASA Earth  
3058 Observatory, 2024). These fires resulted in the deaths of at least 131 people and destroyed  
3059 thousands of homes, leaving at least 1,600 people homeless (UN Resident Coordinator in  
3060 Chile, 2024; *Al Jazeera*, 2024; *El Disconcierto*, 2024). The fires impacted the Lago Peñuelas  
3061 National Reserve where more than 60 km<sup>2</sup> of forest were affected (Oberholtz, *Fox Weather*,  
3062 2024). The National System for Disaster Prevention, Mitigation and Attention (SENAPRED)  
3063 issued a red alert and ordered the evacuation of over 18 nearby towns (Oberholtz, *Fox*  
3064 *Weather*, 2024). The February 2024 wildfires in Valparaíso followed other major disruptive  
3065 wildfires in February 2023, which affected nearby regions of central Chile including Maule,  
3066 Nuble, Bio bío, La Araucanía and Los Rios.

3067  
3068 Several countries with territory in the west of Amazonia experienced anomalies in BA and fire  
3069 behaviour during the 2023-24 fire season, which coincided with drought conditions. Peru's  
3070 Loreto region, which neighbours the Brazilian state of Amazonas, faced its highest BA on  
3071 record in the 2023-2024 fire season signalling the wider impacts of drought conditions in  
3072 western Amazonia (**Figure 2**). The timing of peak anomalies in BA also coincided with those  
3073 in Amazonas, around September-October 2023 (**Figure S2**). The northern Bolivian  
3074 departments of La Paz and Beni experienced similarly-timed anomalies in BA. Remote parts  
3075 of the Colombian Amazon also saw a significant uptick in BA since November 2023 which  
3076 peaked in January 2024 (Mongabay, 2024). As a result of months of record-high temperatures  
3077 and drought conditions since the beginning of El Niño, the region recorded higher C emissions,  
3078 reflecting the severity of the burning at the end of the studied fire season. While the direct  
3079 impacts on society throughout these regions was not as pointed as in the case of fires in Chile,  
3080 the events are likely to have contributed to reductions in regional air quality and also impacted  
3081 forest ecosystems and raised C emissions from fires in South America. At the end of January  
3082 there was a wildfire in the mountains surrounding Bogota that affected the air quality that  
3083 affected thousands of citizens of the capital of Colombia (France-Presse, *VOA News*, 2024).

3084  
3085 In 2023-2024, Venezuela experienced its highest level of fire activity on record, particularly in  
3086 January and February 2024 (ALER, 2024; *Tiempo*, 2024; **Figure 4, Figure S2, Figure S8**),  
3087 notably affecting the states of Anzoátegui, Cojedes, Guárico, and Monagas, areas which  
3088 dominant land cover primarily consists of savannas and extensive grasslands. This surge in  
3089 fires during the dry season was intensified by unusually warm and dry conditions in the  
3090 preceding months. These conditions, likely a result of global warming and changes in  
3091 circulation and rainfall patterns associated with El Niño, making the landscapes more  
3092 vulnerable to fires.

## 3093 **8 Appendix B: Frontiers in Observing and Modelling Extreme** 3094 **Fire Occurrence and Impact**

3095  
3096 This appendix summarises current challenges in the observation and modelling of extreme  
3097 fire events or seasons and identifies new technological and methodological advances that are  
3098 raising opportunities to overcome such challenges. The section begins with a review of the



3099 study of extreme fire *occurrence* and then focuses on the study of extreme fire *impacts* across  
3100 7 impact sectors. Advances in the study of both fire occurrence and fire impact are required  
3101 because the impacts of extreme fires on society and the environment do not necessarily scale  
3102 with observable fire properties (see **Section 6.2**).

3103

## 3104 **8.1 Occurrence**

3105

### 3106 **8.1.1 Definition of Extreme Fire Events**

3107

3108 Studying impactful fires or unusual fire seasons is crucial for understanding changes in  
3109 exposure and vulnerability to fire. However, defining "extreme" events presents several  
3110 challenges. These challenges can be categorised as follows.

3111

3112 Data-Oriented Challenges:

3113 ● **Lack of Consensus on Quantitative Criteria:** Variability in measurable criteria, such  
3114 as fire size, across different studies hinders consistent classification. No statistical  
3115 threshold is universally established to define outliers.

3116 ● **Geographic Variability:** Regional differences complicate universal definitions. Size  
3117 thresholds vary widely, influenced by local fire regimes.

3118 ● **Evolving Definitions:** The term "extreme fire" has expanded over time, encompassing  
3119 more fire types and behaviours. Climate change increases fire severity, suggesting  
3120 definitions need flexibility.

3121 ● **Context Dependence:** Definitions vary with ecosystem types and fire histories,  
3122 lacking standardisation on baselines such as fire return intervals or ecosystem  
3123 damage.

3124

3125 Knowledge-Oriented Challenges:

3126 ● **Lack of Consensus on Qualitative Criteria:** Variability in criteria like fire behaviour  
3127 and impacts reflects differing expert opinions. The subjective nature of significant  
3128 impact complicates a clear definition.

3129 ● **Terminological Overlap and Redundancy:** Terms like "catastrophic fire" and "megafire"  
3130 overlap, causing confusion due to unclear or interchangeable usage.

3131 ● **Influence of Language and Culture:** Interpretations differ across languages and  
3132 cultures, affecting global reporting and definitions.

3133 ● **Societal Influence on Scientific Terminology:** Scientific terminology evolves with  
3134 societal context. Language in scientific communication must remain adaptable and  
3135 relevant to non-scientific audiences.

3136 ● **Scientific Rigour and Clarity:** Clear, consistent, and scientifically rigorous definitions  
3137 are needed for standardised measurements. Existing definitions often fall short.

3138

3139 Defining 'extreme fire' requires a significant and inclusive effort across the fire science  
3140 community. We avoided a strict definition here, instead adopting a broad and flexible definition  
3141 as discussed in **Section 2.1**. To support a formal definition for future iterations of this report,  
3142 standardised criteria and protocols should be developed through transdisciplinary approaches,  
3143 such as through workshops involving input from scientists, fire practitioners, legislators, and  
3144 communities (Chu et al., 2023; Linley et al., 2022; Shuman et al., 2022).

3145

### 3146 **8.1.2 Observation of Extreme Fire Events**

3147

3148 Global-scale data for characterising extreme fire events are primarily sourced from satellite  
3149 observations, notably active fire detections, BA maps, and tracking of smoke plumes.  
3150 However, to accurately define how extreme a fire event is, it is crucial to contextualise present-  
3151 day observations within historical data. Unfortunately, the historical records of satellite-derived  
3152 active fire and BA products are relatively short. The longest coherent observations on a global

3153 scale are derived from the MODIS instruments onboard the Aqua and Terra satellites,  
3154 launched in 1999 and 2002 respectively. Various global BA products, such as MCD64 product  
3155 family (Giglio et al., 2018) and FireCCI51 (Lizundia-Loiola et al., 2020), as well as active fire  
3156 data like the MCD14 product family (Giglio et al., 2016), have been generated based on  
3157 imagery acquired by MODIS. Although these time-series now span over two decades, they  
3158 are still relatively short when compared to the decadal to centurial fire return intervals observed  
3159 in many ecosystems.

3160  
3161 Pre-MODIS satellite data, like that from the AVHRR program, exists and provides a continuous  
3162 imagery archive from 1982 onwards. Although efforts are ongoing to generate a coherent BA  
3163 product from AVHRR data (Otón et al., 2021), there are limits to the global applicability of  
3164 these products. For example, unresolved challenges stemming from coherence issues  
3165 between imagery from different AVHRR sensors result in artefacts and spurious trends in  
3166 various regions worldwide (Giglio and Roy, 2022), although this has been debated by other  
3167 authors (Pullabhotla et al., 2023).

3168  
3169 Efforts are ongoing to extend the MODIS time-series by incorporating active fire data from  
3170 ATSR and VIRS with BA data (e.g. Chen et al. 2023). However, due to the different  
3171 characteristics of these data, creating a coherent, multi-satellite time-series of active fire data  
3172 and/or BA is not straightforward. Concerns also arise with the impending decommissioning of  
3173 MODIS-Terra, raising doubts about the continuity of existing long-term fire records. However,  
3174 operational satellite sensors such as VIIRS onboard NOAA's series of satellites and SLSTR  
3175 onboard the Sentinel-3 satellites offer promising capabilities for medium-resolution BA  
3176 mapping (e.g. Román et al., 2024; Lizundia-Loiola et al., 2022). Urgent attention should be  
3177 directed towards developing methodologies to integrate these new datasets into a coherent,  
3178 long-term BA dataset. Furthermore, advancements in medium-resolution satellite data  
3179 availability and revisit times, particularly from Landsat and Sentinel-2, now enable global BA  
3180 mapping at spatial resolutions as fine as 20-30m (e.g., Roteta et al., 2021; Chuvieco et al.,  
3181 2022), suggesting a potential future direction for coherent long-term global BA monitoring.

3182  
3183 While BA is a key variable to characterise extreme fire occurrence, multiple other aspects of  
3184 extreme fires can be characterised using satellite data. BA products can be used to cluster  
3185 burned pixels in burned patches to obtain the number and size of individual fires (Archibald  
3186 and Roy, 2009). Furthermore, the daily fire rate-of-spread, length of the active fire line and  
3187 spread direction can be extracted from the daily fire expansion (Andela et al., 2019). These  
3188 algorithms, such as the Global Fire Atlas used in this study, give global scale, coherent  
3189 estimates of patterns and trends in fire number, fire size and rate of spread. However, these  
3190 algorithms are sensitive to the temporal accuracy of the per-pixel burned date detection, the  
3191 spatial resolution of the BA product, and any errors within each product. Recent advances  
3192 focusing on clustering VIIRS thermal anomalies and extracting fire rate of spread, fire  
3193 expansion and length of the active fire line show promising results (Andela et al., 2022,  
3194 Hantson et al., 2022, Chen et al., 2022) but have so far not been developed globally. Future  
3195 development towards a global product should allow for a more detailed characterization of fire  
3196 characteristics in near real-time, well-suited for detection and quantification of fire extremes.

3197  
3198 Active fire detections also record the amount of radiation emitted by the fire at the moment of  
3199 satellite overpass (Fire Radiative Power, FRP), within the pixel detected by the satellite. While  
3200 this information is related to the intensity of the fire, the usage of FRP has been difficult as a  
3201 low-intensity fire burning a large extent of the pixel can have a higher FRP than a high-intensity  
3202 fire burning a small fraction of a pixel. These complications have limited a more standardised  
3203 and operational usage of FRP for quantifying fire extremes. Advances in active fire detection  
3204 from higher resolution sensors may allow for a more comprehensive estimate of fire intensity  
3205 when combined with FRP estimates from coarse resolution sensors (Schroeder et al., 2014,  
3206 2016).

3207

3208 A natural starting point for this global assessment of the 2023-24 fire season was global data  
3209 provided by the MODIS BA dataset, though we note that various national, state-level or  
3210 regional systems exist and can add longer-term context to the extremity of fire seasons (e.g.  
3211 Canadell et al., 2021; Short, 2014; Gincheva et al., 2024). Regional datasets generally depend  
3212 on manual logging of fires via field approaches or desk-based identification with high-  
3213 resolution imagery, or alternatively harness different blends of satellite observation with fire  
3214 detection algorithms that can be regionally optimised. These approaches carry their own  
3215 uncertainties and are limited by design to targeted regions, however their major advantage is  
3216 multi-decadal coverage. Advances in compiling regional datasets into gridded records with  
3217 global coverage are bringing these advantages to formats compatible with global scale  
3218 analysis (Gincheva et al. 2024) and will thus be explored in future efforts to characterise  
3219 regional extremes at scale.

3220

### 3221 **8.1.3 Prediction of Extreme Fire Events**

3222

3223 Since the 1970s, fire predictions have relied on empirical fire behaviour models tailored to  
3224 specific ecosystems (Bradshaw et al., 1983; Noble et al., 1980; Stocks et al., 1980; van  
3225 Wagner, 1987), becoming pivotal tools for fire management agencies (San-Miguel-Ayanz et  
3226 al., 2013). The ease of implementation and the availability of weather data have contributed  
3227 significantly to their widespread adoption. However, despite their utility, several studies have  
3228 highlighted the limited effectiveness of the FWI and similar metrics in fuel-limited ecosystems,  
3229 where fires are driven by the short-term superficial drying of intermittently available biomass  
3230 (Yebra et al., 2013). The absence of consideration for actual fuel availability presents a  
3231 constraint to the meaningful application of the FWI in savanna-type ecosystems. Likewise, the  
3232 response of fuel moisture to meteorological factors can be influenced by external factors that  
3233 are challenging to observe and model at scale, such as mortality triggered by insect infestation  
3234 or disease (Canelles et al., 2021). Beyond weather conditions, the remaining prerequisites for  
3235 fire activity—namely, fuel and ignitions—are intricately linked to vegetation state, lightning  
3236 activity, and human behaviours. Improving fire forecasts beyond solely considering fire  
3237 weather could be achievable by accurately describing these components. This has been  
3238 widely recognised in the global vegetation-fire community for several decades (Hantson et al.,  
3239 2016), and consequently great advances have been made to address this through the  
3240 development of fire-enabled DGVMs, as used in this report. However, explicit representation  
3241 of these processes introduces biases and instabilities that, when used in isolation, limits their  
3242 utilage for assessing climate and human drivers of BA extremes (Hantson et al., 2020; Burton,  
3243 Lampe et al., 2023).

3244

3245 The availability of remote observations for fuel, either independently (Yebra et al., 2018) or  
3246 supported by modelling frameworks (McNorton and Di Giuseppe, 2024), has demonstrated  
3247 potential in aiding the development of new fire models and indices that partially incorporate  
3248 fuel considerations into their formulation (Di Giuseppe, 2023, Hantson et al., 2016). However,  
3249 it is the emergence of the data-driven revolution that holds the promise of significantly  
3250 enhancing our predictive capabilities for extreme fires (McNorton et al., 2024). This has driven  
3251 the development of semi-empirical tools at regional and global scales that could improve fire  
3252 predictions, and their effectiveness will be assessed in the next edition of the report. Not only  
3253 can these tools enhance predictive capability for extreme fires, they also present an  
3254 opportunity to disentangle the drivers of the prediction, giving us the capability to address or  
3255 at least understand the causes of the event, as demonstrated by the POF and ConFire  
3256 frameworks used here. The coupling of FireMIP models with observational data (Burton,  
3257 Lampe et al., 2023 and used here), also showcases the potential to bridge the advanced  
3258 modelling capabilities of FireMIP with application-specific approaches such as ConFire and  
3259 POF.

3260

3261 Despite these technological advancements, widespread adoption is unlikely to occur  
3262 suddenly, as there typically exists a delay between the creation of new indices, their

3263 operationalization, and operational implementation by those responsible for fire prevention  
3264 and control. There are also likely to be some stubborn issues with the detail provided large-  
3265 scale observational data available to predictive systems, particularly in the case of fuel loads  
3266 and fuel state (e.g. living versus dead). New global biomass observations, such as those from  
3267 airborne and spaceborne Light Detection and Ranging (Lidar) and Synthetic Aperture Radar  
3268 (SAR), provide insights into fuel loading but they are not currently providing information  
3269 regarding fuel state that would be useful for modelling fuel moisture response to  
3270 meteorological conditions (Santoro et al., 2022; Hunke et al., 2023).

3271  
3272 Another emerging element is the recent availability of fire danger predictive systems at the  
3273 seasonal and subseasonal timescales (Di Giuseppe et al., 2024). Currently, there is limited  
3274 evidence on how these longer-range tools could contribute to prevention planning and  
3275 adaptation strategies. While they exhibit minimal skill beyond two months, they may offer  
3276 valuable pre-seasonal warnings under specific conditions established during important  
3277 atmospheric modes of variability.

3278  
3279 The current report does not include hybrid models for seasonal fire risk, fire propagation  
3280 models, or fire susceptibility/risk mapping tools. Incorporating these approaches could offer  
3281 valuable insights and will be considered in future reports. These advanced models and tools,  
3282 which account for both past and present weather conditions as well as other critical factors  
3283 such as soil moisture and vegetation dryness, can enhance our understanding of fire dynamics  
3284 and improve predictive capabilities. By exploring these methods, future editions of the report  
3285 could provide a more comprehensive overview of fire risk assessment and management  
3286 strategies.

3287

#### 3288 **8.1.4 Attribution Extreme Fires to Global Change**

3289

3290 The prediction and management of extreme fire events have become increasingly complex  
3291 due to the multifaceted impacts of global change. Climate change exacerbates fire risks  
3292 through rising temperatures, altered precipitation patterns, and more frequent and severe  
3293 droughts, as shown in Canada and western Amazonia in this report. These climatic shifts  
3294 affect vegetation productivity, with elevated CO<sub>2</sub> levels potentially increasing biomass and  
3295 thereby providing more fuel for fires. Nutrient deposition and other environmental changes  
3296 influence ecosystem responses, further altering fire potential. Land use changes and  
3297 management practices also significantly influence fire dynamics. For example, human  
3298 activities such as deforestation, urban expansion, and agricultural practices can both mitigate  
3299 and exacerbate fire risks, with socioeconomic factors shown to have a strong influence on  
3300 overall extreme fire likelihood in western Amazonia, and potentially contributing to increases  
3301 in BA in 2023 in some areas of Greece. Effective land management strategies, including  
3302 prescribed burns and forest thinning, are crucial for reducing fuel loads and minimising fire  
3303 impacts. While climate driven estimates of extreme behaviour are plentiful, few modelling  
3304 frameworks take into account most of these dynamic factors and their interactions (Rabin et  
3305 al., 2017).

3306

3307 We have used model-data fusion techniques that account for these factors in this report, and  
3308 have been able to attribute some of their influences in certain places. This report utilises semi-  
3309 empirical models that blend empirical data with process-based understanding to better predict  
3310 fire behaviour. Quantifying uncertainty in these models is essential, especially when dealing  
3311 with extremes. By generating probability distributions, researchers can better understand the  
3312 likelihood of various fire scenarios, informing more effective management and policy  
3313 decisions.

3314

3315 Through uncertainty quantification techniques, we have been able to ascertain where we are  
3316 confident in our attributions. However, uncertainties still remain, many from not considering  
3317 the complex interactions and feedback onto fire, some from fire itself as it consumes fuel, and

3318 affects from weather. Coupled vegetation-fire models explicitly represent many of these  
3319 feedbacks. However, current FireMIP models struggle to accurately simulate extreme fire  
3320 events (Hantson et al., 2020). One key factor hampering improvements in model development  
3321 is our limited understanding of factors driving fire extinguishers in a natural setting. While much  
3322 process based knowledge exists on the factors influencing fire start and fire spread, only  
3323 limited knowledge exists on the myriad of factors that can stop a fire, from changes in fuel  
3324 moisture, structure and heterogeneity to landscape fragmentation and fire fighting, and how  
3325 these interact (e.g. Finney et al., 2012). Without a strong theoretical understanding of these  
3326 factors, process based modelling of extremes at a global scale might be limited in the near  
3327 future. For the 2023 focal events, we have shown that low fuel loads and variations in human  
3328 modification of the landscape can limit fuel spread (**Figure 11, Figure 12, Figure S13, Figure**  
3329 **S14**). However, we only look at a handful of events and further examples are required at larger  
3330 scales to inform improvement of process-based rates of spread in fire models.

3331  
3332 To move forward, we need to combine these concepts in attribution techniques and quantifying  
3333 uncertainty with coupled vegetation fire models, such as in FireMIP. Early attempts of this are  
3334 promising – ConFire (used in **Section 3, 4 and 5**) borrows many of the modelling concepts  
3335 from FireMIP, though it still lacks many feedbacks from fire itself. We have also used the latest  
3336 FireMIP models coupled to an uncertainty framework for broad-scale, uncertainty-based  
3337 attribution (obtained from Burton, Lampe et al., 2023). But they struggle at reproducing the  
3338 tails of distributions where extreme events are found. Another way to develop these  
3339 techniques is to move towards an integrated system that would inform both attribution and  
3340 future projections in a seamless way. We make some progress in this direction here using  
3341 tools such as ConFire, by using the information gained from fire drivers to build future  
3342 projections, however there is more work to do to link statistical approaches for today’s fires to  
3343 future projections.

3344  
3345 The human role in driving fire and extremes is hard to represent. Despite the often reported  
3346 influences people have on both increasing extreme burning or causing the observed decline  
3347 in global BA, the role of humans in the landscape remains hard to capture and on the whole,  
3348 remains one of the most uncertain aspects of this report. Agent-based modelling (ABM) is  
3349 trying to address this by simulating the behaviours and interactions of individual human entities  
3350 (e.g., deforestation, crop residue burning, suppression, etc.) within a given environment (Ford  
3351 et al., 2021). This approach provides a dynamic representation of how different factors  
3352 contribute to fire risk and links well with subsequent sections of the report. These approaches  
3353 could be a major contributor to subsequent issues of this report. However, the integration of  
3354 these advanced modelling techniques into operational use faces challenges, as there is often  
3355 a delay between the development of new approaches and their widespread adoption by fire  
3356 management agencies. This underscores the need for continuous improvement and adoption  
3357 of innovative modelling approaches to address the growing threat of extreme fire events  
3358 effectively.

3359  
3360 In addition to fire weather index (FWI) and BA projections, it is crucial to go beyond these  
3361 metrics to consider wider impacts such as intensity, and emissions. Understanding the  
3362 intensity of fires helps in assessing their destructive potential and the severity of their  
3363 ecological and societal impacts. Emissions from fires, including C dioxide and other  
3364 greenhouse gases, contribute to climate change and air quality issues. Finally, evaluating the  
3365 broader impacts of fires, such as on biodiversity, human health, and economic stability, is  
3366 essential for developing comprehensive adaptation and mitigation strategies. Quantifying and  
3367 understanding the uncertainty in these projections is crucial for developing adaptive strategies  
3368 that can effectively respond to the evolving fire risks posed by global change.

3369  
3370 **8.1.5 Projection of Fire Extremes**  
3371

3372 Projections of extreme fire events under future climate scenarios indicate a significant increase  
3373 in their frequency and intensity. Semi-empirical models used in this report project that extreme  
3374 BA events, currently rare, are likely to become more common by the end of the century. These  
3375 projections highlight the urgent need for robust fire management strategies and policies to  
3376 mitigate the impacts of these increasingly severe fire events on ecosystems, communities,  
3377 and global C dynamics. Quantifying and understanding the uncertainty in these projections is  
3378 crucial for developing adaptive strategies that can effectively respond to the evolving fire risks  
3379 posed by global change. In our ConFire uncertainty quantification framework, we have been  
3380 able to make some confident inferences about the potential state of wildfires in the coming  
3381 decades. However, we have also identified that there is a significant amount of crucial  
3382 information that is currently beyond our reach due to the uncertainties involved. Our ability to  
3383 forecast for the upcoming season, as well as for the next 2-3 decades, requires further  
3384 refinement as we are observing mixed and uncertain responses. Beyond that, we still show  
3385 similar uncertainties in responses of Canada and Western Amazonia under different scenarios  
3386 as highlighted by UNEP (2022a), which uses the previous generation of climate models from  
3387 CMIP5 – shows a large overlap in the potential range of changes in the occurrence of fire  
3388 extremes between SSP370 and SSP585. This does not imply that mitigation efforts for one  
3389 scenario will be ineffective compared to another, but rather indicates a lack of understanding  
3390 regarding the response of extremes to these scenarios. By narrowing down the uncertainty  
3391 ranges, we can better target adaptation efforts and evaluate the effectiveness of mitigation  
3392 strategies. The reduced likelihood of extreme event recurrence in our high mitigation, however,  
3393 does show that we can start separating out how mitigation efforts might affect fire extremism,  
3394 though not in the level of detail needed for policy.

3395  
3396 There are three main ways we may be able to constrain uncertainties in the coming reports.  
3397 The first is development of the underlying GCMs that project future change in the drivers of  
3398 BA. For individual models, this is a slow process and, beyond informing CMIP model  
3399 development, is outside what the State of Wildfires can contribute to. However, bringing in  
3400 more models, including having another model to incorporate any remaining biases in  
3401 simulated fire from the correct models into our uncertainty projection, will help us constrain  
3402 uncertainties more (Kelley et al., 2023). The second is obtaining more information and  
3403 understanding of how fire drivers relate to fire extremes as outlined in the previous section.

3404  
3405 Better ways of describing the statistical relationship between observed and modelled climate,  
3406 land surface and fire today is a third approach. Investigating the dynamical climatic drivers of  
3407 extreme fire conditions in different regions can help to physically disentangle and potentially  
3408 constrain sources of uncertainty in future climate projections, for example by constructing  
3409 physical storylines (Shepherd et al., 2018; Mindlin et al., 2023). These storylines of plausible  
3410 future change, or other similar approaches to quantify and explain uncertainty in projections,  
3411 provide critical information for communities to develop robust adaptation strategies (Lemos et  
3412 al., 2012) and prepare for future losses and damage caused by evolving fire risks posed by  
3413 global change. Next to understanding future uncertainty, further insights into these dynamical  
3414 drivers can support the development of improved physics-informed bias adjustment of climate  
3415 models (Maraun et al. 2017). Currently available methods to bias adjust climate models for  
3416 their use in fire models, such as the ISIMIP3BASD method, have been shown to modify the  
3417 climate change trend, particularly in extreme threshold indices (Casanueva et al 2020, Spuler  
3418 et al 2024) or increase spread in climate model projections (Lafferty and Sriver, 2023). Bias  
3419 adjustment methods should therefore be evaluated carefully and leave scope for future  
3420 method development that physically links present-day biases to future uncertainty.

## 3421 3422 **8.2 Impact** 3423

3424 **8.2.1 Direct Exposure of People and the Built Environment**

3425 The direct exposure of people and the built environment could be studied at scale, however  
3426 these analyses have not been performed routinely and have thus far tended to focus on  
3427 specific regions. The wildland urban interface (WUI) has been the focus of direct fire exposure  
3428 to populations, particularly in urban conflagrations like the Lahaina fire in August 2023. Efforts  
3429 to reduce fire losses in the WUI through prevention, fuel reduction, and mitigation (Calkin et  
3430 al., 2023) are crucial due to increased populations in these areas (Radeloff et al., 2018) and  
3431 rising fire potential, accelerating community impacts (Higuera et al., 2023). US studies showed  
3432 a doubling of direct population exposure to large fires during 2000-2019, mainly due to fires  
3433 encroaching on the WUI (Modaresi Rad et al., 2023). Similar increases were noted in wildfires  
3434 affecting roads and energy infrastructure, complicating transportation and energy reliability.  
3435 Most structure losses in the US occurred in grasslands and shrublands, not forests,  
3436 highlighting the need to look beyond traditional forest-centric assessments. Global WUI  
3437 mapping efforts (Schug et al., 2023) offer opportunities to identify vulnerable areas and  
3438 characterise fire exposure trends (Chen et al., 2024; Tang et al., 2024).

3439 Understanding fire characteristics that result in direct exposure, structure loss, and fatalities is  
3440 essential. For instance, Abatzoglou et al. (2023) found that fires driven by strong downslope  
3441 winds in the western US caused most structure losses and fatalities from 1999-2020, despite  
3442 being only 12% of all fires. These winds push fires downhill into WUI communities,  
3443 overwhelming suppression efforts and fuel treatments. The 2023 fires in Hawaii, Greece, and  
3444 Chile were driven by such conditions (Synolakis and Karagiannis, 2024). Diagnosing  
3445 characteristics of extreme fires, including meteorological conditions (Van Wagtendonk, 2006;  
3446 Lareau et al., 2018) and pre-existing vegetation conditions (Stephens et al., 2022), provides  
3447 insights into fires likely to cause significant impacts, helping prioritise mitigation efforts.

3448 A significant gap in characterising extreme fires and their human impacts (fatalities,  
3449 evacuations, structure loss, secondary morbidity, economic losses, and impacts on food,  
3450 water, energy, and transportation) is the lack of comprehensive national-to-global data.  
3451 Wildfire morbidity data are collected in few countries due to the infrequency of fatal wildfires  
3452 and unclear cataloguing responsibilities (Haynes et al., 2019). Smoke-induced morbidity  
3453 estimates rely on spikes in hospital visits linked to specific events (Johnston et al., 2021).  
3454 California pioneered systematic cataloguing of structure losses in 2013, yielding significant  
3455 insights (Kolden and Henson, 2019; Syphard and Keeley, 2019), but this model has not been  
3456 widely adopted. Canada now catalogues wildfire evacuations, but complexities remain in  
3457 characterising these events (Beverly and Bothell, 2011). Global insurance records document  
3458 insured losses but do not represent broader losses due to high rates of uninsured property  
3459 (Hazra and Gallagher, 2022).

3460 Databases like EM-DAT have attempted to fill this gap but often overgeneralize wildfire  
3461 impacts, relying on variable accuracy news reporting. Expanding and improving quantification  
3462 of wildfire impacts on humans is critical to overcoming the "burned area fallacy" and  
3463 developing effective mitigation models (Kolden, 2020). Remote sensing for documenting  
3464 structure loss and fire incursion into the WUI, combined with high-resolution sensors and air  
3465 quality monitors, can facilitate interdisciplinary research on wildfire smoke and medical  
3466 morbidity (Liang et al., 2021).

3467  
3468 **8.2.2 Air Quality and Health Impacts**  
3469

3470 The impacts of fire on air quality and health could be studied routinely at scale using  
3471 atmospheric models, however these analyses face several challenges. Exposure to outdoor  
3472 pollution is a major global health risk (Murray et al., 2020). Fine particles with a diameter less  
3473 than 2.5  $\mu\text{m}$  (PM<sub>2.5</sub>) are particularly concerning due to their link to cardiovascular diseases.

3474 Fire smoke is increasingly impacting air quality and is considered more toxic per unit of PM  
3475 exposure than other pollution sources (Aguilera et al., 2021). The World Health Organization  
3476 (WHO) has reduced the annual mean exposure limit for PM<sub>2.5</sub> from 10 µg m<sup>-3</sup> to 5 µg m<sup>-3</sup>.  
3477 With 95% of the world's population exposed to PM<sub>2.5</sub> concentrations of at least 10 µg m<sup>-3</sup>  
3478 (Shaddick et al., 2018), the rise in severe wildfire pollution poses an elevated health risk.  
3479

3480 Issues contributing to the challenge of quantifying the impact of fire pollution on human health  
3481 are the same as those for other pollution sources, including, but not limited to, a lack of ground-  
3482 based measurements in many regions of the world, a need for more pollution dispersion and  
3483 transport studies, a deeper understanding of plume dynamics and chemistry, and a partial  
3484 reliance on animal-based human exposure/response models (e.g., Fiore et al. 2012, Fuzzi et  
3485 al. 2015). These issues contribute to three of the major challenges in quantifying the impact  
3486 of extreme fire pollution on human health. The first is accurately measuring the amount of  
3487 pollution that a wide variety of communities are exposed to and then attributing the contribution  
3488 of a wildfire event, that could be 100s or 1000s of km away, to the measured concentration.  
3489 The second is that PM<sub>2.5</sub> is not the only pollutant of concern (the EPA regulates six pollutants  
3490 of concern for American citizens and a wildfire produces them all). The third is accurately  
3491 linking exposure to a wide range of pollutants to their associated short-term and long-term  
3492 health impacts.  
3493

3494 Tools to assess air quality primarily consist of ground-based measurements and modelling.  
3495 Ground based observations provide an accurate measurement of pollution at their location.  
3496 However, measurement locations are spatially sparse. Ongoing efforts to increase spatial  
3497 coverage include deployment of small relatively affordable particulate matter sensors, such as  
3498 the PurpleAir network, by a wide range of communities (not just scientists), and efforts to relate  
3499 surface PM concentrations to measured aerosol optical depth from satellites (Li et al., 2021).  
3500 One additional constraint of observations is that they cannot differentiate pollution sources,  
3501 but modelling can.  
3502

3503 Dispersion modelling uses emission estimates, reanalysis meteorology, and topography to  
3504 provide estimates of ambient pollutant concentrations at varying spatiotemporal scales. A  
3505 challenge for models currently lies in the large uncertainty in fire emissions (Reddington et al.,  
3506 2016; Carter et al., 2020; Pan et al., 2020). Emission data will therefore require calibration  
3507 against observations and adjusting before the contribution of fire to pollution can be quantified.  
3508 Improved emission datasets will increase confidence in these assessments.  
3509

3510 Environmental and personal factors both influence cardiovascular health, making it  
3511 challenging to isolate the effects of fire smoke. Impacts may also not be immediate; some  
3512 effects can be acute, such as exacerbation of asthma, while others emerge over a longer  
3513 period, like the development of cardiovascular disease, and are thus much more difficult to  
3514 directly connect to a specific extreme fire event. Conducting epidemiological studies that link  
3515 fire smoke exposure to specific health outcomes requires comprehensive data collection and  
3516 follow-up. These studies are resource-intensive, time consuming, and subject to potential  
3517 limitations in data.  
3518

### 3519 **8.2.3 Impacts on Indigenous and Traditional Communities**

3520

3521 The impacts of fire on Indigenous and Traditional Communities are not studied routinely and  
3522 at scale, typically focussing on isolated regions and specific communities. Indigenous peoples  
3523 and local communities (IP&LC) are disproportionately exposed to extreme fire impacts  
3524 because of their proximity to the land and resources from which their cultures, livelihoods and  
3525 often food and medicines derive. Once landscapes are degraded through fire the access and  
3526 abundance of various resources can be shifted. At the same time these communities are often  
3527 less supported by the state due to access and their political and economic marginalisation  
3528 linked to systemic socioeconomic disadvantages. These communities suffer not only post-fire



3529 impacts, but can be disincentivized from particular land and resource use activities because  
3530 of the increasing threat of forthcoming wildfires. Whilst the multiple important values (e.g.  
3531 instrumental, intrinsic and relational) associated with landscapes by IP&LCs are threatened  
3532 by fire, there is a lack of systematic pre- and post-fire assessment of these impacts (van  
3533 Leeuwen and Miller-Sabbioni, 2023).

3534  
3535 Historically fire governance has added an additional burden to IP&LC, often prohibiting cultural  
3536 fire use and management to the detriment of local knowledge and values, and in some cases  
3537 also increasing the propensity of wildfire in tropical systems as well as savannahs (Carmenta  
3538 et al., 2019; Daeli et al., 2021; Croker et al., 2023). In some contexts there is a shift towards  
3539 correcting these issues and renewed interest in and support for cultural burning and  
3540 Indigenous approaches to land management. For example, integrated fire management is  
3541 gaining traction globally and sits at the heart of a number of interventions and international  
3542 policy efforts (e.g. Fire Hub, 2023). The premise of Integrated Fire Management (IFM) is to  
3543 maximise the 'good' fire and minimise the occurrence of wildfire often through an approach of  
3544 connecting knowledges (i.e. expert and place-based or Indigenous). Whilst nations sit at  
3545 different stages of development in respect to IFM, and many IP&LC feel there is a long way to  
3546 go, the growing interest is promising (Bilbao et al., 2019; Luque et al., 2020; Rodríguez-Trejo  
3547 et al., 2022). Research is needed to better understand the effectiveness of IFM and what  
3548 mechanisms and processes work best for rebalancing the influence of various forms of  
3549 knowledge on fire management. For instance in North America where fire use is considered a  
3550 form of medicine to the land, and anointed to particular patches of the landscape for care  
3551 (Palmer, 2021). These approaches are perceived as potentially more just as they allow for the  
3552 many meanings and uses of fire to exist and persist. For example, In Australia, the term  
3553 'Country' is used to convey the cultural and spiritual connection of Aboriginal peoples to the  
3554 land and water in specific regions. This link profoundly colours Indigenous peoples' experience  
3555 of extreme fire events such as the Black Summer fires of 2019-20 (Nolan et al., 2021b).

3556

#### 3557 **8.2.4 Economic Impacts**

3558  
3559 The economic impacts of fire are generally not studied routinely and at scale, but rather focus  
3560 on individual regions and fire seasons and arrive some time after the event occurs. Extreme  
3561 wildfires cause economic disturbances worldwide, with impacts varying across regions due to  
3562 different economic structures, environmental conditions, and response strategies. These  
3563 impacts include property and infrastructure loss, business downtimes, supply chain  
3564 disruptions, decreased tourism, health costs, reduced productivity, and damages to  
3565 ecosystem services. While tangible costs (e.g., insured property losses) are easier to  
3566 measure, intangible costs (e.g., lives lost, health impacts from smoke exposure, damage to  
3567 species and habitats) are harder to quantify due to data availability and varying temporal and  
3568 spatial scales. Consequently, assessing the true economic costs of extreme wildfires is  
3569 challenging. Additionally, some sectors may benefit economically from post-fire reconstruction  
3570 and suppression efforts (Nielsen-Pincus et al., 2014; Meier et al., 2023a).

3571  
3572 Research on the economic impacts of wildfires has mainly focused on developed economies  
3573 in Europe, the US, and Australia. For instance, Meier et al. (2023b) estimated economic losses  
3574 from a 1-in-10 year extreme wildfire in Mediterranean Europe: €162–439 million in Portugal,  
3575 €81–219 million in Spain, €41–290 million in Greece, and €18–78 million in Italy. California's  
3576 2018 and 2020 wildfire seasons resulted in approximately \$150 billion and \$19 billion in  
3577 economic damages, respectively (Wang et al., 2021; Safford et al., 2022). Australia's 2019-  
3578 2020 fire season was the costliest natural disaster in the country's history, with an estimated  
3579 GDP decrease of \$10 billion (Wittwer and Waschik, 2021).

3580  
3581 While satellite data can provide proxies for economic impact shortly after events, traditional  
3582 economic indicators such as sectoral GDP, employment, hospitalizations, suppression  
3583 spending, house prices, and tourism revenues are often not publicly available, not

3584 harmonised, or unable to capture long-term effects. Thus, the full economic costs may only  
3585 become apparent years later.

3586

3587 Econometric analysis of wildfires is more challenging than for other natural hazards because  
3588 wildfire occurrence is largely influenced by human activity, land-use choices, and  
3589 socioeconomic factors. While earthquakes are non-human-induced, making causal analysis  
3590 easier, wildfires correlate with many economic outcome variables. Despite these challenges,  
3591 counterfactual analyses or econometric approaches like instrumental variables can provide  
3592 reliable causal estimates of wildfire impacts. These methods promise to enhance  
3593 understanding and mitigation of wildfire economic consequences through more accurate  
3594 analyses, helping target suppression policies and allocate resources effectively.

3595

3596

### 3597 **8.2.5 Loss of Biodiversity, Ecosystem Function and Carbon Storage**

3598 Impacts of extreme fires on biodiversity and rates of post-fire recovery have tended to require  
3599 field-based approaches and are therefore not conducted routinely and at scale. Climate  
3600 change, altered ignition, and suppression patterns are reshaping fire regimes and ecosystem  
3601 functions, impacting biodiversity, ecosystem services, and C storage. Reduced seed quality,  
3602 resprouting exhaustion, organic soil burning, and misaligned reproductive processes hinder  
3603 post-fire regeneration (Burell et al., 2022; Nolan et al., 2021a; Johnstone et al., 2016). Other  
3604 disturbances like drought and insect infestations compound these effects. For example,  
3605 increased fire activity in boreal forests is reducing fire-adapted species like black spruce,  
3606 favouring deciduous species and altering forest structure and C dynamics (Baltzer et al.,  
3607 2021). In western North America, high-severity fires and warmer, drier conditions lead to poor  
3608 forest recovery and transitions to shrublands or grasslands, affecting habitat, water regulation,  
3609 and C storage (Coop et al., 2020). Similarly, in tropical savannas and forests, fire frequency  
3610 can cause ecosystem transitions that are detrimental for C storage and biodiversity (Staver et  
3611 al., 2011). Furthermore, release of ozone and particulate matter from fires including PM2.5  
3612 negatively impacts plant and ecosystem health (Saxena et al., 2017), and reduces leaf area  
3613 index through drought induced by aerosol radiative effects, leading to reduced carbon uptake  
3614 (Tian et al., 2022).

3615 Observing and modelling shifting fire regimes face challenges due to variability, inconsistent  
3616 historical data, and complex ecosystem responses. Short-term observations often miss long-  
3617 term trends, and species-specific reactions are influenced by fire-adaptive traits and genetic  
3618 variability (Grau-Andrés et al., 2024). Fire regimes respond to multiple disturbances,  
3619 complicating analysis (Nolan et al., 2021a; Coop et al., 2020).

3620 Researchers are using new technologies to address these challenges. Advanced remote  
3621 sensing, including satellite imagery and drones, provides detailed data on fire extent and  
3622 severity (Burell et al., 2022; Baltzer et al., 2021). Improved modelling techniques, such as  
3623 process-based simulation models and machine learning, enhance predictive capabilities  
3624 (Coop et al., 2020; Nolan et al., 2021a). Long-term monitoring networks and citizen science  
3625 initiatives contribute to comprehensive datasets (Baltzer et al., 2021; Coop et al., 2020).  
3626 Advances in genomic tools, climate-adaptive management frameworks, and AI further  
3627 improve fire impact predictions (Nolan et al., 2021a; Coop et al., 2020; Grau-Andrés et al.,  
3628 2024). In all cases, efforts to harmonise local to regional-scale observations of impact are  
3629 required, in a similar manner to emerging compilations of regional fire monitoring systems  
3630 (e.g. Gincheva et al. 2024).

3631 A good example of emerging opportunities stemming from the assemblage of large datasets  
3632 and application of AI is the comprehensive meta-analysis by Grau-Andrés et al. (2024), which  
3633 analysed data from published studies to find that intensified fire regimes reduce plant  
3634 abundance, diversity, and health globally. Increased fire severity has stronger effects than

3635 frequency, with forests, especially conifer and mixed forests, being more negatively impacted  
3636 than open-canopy ecosystems. Woody plants are more susceptible than herbs due to slower  
3637 growth and recovery rates. Arid and cold climates exacerbate these impacts, and transitions  
3638 from surface to crown fires significantly reduce plant abundance, diversity, and health.

3639

## 3640 **8.2.6 Nature-based Solutions and Net Zero**

3641 The impacts of extreme fire on nature-based solutions such as reforestation projects are  
3642 known to be of potential high importance, yet studies of these effects remain rare. Terrestrial  
3643 ecosystems remove about 30% of annual anthropogenic C emissions through enhanced  
3644 growth and ecosystem recovery, but land use change offsets this by increasing annual C  
3645 emissions by about 12% (Friedlingstein et al., 2023). Nature-based solutions, including  
3646 forestry projects for planting, restoration, or conservation, are prominent in net zero strategies  
3647 (Seddon et al., 2020). However, these projects are at risk from fires, leading to inaccurate C  
3648 accounting and reversal risks. The spatial clustering of C projects in specific areas can  
3649 exacerbate risk due to climate variability, such as El Niño impacts. In C markets, projects often  
3650 allocate a portion of their credits to a buffer pool to account for reversal risks, but this may not  
3651 be sufficient in regions facing increasing wildfire extremes (Badgley et al., 2022; Anderegg et  
3652 al., 2024).

3653 Despite these challenges, C markets offer opportunities to fund improved management of fire-  
3654 prone ecosystems like savannas (Russel-Smith et al., 2015) and temperate forests (Nikolakis  
3655 et al., 2022), benefiting ecosystems, climate, and local communities. Effective and scalable C  
3656 markets require accurate and transparent monitoring systems for science-based fire  
3657 management, precise C loss accounting from fires, and assessment of reversal risks. Novel  
3658 satellite-based monitoring can provide early warnings, response to wildfire activity, and better  
3659 estimates of ecosystem C stocks. Field studies remain essential for understanding the  
3660 immediate and long-term impacts of fire on ecosystems (Silva et al., 2020), and new models  
3661 forecasting fire risk over decades are needed to improve management strategies and support  
3662 credible C claims.

3663

## 3664 **8.2.7 Water Quality and other Aquatic Impacts**

3665

3666 Impacts of extreme fires on water quality and other aquatic properties have tended to require  
3667 field-based approaches and are therefore not conducted routinely and at scale. Fire impacts  
3668 freshwater ecosystems mainly through (i) the loss of vegetation and litter cover and (ii) the  
3669 enhanced input of soil, sediment, and ash. This leads to reduced rainfall interception,  
3670 increased runoff, and greater rainfall reaching streams, lakes, and reservoirs (Smith et al.,  
3671 2011). Increased runoff from burned hillslopes can cause erosion, debris flows, and localised  
3672 flooding (Shakesby and Doerr, 2006).

3673

3674 Wildfire ash, enriched in nutrients and contaminants (e.g., metals, polycyclic aromatic  
3675 hydrocarbons) compared to vegetation and soil (Bodi et al., 2014; Sánchez-García et al.,  
3676 2023), affects water quality by increasing turbidity, temperature, nutrient, and toxin content,  
3677 and decreasing dissolved oxygen. These changes can cause increased mortality in freshwater  
3678 ecosystems, algal blooms, and water quality issues for supply catchments (Smith et al., 2011).  
3679 For example, the 2016 Horse River Fire in Canada led to \$9 million in additional water  
3680 treatment costs (Pomeroy et al., 2019). The impacts depend on the burned ecosystem type,  
3681 fire size and severity, vegetation recovery rate, and post-fire rainfall patterns (Shakesby and  
3682 Doerr, 2006; Nunes et al., 2018).

3683

3684 Fire emissions to the atmosphere contain compounds that can enrich or toxify aquatic  
3685 ecosystems (Hamilton et al., 2022; Perron et al., 2022). While 2023 fire impacts on marine

3686 ecosystems are not yet well-documented, past extreme fires have disturbed ocean  
3687 productivity far from the fire source. For instance, large Siberian fires in 2014 boosted Arctic  
3688 phytoplankton blooms by adding reactive nitrogen (Ardyna et al., 2022). Similarly, 2019-2020  
3689 Eurasian fires increased East Siberian Sea productivity by over 200% through nutrient  
3690 deposition and ice melting (Seok et al., 2024). The 2017 Thomas fires in California and the  
3691 2019/2020 Black Summer fires in Australia also caused significant changes in marine  
3692 productivity and coastal ecosystems (Kramer et al., 2020; Ladd et al., 2023; Tang et al., 2021).  
3693 The latter fueled a large phytoplankton bloom, temporarily offsetting the carbon emitted by the  
3694 fires (Tang et al., 2021), though this effect fluctuates with each fire season (Hamilton et al.,  
3695 2022; Wang et al., 2022).

3696

## 3697 **9 Competing Interests Statement**

3698

3699 SV is a member of the editorial board of Earth System Science Data. The authors declare no  
3700 further conflict of interest.

3701

## 3702 **10 Acknowledgements**

3703

3704 The authors thank the following for their contributions to the identification and description of  
3705 key events in the 2023-24 fire season: Robert Ang'ila (Karatina University, Kenya); Miltiadis  
3706 Athanasiou (Institute of Mediterranean Forest Ecosystems, Greece); Davide Ascoli (University  
3707 of Turin); Chris Collins (Tasmania Fire Service, Australia); Abigail Croker (Imperial College,  
3708 London); Helen De Klerk (Stellenbosch University); Kebonyethata Dintwe (University of  
3709 Botswana); David Field (NSW Rural Fire Service, Australia); Ronald Heath (Forestry South  
3710 Africa); Konstantinos Kaoukis (Institute of Mediterranean Forest Ecosystems, Greece); Agnes  
3711 Kristina (Department of Fire and Emergency Services, Australia); Niall MacLennan (Scottish  
3712 Fire and Rescue Service); John Mendelsohn (Okavango Research Institute); Grant Pearce  
3713 (Fire and Emergency NZ, New Zealand); Galia Selaya (Ecosconsult, Bolivia); Russell  
3714 Stephens Peacock (QLD Fire and Emergency Services, Australia); Simeon Telfer (SA Country  
3715 Fire Service, Australia); Emmanuela Zevgoli (Agricultural University of Athens, Greece);  
3716 Hellenic Agricultural Organization "DIMITRA"; The Chico Mendes Institute for Biodiversity  
3717 Conservation (ICMBio, Brazil, Santarém Office). The authors thank Andrew Ciavarella (Met  
3718 Office) for guidance on using the HadGEM3-A data for the fire weather index. The authors  
3719 thank Anna Bradley (UK Met Office) for JULES-ES-ISIMIP data processing and submission to  
3720 ISIMIP repository. The authors thank the working groups "FLARE: Fire science Learning  
3721 AcRoss the Earth System" and "TerraFIRMA: Dummies Guide to using Fire Models" for  
3722 contributing to defining the report scope and establishing contributor links.

3723

## 3724 **11 Author Contributions**

3725

3726 **Conceptualization:** Jones, M. W., Kelley, D. I., Burton, C. A., Di Giuseppe, F.

3727 **Project Administration:** Jones, M. W., Kelley, D. I., Burton, C. A., Di Giuseppe, F.

3728 **Data Curation:** Jones, M. W., Kelley, D. I., Burton, C. A., Di Giuseppe, F., Barbosa, M. L. F.,  
3729 Brambleby, E., Lampe, S., Mataveli, G., McNorton, J., Spuler, F., Wessel, J., Parrington, M.

3730 **Formal Analysis:** Jones, M. W., Kelley, D. I., Burton, C. A., Di Giuseppe, F., Brambleby, E.,  
3731 Lampe, S., Mataveli, G., McNorton, J., Spuler, F., Wessel, J., Parrington, M.

3732 Jones, M. W., Kelley, D. I., Burton, C. A., Di Giuseppe, F., Barbosa, M. L. F., Brambleby, E.,  
3733 Hartley, A., Lampe, S., McNorton, J., Spuler, F., Wessel, J., Parrington, M., Hamilton, D. S.

3734 **Resources/Software:** Andela, N., Giglio, L., Parrington, M., van der Werf, G. R., Barbosa, M.  
3735 L. F., Brambleby, E., Hartley, A., Lampe, S., McNorton, J., Spuler, F., Wessel, J., Burke, E.,  
3736 San-Miguel-Ayanz, J., Qu, Y.

3737 **Visualisation:** Jones, M. W., Kelley, D. I., Burton, C. A., Di Giuseppe, F., Mataveli, G.,  
3738 McNorton, J., Qu, Y., Lombardi, A.

3739 **Writing – Original Draft Preparation:** Jones, M. W., Kelley, D. I., Burton, C. A., Di Giuseppe,  
3740 F., McNorton, J., Anderson, L., Archibald, S., Armenteras, D., Clarke, H., Doerr, S.,  
3741 Fernandes, P., Harris, S., Jain, P., Kolden, C., Ribeiro, N., Saharjo, B., Shuman, J., Tanpipat,  
3742 V., Xanthopoulos, G., Carmenta, R., Hamilton, D. S., Hantson, S., Meier, S., Perron, M. M. G.,  
3743 Parrington, M., Hartley, A., J., Spuler, F., Wessel  
3744 **Writing – Review & Editing:** All authors.  
3745

## 3746 **12 Data Availability**

3747

3748 BA data from NASA's MODIS BA product (MCD64A1) are extended from Giglio et al. (2018)  
3749 and are available at Giglio et al. (2021, <https://lpdaac.usgs.gov/products/mcd64a1v061/>, last  
3750 access: 9 July 2024). GFED4.1s fire C emissions data are extended from van der Werf and  
3751 are available at <https://globalfiredata.org/> (last access: 9 July 2024). GFAS fire C emissions  
3752 data are extended from Kaiser et al. (2012) and are available at  
3753 [https://confluence.ecmwf.int/display/CKB/CAMS+global+biomass+burning+emissions+base  
3754 d+on+fire+radiative+power+%28GFAS%29%3A+data+documentation](https://confluence.ecmwf.int/display/CKB/CAMS+global+biomass+burning+emissions+base+d+on+fire+radiative+power+%28GFAS%29%3A+data+documentation) (last access: 9 July  
3755 2024). Global Fire Atlas are extended from Andela et al. (2019) and are available at Andela  
3756 and Jones (2024, <https://doi.org/10.5281/zenodo.11400062>, last access: 9 July 2024).  
3757 Regional summaries of the MODIS BA, GFED4.1s, GFAS, and the Global Fire Atlas are  
3758 presented here are available at Jones et al. (2024, <https://doi.org/10.5281/zenodo.11400539>,  
3759 last access: 9 July 2024). Studies utilising our regional summaries should cite both the current  
3760 article and the primary reference for the variable(s) of interest: Giglio et al. (2018) for BA; van  
3761 der Werf et al. (2017) for GFED4.1s fire C emissions; Kaiser et al. (2012) for GFAS fire C  
3762 emissions; Andela et al. (2019) for the Global Fire Atlas.  
3763

3764 Driving data, re-gridded BA target data for ConFire and ConFire outputs are available at Kelley  
3765 et al. (2024, <https://doi.org/10.5281/zenodo.11420742>, last access: 9 July 2024). Historical  
3766 (1960-2013) HadGEM3-A are available through the Centre for Environmental Data Analysis  
3767 (CEDA) archive of the NERC's Environmental Data Service (EDS) at  
3768 <http://catalogue.ceda.ac.uk/uuid/99b29b4bfeae470599fb96243e90cde3> (last access: 9 July  
3769 2024). FireMIP / ISIMIP driving and output data is available from the Inter-Sectoral Impact  
3770 Model Intercomparison Project (ISIMIP) repository at <https://data.ISIMIP.org/> (last access: 9  
3771 July 2024).  
3772

## 3773 **13 Code Availability**

3774

3775 ConFire attribution framework code (Kelley et al., 2021; Barbosa, 2024), was incorporated into  
3776 the FLAME repository ([https://github.com/douglask3/Bayesian\\_fire\\_models/tree/ConFire](https://github.com/douglask3/Bayesian_fire_models/tree/ConFire)) and  
3777 will be archived with a doi upon publication. Configuration settings for **Section 3** are in  
3778 namelists/nrt.ini, while **Section 4** and **Section 5** are in namelists/ISIMIP.ini. Scripts for  
3779 reproducing plots can be found in State of Wildfire GitHub repo (currently available at  
3780 [https://github.com/douglask3/State\\_of\\_Wildfires\\_report](https://github.com/douglask3/State_of_Wildfires_report), with an archived doi available upon  
3781 final publication).  
3782

3783 The code used to produce the FWI attribution results is available in State of Wildfire GitHub  
3784 repo (currently available at [https://github.com/douglask3/State\\_of\\_Wildfires\\_report](https://github.com/douglask3/State_of_Wildfires_report), with an  
3785 archived doi available upon final publication). FWI code can be accessed via the ECMWF  
3786 GitHub (<https://github.com/ecmwf-projects/geff>). Met Office implementation of the FWI is  
3787 based on this code, and can be accessed at  
3788 <https://github.com/MetOffice/impactstoolbox/tree/main> with registration. All details of the data  
3789 and code used for the FireMIP attribution results is documented in Burton, Lampe et al. (2023).  
3790

3791 The current version of ibicus, used for JULES-ES bias correction, is available from PyPI  
3792 (<https://pypi.org/project/ibicus/>, last access: 9 July 2024) under the Apache License version

3793 2.0, and is described in detail in <https://ibicus.readthedocs.io/en/latest/> (last access: 9 July  
3794 2024). The source code is available via GitHub (<https://github.com/ecmwf-projects/ibicus>, last  
3795 access: 9 July 2024). Ibicus is also archived on Zenodo by Spuler and Wessel (2023;  
3796 <https://doi.org/10.5281/zenodo.8101898>, last access: 9 July 2024). Model code and  
3797 evaluation for bias-correction of JULES-ES model output can be found at the State of Wildfire  
3798 GitHub repo (currently available at [https://github.com/jakobwes/State-of-Wildfires---Bias-](https://github.com/jakobwes/State-of-Wildfires---Bias-Adjustment)  
3799 [Adjustment](https://github.com/jakobwes/State-of-Wildfires---Bias-Adjustment), with an archived doi available upon final publication).

3800

### 3801 **13.1 Financial support**

3802

3803 MWJ was funded by the UK Natural Environment Research Council (NERC) (NE/V01417X/1).  
3804 DIK was supported by NERC as part of the LTSM2 TerraFIRMA project and NC-International  
3805 programme (NE/X006247/1) delivering National Capability. CAB was funded by the Met Office  
3806 Climate Science for Service Partnership (CSSP) Brazil project which is supported by the  
3807 Department for Science, Innovation & Technology (DSIT), and by the Met Office Hadley  
3808 Centre Climate Programme funded by DSIT. PMF acknowledges support by National Funds  
3809 by FCT - Portuguese Foundation for Science and Technology (project UIDB/04033/2020,  
3810 <https://doi.org/10.54499/UIDB/04033/2020>). FDG and JMC are both funded by a service  
3811 contract (n 942604) issued by the Joint Research Center on behalf of the European  
3812 Commission. LOA acknowledges support by the São Paulo Research Foundation  
3813 (FAPESP)(projects: 2021/07660-2 and 2020/16457-3) and by the National Council for  
3814 Scientific and Technological Development (CNPq), productivity scholarship (process:  
3815 314473/2020-3). GM acknowledges support by FAPESP (grants 2019/25701-8, 2020/15230-  
3816 5 and 2023/03206-0). SL was supported by a PhD Fundamental Research Grant by Fonds  
3817 Wetenschappelijk Onderzoek - Vlaanderen (11M7723N). SM gratefully acknowledges the  
3818 support of the Dragon Capital Chair on Biodiversity Economics. ECh is being supported by  
3819 the European Space Agency's Climate Change Initiative (ESA CCI) programme (FireCCI:  
3820 Contract No. 4000126706/19/I-NB). CAK acknowledges support from USDA NIFA (award  
3821 2022-67019-36435). YQ was supported by the China Scholarship Council (CSC) under grant  
3822 number 201906040220. MMGP was supported by a Marie Skłodowska-Curie Actions 2021  
3823 Postdoctoral Fellow funding number 101064063. HC was funded by the Westpac Scholars  
3824 Trust via a Westpac Research Fellowship. SHD acknowledges support from NERC (grant  
3825 NE/X005143/1) and the FirEURisk project, which has received funding from the European  
3826 Union's Horizon 2020 research and innovation programme under grant agreement No  
3827 101003890. EB was supported by the NERC ARIES Doctoral Training Partnership (grant  
3828 number NE/S007334/1). JKS acknowledges support from the National Aeronautics and Space  
3829 Administration (NASA) FireSense Project. NA was supported by the Sense4Fire project as  
3830 part of ESA's C Cycle Cluster (ESA contract number: 4000134840/21/I-NB). MLFB was  
3831 supported by the Coordination for the Improvement of Higher Education Personnel (CAPES),  
3832 Finance Code 001. The contribution of SV was funded by the European Research Council  
3833 through a Consolidator grant under the European Union's Horizon 2020 research and  
3834 innovation program (grant agreement No. 101000987). RC is grateful to the Tyndall Centre  
3835 for Climate Change Research for financial support.

3836

### 3837 **14 References**

3838

3839 Abatzoglou, J. T., Williams, A. P., Boschetti, L., Zubkova, M., and Kolden, C. A.: Global patterns of interannual climate–fire  
3840 relationships, *Glob Change Biol*, 24, 5164–5175, <https://doi.org/10.1111/gcb.14405>, 2018.

3841 Abatzoglou, J. T., Williams, A. P., and Barbero, R.: Global Emergence of Anthropogenic Climate Change in Fire Weather Indices,  
3842 *Geophys. Res. Lett.*, 46, 326–336, <https://doi.org/10.1029/2018GL080959>, 2019.



- 3843 Abatzoglou, J. T., Juang, C. S., Williams, A. P., Kolden, C. A., and Westerling, A. L.: Increasing Synchronous Fire Danger in  
3844 Forests of the Western United States, *Geophysical Research Letters*, 48, e2020GL091377,  
3845 <https://doi.org/10.1029/2020GL091377>, 2021.
- 3846 Abatzoglou, J. T., Kolden, C. A., Williams, A. P., Sadegh, M., Balch, J. K., and Hall, A.: Downslope Wind-Driven Fires in the  
3847 Western United States, *Earth's Future*, 11, e2022EF003471, <https://doi.org/10.1029/2022EF003471>, 2023.
- 3848 Abram, N. J., Henley, B. J., Sen Gupta, A., Lippmann, T. J. R., Clarke, H., Dowdy, A. J., Sharples, J. J., Nolan, R. H., Zhang, T.,  
3849 Wooster, M. J., Wurtzel, J. B., Meissner, K. J., Pitman, A. J., Ukkola, A. M., Murphy, B. P., Tapper, N. J., and Boer, M. M.:  
3850 Connections of climate change and variability to large and extreme forest fires in southeast Australia, *Commun Earth Environ*, 2,  
3851 8, <https://doi.org/10.1038/s43247-020-00065-8>, 2021.
- 3852 Adzhar, R., Kelley, D. I., Dong, N., George, C., Torello Raventos, M., Veenendaal, E., Feldpausch, T. R., Phillips, O. L., Lewis,  
3853 S. L., Sonké, B., Taedoumg, H., Schwantes Marimon, B., Domingues, T., Arroyo, L., Djagbletey, G., Saiz, G., and Gerard, F.:  
3854 MODIS Vegetation Continuous Fields tree cover needs calibrating in tropical savannas, *Biogeosciences*, 19, 1377–1394,  
3855 <https://doi.org/10.5194/bg-19-1377-2022>, 2022.
- 3856 AfricaNews: Wildfires force evacuations of South African coastal towns, available at:  
3857 <https://www.africanews.com/2024/01/31/wildfires-force-evacuations-of-south-african-coastal-towns/>, last access: 9 July 2024,  
3858 Africanews, 31st January, 2024.
- 3859 Aguilera, R., Corringham, T., Gershunov, A., and Benmarhnia, T.: Wildfire smoke impacts respiratory health more than fine  
3860 particles from other sources: observational evidence from Southern California, *Nat Commun*, 12, 1493,  
3861 <https://doi.org/10.1038/s41467-021-21708-0>, 2021.
- 3862 Agustí-Panareda, A., Diamantakis, M., Massart, S., Chevallier, F., Muñoz-Sabater, J., Barré, J., Curcoll, R., Engelen, R.,  
3863 Langerock, B., Law, R. M., Loh, Z., Morguí, J. A., Parrington, M., Peuch, V.-H., Ramonet, M., Roehl, C., Vermeulen, A. T.,  
3864 Warneke, T., and Wunch, D.: Modelling CO<sub>2</sub> weather – why horizontal resolution matters, *Atmospheric Chemistry and Physics*,  
3865 19, 7347–7376, <https://doi.org/10.5194/acp-19-7347-2019>, 2019.
- 3866 Al Jazeera: 2023a From Algeria to Syria, heatwaves scorch Middle East, North Africa, available at:  
3867 <https://www.aljazeera.com/news/2023/7/19/from-algeria-to-syria-heatwaves-scorch-middle-east-north-africa>, last access: 9 July  
3868 2024, Al Jazeera, 19th July, 2023a.
- 3869 Al Jazeera: 2023b Wildfires in Algeria kill dozens, force hundreds to flee homes, available at:  
3870 <https://www.aljazeera.com/news/2023/7/24/deadly-algeria-wildfires-amid-extreme-heat-high-winds>, last access: 9 July 2024, Al  
3871 Jazeera, 24th July, 2023b.
- 3872 Al Jazeera: More than 60 people killed as forest fires rage in Chile, available at: [https://www.aljazeera.com/news/2024/2/3/chile-](https://www.aljazeera.com/news/2024/2/3/chile-declares-state-of-emergency-over-raging-forest-fires)  
3873 [declares-state-of-emergency-over-raging-forest-fires](https://www.aljazeera.com/news/2024/2/3/chile-declares-state-of-emergency-over-raging-forest-fires), last access: 9 July 2024, Al Jazeera, 4th February, 2024.
- 3874 ALER: Alarmantes cifras de incendios forestales se registran en Venezuela durante el primer trimestre de 2024 – ALER, available  
3875 at: [https://aler.org/nota\\_informativa/alarmanentes-cifras-de-incendios-forestales-se-registran-en-venezuela-durante-el-primer-](https://aler.org/nota_informativa/alarmanentes-cifras-de-incendios-forestales-se-registran-en-venezuela-durante-el-primer-trimestre-de-2024/)  
3876 [trimestre-de-2024/](https://aler.org/nota_informativa/alarmanentes-cifras-de-incendios-forestales-se-registran-en-venezuela-durante-el-primer-trimestre-de-2024/), last access: 9 July 2024, 2024.
- 3877 Alvarado, S. T., Andela, N., Silva, T. S. F., and Archibald, S.: Thresholds of fire response to moisture and fuel load differ between  
3878 tropical savannas and grasslands across continents, *Global Ecol Biogeogr*, 29, 331–344, <https://doi.org/10.1111/geb.13034>,  
3879 2020.
- 3880 Andela, N. and Jones, M. W.: Update of: The Global Fire Atlas of individual fire size, duration, speed and direction,  
3881 <https://doi.org/10.5281/zenodo.11400062>, 2024.
- 3882 Andela, N., Morton, D. C., Giglio, L., Chen, Y., van der Werf, G. R., Kasibhatla, P. S., DeFries, R. S., Collatz, G. J., Hantson, S.,  
3883 Kloster, S., Bachelet, D., Forrest, M., Lasslop, G., Li, F., Mangeon, S., Melton, J. R., Yue, C., and Randerson, J. T.: A human-  
3884 driven decline in global burned area, *Science*, 356, 1356–1362, <https://doi.org/10.1126/science.aal4108>, 2017.
- 3885 Andela, N., Morton, D. C., Giglio, L., Paugam, R., Chen, Y., and Hantson, S.: The Global Fire Atlas of individual fire size, duration,  
3886 speed and direction, 24, 2019.

- 3887 Andela, N., Morton, D. C., Schroeder, W., Chen, Y., Brando, P. M., and Randerson, J. T.: Tracking and classifying Amazon fire  
3888 events in near real time, *Science Advances*, 8, eabd2713, <https://doi.org/10.1126/sciadv.abd2713>, 2022.
- 3889 Anderegg, W. R. L., Trugman, A. T., Vargas, G., Wu, C., and Yang, L.: Current forest carbon offset buffer pools do not adequately  
3890 insure against disturbance-driven carbon losses, <https://doi.org/10.1101/2024.03.28.587000>, 31 March 2024.
- 3891 Antara News: ASEAN inaugurates ACC THPC to combat haze pollution, available at:  
3892 <https://en.antaranews.com/news/292902/asean-inaugurates-acc-thpc-to-combat-haze-pollution>, last access: 9 July 2024, Antara  
3893 News, 2023.
- 3894 Aragão, L. E. O. C., Anderson, L. O., Fonseca, M. G., Rosan, T. M., Vedovato, L. B., Wagner, F. H., Silva, C. V. J., Silva Junior,  
3895 C. H. L., Arai, E., Aguiar, A. P., Barlow, J., Berenguer, E., Deeter, M. N., Domingues, L. G., Gatti, L., Gloor, M., Malhi, Y., Marengo,  
3896 J. A., Miller, J. B., Phillips, O. L., and Saatchi, S.: 21st Century drought-related fires counteract the decline of Amazon  
3897 deforestation carbon emissions, *Nat Commun*, 9, 536, <https://doi.org/10.1038/s41467-017-02771-y>, 2018.
- 3898 Aragão, L. E. O. C., Malhi, Y., Roman-Cuesta, R. M., Saatchi, S., Anderson, L. O., and Shimabukuro, Y. E.: Spatial patterns and  
3899 fire response of recent Amazonian droughts, *Geophysical Research Letters*, 34, <https://doi.org/10.1029/2006GL028946>, 2007.
- 3900 ArcGIS Hub: World Continents, available at: <https://hub.arcgis.com/maps/CESJ:world-continents>, last access: 9 July 2024, 2024.
- 3901 Archibald, S. and Roy, D. P.: Identifying individual fires from satellite-derived burned area data, in: 2009 IEEE International  
3902 Geoscience and Remote Sensing Symposium, 2009 IEEE International Geoscience and Remote Sensing Symposium, III-160-  
3903 III-163, <https://doi.org/10.1109/IGARSS.2009.5417974>, 2009.
- 3904 Archibald, S., Roy, D. P., van WILGEN, B. W., and Scholes, R. J.: What limits fire? An examination of drivers of burnt area in  
3905 Southern Africa, *Global Change Biology*, 15, 613–630, <https://doi.org/10.1111/j.1365-2486.2008.01754.x>, 2009.
- 3906 Ardyna, M., Hamilton, D. S., Harmel, T., Lacour, L., Bernstein, D. N., Laliberté, J., Horvat, C., Laxenaire, R., Mills, M. M., van  
3907 Dijken, G., Polyakov, I., Claustre, H., Mahowald, N., and Arrigo, K. R.: Wildfire aerosol deposition likely amplified a summertime  
3908 Arctic phytoplankton bloom, *Commun Earth Environ*, 3, 1–8, <https://doi.org/10.1038/s43247-022-00511-9>, 2022.
- 3909 Arino, O., Rosaz, J.-M., and Goloub, P.: The ATSR World Fire Atlas A synergy with ‘Polder’ aerosol products, *Earth Observation  
3910 Quarterly*, 64, 30, 1999.
- 3911 Armero, A. J.: El fuego en Las Hurdes y Sierra de Gata deja a Pinofranqueado sin agua potable, available at:  
3912 <https://www.hoy.es/extremadura/fuego-hurdes-sierra-gata-deja-pinofranqueado-agua-20230624190605-nt.html>, last access: 9  
3913 July 2024, Hoy, 2023.
- 3914 Artés, T., Oom, D., de Rigo, D., Durrant, T. H., Maianti, P., Libertà, G., and San-Miguel-Ayanz, J.: A global wildfire dataset for the  
3915 analysis of fire regimes and fire behaviour, *Sci Data*, 6, 296, <https://doi.org/10.1038/s41597-019-0312-2>, 2019.
- 3916 Athanasiou, M.: Preliminary findings on the behaviour and spread of the wildfire of August 2023 in Evros, Greece (in Greek with  
3917 English abstract). Project “Learning from the Evros wildfire: Firefighting effectiveness evaluation and proposals”. WWF Greece,  
3918 Athens, 76 p., WWF Greece, Athens, 2024.
- 3919 Atlas of Namibia: Atlas of Namibia Chapter 8: Conservation, available at: <https://atlasofnamibia.online/chapter-8/conservation>,  
3920 last access: 9 July 2024, 2021.
- 3921 Austen, I.: As ‘Zombie Fires’ Smolder, Canada Braces for Another Season of Flames, available at:  
3922 <https://www.nytimes.com/2024/03/04/canada-zombie-fires-wildfire.html>, last access: 9 July 2024, New York Times, 4th March,  
3923 2024.
- 3924 B. Ankhtuya: Bush fire in Dornod spreads to Russia - News.MN, available at: <https://news.mn/en/791879/>, last access: 9 July  
3925 2024, News.MN, 2020.
- 3926 Badgley, G., Chay, F., Chegwidan, O. S., Hamman, J. J., Freeman, J., and Cullenward, D.: California’s forest carbon offsets  
3927 buffer pool is severely undercapitalized, *Front. For. Glob. Change*, 5, <https://doi.org/10.3389/ffgc.2022.930426>, 2022.



- 3928 Baltzer, J. L., Day, N. J., Walker, X. J., Greene, D., Mack, M. C., Alexander, H. D., Arseneault, D., Barnes, J., Bergeron, Y.,  
3929 Boucher, Y., Bourgeau-Chavez, L., Brown, C. D., Carrière, S., Howard, B. K., Gauthier, S., Parisien, M.-A., Reid, K. A., Rogers,  
3930 B. M., Roland, C., Sirois, L., Stehn, S., Thompson, D. K., Turetsky, M. R., Veraverbeke, S., Whitman, E., Yang, J., and Johnstone,  
3931 J. F.: Increasing fire and the decline of fire adapted black spruce in the boreal forest, *Proceedings of the National Academy of*  
3932 *Sciences*, 118, e2024872118, <https://doi.org/10.1073/pnas.2024872118>, 2021.
- 3933 Barbosa, M. L. F.: *Tracing the Ashes: Uncovering Burned Area Patterns and Drivers Over the Brazilian Biomes* (PhD Thesis  
3934 supervised by Liana Anderson), Instituto Nacional de Pesquisas Espaciais, São José dos Campos, 2024.
- 3935 Barlow, J., Parry, L., Gardner, T. A., Ferreira, J., Aragão, L. E. O. C., Carmenta, R., Berenguer, E., Vieira, I. C. G., Souza, C.,  
3936 and Cochrane, M. A.: The critical importance of considering fire in REDD+ programs, *Biological Conservation*, 154, 1–8,  
3937 <https://doi.org/10.1016/j.biocon.2012.03.034>, 2012.
- 3938 Barlow, J., França, F., Gardner, T. A., Hicks, C. C., Lennox, G. D., Berenguer, E., Castello, L., Economo, E. P., Ferreira, J.,  
3939 Guénard, B., Gontijo Leal, C., Isaac, V., Lees, A. C., Parr, C. L., Wilson, S. K., Young, P. J., and Graham, N. A. J.: The future of  
3940 hyperdiverse tropical ecosystems, *Nature*, 559, 517–526, <https://doi.org/10.1038/s41586-018-0301-1>, 2018.
- 3941 Barlow, J., Berenguer, E., Carmenta, R., and França, F.: Clarifying Amazonia's burning crisis, *Glob Change Biol*, 26, 319–321,  
3942 <https://doi.org/10.1111/gcb.14872>, 2020.
- 3943 Barnes, C., Boulanger, Y., Keeping, T., Gachon, P., Gillett, N., Boucher, J., Roberge, F., Kew, S., Haas, O., Heinrich, D.,  
3944 Vahlberg, M., Singh, R., Elbe, M., Sivanu, S., Arrighi, J., Van Aalst, M., Otto, F., Zachariah, M., Krikken, F., Wang, X., Erni, S.,  
3945 Pietropalo, E., Avis, A., Bisailon, A., and Kimutai, J.: Climate change more than doubled the likelihood of extreme fire weather  
3946 conditions in Eastern Canada, available at: <http://spiral.imperial.ac.uk/handle/10044/1/105981>, last access: 9 July 2024,  
3947 <https://doi.org/10.25561/105981>, 2023.
- 3948 BBC News: Why is Canada having so many wildfires this season?, available at: [https://www.bbc.com/news/world-us-canada-](https://www.bbc.com/news/world-us-canada-69011493)  
3949 [69011493](https://www.bbc.com/news/world-us-canada-69011493), last access: 9 July 2024, BBC News, 15th May, 2024.
- 3950 Bedia, J., Herrera, S., Gutiérrez, J. M., Benali, A., Brands, S., Mota, B., and Moreno, J. M.: Global patterns in the sensitivity of  
3951 burned area to fire-weather: Implications for climate change, *Agricultural and Forest Meteorology*, 214–215, 369–379,  
3952 <https://doi.org/10.1016/j.agrformet.2015.09.002>, 2015.
- 3953 Bedia, J., Golding, N., Casanueva, A., Iturbide, M., Buontempo, C., and Gutiérrez, J. M.: Seasonal predictions of Fire Weather  
3954 Index: Paving the way for their operational applicability in Mediterranean Europe, *Climate Services*, 9, 101–110,  
3955 <https://doi.org/10.1016/j.cliser.2017.04.001>, 2018.
- 3956 Belcher, C. M., Brown, I., Clay, G. D., Doerr, S. H., Elliott, A., Gazzard, R., Kettridge, N., Morison, J., Perry, M., Santin, C., and  
3957 Smith, T. E. L.: UK Wildfires and their Climate Challenges, Expert Led Report Prepared for the Third UK Climate Change Risk  
3958 Assessment (CCRA3), available at: [https://www.ukclimaterisk.org/wp-content/uploads/2021/06/UK-Wildfires-and-their-Climate-](https://www.ukclimaterisk.org/wp-content/uploads/2021/06/UK-Wildfires-and-their-Climate-Challenges.pdf)  
3959 [Challenges.pdf](https://www.ukclimaterisk.org/wp-content/uploads/2021/06/UK-Wildfires-and-their-Climate-Challenges.pdf), last access: 9 July 2024, University of Exeter Global Systems Institute, Exeter, 2021.
- 3960 Betts, R. A., Belcher, S. E., Hermanson, L., Klein Tank, A., Lowe, J. A., Jones, C. D., Morice, C. P., Rayner, N. A., Scaife, A. A.,  
3961 and Stott, P. A.: Approaching 1.5 °C: how will we know we've reached this crucial warming mark?, *Nature*, 624, 33–35,  
3962 <https://doi.org/10.1038/d41586-023-03775-z>, 2023.
- 3963 Beverly, J. L. and Bothwell, P.: Wildfire evacuations in Canada 1980–2007, *Nat Hazards*, 59, 571–596,  
3964 <https://doi.org/10.1007/s11069-011-9777-9>, 2011.
- 3965 Bhandari, S. R.: Culprits behind dense smog in northern Thailand, Laos: corn and wildfires, available at:  
3966 <https://www.rfa.org/english/news/environment/smog-04172023135125.html>, last access: 9 July 2024, Radio Free Asia, 2023.
- 3967 Bilbao, B., Mistry, J., Millán, A., and Berardi, A.: Sharing Multiple Perspectives on Burning: Towards a Participatory and  
3968 Intercultural Fire Management Policy in Venezuela, Brazil, and Guyana, *Fire*, 2, 39, <https://doi.org/10.3390/fire2030039>, 2019.
- 3969 Bistinas, I., Harrison, S. P., Prentice, I. C., and Pereira, J. M. C.: Causal relationships versus emergent patterns in the global  
3970 controls of fire frequency, *Biogeosciences*, 11, 5087–5101, <https://doi.org/10.5194/bg-11-5087-2014>, 2014.

- 3971 Bodí, M. B., Martin, D. A., Balfour, V. N., Santín, C., Doerr, S. H., Pereira, P., Cerdà, A., and Mataix-Solera, J.: Wildland fire ash:  
3972 Production, composition and eco-hydro-geomorphic effects, *Earth-Science Reviews*, 130, 103–127,  
3973 <https://doi.org/10.1016/j.earscirev.2013.12.007>, 2014.
- 3974 Borneo Bulletin: Mongolia battles wildfire in eastern region, available at: <https://borneobulletin.com.bn/mongolia-battles-wildfire-in-eastern-region/>, last access: 9 July 2024, Mongolia battles wildfire in eastern region, 2023.
- 3976 Boschetti, L. and Roy, D. P.: Defining a fire year for reporting and analysis of global interannual fire variability, *Journal of*  
3977 *Geophysical Research: Biogeosciences*, 113, <https://doi.org/10.1029/2008JG000686>, 2008.
- 3978 Boucher, O., Servonnat, J., Albright, A. L., Aumont, O., Balkanski, Y., Bastrikov, V., Bekki, S., Bonnet, R., Bony, S., Bopp, L.,  
3979 Braconnot, P., Brockmann, P., Cadule, P., Caubel, A., Cheruy, F., Codron, F., Cozic, A., Cugnet, D., D'Andrea, F., Davini, P., de  
3980 Lavergne, C., Denvil, S., Deshayes, J., Devilliers, M., Ducharne, A., Dufresne, J.-L., Dupont, E., Éthé, C., Fairhead, L., Falletti,  
3981 L., Flavoni, S., Foujols, M.-A., Gardoll, S., Gastineau, G., Ghattas, J., Grandpeix, J.-Y., Guenet, B., Guez, E., Lionel, Guilyardi,  
3982 E., Guimberteau, M., Hauglustaine, D., Hourdin, F., Idelkadi, A., Joussaume, S., Kageyama, M., Khodri, M., Krinner, G., Lebas,  
3983 N., Levavasseur, G., Lévy, C., Li, L., Lott, F., Lurton, T., Luysaert, S., Madec, G., Madeleine, J.-B., Maignan, F., Marchand, M.,  
3984 Marti, O., Mellul, L., Meurdesoif, Y., Mignot, J., Musat, I., Ottlé, C., Peylin, P., Planton, Y., Polcher, J., Rio, C., Rochetin, N.,  
3985 Rousset, C., Sepulchre, P., Sima, A., Swingedouw, D., Thiéblemont, R., Traore, A. K., Vancoppenolle, M., Vial, J., Vialard, J.,  
3986 Viovy, N., and Vuichard, N.: Presentation and Evaluation of the IPSL-CM6A-LR Climate Model, *Journal of Advances in Modeling*  
3987 *Earth Systems*, 12, e2019MS002010, <https://doi.org/10.1029/2019MS002010>, 2020.
- 3988 Boulanger, Y., Arseneault, D., Bélisle, A. C., Bergeron, Y., Boucher, J., Boucher, Y., Danneyrolles, V., Erni, S., Gachon, P.,  
3989 Girardin, M. P., Grant, E., Grondin, P., Jetté, J.-P., Labadie, G., Leblond, M., Leduc, A., Puigdevall, J. P., St-Laurent, M.-H.,  
3990 Tremblay, J. A., and Waldron, K.: The 2023 wildfire season in Québec: an overview of extreme conditions, impacts, lessons  
3991 learned and considerations for the future, <https://doi.org/10.1101/2024.02.20.581257>, 22 February 2024.
- 3992 Boussetta, S., Balsamo, G., Arduini, G., Dutra, E., McNorton, J., Choulga, M., Agustí-Panareda, A., Beljaars, A., Wedi, N., Munõz-  
3993 Sabater, J., de Rosnay, P., Sandu, I., Hadade, I., Carver, G., Mazzetti, C., Prudhomme, C., Yamazaki, D., and Zsoter, E.: ECLand:  
3994 The ECMWF Land Surface Modelling System, *Atmosphere*, 12, 723, <https://doi.org/10.3390/atmos12060723>, 2021.
- 3995 Bradshaw, L. S., Deeming, J. E., Burgan, R. E., and compilers.Cohen, J. D.: The 1978 National Fire-Danger Rating System:  
3996 technical documentation, General Technical Report INT-169. Ogden, UT: U.S. Department of Agriculture, Forest Service,  
3997 Intermountain Forest and Range Experiment Station. 44 p., 169, <https://doi.org/10.2737/INT-GTR-169>, 1984a.
- 3998 Bradshaw, L. S., Deeming, J., Burgan, R., and Cohen, J.: The 1978 National Fire-Danger Rating System: Technical  
3999 Documentation, U.S. Department of Agriculture, Forest Service, Intermountain Forest and Range Experiment Station, 52 pp.,  
4000 1984b.
- 4001 Bureau of Meteorology: Annual Australian Climate Statement 2023, scheme=AGLSTERMS.AglsAgent;  
4002 corporateName=Australian Government - Bureau of Meteorology, 2024.
- 4003 Burrell, A. L., Sun, Q., Baxter, R., Kukavskaya, E. A., Zhila, S., Shestakova, T., Rogers, B. M., Kaduk, J., and Barrett, K.: Climate  
4004 change, fire return intervals and the growing risk of permanent forest loss in boreal Eurasia, *Science of The Total Environment*,  
4005 831, 154885, <https://doi.org/10.1016/j.scitotenv.2022.154885>, 2022.
- 4006 Burton, C., Lampe, S., Kelley, D., Thiery, W., Hantson, S., Christidis, N., Gudmundsson, L., Forrest, M., Burke, E., Chang, J.,  
4007 Huang, H., Ito, A., Kou-Giesbrecht, S., Lasslop, G., Li, W., Nieradzki, L., Li, F., Chen, Y., Randerson, J., Reyer, C., and Mengel,  
4008 M.: Global burned area increasingly explained by climate change, <https://doi.org/10.21203/rs.3.rs-3168150/v1>, 20 July 2023.
- 4009 Cai, W., Cowan, T., and Raupach, M.: Positive Indian Ocean Dipole events precondition southeast Australia bushfires,  
4010 *Geophysical Research Letters*, 36, <https://doi.org/10.1029/2009GL039902>, 2009.
- 4011 California Department of Forestry and Fire Protection: CAL FIRE Damage Inspection (DINS) Data, available at:  
4012 <https://www.arcgis.com/sharing/rest/content/items/994d3dc4569640caadbcc3198d5a3da1>, last access: 9 July 2024, 2024.

- 4013 Calkin, D. E., Barrett, K., Cohen, J. D., Finney, M. A., Pyne, S. J., and Quarles, S. L.: Wildland-urban fire disasters aren't actually  
4014 a wildfire problem, *Proceedings of the National Academy of Sciences*, 120, e2315797120,  
4015 <https://doi.org/10.1073/pnas.2315797120>, 2023.
- 4016 Canadell, J. G., Meyer, C. P. (Mick), Cook, G. D., Dowdy, A., Briggs, P. R., Knauer, J., Pepler, A., and Haverd, V.: Multi-decadal  
4017 increase of forest burned area in Australia is linked to climate change, *Nat Commun*, 12, 6921, [https://doi.org/10.1038/s41467-  
4018 021-27225-4](https://doi.org/10.1038/s41467-021-27225-4), 2021.
- 4019 Canadian Environmental Protection Act Federal-Provincial Working Group on Air Quality: National ambient air quality objectives  
4020 for particulate matter. Part 1, Science assessment document: executive summary / a report by the Canadian Environmental  
4021 Protection Act (CEPA)/Federal-Provincial Advisory Committee (FPAC) Working Group on Air Quality Objectives and  
4022 Guidelines.25p., Health Canada, Environmental Health Directorate, Ottawa, Ontario, 25 pp., 1998.
- 4023 Canadian Interagency Forest Fire Centre: CIFFC Canada Report 2023 Fire Season, available at:  
4024 [https://ciffc.ca/sites/default/files/2024-03/CIFFC\\_2023CanadaReport\\_FINAL.pdf](https://ciffc.ca/sites/default/files/2024-03/CIFFC_2023CanadaReport_FINAL.pdf), last access: 9 July 2024, Canadian Interagency  
4025 Forest Fire Centre, Canada, 2023.
- 4026 Canelles, Q., Aquilué, N., James, P. M. A., Lawler, J., and Brotons, L.: Global review on interactions between insect pests and  
4027 other forest disturbances, *Landscape Ecol*, 36, 945–972, <https://doi.org/10.1007/s10980-021-01209-7>, 2021.
- 4028 Cardil, A., Rodrigues, M., Tapia, M., Barbero, R., Ramírez, J., Stoof, C. R., Silva, C. A., Mohan, M., and de-Miguel, S.: Climate  
4029 teleconnections modulate global burned area, *Nat Commun*, 14, 427, <https://doi.org/10.1038/s41467-023-36052-8>, 2023.
- 4030 Carmenta, R., Coudel, E., and Steward, A. M.: Forbidden fire: Does criminalising fire hinder conservation efforts in swidden  
4031 landscapes of the Brazilian Amazon?, *Geographical Journal*, 185, 23–37, <https://doi.org/10.1111/geoj.12255>, 2019.
- 4032 Carmenta, R., Cammelli, F., Dressler, W., Verbicaro, C., and Zaehring, J. G.: Between a rock and a hard place: The burdens  
4033 of uncontrolled fire for smallholders across the tropics, *World Development*, 145, 105521,  
4034 <https://doi.org/10.1016/j.worlddev.2021.105521>, 2021.
- 4035 Carter, T. S., Heald, C. L., Jimenez, J. L., Campuzano-Jost, P., Kondo, Y., Moteki, N., Schwarz, J. P., Wiedinmyer, C., Darmenov,  
4036 A. S., Da Silva, A. M., and Kaiser, J. W.: How emissions uncertainty influences the distribution and radiative impacts of smoke  
4037 from fires in North America, *Atmos. Chem. Phys.*, 20, 2073–2097, <https://doi.org/10.5194/acp-20-2073-2020>, 2020.
- 4038 Carvalho, A., Flannigan, M. D., Logan, K., Miranda, A. I., and Borrego, C.: Fire activity in Portugal and its relationship to weather  
4039 and the Canadian Fire Weather Index System, *Int. J. Wildland Fire*, 17, 328–338, <https://doi.org/10.1071/WF07014>, 2008.
- 4040 Casanueva, A., Herrera, S., Iturbide, M., Lange, S., Jury, M., Dosio, A., Maraun, D., and Gutiérrez, J. M.: Testing bias adjustment  
4041 methods for regional climate change applications under observational uncertainty and resolution mismatch, *Atmospheric Science  
4042 Letters*, 21, e978, <https://doi.org/10.1002/asl.978>, 2020.
- 4043 Cátedra Cambio Climático de la Universidad de Oviedo: Evaluación de los Impactos Medioambientales Producidos por el  
4044 Incendio de Foyedo (Asturias) Ocurrido en Primavera de 2023, available at: [https://cucc-uo.es/evaluacion-de-los-impactos-  
4045 medioambientales-producidos-por-el-incendio-de-foyedo-asturias-ocurrido-en-primavera-de-2023/](https://cucc-uo.es/evaluacion-de-los-impactos-medioambientales-producidos-por-el-incendio-de-foyedo-asturias-ocurrido-en-primavera-de-2023/), last access: 9 July 2024,  
4046 2023.
- 4047 CBC News: Kelowna declares state of emergency after wildfire jumps Okanagan Lake, prompting more evacuations, available  
4048 at: <https://www.cbc.ca/news/canada/british-columbia/what-you-need-to-know-about-bc-wildfires-aug-17-2023-1.6938796>, last  
4049 access: 9 July 2024, CBC News, 17th August, 2023.
- 4050 Cecil, D. J., Buechler, D. E., and Blakeslee, R. J.: Gridded lightning climatology from TRMM-LIS and OTD: Dataset description,  
4051 *Atmospheric Research*, 135–136, 404–414, <https://doi.org/10.1016/j.atmosres.2012.06.028>, 2014.
- 4052 Centre for Research on the Epidemiology of Disasters: EM-DAT International Disaster Database, available at:  
4053 <https://public.emdat.be/>, last access: 9 July 2024, 2024.
- 4054 Chen, B., Wu, S., Jin, Y., Song, Y., Wu, C., Venevsky, S., Xu, B., Webster, C., and Gong, P.: Wildfire risk for global wildland–  
4055 urban interface areas, *Nat Sustain*, 7, 474–484, <https://doi.org/10.1038/s41893-024-01291-0>, 2024.

- 4056 Chen, T. and Guestrin, C.: XGBoost: A Scalable Tree Boosting System, in: Proceedings of the 22nd ACM SIGKDD International  
4057 Conference on Knowledge Discovery and Data Mining, New York, NY, USA, 785–794, <https://doi.org/10.1145/2939672.2939785>,  
4058 2016.
- 4059 Chen, Y., Morton, D. C., Andela, N., van der Werf, G. R., Giglio, L., and Randerson, J. T.: A pan-tropical cascade of fire driven  
4060 by El Niño/Southern Oscillation, *Nature Clim Change*, 7, 906–911, <https://doi.org/10.1038/s41558-017-0014-8>, 2017.
- 4061 Chen, Y., Hantson, S., Andela, N., Coffield, S. R., Graff, C. A., Morton, D. C., Ott, L. E., Fofoula-Georgiou, E., Smyth, P.,  
4062 Goulden, M. L., and Randerson, J. T.: California wildfire spread derived using VIIRS satellite observations and an object-based  
4063 tracking system, *Sci Data*, 9, 249, <https://doi.org/10.1038/s41597-022-01343-0>, 2022.
- 4064 Chen, Y., Hall, J., van Wees, D., Andela, N., Hantson, S., Giglio, L., van der Werf, G. R., Morton, D. C., and Randerson, J. T.:  
4065 Multi-decadal trends and variability in burned area from the fifth version of the Global Fire Emissions Database (GFED5), *Earth  
4066 System Science Data*, 15, 5227–5259, <https://doi.org/10.5194/essd-15-5227-2023>, 2023.
- 4067 Christidis, N., Stott, P. A., Scaife, A. A., Arribas, A., Jones, G. S., Copsey, D., Knight, J. R., and Tennant, W. J.: A New HadGEM3-  
4068 A-Based System for Attribution of Weather- and Climate-Related Extreme Events, *Journal of Climate*, 26, 2756–2783,  
4069 <https://doi.org/10.1175/JCLI-D-12-00169.1>, 2013.
- 4070 Chu, L., Grafton, R. Q., and Nelson, H.: Accounting for forest fire risks: global insights for climate change mitigation, *Mitig Adapt  
4071 Strateg Glob Change*, 28, 48, <https://doi.org/10.1007/s11027-023-10087-0>, 2023.
- 4072 Chuvieco, E., Mouillot, F., van der Werf, G. R., San Miguel, J., Tanase, M., Koutsias, N., García, M., Yebra, M., Padilla, M., Gitas,  
4073 I., Heil, A., Hawbaker, T. J., and Giglio, L.: Historical background and current developments for mapping burned area from satellite  
4074 Earth observation, *Remote Sensing of Environment*, 225, 45–64, <https://doi.org/10.1016/j.rse.2019.02.013>, 2019.
- 4075 Chuvieco, E., Roteta, E., Sali, M., Stroppiana, D., Boettcher, M., Kirches, G., Storm, T., Khairoun, A., Pettinari, M. L., Franquesa,  
4076 M., and Albergel, C.: Building a small fire database for Sub-Saharan Africa from Sentinel-2 high-resolution images, *Science of  
4077 The Total Environment*, 845, 157139, <https://doi.org/10.1016/j.scitotenv.2022.157139>, 2022.
- 4078 Chuvieco, E., Yebra, M., Martino, S., Thonicke, K., Gómez-Giménez, M., San-Miguel, J., Oom, D., Velea, R., Mouillot, F., Molina,  
4079 J. R., Miranda, A. I., Lopes, D., Salis, M., Bugaric, M., Sofiev, M., Kadantsev, E., Gitas, I. Z., Stavrakoudis, D., Eftychidis, G., Bar-  
4080 Massada, A., Neidermeier, A., Pampanoni, V., Pettinari, M. L., Arrogante-Funes, F., Ochoa, C., Moreira, B., and Viegas, D.:  
4081 Towards an Integrated Approach to Wildfire Risk Assessment: When, Where, What and How May the Landscapes Burn, *Fire*, 6,  
4082 215, <https://doi.org/10.3390/fire6050215>, 2023.
- 4083 Ciais, P., Bastos, A., Chevallier, F., Lauerwald, R., Poulter, B., Canadell, J. G., Hugelius, G., Jackson, R. B., Jain, A., Jones, M.,  
4084 Kondo, M., Luijckx, I. T., Patra, P. K., Peters, W., Pongratz, J., Petrescu, A. M. R., Piao, S., Qiu, C., Von Randow, C., Regnier, P.,  
4085 Saunois, M., Scholes, R., Shvidenko, A., Tian, H., Yang, H., Wang, X., and Zheng, B.: Definitions and methods to estimate  
4086 regional land carbon fluxes for the second phase of the REgional Carbon Cycle Assessment and Processes Project (RECCAP-  
4087 2), *Geoscientific Model Development*, 15, 1289–1316, <https://doi.org/10.5194/gmd-15-1289-2022>, 2022.
- 4088 Ciavarella, A., Christidis, N., Andrews, M., Groenendijk, M., Rostron, J., Elkington, M., Burke, C., Lott, F. C., and Stott, P. A.:  
4089 Upgrade of the HadGEM3-A based attribution system to high resolution and a new validation framework for probabilistic event  
4090 attribution, *Weather and Climate Extremes*, 20, 9–32, <https://doi.org/10.1016/j.wace.2018.03.003>, 2018.
- 4091 Citizen Digital: Wildfires ravage over 40,000 acres of Aberdare forest, available at: <https://www.citizen.digital/news/wildfires-ravage-over-40000-acres-of-aberdare-forest-n314597>,  
4092 last access: 9 July 2024, Citizen Digital, 2023.
- 4093 Clarke, B., Barnes, C., Rodrigues, R., Zachariah, M., Stewart, S., Raju, E., Baumgart, N., Heinrich, D., Libonati, R., Santos, D.,  
4094 Albuquerque, R., Alves, L., Pinto, I., Otto, F., Kimutai, J., Philip, S., Kew, S., Bazo, J., and Wynter, A.: Climate change, not El  
4095 Niño, main driver of extreme drought in highly vulnerable Amazon River Basin, Imperial College London,  
4096 <https://doi.org/10.25561/108761>, 2024.
- 4097 Collins, L., Clarke, H., Clarke, M. F., McColl Gausden, S. C., Nolan, R. H., Penman, T., and Bradstock, R.: Warmer and drier  
4098 conditions have increased the potential for large and severe fire seasons across south-eastern Australia, *Global Ecology and  
4099 Biogeography*, 31, 1933–1948, <https://doi.org/10.1111/geb.13514>, 2022.

- 4100 Comisión Nacional Forestal: CONAFOR Reporte semanal de incendios 2024, available at:  
4101 <https://www.gob.mx/conafor/documentos/reporte-semanal-de-incendios>, last access: 9 July 2024, 2024.
- 4102 Conlisk, E., Butsic, V., Syphard, A. D., Evans, S., and Jennings, M.: Evidence of increasing wildfire damage with decreasing  
4103 property price in Southern California fires, PLoS ONE, 19, e0300346, <https://doi.org/10.1371/journal.pone.0300346>, 2024.
- 4104 Coop, J. D., Parks, S. A., Stevens-Rumann, C. S., Crausbay, S. D., Higuera, P. E., Hurteau, M. D., Tepley, A., Whitman, E.,  
4105 Assal, T., Collins, B. M., Davis, K. T., Dobrowski, S., Falk, D. A., Fornwalt, P. J., Fulé, P. Z., Harvey, B. J., Kane, V. R., Littlefield,  
4106 C. E., Margolis, E. Q., North, M., Parisien, M.-A., Prichard, S., and Rodman, K. C.: Wildfire-Driven Forest Conversion in Western  
4107 North American Landscapes, BioScience, 70, 659–673, <https://doi.org/10.1093/biosci/biaa061>, 2020.
- 4108 Copernicus Climate Change Service: The European heatwave of July 2023 in a longer-term context, available at:  
4109 <https://climate.copernicus.eu/european-heatwave-july-2023-longer-term-context>, last access: 9 July 2024, 2023.
- 4110 Copernicus Climate Change Service (C3S): ERA5 hourly data on single levels from 1940 to present,  
4111 <https://doi.org/10.24381/CDS.ADBB2D47>, 2018.
- 4112 Copernicus Climate Change Service (C3S): 2023a European State of the Climate 2023, available at:  
4113 <https://climate.copernicus.eu/esotc/2023>, last access: 9 July 2024, 2024a.
- 4114 Copernicus Climate Change Service (C3S): C3S Seasonal Charts, available at:  
4115 [https://climate.copernicus.eu/charts/packages/c3s\\_seasonal/](https://climate.copernicus.eu/charts/packages/c3s_seasonal/), last access: 9 July 2024, 2024b.
- 4116 Copernicus Emergency Management Service: Copernicus EMS Fire danger indices historical data from the Copernicus  
4117 Emergency Management Service, <https://doi.org/10.24381/CDS.0E89C522>, 2019.
- 4118 Copernicus Emergency Management Service: 2023a Copernicus EMS Rapid Mapping Activation Viewer: EMSR715 - Wildfire in  
4119 Valparaiso region, Chile, available at: <https://rapidmapping.emergency.copernicus.eu/EMSR715/download>, last access: 9 July  
4120 2024, 2023a.
- 4121 Copernicus Emergency Management Service: 2023b Copernicus EMS Rapid Mapping Activation Viewer: EMSR667 - Wildfire in  
4122 Caceres, Spain, available at: <https://rapidmapping.emergency.copernicus.eu/EMSR667>, last access: 9 July 2024, 2023b.
- 4123 Copernicus Emergency Management Service: 2023c Copernicus EMS Situational Reporting: EMSR685 - Fire in Tenerife, Spain,  
4124 available at: <https://storymaps.arcgis.com/stories/0f6c7842e2aa412db35d4f14ecc292ec>, last access: 9 July 2024, ArcGIS  
4125 StoryMaps, 2023c.
- 4126 Crisis24: South Africa: Emergency crews continue to respond to wildfires across parts of Western Cape as of Jan. 30 /update 1,  
4127 available at: [https://crisis24.garda.com/alerts/2024/01/south-africa-emergency-crews-continue-to-respond-to-wildfires-across-](https://crisis24.garda.com/alerts/2024/01/south-africa-emergency-crews-continue-to-respond-to-wildfires-across-parts-of-western-cape-as-of-jan-30-update-1)  
4128 [parts-of-western-cape-as-of-jan-30-update-1](https://crisis24.garda.com/alerts/2024/01/south-africa-emergency-crews-continue-to-respond-to-wildfires-across-parts-of-western-cape-as-of-jan-30-update-1), last access: 9 July 2024, South Africa: Emergency crews continue to respond to  
4129 wildfires across parts of Western Cape as of Jan. 30 /update 1 | Crisis24, 2024.
- 4130 Croker, A. R., Woods, J., and Kountouris, Y.: Community-Based Fire Management in East and Southern African Savanna-  
4131 Protected Areas: A Review of the Published Evidence, Earth's Future, 11, e2023EF003552,  
4132 <https://doi.org/10.1029/2023EF003552>, 2023.
- 4133 Cunningham, C. X., Williamson, G. J., and Bowman, D. M. J. S.: Increasing frequency and intensity of the most extreme wildfires  
4134 on Earth, Nat Ecol Evol, 1–6, <https://doi.org/10.1038/s41559-024-02452-2>, 2024a.
- 4135 Cunningham, C. X., Williamson, G. J., Nolan, R. H., Teckentrup, L., Boer, M. M., and Bowman, D. M. J. S.: Pyrogeography in  
4136 flux: Reorganization of Australian fire regimes in a hotter world, Global Change Biology, 30, e17130,  
4137 <https://doi.org/10.1111/gcb.17130>, 2024b.
- 4138 Cunningham, D., Cunningham, P., and Fagan, M. E.: Evaluating Forest Cover and Fragmentation in Costa Rica with a Corrected  
4139 Global Tree Cover Map, Remote Sensing, 12, 3226, <https://doi.org/10.3390/rs12193226>, 2020.



- 4140 Daeli, W., Carmenta, R., Monroe, M. C., and Adams, A. E.: Where Policy and Culture Collide: Perceptions and Responses of  
4141 Swidden Farmers to the Burn Ban in West Kalimantan, Indonesia, *Hum Ecol*, 49, 159–170, [https://doi.org/10.1007/s10745-021-](https://doi.org/10.1007/s10745-021-00227-y)  
4142 [00227-y](https://doi.org/10.1007/s10745-021-00227-y), 2021.
- 4143 Deeming, J. E., Burgan, R. E., and Cohen, J. D.: The National Fire-Danger Rating System - 1978, Gen. Tech. Rep. INT-GTR-39.  
4144 Ogden, UT: U.S. Department of Agriculture, Forest Service, Intermountain Forest and Range Experiment Station. 63 p., 39, 1977.
- 4145 Di Giuseppe, F.: Accounting for fuel in fire danger forecasts: the fire occurrence probability index (FOPI), *Environ. Res. Lett.*, 18,  
4146 064029, <https://doi.org/10.1088/1748-9326/acd2ee>, 2023.
- 4147 Di Giuseppe, F., Vitolo, C., Krzeminski, B., Barnard, C., Maciel, P., and San-Miguel, J.: Fire Weather Index: the skill provided by  
4148 the European Centre for Medium-Range Weather Forecasts ensemble prediction system, *Natural Hazards and Earth System*  
4149 *Sciences*, 20, 2365–2378, <https://doi.org/10.5194/nhess-20-2365-2020>, 2020.
- 4150 Di Giuseppe, F., Benedetti, A., Coughlan, R., Vitolo, C., and Vuckovic, M.: A Global Bottom-Up Approach to Estimate Fuel  
4151 Consumed by Fires Using Above Ground Biomass Observations, *Geophysical Research Letters*, 48, e2021GL095452,  
4152 <https://doi.org/10.1029/2021GL095452>, 2021.
- 4153 Di Giuseppe, F., Vitolo, C., Barnard, C., Libertá, G., Maciel, P., San-Miguel-Ayanz, J., Villaume, S., and Wetterhall, F.: Global  
4154 seasonal prediction of fire danger, *Sci Data*, 11, 128, <https://doi.org/10.1038/s41597-024-02948-3>, 2024.
- 4155 Di Giuseppe, F., F. Pappenberger, F. Wetterhall, B. Krzeminski, A. Camia, G. Libertá, and J. San Miguel, 2016: The Potential  
4156 Predictability of Fire Danger Provided by Numerical Weather Prediction. *J. Appl. Meteor. Climatol.*, 55, 2469–2491,  
4157 <https://doi.org/10.1175/JAMC-D-15-0297.1>.
- 4158 DiMiceli, C., Carroll, M., Sohlberg, R., Kim, D.-H., Kelly, M., and Townshend, J.: MOD44B MODIS/Terra Vegetation Continuous  
4159 Fields Yearly L3 Global 250m SIN Grid V006, <https://doi.org/10.5067/MODIS/MOD44B.006>, 2015.
- 4160 DiMiceli, C., Carroll, M., Sohlberg, R., Huang, C., Hansen, M., and Townshend, J.: Annual Global Automated MODIS Vegetation  
4161 Continuous Fields (MOD44B) at 250 m Spatial Resolution for Data Years Beginning Day 65, 2000-2010, Collection 5 Percent  
4162 Tree Cover, University of Maryland, 2017.
- 4163 DiMiceli, C., Sohlberg, R., and Townshend, J.: MODIS/Terra Vegetation Continuous Fields Yearly L3 Global 250m SIN Grid  
4164 V061, <https://doi.org/10.5067/MODIS/MOD44B.061>, 2022.
- 4165 Direção Nacional de Gestão do Programa de Fogos Rurais: 8.º Relatório Provisório de Incêndios Rurais – 2023 - 1 de Janeiro a  
4166 15 de Outubro, available at: <https://www.icnf.pt/api/file/doc/058d65a2c60898dc>, last access: 9 July 2024, 2023.
- 4167 Dong, X., Li, F., Lin, Z., Harrison, S. P., Chen, Y., and Kug, J.-S.: Climate influence on the 2019 fires in Amazonia, *Science of*  
4168 *The Total Environment*, 794, 148718, <https://doi.org/10.1016/j.scitotenv.2021.148718>, 2021.
- 4169 Dowdy, A. J.: Seamless climate change projections and seasonal predictions for bushfires in Australia, *JSHES*, 70, 120–138,  
4170 <https://doi.org/10.1071/ES20001>, 2020.
- 4171 Economia Online: Violento incêndio em Odemira agita turismo e economia local, available at:  
4172 <https://eco.sapo.pt/2023/08/08/violento-incendio-em-odemira-agita-turismo-e-economia-local/>, last access: 9 July 2024, ECO,  
4173 2023.
- 4174 Educación Forestal: Grandes Incendios Forestales en España durante 2023: Incendio de Villanueva de Viver, Iniciado el  
4175 23/03/2023, available at: [https://edu.forestry.es/p/grandes-incendios-forestales-en-espana\\_23.html#01](https://edu.forestry.es/p/grandes-incendios-forestales-en-espana_23.html#01), last access: 9 July 2024,  
4176 2023.
- 4177 Educación Forestal: Grandes Incendios Forestales en España durante 2023: Incendios en Asturias-Cantabria, Iniciado el  
4178 28/03/2023, available at: [https://edu.forestry.es/p/grandes-incendios-forestales-en-espana\\_23.html#03](https://edu.forestry.es/p/grandes-incendios-forestales-en-espana_23.html#03), last access: 9 July 2024,  
4179 2024.

- 4180 El Desconcierto: Saldo de incendios forestales: 131 muertos, 7.000 viviendas destruidas y 5.000 damnificados, available at:  
 4181 <https://www.eldesconcierto.cl/nacional/2024/02/11/saldo-de-incendios-forestales-131-muertos-7-000-viviendas-destruidas-y-5-000-damnificados.html>, last access: 9 July 2024, El Desconcierto / Periodismo digital independiente, 2024.  
 4182
- 4183 Erraji, A.: 182 Wildfires Reported Across Morocco in 2023, available at:  
 4184 <https://www.moroccoworldnews.com/2023/07/356405/182-wildfires-reported-nationwide-in-2023>, last access: 9 July 2024,  
 4185 Morocco World News, 2023.
- 4186 Espinoza, J.-C., Jimenez, J. C., Marengo, J. A., Schongart, J., Ronchail, J., Lavado-Casimiro, W., and Ribeiro, J. V. M.: The new  
 4187 record of drought and warmth in the Amazon in 2023 related to regional and global climatic features, *Sci Rep*, 14, 8107,  
 4188 <https://doi.org/10.1038/s41598-024-58782-5>, 2024.
- 4189 Estado do Amazonas: Plano Estadual de Prevenção e Controle do Desmatamento e Queimadas do Estado do Amazonas  
 4190 PPCDQ-AM 2020-2022, 2020.
- 4191 EU Eurostat: Countries - GISCO - Eurostat, available at: [https://ec.europa.eu/eurostat/web/gisco/geodata/reference-](https://ec.europa.eu/eurostat/web/gisco/geodata/reference-data/administrative-units-statistical-units/countries)  
 4192 [data/administrative-units-statistical-units/countries](https://ec.europa.eu/eurostat/web/gisco/geodata/reference-data/administrative-units-statistical-units/countries), last access: 9 July 2024, 2020.
- 4193 euronews: Wildfires tear through Algeria and Tunisia as temperatures near 50C, available at:  
 4194 [https://www.euronews.com/green/2023/07/25/north-africa-heatwave-wildfires-kill-dozens-and-force-over-1500-people-to-](https://www.euronews.com/green/2023/07/25/north-africa-heatwave-wildfires-kill-dozens-and-force-over-1500-people-to-evacuate)  
 4195 [evacuate](https://www.euronews.com/green/2023/07/25/north-africa-heatwave-wildfires-kill-dozens-and-force-over-1500-people-to-evacuate), last access: 9 July 2024, euronews, 2023.
- 4196 European Centre for Medium-Range Weather Forecasts: CAMS global biomass burning emissions based on fire radiative power  
 4197 (GFAS): data documentation, available at:  
 4198 [https://confluence.ecmwf.int/display/CKB/CAMS+global+biomass+burning+emissions+based+on+fire+radiative+power+%28GF](https://confluence.ecmwf.int/display/CKB/CAMS+global+biomass+burning+emissions+based+on+fire+radiative+power+%28GFAS%29%3A+data+documentation)  
 4199 [AS%29%3A+data+documentation](https://confluence.ecmwf.int/display/CKB/CAMS+global+biomass+burning+emissions+based+on+fire+radiative+power+%28GFAS%29%3A+data+documentation), last access: 9 July 2024, CAMS global biomass burning emissions based on fire radiative  
 4200 power (GFAS): data documentation, 2024.
- 4201 European Commission EU Science Hub: Wildfires in the Mediterranean: EFFIS data reveal extent this summer, available at:  
 4202 [https://joint-research-centre.ec.europa.eu/jrc-news-and-updates/wildfires-mediterranean-effis-data-reveal-extent-summer-2023-](https://joint-research-centre.ec.europa.eu/jrc-news-and-updates/wildfires-mediterranean-effis-data-reveal-extent-summer-2023-09-08_en)  
 4203 [09-08\\_en](https://joint-research-centre.ec.europa.eu/jrc-news-and-updates/wildfires-mediterranean-effis-data-reveal-extent-summer-2023-09-08_en), last access: 9 July 2024, 2023.
- 4204 European Commission Joint Research Centre: Forest fires in Europe, Middle East and North Africa 2022., Publications Office,  
 4205 LU, 2023.
- 4206 European Forest Fire Information System: EFFIS - Statistics Portal, available at: [https://forest-](https://forest-fire.emergency.copernicus.eu/apps/effis.statistics/)  
 4207 [fire.emergency.copernicus.eu/apps/effis.statistics/](https://forest-fire.emergency.copernicus.eu/apps/effis.statistics/), last access: 9 July 2024, Copernicus Forest Fire, 2024.
- 4208 Feng, M., Sexton, J. O., Huang, C., Anand, A., Channan, S., Song, X.-P., Song, D.-X., Kim, D.-H., Noojipady, P., and Townshend,  
 4209 J. R.: Earth science data records of global forest cover and change: Assessment of accuracy in 1990, 2000, and 2005 epochs,  
 4210 *Remote Sensing of Environment*, 184, 73–85, <https://doi.org/10.1016/j.rse.2016.06.012>, 2016.
- 4211 Fernandes, P. M. and Botelho, H. S.: A review of prescribed burning effectiveness in fire hazard reduction, *Int. J. Wildland Fire*,  
 4212 12, 117–128, <https://doi.org/10.1071/wf02042>, 2003.
- 4213 Ferreira Barbosa, M. L., Haddad, I., da Silva Nascimento, A. L., Máximo da Silva, G., Moura da Veiga, R., Hoffmann, T. B.,  
 4214 Rosane de Souza, A., Dalagnol, R., Susin Streher, A., Souza Pereira, F. R., Oliveira e Cruz de Aragão, L. E., and Oighenstein  
 4215 Anderson, L.: Compound impact of land use and extreme climate on the 2020 fire record of the Brazilian Pantanal, *Global Ecology*  
 4216 *and Biogeography*, 31, 1960–1975, <https://doi.org/10.1111/geb.13563>, 2022.
- 4217 Field, R. D., van der Werf, G. R., Fanin, T., Fetzer, E. J., Fuller, R., Jethva, H., Levy, R., Livesey, N. J., Luo, M., Torres, O., and  
 4218 Worden, H. M.: Indonesian fire activity and smoke pollution in 2015 show persistent nonlinear sensitivity to El Niño-induced  
 4219 drought, *Proceedings of the National Academy of Sciences*, 113, 9204–9209, <https://doi.org/10.1073/pnas.1524888113>, 2016.
- 4220 Finney, D. L., Doherty, R. M., Wild, O., Stevenson, D. S., MacKenzie, I. A., and Blyth, A. M.: A projected decrease in lightning  
 4221 under climate change, *Nature Clim Change*, 8, 210–213, <https://doi.org/10.1038/s41558-018-0072-6>, 2018.

- 4222 Finney, M. A., Cohen, J. D., McAllister, S. S., and Jolly, W. M.: On the need for a theory of wildland fire spread, *Int. J. Wildland*  
4223 *Fire*, 22, 25–36, <https://doi.org/10.1071/WF11117>, 2012.
- 4224 Fiore, A. M., Naik, V., Spracklen, D. K., Steiner, A., Unger, N., Prather, M., Bergmann, D., Cameron-Smith, P. J., Cionni, I.,  
4225 Collins, W. J., Dalsøren, S., Eyring, V., Folberth, G. A., Ginoux, P., Horowitz, L. W., Josse, B., Lamarque, J.-F., A. MacKenzie,  
4226 I., Nagashima, T., O'Connor, F. M., Righi, M., Rumbold, S. T., Shindell, D. T., Skeie, R. B., Sudo, K., Szopa, S., Takemura, T.,  
4227 and Zeng, G.: Global air quality and climate, *Chemical Society Reviews*, 41, 6663–6683, <https://doi.org/10.1039/C2CS35095E>,  
4228 2012.
- 4229 Fire Hub - The Global Fire Management Hub: 1st Technical Workshop – Summary Report, available at:  
4230 <https://openknowledge.fao.org/server/api/core/bitstreams/491e9112-8106-4b02-97f1-0a27f3e1f6d6/content>, last access: 9 July  
4231 2024, FAO Headquarters, 2023.
- 4232 Fire Safety Research Institute, Kerber, S., and Alkonis, D.: Lahaina Fire Comprehensive Timeline Report, available at:  
4233 <https://fsri.org/research-update/lahaina-fire-comprehensive-timeline-report-released-attorney-general-hawaii>, last access: 9 July  
4234 2024, UL Research Institutes, <https://doi.org/10.54206/102376/VQKQ5427>, 2024.
- 4235 Fisher, R.: Vastly bigger than the Black Summer: 84 million hectares of northern Australia burned in 2023, available at:  
4236 [http://theconversation.com/vastly-bigger-than-the-black-summer-84-million-hectares-of-northern-australia-burned-in-2023-](http://theconversation.com/vastly-bigger-than-the-black-summer-84-million-hectares-of-northern-australia-burned-in-2023-227996)  
4237 227996, last access: 9 July 2024, The Conversation, 2024.
- 4238 Food and Agriculture Organization of the United Nations: Global Fire Management Hub, available at: [https://www.fao.org/forestry-](https://www.fao.org/forestry-fao/firemanagement/101248/en/)  
4239 [fao/firemanagement/101248/en/](https://www.fao.org/forestry-fao/firemanagement/101248/en/), last access: 9 July 2024, Global Fire Management Hub, 2024.
- 4240 Ford, A. E. S., Harrison, S. P., Kountouris, Y., Millington, J. D. A., Mistry, J., Perkins, O., Rabin, S. S., Rein, G., Schreckenber,  
4241 K., Smith, C., Smith, T. E. L., and Yadav, K.: Modelling Human-Fire Interactions: Combining Alternative Perspectives and  
4242 Approaches, *Frontiers in Environmental Science*, 9, 418, <https://doi.org/10.3389/fenvs.2021.649835>, 2021.
- 4243 Forster, P. M., Smith, C., Walsh, T., Lamb, W. F., Lamboll, R., Hall, B., Hauser, M., Ribes, A., Rosen, D., Gillett, N. P., Palmer,  
4244 M. D., Rogelji, J., von Schuckmann, K., Trewin, B., Allen, M., Andrew, R., Betts, R. A., Borger, A., Boyer, T., Broersma, J. A.,  
4245 Buontempo, C., Burgess, S., Cagnazzo, C., Cheng, L., Friedlingstein, P., Gettelman, A., Gütschow, J., Ishii, M., Jenkins, S., Lan,  
4246 X., Morice, C., Mühle, J., Kadow, C., Kennedy, J., Killick, R. E., Krummel, P. B., Minx, J. C., Myhre, G., Naik, V., Peters, G. P.,  
4247 Pirani, A., Pongratz, J., Schleussner, C.-F., Seneviratne, S. I., Szopa, S., Thorne, P., Kovilakam, M. V. M., Majamäki, E.,  
4248 Jalkanen, J.-P., van Marle, M., Hoesly, R. M., Rohde, R., Schumacher, D., van der Werf, G., Vose, R., Zickfeld, K., Zhang, X.,  
4249 Masson-Delmotte, V., and Zhai, P.: Indicators of Global Climate Change 2023: annual update of key indicators of the state of the  
4250 climate system and human influence, *Earth System Science Data*, 16, 2625–2658, <https://doi.org/10.5194/essd-16-2625-2024>,  
4251 2024.
- 4252 France-Presse, A.: Colombia Declares Emergency Over Forest Fires, available at: [https://www.voanews.com/a/colombia-](https://www.voanews.com/a/colombia-declares-emergency-over-forest-fires/7456551.html)  
4253 [declares-emergency-over-forest-fires/7456551.html](https://www.voanews.com/a/colombia-declares-emergency-over-forest-fires/7456551.html), last access: 9 July 2024, Voice of America, 2024.
- 4254 Frazier, A. E. and Hemingway, B. L.: A Technical Review of Planet Smallsat Data: Practical Considerations for Processing and  
4255 Using PlanetScope Imagery, *Remote Sensing*, 13, 3930, <https://doi.org/10.3390/rs13193930>, 2021.
- 4256 Friedlingstein, P., O'Sullivan, M., Jones, M. W., Andrew, R. M., Bakker, D. C. E., Hauck, J., Landschützer, P., Le Quééré, C.,  
4257 Lujikx, I. T., Peters, G. P., Peters, W., Pongratz, J., Schwingshackl, C., Sitch, S., Canadell, J. G., Ciais, P., Jackson, R. B., Alin,  
4258 S. R., Anthoni, P., Barbero, L., Bates, N. R., Becker, M., Bellouin, N., Decharme, B., Bopp, L., Brasika, I. B. M., Cadule, P.,  
4259 Chamberlain, M. A., Chandra, N., Chau, T.-T.-T., Chevallier, F., Chini, L. P., Cronin, M., Dou, X., Enyo, K., Evans, W., Falk, S.,  
4260 Feely, R. A., Feng, L., Ford, D. J., Gasser, T., Ghattas, J., Gkritzalis, T., Grassi, G., Gregor, L., Gruber, N., Gürses, Ö., Harris, I.,  
4261 Hefner, M., Heinke, J., Houghton, R. A., Hurtt, G. C., Iida, Y., Ilyina, T., Jacobson, A. R., Jain, A., Jarniková, T., Jersild, A., Jiang,  
4262 F., Jin, Z., Joos, F., Kato, E., Keeling, R. F., Kennedy, D., Klein Goldewijk, K., Knauer, J., Korsbakken, J. I., Körtzinger, A., Lan,  
4263 X., Lefèvre, N., Li, H., Liu, J., Liu, Z., Ma, L., Marland, G., Mayot, N., McGuire, P. C., McKinley, G. A., Meyer, G., Morgan, E. J.,  
4264 Munro, D. R., Nakaoka, S.-I., Niwa, Y., O'Brien, K. M., Olsen, A., Omar, A. M., Ono, T., Paulsen, M., Pierrot, D., Pocock, K.,  
4265 Poulter, B., Powis, C. M., Rehder, G., Resplandy, L., Robertson, E., Rödenbeck, C., Rosan, T. M., Schwinger, J., Séférian, R.,  
4266 et al.: Global Carbon Budget 2023, *Earth System Science Data*, 15, 5301–5369, <https://doi.org/10.5194/essd-15-5301-2023>,  
4267 2023.



- 4268 Frieler, K., Volkholz, J., Lange, S., Schewe, J., Mengel, M., del Rocío Rivas López, M., Otto, C., Reyer, C. P. O., Karger, D. N.,  
4269 Malle, J. T., Treu, S., Menz, C., Blanchard, J. L., Harrison, C. S., Petrik, C. M., Eddy, T. D., Ortega-Cisneros, K., Novaglio, C.,  
4270 Rousseau, Y., Watson, R. A., Stock, C., Liu, X., Heneghan, R., Tittensor, D., Maury, O., Büchner, M., Vogt, T., Wang, T., Sun,  
4271 F., Sauer, I. J., Koch, J., Vanderkelen, I., Jägermeyr, J., Müller, C., Rabin, S., Klar, J., Vega del Valle, I. D., Lasslop, G., Chadburn,  
4272 S., Burke, E., Gallego-Sala, A., Smith, N., Chang, J., Hantson, S., Burton, C., Gädeke, A., Li, F., Gosling, S. N., Müller Schmied,  
4273 H., Hattermann, F., Wang, J., Yao, F., Hickler, T., Marcé, R., Pierson, D., Thiery, W., Mercado-Bettín, D., Ladwig, R., Ayala-  
4274 Zamora, A. I., Forrest, M., and Bechtold, M.: Scenario setup and forcing data for impact model evaluation and impact attribution  
4275 within the third round of the Inter-Sectoral Impact Model Intercomparison Project (ISIMIP3a), *Geoscientific Model Development*,  
4276 17, 1–51, <https://doi.org/10.5194/gmd-17-1-2024>, 2024.
- 4277 Fuller, D. O. and Murphy, K.: The ENSO-Fire Dynamic in Insular Southeast Asia, *Climatic Change*, 74, 435–455,  
4278 <https://doi.org/10.1007/s10584-006-0432-5>, 2006.
- 4279 Fuzzi, S., Baltensperger, U., Carslaw, K., Decesari, S., Denier van der Gon, H., Facchini, M. C., Fowler, D., Koren, I., Langford,  
4280 B., Lohmann, U., Nemitz, E., Pandis, S., Riipinen, I., Rudich, Y., Schaap, M., Slowik, J. G., Spracklen, D. V., Vignati, E., Wild,  
4281 M., Williams, M., and Gilardoni, S.: Particulate matter, air quality and climate: lessons learned and future needs, *Atmospheric*  
4282 *Chemistry and Physics*, 15, 8217–8299, <https://doi.org/10.5194/acp-15-8217-2015>, 2015.
- 4283 Garnett, S. T., Burgess, N. D., Fa, J. E., Fernández-Llamazares, Á., Molnár, Z., Robinson, C. J., Watson, J. E. M., Zander, K. K.,  
4284 Austin, B., Brondizio, E. S., Collier, N. F., Duncan, T., Ellis, E., Geyle, H., Jackson, M. V., Jonas, H., Malmer, P., McGowan, B.,  
4285 Sivongxay, A., and Leiper, I.: A spatial overview of the global importance of Indigenous lands for conservation, *Nat Sustain*, 1,  
4286 369–374, <https://doi.org/10.1038/s41893-018-0100-6>, 2018.
- 4287 Gatti, L. V., Basso, L. S., Miller, J. B., Gloor, M., Gatti Domingues, L., Cassol, H. L. G., Tejada, G., Aragão, L. E. O. C., Nobre,  
4288 C., Peters, W., Marani, L., Arai, E., Sanches, A. H., Corrêa, S. M., Anderson, L., Von Randow, C., Correia, C. S. C., Crispim, S.  
4289 P., and Neves, R. A. L.: Amazonia as a carbon source linked to deforestation and climate change, *Nature*, 595, 388–393,  
4290 <https://doi.org/10.1038/s41586-021-03629-6>, 2021.
- 4291 Gauldie, R.: Coming to the rescEU: European firefighting, available at: <https://www.airmedandrescue.com/latest/long-read/coming-resceu-european-firefighting>, last access: 9 July 2024, *AirMed&Rescue*, 2024.
- 4293 Gelman, A., Carlin, J. B., Stern, H. S., Dunson, D. B., Vehtari, A., and Rubin, D. B.: *Bayesian Data Analysis*, 0 ed., Chapman and  
4294 Hall/CRC, <https://doi.org/10.1201/b16018>, 2013.
- 4295 Giglio, L. and Roy, D. P.: Assessment of satellite orbit-drift artifacts in the long-term AVHRR FireCCILT11 global burned area  
4296 data set, *Science of Remote Sensing*, 5, 100044, <https://doi.org/10.1016/j.srs.2022.100044>, 2022.
- 4297 Giglio, L., Randerson, J. T., and van der Werf, G. R.: Analysis of daily, monthly, and annual burned area using the fourth-  
4298 generation global fire emissions database (GFED4), *Journal of Geophysical Research: Biogeosciences*, 118, 317–328,  
4299 <https://doi.org/10.1002/jgrg.20042>, 2013.
- 4300 Giglio, L., Schroeder, W., and Justice, C. O.: The collection 6 MODIS active fire detection algorithm and fire products, *Remote*  
4301 *Sensing of Environment*, 178, 31–41, <https://doi.org/10.1016/j.rse.2016.02.054>, 2016.
- 4302 Giglio, L., Boschetti, L., Roy, D. P., Humber, M. L., and Justice, C. O.: The Collection 6 MODIS burned area mapping algorithm  
4303 and product, *Remote Sensing of Environment*, 217, 72–85, <https://doi.org/10.1016/j.rse.2018.08.005>, 2018.
- 4304 Giglio, L., Justice, C., Boschetti, L., and Roy, D.: MODIS/Terra+Aqua Burned Area Monthly L3 Global 500m SIN Grid V061,  
4305 <https://doi.org/10.5067/MODIS/MCD64A1.061>, 2021.
- 4306 Gincheva, A., Pausas, J. G., Edwards, A., Provenzale, A., Cerdà, A., Hanes, C., Royé, D., Chuvieco, E., Mouillot, F., Vissio, G.,  
4307 Rodrigo, J., Bedía, J., Abatzoglou, J. T., Senciales González, J. M., Short, K. C., Baudena, M., Llasat, M. C., Magnani, M., Boer,  
4308 M. M., González, M. E., Torres-Vázquez, M. Á., Fiorucci, P., Jacklyn, P., Libonati, R., Trigo, R. M., Herrera, S., Jerez, S., Wang,  
4309 X., and Turco, M.: A monthly gridded burned area database of national wildland fire data, *Sci Data*, 11, 352,  
4310 <https://doi.org/10.1038/s41597-024-03141-2>, 2024.

- 4311 Grau-Andrés, R., Moreira, B., and Pausas, J. G.: Global plant responses to intensified fire regimes, *Global Ecology and*  
4312 *Biogeography*, n/a, e13858, <https://doi.org/10.1111/geb.13858>, 2024.
- 4313 Haas, O., Prentice, I. C., and Harrison, S. P.: Global environmental controls on wildfire burnt area, size, and intensity, *Environ.*  
4314 *Res. Lett.*, 17, 065004, <https://doi.org/10.1088/1748-9326/ac6a69>, 2022.
- 4315 Hamilton, D. S., Perron, M. M. G., Bond, T. C., Bowie, A. R., Buchholz, R. R., Guieu, C., Ito, A., Maenhaut, W., Myriokefalitakis,  
4316 S., Olgun, N., Rathod, S. D., Schepanski, K., Tagliabue, A., Wagner, R., and Mahowald, N. M.: Earth, Wind, Fire, and Pollution:  
4317 Aerosol Nutrient Sources and Impacts on Ocean Biogeochemistry, *Annual Review of Marine Science*, 14, 303–330,  
4318 <https://doi.org/10.1146/annurev-marine-031921-013612>, 2022.
- 4319 Hantson, S., Padilla, M., Corti, D., and Chuvieco, E.: Strengths and weaknesses of MODIS hotspots to characterize global fire  
4320 occurrence, *Remote Sensing of Environment*, 131, 152–159, <https://doi.org/10.1016/j.rse.2012.12.004>, 2013.
- 4321 Hantson, S., Arneeth, A., Harrison, S. P., Kelley, D. I., Prentice, I. C., Rabin, S. S., Archibald, S., Mouillot, F., Arnold, S. R., Artaxo,  
4322 P., Bachelet, D., Ciais, P., Forrest, M., Friedlingstein, P., Hickler, T., Kaplan, J. O., Kloster, S., Knorr, W., Lasslop, G., Li, F.,  
4323 Mangeon, S., Melton, J. R., Meyn, A., Sitch, S., Spessa, A., van der Werf, G. R., Voulgarakis, A., and Yue, C.: The status and  
4324 challenge of global fire modelling, *Biogeosciences*, 13, 3359–3375, <https://doi.org/10.5194/bg-13-3359-2016>, 2016.
- 4325 Hantson, S., Kelley, D. I., Arneeth, A., Harrison, S. P., Archibald, S., Bachelet, D., Forrest, M., Hickler, T., Lasslop, G., Li, F.,  
4326 Mangeon, S., Melton, J. R., Nieradzki, L., Rabin, S. S., Prentice, I. C., Sheehan, T., Sitch, S., Teckentrup, L., Voulgarakis, A.,  
4327 and Yue, C.: Quantitative assessment of fire and vegetation properties in simulations with fire-enabled vegetation models from  
4328 the Fire Model Intercomparison Project, *Geoscientific Model Development*, 13, 3299–3318, [https://doi.org/10.5194/gmd-13-3299-](https://doi.org/10.5194/gmd-13-3299-2020)  
4329 [2020](https://doi.org/10.5194/gmd-13-3299-2020), 2020.
- 4330 Hantson, S., Andela, N., Goulden, M. L., and Randerson, J. T.: Human-ignited fires result in more extreme fire behavior and  
4331 ecosystem impacts, *Nat Commun*, 13, 2717, <https://doi.org/10.1038/s41467-022-30030-2>, 2022.
- 4332 Harris, S. and Lucas, C.: Understanding the variability of Australian fire weather between 1973 and 2017, *PLOS ONE*, 14,  
4333 e0222328, <https://doi.org/10.1371/journal.pone.0222328>, 2019.
- 4334 Harrison, S. P., Bartlein, P. J., Brovkin, V., Houweling, S., Kloster, S., and Prentice, I. C.: The biomass burning contribution to  
4335 climate–carbon-cycle feedback, *Earth Syst. Dynam.*, 9, 663–677, <https://doi.org/10.5194/esd-9-663-2018>, 2018.
- 4336 Haynes, K., Short, K., Xanthopoulos, G., Viegas, D., Ribeiro, L. M., and Bianchi, R.: Wildfires and WUI Fire Fatalities, in:  
4337 *Encyclopedia of Wildfires and Wildland-Urban Interface (WUI) Fires*, edited by: Manzello, S. L., Springer International Publishing,  
4338 Cham, 1–16, [https://doi.org/10.1007/978-3-319-51727-8\\_92-1](https://doi.org/10.1007/978-3-319-51727-8_92-1), 2019.
- 4339 Hazra, D. and Gallagher, P.: Role of insurance in wildfire risk mitigation, *Economic Modelling*, 108, 105768,  
4340 <https://doi.org/10.1016/j.econmod.2022.105768>, 2022.
- 4341 Hegerl, G. C., Hoegh-Guldberg, O., Casassa, G., Hoerling, M., Kovats, S., Parmesan, C., Pierce, D., and Stott, P.: IPCC WGI  
4342 Expert Meeting on Detection and Attribution Related to Anthropogenic Climate Change: Good Practice Guidance Paper on  
4343 Detection and Attribution Related to Anthropogenic Climate Change, available at: [https://archive.ipcc.ch/pdf/supporting-](https://archive.ipcc.ch/pdf/supporting-material/ipcc_good_practice_guidance_paper_anthropogenic.pdf)  
4344 [material/ipcc\\_good\\_practice\\_guidance\\_paper\\_anthropogenic.pdf](https://archive.ipcc.ch/pdf/supporting-material/ipcc_good_practice_guidance_paper_anthropogenic.pdf), last access: 9 July 2024, edited by: Stocker, T., Field, C.,  
4345 Dahe, Q., Barros, V., Plattner, G.-K., Tignor, M., Midgley, P., and Ebi, K., Geneva, 2009.
- 4346 Held, I. M., Guo, H., Adcroft, A., Dunne, J. P., Horowitz, L. W., Krasting, J., Shevliakova, E., Winton, M., Zhao, M., Bushuk, M.,  
4347 Wittenberg, A. T., Wyman, B., Xiang, B., Zhang, R., Anderson, W., Balaji, V., Donner, L., Dunne, K., Durachta, J., Gauthier, P.  
4348 P. G., Ginoux, P., Golaz, J.-C., Griffies, S. M., Hallberg, R., Harris, L., Harrison, M., Hurlin, W., John, J., Lin, P., Lin, S.-J.,  
4349 Malyshev, S., Menzel, R., Milly, P. C. D., Ming, Y., Naik, V., Paynter, D., Paulot, F., Ramaswamy, V., Reichl, B., Robinson, T.,  
4350 Rosati, A., Seman, C., Silvers, L. G., Underwood, S., and Zadeh, N.: Structure and Performance of GFDL's CM4.0 Climate Model,  
4351 *Journal of Advances in Modeling Earth Systems*, 11, 3691–3727, <https://doi.org/10.1029/2019MS001829>, 2019.
- 4352 Higuera, P. E. and Abatzoglou, J. T.: Record-setting climate enabled the extraordinary 2020 fire season in the western United  
4353 States, *Glob. Change Biol.*, 27, 1–2, <https://doi.org/10.1111/gcb.15388>, 2021.

- 4354 Higuera, P. E., Cook, M. C., Balch, J. K., Stavros, E. N., Mahood, A. L., and St. Denis, L. A.: Shifting social-ecological fire regimes  
 4355 explain increasing structure loss from Western wildfires, *PNAS Nexus*, 2, pgad005, <https://doi.org/10.1093/pnasnexus/pgad005>,  
 4356 2023.
- 4357 Hollis, J. J., Matthews, S., Fox-Hughes, P., Grootemaat, S., Heemstra, S., Kenny, B. J., and Sauvage, S.: Introduction to the  
 4358 Australian Fire Danger Rating System, *Int. J. Wildland Fire*, 33, <https://doi.org/10.1071/WF23140>, 2024.
- 4359 Hough, A.: The battle for Scarborough, available at: <https://www.iol.co.za/capetimes/news/the-battle-for-scarborough-f9d4ce5c-223e-4fd9-97e3-ce23c58b12b9>, last access: 9 July 2024, IOL News, 2023.  
 4360
- 4361 Hunka, N., Santoro, M., Armston, J., Dubayah, R., McRoberts, R. E., Næsset, E., Quegan, S., Urbazaev, M., Pascual, A., May,  
 4362 P. B., Minor, D., Leitold, V., Basak, P., Liang, M., Melo, J., Herold, M., Málaga, N., Wilson, S., Montesinos, P. D., Arana, A.,  
 4363 Paiva, R. E. D. L. C., Ferrand, J., Keoka, S., Guerra-Hernández, J., and Duncanson, L.: On the NASA GEDI and ESA CCI  
 4364 biomass maps: aligning for uptake in the UNFCCC global stocktake, *Environ. Res. Lett.*, 18, 124042,  
 4365 <https://doi.org/10.1088/1748-9326/ad0b60>, 2023.
- 4366 Inness, A., Ades, M., Agustí-Panareda, A., Barré, J., Benedictow, A., Blechschmidt, A.-M., Dominguez, J. J., Engelen, R., Eskes,  
 4367 H., Flemming, J., Huijnen, V., Jones, L., Kipling, Z., Massart, S., Parrington, M., Peuch, V.-H., Razinger, M., Remy, S., Schulz,  
 4368 M., and Suttie, M.: The CAMS reanalysis of atmospheric composition, *Atmospheric Chemistry and Physics*, 19, 3515–3556,  
 4369 <https://doi.org/10.5194/acp-19-3515-2019>, 2019.
- 4370 Instituto Chico Mendes de Conservação da Biodiversidade: Plano de Manejo Floresta Nacional do Tapajós, available at:  
 4371 [https://www.gov.br/icmbio/pt-br/assuntos/biodiversidade/unidade-de-conservacao/unidades-de-biomas/amazonia/lista-de-  
 4372 ucs/flona-do-tapajos/arquivos/plano\\_de\\_manejo\\_flona\\_do\\_tapajos\\_2019\\_vol2.pdf](https://www.gov.br/icmbio/pt-br/assuntos/biodiversidade/unidade-de-conservacao/unidades-de-biomas/amazonia/lista-de-ucs/flona-do-tapajos/arquivos/plano_de_manejo_flona_do_tapajos_2019_vol2.pdf), last access: 9 July 2024, 2019.
- 4373 Instituto da Conservação da Natureza e das Florestas: IR de Carrascal (Sarzedas) Castelo Branco - Proença-a-Nova Relatório  
 4374 de Estabilização de Emergência Pós-Incêndio, available at: <https://www.icnf.pt/api/file/doc/058d65a2c60898dc>, last access: 9  
 4375 July 2024, 2023.
- 4376 Intergovernmental Panel on Climate Change (IPCC) (Ed.): 2023a Changing State of the Climate System, in: *Climate Change*  
 4377 2021 – The Physical Science Basis: Working Group I Contribution to the Sixth Assessment Report of the Intergovernmental Panel  
 4378 on Climate Change, Cambridge University Press, Cambridge, 287–422, <https://doi.org/10.1017/9781009157896.004>, 2023a.
- 4379 Intergovernmental Panel on Climate Change (IPCC) (Ed.): 2023b Key Risks across Sectors and Regions, in: *Climate Change*  
 4380 2022 – Impacts, Adaptation and Vulnerability: Working Group II Contribution to the Sixth Assessment Report of the  
 4381 Intergovernmental Panel on Climate Change, Cambridge University Press, Cambridge, 2411–2538,  
 4382 <https://doi.org/10.1017/9781009325844.025>, 2023b.
- 4383 Intergovernmental Panel on Climate Change (IPCC) (Ed.): 2023c Point of Departure and Key Concepts, in: *Climate Change 2022*  
 4384 – Impacts, Adaptation and Vulnerability: Working Group II Contribution to the Sixth Assessment Report of the Intergovernmental  
 4385 Panel on Climate Change, Cambridge University Press, Cambridge, 121–196, <https://doi.org/10.1017/9781009325844.003>,  
 4386 2023c.
- 4387 International Federation of Red Cross and Red Crescent Societies: Mongolia: IFRC network mid-year report, January - June  
 4388 2023 (14 December 2023) - Mongolia, available at: [https://reliefweb.int/report/mongolia/mongolia-ifrc-network-mid-year-report-  
 4389 january-june-2023-14-december-2023](https://reliefweb.int/report/mongolia/mongolia-ifrc-network-mid-year-report-january-june-2023-14-december-2023), last access: 9 July 2024, 2023.
- 4390 Istituto Superiore per la Protezione e la Ricerca Ambientale (ISPRA): Gli incendi boschivi in Italia: stagione degli incendi 2023,  
 4391 Roma, 2023.
- 4392 Jain, P., Barber, Q. E., Taylor, S., Whitman, E., Castellanos Acuna, D., Boulanger, Y., Chavardès, R. D., Chen, J., Englefield, P.,  
 4393 Flannigan, M., Girardin, M. P., Hanes, C. C., Little, J., Morrison, K., Skakun, R. S., Thompson, D. K., Wang, X., and Parisien, M.-  
 4394 A.: Canada Under Fire – Drivers and Impacts of the Record-Breaking 2023 Wildfire Season,  
 4395 <https://doi.org/10.22541/essoar.170914412.27504349/v1>.

- 4396 Jimémez-Muñoz, J. C., Mattar, C., Barichivich, J., Santamaría-Artigas, A., Takahashi, K., Malhi, Y., Sobrino, J. A., and Schrier,  
4397 G. van der: Record-breaking warming and extreme drought in the Amazon rainforest during the course of El Niño 2015–2016,  
4398 *Sci Rep*, 6, 33130, <https://doi.org/10.1038/srep33130>, 2016.
- 4399 Johnson, S. J., Stockdale, T. N., Ferranti, L., Balmaseda, M. A., Molteni, F., Magnusson, L., Tietsche, S., Decremer, D.,  
4400 Weisheimer, A., Balsamo, G., Keeley, S. P. E., Mogensen, K., Zuo, H., and Monge-Sanz, B. M.: SEAS5: the new ECMWF  
4401 seasonal forecast system, *Geoscientific Model Development*, 12, 1087–1117, <https://doi.org/10.5194/gmd-12-1087-2019>, 2019.
- 4402 Johnston, F. H., Henderson, S. B., Chen, Y., Randerson, J. T., Marlier, M., DeFries, R. S., Kinney, P., Bowman, D. M. J. S., and  
4403 Brauer, M.: Estimated Global Mortality Attributable to Smoke from Landscape Fires, *Environmental Health Perspectives*, 120,  
4404 695–701, <https://doi.org/10.1289/ehp.1104422>, 2012.
- 4405 Johnston, F. H., Borchers-Arriagada, N., Morgan, G. G., Jalaludin, B., Palmer, A. J., Williamson, G. J., and Bowman, D. M. J. S.:  
4406 Unprecedented health costs of smoke-related PM2.5 from the 2019–20 Australian megafires, *Nat Sustain*, 4, 42–47,  
4407 <https://doi.org/10.1038/s41893-020-00610-5>, 2021.
- 4408 Jones, M. W., Abatzoglou, J. T., Veraverbeke, S., Andela, N., Lasslop, G., Forkel, M., Smith, A. J. P., Burton, C., Betts, R. A.,  
4409 van der Werf, G. R., Sitch, S., Canadell, J. G., Santín, C., Kolden, C., Doerr, S. H., and Le Quéré, C.: Global and Regional Trends  
4410 and Drivers of Fire Under Climate Change, *Reviews of Geophysics*, 60, e2020RG000726,  
4411 <https://doi.org/10.1029/2020RG000726>, 2022.
- 4412 Jones, M. W., Brambleby, E., Andela, N., van der Werf, G. R., Parrington, M., and Giglio, L.: State of Wildfires 2023-24: Anomalies  
4413 in Burned Area, Fire Emissions, and Individual Fire Characteristics by Continent, Biome, Country, and Administrative Region,  
4414 <https://doi.org/10.5281/zenodo.11400540>, 2024.
- 4415 Joshi, M.: El Niño could push global warming past 1.5°C – but what is it and how does it affect the weather in Europe?, available  
4416 at: [http://theconversation.com/el-nino-could-push-global-warming-past-1-5-but-what-is-it-and-how-does-it-affect-the-weather-in-](http://theconversation.com/el-nino-could-push-global-warming-past-1-5-but-what-is-it-and-how-does-it-affect-the-weather-in-europe-208412)  
4417 [europe-208412](http://theconversation.com/el-nino-could-push-global-warming-past-1-5-but-what-is-it-and-how-does-it-affect-the-weather-in-europe-208412), last access: 9 July 2024, *The Conversation*, 2023.
- 4418 Juntaex.es: El incendio de Pinofranqueado y Gata ha afectado a 10.863 hectáreas según las primeras estimaciones, available  
4419 at: <https://www.juntaex.es/w/superficie-incendio-hurdes-gata>, last access: 9 July 2024, *Juntaex.es*, 2023.
- 4420 Kaiser, J. W., Heil, A., Andreae, M. O., Benedetti, A., Chubarova, N., Jones, L., Morcrette, J.-J., Razinger, M., Schultz, M. G.,  
4421 Suttie, M., and van der Werf, G. R.: Biomass burning emissions estimated with a global fire assimilation system based on  
4422 observed fire radiative power, *Biogeosciences*, 9, 527–554, <https://doi.org/10.5194/bg-9-527-2012>, 2012.
- 4423 Keeley, J. E.: Fire intensity, fire severity and burn severity: a brief review and suggested usage, *Int. J. Wildland Fire*, 18, 116–  
4424 126, <https://doi.org/10.1071/WF07049>, 2009.
- 4425 Kelley, D., Gerard, F., Dong, N., Burton, C., Argles, A., Li, G., Whitley, R., Marthews, T., Roberston, E., Weedon, G., Lasslop, G.,  
4426 Ellis, R., Bistinas, I., and Veendendaal, E.: Observational constraints of fire, environmental and anthropogenic on pantropical tree  
4427 cover, <https://doi.org/10.21203/rs.3.rs-3413013/v1>, 16 October 2023.
- 4428 Kelley, D. I., Harrison, S. P., and Prentice, I. C.: Improved simulation of fire–vegetation interactions in the Land surface Processes  
4429 and eXchanges dynamic global vegetation model (LPX-Mv1), *Geoscientific Model Development*, 7, 2411–2433,  
4430 <https://doi.org/10.5194/gmd-7-2411-2014>, 2014.
- 4431 Kelley, D. I., Bistinas, I., Whitley, R., Burton, C., Marthews, T. R., and Dong, N.: How contemporary bioclimatic and human  
4432 controls change global fire regimes, *Nat. Clim. Chang.*, 9, 690–696, <https://doi.org/10.1038/s41558-019-0540-7>, 2019.
- 4433 Kelley, D. I., Burton, C., Huntingford, C., Brown, M. A. J., Whitley, R., and Dong, N.: Technical note: Low meteorological influence  
4434 found in 2019 Amazonia fires, *Biogeosciences*, 18, 787–804, <https://doi.org/10.5194/bg-18-787-2021>, 2021.
- 4435 Kelley, D. I., Ferreira Barbosa, M. L., Burke, E., Burton, C. A., Bradley, A., Jones, M. W., Spuler, F., Wessel, J., McNorton, J., and  
4436 Di Giuseppe, F.: State of Wildfires 2023-24: ConFire data, <https://doi.org/10.5281/zenodo.11420743>, 2024.

- 4437 Klein Goldewijk, K., Beusen, A., Van Drecht, G., and De Vos, M.: The HYDE 3.1 spatially explicit database of human-induced  
4438 global land-use change over the past 12,000 years: HYDE 3.1 Holocene land use, *Global Ecology and Biogeography*, 20, 73–  
4439 86, <https://doi.org/10.1111/j.1466-8238.2010.00587.x>, 2011.
- 4440 Kolden, C.: Wildfires: count lives and homes, not hectares burnt, *Nature*, 586, 9–9, <https://doi.org/10.1038/d41586-020-02740-4>,  
4441 2020.
- 4442 Kolden, C. A. and Henson, C.: A Socio-Ecological Approach to Mitigating Wildfire Vulnerability in the Wildland Urban Interface:  
4443 A Case Study from the 2017 Thomas Fire, *Fire*, 2, 9, <https://doi.org/10.3390/fire2010009>, 2019.
- 4444 Kolden, C. A., Abatzoglou, J. T., Jones, M. W., and Jain, P.: Wildfires in 2023, *Nat Rev Earth Environ*, 5, 238–240,  
4445 <https://doi.org/10.1038/s43017-024-00544-y>, 2024.
- 4446 Kramer, S. J., Bisson, K. M., and Fischer, A. D.: Observations of Phytoplankton Community Composition in the Santa Barbara  
4447 Channel During the Thomas Fire, *Journal of Geophysical Research: Oceans*, 125, e2020JC016851,  
4448 <https://doi.org/10.1029/2020JC016851>, 2020.
- 4449 Ladd, T. M., Catlett, D., Maniscalco, M. A., Kim, S. M., Kelly, R. L., John, S. G., Carlson, C. A., and Iglesias-Rodríguez, M. D.:  
4450 Food for all? Wildfire ash fuels growth of diverse eukaryotic plankton, *Proceedings of the Royal Society B: Biological Sciences*,  
4451 290, 20231817, <https://doi.org/10.1098/rspb.2023.1817>, 2023.
- 4452 Lafferty, D. C. and Sriver, R. L.: Downscaling and bias-correction contribute considerable uncertainty to local climate projections  
4453 in CMIP6, *npj Clim Atmos Sci*, 6, 1–13, <https://doi.org/10.1038/s41612-023-00486-0>, 2023.
- 4454 Lange, S.: Trend-preserving bias adjustment and statistical downscaling with ISIMIP3BASD (v1.0), *Geoscientific Model  
4455 Development*, 12, 3055–3070, <https://doi.org/10.5194/gmd-12-3055-2019>, 2019.
- 4456 Lapola, D. M., Pinho, P., Barlow, J., Aragão, L. E. O. C., Berenguer, E., Carmenta, R., Liddy, H. M., Seixas, H., Silva, C. V. J.,  
4457 Silva-Junior, C. H. L., Alencar, A. A. C., Anderson, L. O., Armenteras, D., Brovkin, V., Calders, K., Chambers, J., Chini, L., Costa,  
4458 M. H., Faria, B. L., Fearnside, P. M., Ferreira, J., Gatti, L., Gutierrez-Velez, V. H., Han, Z., Hibbard, K., Koven, C., Lawrence, P.,  
4459 Pongratz, J., Portela, B. T. T., Rounsevell, M., Ruane, A. C., Schaldach, R., da Silva, S. S., von Randow, C., and Walker, W. S.:  
4460 The drivers and impacts of Amazon forest degradation, *Science*, 379, eabp8622, <https://doi.org/10.1126/science.abp8622>, 2023.
- 4461 Lareau, N. P., Nauslar, N. J., and Abatzoglou, J. T.: The Carr Fire Vortex: A Case of Pyrotornadogenesis?, *Geophysical Research  
4462 Letters*, 45, <https://doi.org/10.1029/2018GL080667>, 2018.
- 4463 Las Provincias: Las terribles cifras del incendio de Villanueva de Viver, available at:  
4464 <https://www.lasprovincias.es/sucesos/terribles-cifras-incendio-villanueva-viver-20230602133033-nt.html>, last access: 9 July  
4465 2024, Las Provincias, 2023.
- 4466 Laurent, P., Mouillot, F., Yue, C., Ciais, P., Moreno, M. V., and Nogueira, J. M. P.: FRY, a global database of fire patch functional  
4467 traits derived from space-borne burned area products, *Sci Data*, 5, 180132, <https://doi.org/10.1038/sdata.2018.132>, 2018.
- 4468 Le Monde: Russia: Forest fires break out in Siberia amid heatwave, available at:  
4469 [https://www.lemonde.fr/en/russia/article/2023/05/08/russia-forest-fires-break-out-in-siberia-amid-heatwave\\_6025902\\_140.html](https://www.lemonde.fr/en/russia/article/2023/05/08/russia-forest-fires-break-out-in-siberia-amid-heatwave_6025902_140.html),  
4470 last access: 9 July 2024, Le Monde.fr, 8th May, 2023.
- 4471 van Leeuwen, S. and Miller-Sabbioni, C.: Australia's Megafires: Biodiversity Impacts and Lessons from 2019-2020, in: Australia's  
4472 Megafires: Biodiversity Impacts and Lessons from 2019-20, Rumpff, L.; Legge, S. M.; van Leeuwen, S.; Wintle, B. A.; Woinarski,  
4473 J. C. Z., 2023.
- 4474 Lemos, M. C., Kirchhoff, C. J., and Ramprasad, V.: Narrowing the climate information usability gap, *Nature Clim Change*, 2, 789–  
4475 794, <https://doi.org/10.1038/nclimate1614>, 2012.
- 4476 Li, S., Sparrow, S. N., Otto, F. E. L., Rifai, S. W., Oliveras, I., Krikken, F., Anderson, L. O., Malhi, Y., and Wallom, D.:  
4477 Anthropogenic climate change contribution to wildfire-prone weather conditions in the Cerrado and Arc of deforestation, *Environ.  
4478 Res. Lett.*, 16, 094051, <https://doi.org/10.1088/1748-9326/ac1e3a>, 2021a.



- 4479 Li, Y., Sulla-Menashe, D., Motesharrei, S., Song, X.-P., Kalnay, E., Ying, Q., Li, S., and Ma, Z.: Inconsistent estimates of forest  
4480 cover change in China between 2000 and 2013 from multiple datasets: differences in parameters, spatial resolution, and  
4481 definitions, *Sci Rep*, 7, 8748, <https://doi.org/10.1038/s41598-017-07732-5>, 2017.
- 4482 Li, Y., Yuan, S., Fan, S., Song, Y., Wang, Z., Yu, Z., Yu, Q., and Liu, Y.: Satellite Remote Sensing for Estimating PM2.5 and Its  
4483 Components, *Curr Pollution Rep*, 7, 72–87, <https://doi.org/10.1007/s40726-020-00170-4>, 2021b.
- 4484 Liang, Y., Sengupta, D., Campmier, M. J., Lunderberg, D. M., Apte, J. S., and Goldstein, A. H.: Wildfire smoke impacts on indoor  
4485 air quality assessed using crowdsourced data in California, *Proc. Natl. Acad. Sci. U.S.A.*, 118, e2106478118,  
4486 <https://doi.org/10.1073/pnas.2106478118>, 2021.
- 4487 Lin, Y. C., Jenkins, S. F., Chow, J. R., Biass, S., Woo, G., and Lallemand, D.: Modeling Downward Counterfactual Events:  
4488 Unrealized Disasters and why they Matter, *Front. Earth Sci.*, 8, <https://doi.org/10.3389/feart.2020.575048>, 2020.
- 4489 Linley, G. D., Jolly, C. J., Doherty, T. S., Geary, W. L., Armenteras, D., Belcher, C. M., Bliege Bird, R., Duane, A., Fletcher, M.-  
4490 S., Giorgis, M. A., Haslem, A., Jones, G. M., Kelly, L. T., Lee, C. K. F., Nolan, R. H., Parr, C. L., Pausas, J. G., Price, J. N., Regos,  
4491 A., Ritchie, E. G., Ruffault, J., Williamson, G. J., Wu, Q., and Nimmo, D. G.: What do you mean, 'megafire'?, *Global Ecology and*  
4492 *Biogeography*, 31, 1906–1922, <https://doi.org/10.1111/geb.13499>, 2022.
- 4493 Lizundia-Loiola, J., Otón, G., Ramo, R., and Chuvieco, E.: A spatio-temporal active-fire clustering approach for global burned  
4494 area mapping at 250 m from MODIS data, *Remote Sensing of Environment*, 236, 111493,  
4495 <https://doi.org/10.1016/j.rse.2019.111493>, 2020.
- 4496 Lizundia-Loiola, J., Franquesa, M., Khairoun, A., and Chuvieco, E.: Global burned area mapping from Sentinel-3 Synergy and  
4497 VIIRS active fires, *Remote Sensing of Environment*, 282, 113298, <https://doi.org/10.1016/j.rse.2022.113298>, 2022.
- 4498 Lundberg, S. M. and Lee, S.-I.: A unified approach to interpreting model predictions, in: *Proceedings of the 31st International*  
4499 *Conference on Neural Information Processing Systems*, Red Hook, NY, USA, 4768–4777, 2017.
- 4500 Luque, M. A. M., Leon, E., Ardila, J. G. B., Gutiérrez, G., Bilbao, B., Rivera-Lombardi, R., and Milán, A.: Community Forest  
4501 Brigades and their implementation as part of a new vision in the integrated fire management in the Bolivarian Republic of  
4502 Venezuela, *Biodiversidade Brasileira*, 10, 49–49, <https://doi.org/10.37002/biodiversidadebrasileira.v10i1.1624>, 2020.
- 4503 Majasalmi, T. and Rautiainen, M.: Representation of tree cover in global land cover products: Finland as a case study area,  
4504 *Environ Monit Assess*, 193, 121, <https://doi.org/10.1007/s10661-021-08898-2>, 2021.
- 4505 MapBiomias Brasil: Plataforma - Monitor do Fogo, available at: <https://plataforma.brasil.mapbiomas.org/monitor-do-fogo>, last  
4506 access: 9 July 2024, 2024.
- 4507 Maraun, D., Shepherd, T. G., Widmann, M., Zappa, G., Walton, D., Gutiérrez, J. M., Hagemann, S., Richter, I., Soares, P. M. M.,  
4508 Hall, A., and Mearns, L. O.: Towards process-informed bias correction of climate change simulations, *Nature Clim Change*, 7,  
4509 764–773, <https://doi.org/10.1038/nclimate3418>, 2017.
- 4510 Mariani, M., Fletcher, M.-S., Holz, A., and Nyman, P.: ENSO controls interannual fire activity in southeast Australia, *Geophysical*  
4511 *Research Letters*, 43, 10,891-10,900, <https://doi.org/10.1002/2016GL070572>, 2016.
- 4512 Mataveli, G., Jones, M. W., Carmenta, R., Sanchez, A., Dutra, D. J., Chaves, M., de Oliveira, G., Anderson, L. O., and Aragão,  
4513 L. E. O. C.: Deforestation falls but rise of wildfires continues degrading Brazilian Amazon forests, *Global Change Biology*, 30,  
4514 e17202, <https://doi.org/10.1111/gcb.17202>, 2024.
- 4515 Mathison, C., Burke, E., Hartley, A. J., Kelley, D. I., Burton, C., Robertson, E., Gedney, N., Williams, K., Wiltshire, A., Ellis, R. J.,  
4516 Sellar, A. A., and Jones, C. D.: Description and evaluation of the JULES-ES set-up for ISIMIP2b, *Geoscientific Model*  
4517 *Development*, 16, 4249–4264, <https://doi.org/10.5194/gmd-16-4249-2023>, 2023.
- 4518 Matthews, S.: A comparison of fire danger rating systems for use in forests, *Australian Meteorological and Oceanographic*  
4519 *Journal*, 58, 41–48, <https://doi.org/10.22499/2.5801.005>, 2009.

- 4520 Mauritsen, T., Bader, J., Becker, T., Behrens, J., Bittner, M., Brokopf, R., Brovkin, V., Claussen, M., Crueger, T., Esch, M., Fast,  
4521 I., Fiedler, S., Fläschner, D., Gayler, V., Giorgetta, M., Goll, D. S., Haak, H., Hagemann, S., Hedemann, C., Hohenegger, C.,  
4522 Ilyina, T., Jahns, T., Jimenez-de-la-Cuesta, D., Jungclaus, J., Kleinen, T., Kloster, S., Kracher, D., Kinne, S., Kleberg, D., Lasslop,  
4523 G., Kornblueh, L., Marotzke, J., Matei, D., Meraner, K., Mikolajewicz, U., Modali, K., Möbis, B., Müller, W. A., Nabel, J. E. M. S.,  
4524 Nam, C. C. W., Notz, D., Nyawira, S.-S., Paulsen, H., Peters, K., Pincus, R., Pohlmann, H., Pongratz, J., Popp, M., Raddatz, T.  
4525 J., Rast, S., Redler, R., Reick, C. H., Rohrschneider, T., Schemann, V., Schmidt, H., Schnur, R., Schulzweida, U., Six, K. D.,  
4526 Stein, L., Stemmler, I., Stevens, B., von Storch, J.-S., Tian, F., Voigt, A., Vrese, P., Wieners, K.-H., Wilkenskjeld, S., Winkler, A.,  
4527 and Roeckner, E.: Developments in the MPI-M Earth System Model version 1.2 (MPI-ESM1.2) and Its Response to Increasing  
4528 CO<sub>2</sub>, *Journal of Advances in Modeling Earth Systems*, 11, 998–1038, <https://doi.org/10.1029/2018MS001400>, 2019.
- 4529 McNorton, J., Agustí-Panareda, A., Arduini, G., Balsamo, G., Boussez, N., Boussetta, S., Chericoni, M., Choulga, M., Engelen,  
4530 R., and Guevara, M.: An Urban Scheme for the ECMWF Integrated Forecasting System: Global Forecasts and Residential CO<sub>2</sub>  
4531 Emissions, *Journal of Advances in Modeling Earth Systems*, 15, e2022MS003286, <https://doi.org/10.1029/2022MS003286>, 2023.
- 4532 McNorton, J. R. and Di Giuseppe, F.: A global fuel characteristic model and dataset for wildfire prediction, *Biogeosciences*, 21,  
4533 279–300, <https://doi.org/10.5194/bg-21-279-2024>, 2024.
- 4534 McNorton, J. R., Giuseppe, F. D., Pinnington, E. M., Chantry, M., and Barnard, C.: A Global Probability-of-Fire (PoF) Forecast,  
4535 <https://doi.org/10.22541/essoar.170542063.30086889/v1>.
- 4536 Meadley, J.: Thailand Enhances Measures Against Forest Fires, Encroachment Increases in Laos, available at:  
4537 <https://laotiantimes.com/2024/01/31/thailand-enhances-measures-against-forest-fires-encroachment-increases-in-laos/>, last  
4538 access: 9 July 2024, *Laotian Times*, 2024.
- 4539 Mediterranean Center for Environmental Studies: Postfire/Informes de Impacto: Informe sobre el impacto del incendio forestal  
4540 de Villanueva de Viver, 2023, available at: [https://www.ceam.es/es/news/postfire-informes-de-impacto-informe-sobre-el-impacto-  
4541 del-incendio-forestal-de-villanueva-de-viver-2023/](https://www.ceam.es/es/news/postfire-informes-de-impacto-informe-sobre-el-impacto-del-incendio-forestal-de-villanueva-de-viver-2023/), last access: 9 July 2024, 2023.
- 4542 Meier, S., Elliott, R. J. R., and Strobl, E.: 2023a The regional economic impact of wildfires: Evidence from Southern Europe,  
4543 *Journal of Environmental Economics and Management*, 118, 102787, <https://doi.org/10.1016/j.jeem.2023.102787>, 2023a.
- 4544 Meier, S., Strobl, E., Elliott, R. J. R., and Kettridge, N.: 2023b Cross-country risk quantification of extreme wildfires in  
4545 Mediterranean Europe, *Risk Analysis*, 43, 1745–1762, <https://doi.org/10.1111/risa.14075>, 2023b.
- 4546 Mengel, M., Treu, S., Lange, S., and Frieler, K.: ATTRICI v1.1 – counterfactual climate for impact attribution, *Geoscientific Model  
4547 Development*, 14, 5269–5284, <https://doi.org/10.5194/gmd-14-5269-2021>, 2021.
- 4548 Mills, G., Salkin, O., Fearon, M., Harris, S., Brown, T., and Reinbold, H.: Meteorological drivers of the eastern Victorian Black  
4549 Summer (2019–2020) fires, *J. South. Hemisph. Earth Syst. Sci.*, 72, 139–163, <https://doi.org/10.1071/ES22011>, 2022.
- 4550 Mindlin, J., Vera, C. S., Shepherd, T. G., and Osman, M.: Plausible Drying and Wetting Scenarios for Summer in Southeastern  
4551 South America, *Journal of Climate*, 36, 7973–7991, <https://doi.org/10.1175/JCLI-D-23-0134.1>, 2023.
- 4552 Ministério Público Federal: Procuradoria da República no Amazonas. Reference: PA-PPB nº 1.13.000.001219/2021-55, 2023.
- 4553 Modaresi Rad, A., Abatzoglou, J. T., Kreitler, J., Alizadeh, M. R., AghaKouchak, A., Hudyma, N., Nauslar, N. J., and Sadegh, M.:  
4554 Human and infrastructure exposure to large wildfires in the United States, *Nat Sustain*, 6, 1343–1351,  
4555 <https://doi.org/10.1038/s41893-023-01163-z>, 2023.
- 4556 Mongabay: Gobierno colombiano declara situación de desastre y calamidad en el país ante el grave impacto de incendios  
4557 forestales, available at: [https://es.mongabay.com/2024/01/gobierno-colombiano-declara-situacion-de-desastre-y-calamidad-en-  
4558 el-pais-ante-el-grave-impacto-de-incendios-forestales/](https://es.mongabay.com/2024/01/gobierno-colombiano-declara-situacion-de-desastre-y-calamidad-en-el-pais-ante-el-grave-impacto-de-incendios-forestales/), last access: 9 July 2024, *Noticias ambientales*, 2024.
- 4559 Moreira, F., Ascoli, D., Safford, H., Adams, M. A., Moreno, J. M., Pereira, J. M. C., Catry, F. X., Armesto, J., Bond, W., González,  
4560 M. E., Curt, T., Koutsias, N., McCaw, L., Price, O., Pausas, J. G., Rigolot, E., Stephens, S., Tavsanoglu, C., Vallejo, V. R., Wilgen,  
4561 B. W. V., Xanthopoulos, G., and Fernandes, P. M.: Wildfire management in Mediterranean-type regions: paradigm change  
4562 needed, *Environ. Res. Lett.*, 15, 011001, <https://doi.org/10.1088/1748-9326/ab541e>, 2020.

4563 Muñoz-Sabater, J., Dutra, E., Agustí-Panareda, A., Albergel, C., Arduini, G., Balsamo, G., Boussetta, S., Choulga, M., Harrigan,  
4564 S., Hersbach, H., Martens, B., Miralles, D. G., Piles, M., Rodríguez-Fernández, N. J., Zsoter, E., Buontempo, C., and Thépaut,  
4565 J.-N.: ERA5-Land: a state-of-the-art global reanalysis dataset for land applications, *Earth System Science Data*, 13, 4349–4383,  
4566 <https://doi.org/10.5194/essd-13-4349-2021>, 2021.

4567 Murray, C. J. L., Aravkin, A. Y., Zheng, P., Abbafati, C., Abbas, K. M., Abbasi-Kangevari, M., Abd-Allah, F., Abdelalim, A.,  
4568 Abdollahi, M., Abdollahpour, I., Abegaz, K. H., Abolhassani, H., Aboyans, V., Abreu, L. G., Abrigo, M. R. M., Abualhasan, A.,  
4569 Abu-Raddad, L. J., Abushouk, A. I., Adabi, M., Adeganmbi, V., Adeoye, A. M., Adetokunboh, O. O., Adham, D., Advani, S. M.,  
4570 Agarwal, G., Aghamir, S. M. K., Agrawal, A., Ahmad, T., Ahmadi, K., Ahmadi, M., Ahmadi, H., Ahmed, M. B., Akalu, T. Y.,  
4571 Akinyemi, R. O., Akinyemiju, T., Akombi, B., Akunna, C. J., Alahdab, F., Al-Aly, Z., Alam, K., Alam, S., Alam, T., Alanezi, F. M.,  
4572 Alanzi, T. M., Alemu, B., Wassihun, Alhabib, K. F., Ali, M., Ali, S., Alicandro, G., Alinia, C., Alipour, V., Alizade, H., Aljunid, S. M.,  
4573 Alla, F., Allebeck, P., Almasi-Hashiani, A., Al-Mekhlafi, H. M., Alonso, J., Altirkawi, K. A., Amini-Rarani, M., Amiri, F., Amugsi, D.  
4574 A., Ancuceanu, R., Anderlini, D., Anderson, J. A., Andrei, C. L., Andrei, T., Angus, C., Anjomshoa, M., Ansari, F., Ansari-  
4575 Moghaddam, A., Antonazzo, I. C., Antonio, C. A. T., Antony, C. M., Antriyandarti, E., Anvari, D., Anwer, R., Appiah, S. C. Y.,  
4576 Arabloo, J., Arab-Zozani, M., Ariani, F., Armoon, B., Ärnlöv, J., Arzani, A., Asadi-Aliabadi, M., Asadi-Pooya, A. A., Ashbaugh, C.,  
4577 Assmus, M., Atafar, Z., Atnafu, D. D., Atout, M. M. W., Ausloos, F., Ausloos, M., Quintanilla, B. P. A., Ayano, G., Ayanore, M. A.,  
4578 Azari, S., Azarian, G., Azene, Z. N., et al.: Global burden of 87 risk factors in 204 countries and territories, 1990–2019: a  
4579 systematic analysis for the Global Burden of Disease Study 2019, *The Lancet*, 396, 1223–1249, [https://doi.org/10.1016/S0140-  
4580 6736\(20\)30752-2](https://doi.org/10.1016/S0140-6736(20)30752-2), 2020.

4581 NASA Earth Observatory: Tracking Canada's Extreme 2023 Fire Season, available at:  
4582 <https://earthobservatory.nasa.gov/images/151985/tracking-canadas-extreme-2023-fire-season>, last access: 9 July 2024, 2023.

4583 NASA Earth Observatory: Fires Rage in Central Chile, available at: [https://earthobservatory.nasa.gov/images/152411/fires-rage-  
4584 in-central-chile](https://earthobservatory.nasa.gov/images/152411/fires-rage-in-central-chile), last access: 9 July 2024, 2024.

4585 NASA Earth Science Data Systems: MODIS/Aqua+Terra Thermal Anomalies/Fire locations 1km FIRMS V006 and V0061 (Vector  
4586 data), available at: <https://www.earthdata.nasa.gov/learn/find-data/near-real-time/firms/mcd14ml>, last access: 9 July 2024, 2020.

4587 NASA FIRMS: NASA Fire Information for Resource Management System, available at:  
4588 <https://firms.modaps.eosdis.nasa.gov/map/>, last access: 9 July 2024, 2024.

4589 National Institute for Space Research: INPE Programa Queimadas - Banco de Dados de Queimadas, available at:  
4590 <https://terrabrazilis.dpi.inpe.br/queimadas/portal/>, last access: 9 July 2024, 2024.

4591 National Interagency Fire Center: National Interagency Fire Center Situation Report for August 31, 2023, available at:  
4592 [https://www.nifc.gov/sites/default/files/NICC/1-Incident%20Information/IMSR/2023/August/IMSR\\_CY23\\_08\\_31\\_23\\_0.pdf](https://www.nifc.gov/sites/default/files/NICC/1-Incident%20Information/IMSR/2023/August/IMSR_CY23_08_31_23_0.pdf), last  
4593 access: 9 July 2024, National Interagency Fire Center, 2023.

4594 National Interagency Fire Center: 2024a Statistics - Current National Statistics, available at: [https://www.nifc.gov/fire-  
4595 information/statistics](https://www.nifc.gov/fire-information/statistics), last access: 9 July 2024, 2024a.

4596 National Interagency Fire Center: 2024b InciWeb Information, available at: [https://www.nifc.gov/fire-information/pio-bulletin-  
4597 board/inciweb](https://www.nifc.gov/fire-information/pio-bulletin-board/inciweb), last access: 9 July 2024, 2024b.

4598 National Oceanic and Atmospheric Administration: National Centers for Environmental Information, Monthly Wildfires Report,  
4599 available at: <https://www.ncei.noaa.gov/access/monitoring/monthly-report/fire/202308>, last access: 9 July 2024, National Oceanic  
4600 and Atmospheric Administration, 2023.

4601 National Oceanic and Atmospheric Administration: Fires Rage Across Texas Panhandle, available at:  
4602 <https://www.nesdis.noaa.gov/news/fires-rage-across-texas-panhandle>, last access: 9 July 2024, National Environmental  
4603 Satellite, Data, and Information Service, 2024.

4604 Neris, J., Santin, C., Lew, R., Robichaud, P. R., Elliot, W. J., Lewis, S. A., Sheridan, G., Rohlf, A.-M., Ollivier, Q., Oliveira, L.,  
4605 and Doerr, S. H.: Designing tools to predict and mitigate impacts on water quality following the Australian 2019/2020 wildfires:  
4606 Insights from Sydney's largest water supply catchment, *Integrated Environmental Assessment and Management*, 17, 1151–1161,  
4607 <https://doi.org/10.1002/ieam.4406>, 2021.



- 4608 Nielsen-Pincus, M., Moseley, C., and Gebert, K.: Job growth and loss across sectors and time in the western US: The impact of  
4609 large wildfires, *Forest Policy and Economics*, 38, 199–206, <https://doi.org/10.1016/j.forpol.2013.08.010>, 2014.
- 4610 Nikolakis, W., Welham, C., and Greene, G.: Diffusion of indigenous fire management and carbon-credit programs: Opportunities  
4611 and challenges for “scaling-up” to temperate ecosystems, *Front. For. Glob. Change*, 5, <https://doi.org/10.3389/ffgc.2022.967653>,  
4612 2022.
- 4613 Noble, I. R., Gill, A. M., and Bary, G. a. V.: McArthur’s fire-danger meters expressed as equations, *Australian Journal of Ecology*,  
4614 5, 201–203, <https://doi.org/10.1111/j.1442-9993.1980.tb01243.x>, 1980.
- 4615 Nolan, R. H., Collins, L., Leigh, A., Ooi, M. K. J., Curran, T. J., Fairman, T. A., Resco de Dios, V., and Bradstock, R.: 2021a Limits  
4616 to post-fire vegetation recovery under climate change, *Plant, Cell & Environment*, 44, 3471–3489,  
4617 <https://doi.org/10.1111/pce.14176>, 2021a.
- 4618 Nolan, R. H., Bowman, D. M. J. S., Clarke, H., Haynes, K., Ooi, M. K. J., Price, O. F., Williamson, G. J., Whittaker, J., Bedward,  
4619 M., Boer, M. M., Cavanagh, V. I., Collins, L., Gibson, R. K., Griebel, A., Jenkins, M. E., Keith, D. A., McIlwee, A. P., Penman, T.  
4620 D., Samson, S. A., Tozer, M. G., and Bradstock, R. A.: 2021b What Do the Australian Black Summer Fires Signify for the Global  
4621 Fire Crisis?, *Fire*, 4, 97, <https://doi.org/10.3390/fire4040097>, 2021b.
- 4622 Nunes, J. P., Doerr, S. H., Sheridan, G., Neris, J., Santín, C., Emelko, M. B., Silins, U., Robichaud, P. R., Elliot, W. J., and Keizer,  
4623 J.: Assessing water contamination risk from vegetation fires: Challenges, opportunities and a framework for progress,  
4624 *Hydrological Processes*, 32, 687–694, <https://doi.org/10.1002/hyp.11434>, 2018.
- 4625 Oberholtz, C.: Drone video shows wildfire devastation in Chile as death toll soars to 112 with hundreds still missing, available at:  
4626 <https://www.foxweather.com/weather-news/valparaiso-chile-forest-fires-evacuations-damage>, last access: 9 July 2024, FOX  
4627 Weather, 2024.
- 4628 O’Dell, K., Ford, B., Fischer, E. V., and Pierce, J. R.: Contribution of Wildland-Fire Smoke to US PM<sub>2.5</sub> and Its Influence on  
4629 Recent Trends, *Environ. Sci. Technol.*, 53, 1797–1804, <https://doi.org/10.1021/acs.est.8b05430>, 2019.
- 4630 OECD: Taming Wildfires in the Context of Climate Change, OECD, <https://doi.org/10.1787/dd00c367-en>, 2023.
- 4631 Oklahoma Department of Emergency Management: April 1 Situation Update 2 Wildfires Impacting State, available at:  
4632 <https://oklahoma.gov/oem/emergencies-and-disasters/2023/march-31-wildfire-event/april-1-situation-update-2.html>, last access:  
4633 9 July 2024, Oklahoma Department of Emergency Management, 2023.
- 4634 Olson, D. M., Dinerstein, E., Wikramanayake, E. D., Burgess, N. D., Powell, G. V. N., Underwood, E. C., D’amico, J. A., Itoua, I.,  
4635 Strand, H. E., Morrison, J. C., Loucks, C. J., Allnutt, T. F., Ricketts, T. H., Kura, Y., Lamoreux, J. F., Wettengel, W. W., Hedao,  
4636 P., and Kassem, K. R.: Terrestrial Ecoregions of the World: A New Map of Life on Earth, *BioScience*, 51, 933,  
4637 [https://doi.org/10.1641/0006-3568\(2001\)051\[0933:TEOTWA\]2.0.CO;2](https://doi.org/10.1641/0006-3568(2001)051[0933:TEOTWA]2.0.CO;2), 2001.
- 4638 Otón, G., Lizundia-Loiola, J., Pettinari, M. L., and Chuvieco, E.: Development of a consistent global long-term burned area product  
4639 (1982–2018) based on AVHRR-LTDR data, *International Journal of Applied Earth Observation and Geoinformation*, 103, 102473,  
4640 <https://doi.org/10.1016/j.jag.2021.102473>, 2021.
- 4641 Pai, S. J., Carter, T. S., Heald, C. L., and Kroll, J. H.: Updated World Health Organization Air Quality Guidelines Highlight the  
4642 Importance of Non-anthropogenic PM<sub>2.5</sub>, *Environ. Sci. Technol. Lett.*, 9, 501–506, <https://doi.org/10.1021/acs.estlett.2c00203>,  
4643 2022.
- 4644 Palmer, J.: Fire as Medicine: Learning from Native American Fire Stewardship, available at: [http://eos.org/features/fire-as-](http://eos.org/features/fire-as-medicine-learning-from-native-american-fire-stewardship)  
4645 [medicine-learning-from-native-american-fire-stewardship](http://eos.org/features/fire-as-medicine-learning-from-native-american-fire-stewardship), last access: 9 July 2024, Eos, 2021.
- 4646 Pan, X., Chin, M., Ichoku, C. M., and Field, R. D.: Connecting Indonesian Fires and Drought With the Type of El Niño and Phase  
4647 of the Indian Ocean Dipole During 1979–2016, *Journal of Geophysical Research: Atmospheres*, 123, 7974–7988,  
4648 <https://doi.org/10.1029/2018JD028402>, 2018.

- 4649 Pan, X., Ichoku, C., Chin, M., Bian, H., Darmenov, A., Colarco, P., Ellison, L., Kucsera, T., da Silva, A., Wang, J., Oda, T., and  
4650 Cui, G.: Six global biomass burning emission datasets: intercomparison and application in one global aerosol model, *Atmospheric  
4651 Chemistry and Physics*, 20, 969–994, <https://doi.org/10.5194/acp-20-969-2020>, 2020.
- 4652 Perron, M. M. G., Meyerink, S., Corkill, M., Strzelec, M., Proemse, B. C., Gault-Ringold, M., Sanz Rodriguez, E., Chase, Z., and  
4653 Bowie, A. R.: Trace elements and nutrients in wildfire plumes to the southeast of Australia, *Atmospheric Research*, 270, 106084,  
4654 <https://doi.org/10.1016/j.atmosres.2022.106084>, 2022.
- 4655 Perry, M. C., Vanvyve, E., Betts, R. A., and Palin, E. J.: Past and future trends in fire weather for the UK, *Natural Hazards and  
4656 Earth System Sciences*, 22, 559–575, <https://doi.org/10.5194/nhess-22-559-2022>, 2022.
- 4657 Phillips, C. A., Rogers, B. M., Elder, M., Cooperdock, S., Moubarak, M., Randerson, J. T., and Frumhoff, P. C.: Escalating carbon  
4658 emissions from North American boreal forest wildfires and the climate mitigation potential of fire management, *Science Advances*,  
4659 8, eabl7161, <https://doi.org/10.1126/sciadv.abl7161>, 2022.
- 4660 Polade, S. D., Pierce, D. W., Cayan, D. R., Gershunov, A., and Dettinger, M. D.: The key role of dry days in changing regional  
4661 climate and precipitation regimes, *Sci Rep*, 4, 4364, <https://doi.org/10.1038/srep04364>, 2014.
- 4662 Pomeroy, J. W., DeBeer, C. M., Adapa, P., Phare, M. A., Overduin, N., Miltenberger, M., Maas, M., Pentland, R., Brandes, O.  
4663 M., and Sandford, R. W.: Water Security for Canadians: Solutions for Canada’s Emerging Water Crisis, available at:  
4664 <https://landusekn.ca/resource/water-security-canadians-solutions-canada%E2%80%99s-emerging-water-crisis>, last access: 9  
4665 July 2024, 2019.
- 4666 Pullabhotla, H., Zahid, M., Heft-Neal, S., Rathi, V., and Burke, M.: Reply to Giglio and Roy: Aggregate infant mortality estimates  
4667 robust to choice of burned area product, *Proceedings of the National Academy of Sciences*, 120, e2318188120,  
4668 <https://doi.org/10.1073/pnas.2318188120>, 2023.
- 4669 Pyne, S. J.: *Fire in America: A Cultural History of Wildland and Rural Fire*, University of Washington Press, 2017.
- 4670 Rabin, S. S., Melton, J. R., Lasslop, G., Bachelet, D., Forrest, M., Hantson, S., Kaplan, J. O., Li, F., Mangeon, S., Ward, D. S.,  
4671 Yue, C., Arora, V. K., Hickler, T., Kloster, S., Knorr, W., Nieradzik, L., Spessa, A., Folberth, G. A., Sheehan, T., Voulgarakis, A.,  
4672 Kelley, D. I., Prentice, I. C., Sitch, S., Harrison, S., and Arneth, A.: The Fire Modeling Intercomparison Project (FireMIP), phase  
4673 1: experimental and analytical protocols with detailed model descriptions, *Geoscientific Model Development*, 10, 1175–1197,  
4674 <https://doi.org/10.5194/gmd-10-1175-2017>, 2017.
- 4675 Radeloff, V. C., Helmers, D. P., Kramer, H. A., Mockrin, M. H., Alexandre, P. M., Bar-Massada, A., Butsic, V., Hawbaker, T. J.,  
4676 Martinuzzi, S., Syphard, A. D., and Stewart, S. I.: Rapid growth of the US wildland-urban interface raises wildfire risk, *Proceedings  
4677 of the National Academy of Sciences*, 115, 3314–3319, <https://doi.org/10.1073/pnas.1718850115>, 2018.
- 4678 Rádio e Televisão de Portugal: Prejuízos dos incêndios no Porto Moniz e Calheta rondam os 3 milhões de euros (áudio), available  
4679 at: <https://madeira.rtp.pt/politica/prejuizos-dos-incendios-no-porto-moniz-e-calheta-rondam-os-3-milhoes-de-euros-audio/>, last  
4680 access: 9 July 2024, 2023.
- 4681 Reddington, C. L., Spracklen, D. V., Artaxo, P., Ridley, D. A., Rizzo, L. V., and Arana, A.: Analysis of particulate emissions from  
4682 tropical biomass burning using a global aerosol model and long-term surface observations, *Atmospheric Chemistry and Physics*,  
4683 16, 11083–11106, <https://doi.org/10.5194/acp-16-11083-2016>, 2016.
- 4684 Ren, X., Zhang, L., Cai, W., and Wu, L.: Moderate Indian Ocean Dipole Dominates Spring Fire Weather Conditions in Southern  
4685 Australia, *Environ. Res. Lett.*, <https://doi.org/10.1088/1748-9326/ad4fa5>, 2024.
- 4686 Reuters: 2023a Deadly fires rage along Algeria coast, spread to Tunisia, available at:  
4687 <https://www.reuters.com/world/africa/deadly-fires-rage-along-algeria-coast-spread-tunisia-2023-07-25/>, last access: 9 July 2024,  
4688 Reuters, 25th July, 2023a.
- 4689 Reuters: 2023b Syria struggles to contain wildfires as temperatures rise, available at: <https://www.reuters.com/world/middle-east/syria-struggles-contain-wildfires-temperatures-rise-2023-07-18/>, last access: 9 July 2024, Reuters, 18th July, 2023b.  
4690

- 4691 Roads, J., Tripp, P., Juang, H., Wang, J., Fujioka, F., and Chen, S.: NCEP-ECPC monthly to seasonal US fire danger forecasts, *International Journal of Wildland Fire* 19:399-414, 19, 399–414, <https://doi.org/10.1071/WF07079>, 2010.
- 4692
- 4693 Rodríguez-Trejo, D. A., Ponce-Calderón, L. P., Tchikoué, H., Martínez-Domínguez, R., Martínez-Muñoz, P., and Pulido-Luna, J. A.: Towards integrated fire management in Mexico's Megalopolis region: a diagnosis, *TFI*, 80–86, <https://doi.org/10.55515/NWAM8441>, 2022.
- 4694
- 4695
- 4696 Román, M. O., Justice, C., Paynter, I., Boucher, P. B., Devadiga, S., Endsley, A., Erb, A., Friedl, M., Gao, H., Giglio, L., Gray, J. M., Hall, D., Hulley, G., Kimball, J., Knyazikhin, Y., Lyapustin, A., Myneni, R. B., Noojipady, P., Pu, J., Riggs, G., Sarkar, S., Schaaf, C., Shah, D., Tran, K. H., Vermote, E., Wang, D., Wang, Z., Wu, A., Ye, Y., Shen, Y., Zhang, S., Zhang, S., Zhang, X., Zhao, M., Davidson, C., and Wolfe, R.: Continuity between NASA MODIS Collection 6.1 and VIIRS Collection 2 land products, *Remote Sensing of Environment*, 302, 113963, <https://doi.org/10.1016/j.rse.2023.113963>, 2024.
- 4697
- 4698
- 4699
- 4700
- 4701 Romps, D. M.: Evaluating the Future of Lightning in Cloud-Resolving Models, *Geophysical Research Letters*, 46, 14863–14871, <https://doi.org/10.1029/2019GL085748>, 2019.
- 4702
- 4703 Rosan, T. M., Sitch, S., Mercado, L. M., Heinrich, V., Friedlingstein, P., and Aragão, L. E. O. C.: Fragmentation-Driven Divergent Trends in Burned Area in Amazonia and Cerrado, *Front. For. Glob. Change*, 5, <https://doi.org/10.3389/ffgc.2022.801408>, 2022.
- 4704
- 4705 Roteta, E., Bastarrika, A., Ibisate, A., and Chuvieco, E.: A Preliminary Global Automatic Burned-Area Algorithm at Medium Resolution in Google Earth Engine, *Remote Sensing*, 13, 4298, <https://doi.org/10.3390/rs13214298>, 2021.
- 4706
- 4707 Roy, D. P., Boschetti, L., Justice, C. O., and Ju, J.: The collection 5 MODIS burned area product — Global evaluation by comparison with the MODIS active fire product, *Remote Sensing of Environment*, 112, 3690–3707, <https://doi.org/10.1016/j.rse.2008.05.013>, 2008.
- 4708
- 4709
- 4710 Russell-Smith, J., Yates, C. P., Edwards, A. C., Whitehead, P. J., Murphy, B. P., and Lawes, M. J.: Deriving Multiple Benefits from Carbon Market-Based Savanna Fire Management: An Australian Example, *PLoS ONE*, 10, e0143426, <https://doi.org/10.1371/journal.pone.0143426>, 2015.
- 4711
- 4712
- 4713 Sabljak, E.: Scotland's wildfires in maps and charts across all councils, available at: <https://www.heraldsotland.com/news/23498843.scotlands-wildfires-maps-charts-across-councils/>, last access: 9 July 2024, 2023.
- 4714
- 4715
- 4716 Safford, H. D., Paulson, A. K., Steel, Z. L., Young, D. J. N., and Wayman, R. B.: The 2020 California fire season: A year like no other, a return to the past or a harbinger of the future?, *Global Ecol Biogeogr*, 31, 2005–2025, <https://doi.org/10.1111/geb.13498>, 2022.
- 4717
- 4718
- 4719 Sánchez-García, C., Santín, C., Neris, J., Sigmund, G., Otero, X. L., Manley, J., González-Rodríguez, G., Belcher, C. M., Cerdà, A., Marcotte, A. L., Murphy, S. F., Rhoades, C. C., Sheridan, G., Strydom, T., Robichaud, P. R., and Doerr, S. H.: Chemical characteristics of wildfire ash across the globe and their environmental and socio-economic implications, *Environment International*, 178, 108065, <https://doi.org/10.1016/j.envint.2023.108065>, 2023.
- 4720
- 4721
- 4722
- 4723 San-Miguel-Ayanz, J., Schulte, E., Schmuck, G., and Camia, A.: The European Forest Fire Information System in the context of environmental policies of the European Union, *Forest Policy and Economics*, 29, 19–25, <https://doi.org/10.1016/j.forpol.2011.08.012>, 2013.
- 4724
- 4725
- 4726 Santoro, M. and Cartus, O.: ESA Biomass Climate Change Initiative (Biomass\_cci): Global datasets of forest above-ground biomass for the years 2010, 2017 and 2018, v3, <https://doi.org/10.5285/5F331C418E9F4935B8EB1B836F8A91B8>, 2021.
- 4727
- 4728 Santoro, M., Cartus, O., Wegmüller, U., Besnard, S., Carvalhais, N., Araza, A., Herold, M., Liang, J., Cavlovic, J., and Engdahl, M. E.: Global estimation of above-ground biomass from spaceborne C-band scatterometer observations aided by LiDAR metrics of vegetation structure, *Remote Sensing of Environment*, 279, 113114, <https://doi.org/10.1016/j.rse.2022.113114>, 2022.
- 4729
- 4730
- 4731 Scholten, R. C., Jandt, R., Miller, E. A., Rogers, B. M., and Veraverbeke, S.: Overwintering fires in boreal forests, *Nature*, 593, 399–404, <https://doi.org/10.1038/s41586-021-03437-y>, 2021.
- 4732

- 4733 Schroeder, W., Oliva, P., Giglio, L., and Csiszar, I. A.: The New VIIRS 375 m active fire detection data product: Algorithm  
4734 description and initial assessment, *Remote Sensing of Environment*, 143, 85–96, <https://doi.org/10.1016/j.rse.2013.12.008>, 2014.
- 4735 Schroeder, W., Oliva, P., Giglio, L., Quayle, B., Lorenz, E., and Morelli, F.: Active fire detection using Landsat-8/OLI data, *Remote  
4736 Sensing of Environment*, 185, 210–220, <https://doi.org/10.1016/j.rse.2015.08.032>, 2016.
- 4737 Schug, F., Bar-Massada, A., Carlson, A. R., Cox, H., Hawbaker, T. J., Helmers, D., Hostert, P., Kaim, D., Kasraee, N. K.,  
4738 Martinuzzi, S., Mockrin, M. H., Pfoch, K. A., and Radeloff, V. C.: The global wildland–urban interface, *Nature*, 621, 94–99,  
4739 <https://doi.org/10.1038/s41586-023-06320-0>, 2023.
- 4740 Seddon, N., Chausson, A., Berry, P., Girardin, C. A. J., Smith, A., and Turner, B.: Understanding the value and limits of nature-  
4741 based solutions to climate change and other global challenges, *Philosophical Transactions of the Royal Society B: Biological  
4742 Sciences*, 375, 20190120, <https://doi.org/10.1098/rstb.2019.0120>, 2020.
- 4743 Seok, M.-W., Ko, Y. H., Park, K.-T., and Kim, T.-W.: Possible enhancement in ocean productivity associated with wildfire-derived  
4744 nutrient and black carbon deposition in the Arctic Ocean in 2019–2021, *Marine Pollution Bulletin*, 201, 116149,  
4745 <https://doi.org/10.1016/j.marpolbul.2024.116149>, 2024.
- 4746 Sexton, J. O., Noojipady, P., Song, X.-P., Feng, M., Song, D.-X., Kim, D.-H., Anand, A., Huang, C., Channan, S., Pimm, S. L.,  
4747 and Townshend, J. R.: Conservation policy and the measurement of forests, *Nature Clim Change*, 6, 192–196,  
4748 <https://doi.org/10.1038/nclimate2816>, 2016.
- 4749 Seneviratne, S.I., X. Zhang, M. Adnan, W. Badi, C. Dereczynski, A. Di Luca, S. Ghosh, I. Iskandar, J. Kossin, S. Lewis, F. Otto,  
4750 I. Pinto, M. Satoh, S.M. Vicente-Serrano, M. Wehner, and B. Zhou, 2021: Weather and Climate Extreme Events in a Changing  
4751 Climate. In *Climate Change 2021: The Physical Science Basis. Contribution of Working Group I to the Sixth Assessment Report  
4752 of the Intergovernmental Panel on Climate Change [Masson-Delmotte, V., P. Zhai, A. Pirani, S.L. Connors, C. Péan, S. Berger,  
4753 N. Caud, Y. Chen, L. Goldfarb, M.I. Gomis, M. Huang, K. Leitzell, E. Lonnoy, J.B.R. Matthews, T.K. Maycock, T. Waterfield, O.  
4754 Yelekçi, R. Yu, and B. Zhou (eds.)]. Cambridge University Press, Cambridge, United Kingdom and New York, NY, USA, pp.  
4755 1513–1766, doi: 10.1017/9781009157896.013.*
- 4756 Shaddick, G., Thomas, M. L., Amini, H., Broday, D., Cohen, A., Frostad, J., Green, A., Gumy, S., Liu, Y., Martin, R. V., Pruss-  
4757 Ustun, A., Simpson, D., van Donkelaar, A., and Brauer, M.: Data Integration for the Assessment of Population Exposure to  
4758 Ambient Air Pollution for Global Burden of Disease Assessment, *Environ. Sci. Technol.*, 52, 9069–9078,  
4759 <https://doi.org/10.1021/acs.est.8b02864>, 2018.
- 4760 Shakesby, R. A. and Doerr, S. H.: Wildfire as a hydrological and geomorphological agent, *Earth-Science Reviews*, 74, 269–307,  
4761 <https://doi.org/10.1016/j.earscirev.2005.10.006>, 2006.
- 4762 Shepherd, T. G., Boyd, E., Calel, R. A., Chapman, S. C., Dessai, S., Dima-West, I. M., Fowler, H. J., James, R., Maraun, D.,  
4763 Martius, O., Senior, C. A., Sobel, A. H., Stainforth, D. A., Tett, S. F. B., Trenberth, K. E., van den Hurk, B. J. J. M., Watkins, N.  
4764 W., Wilby, R. L., and Zenghelis, D. A.: Storylines: an alternative approach to representing uncertainty in physical aspects of  
4765 climate change, *Climatic Change*, 151, 555–571, <https://doi.org/10.1007/s10584-018-2317-9>, 2018.
- 4766 Shingler, B.: It's the middle of winter, and more than 100 wildfires are still smouldering, available at:  
4767 <https://www.cbc.ca/news/climate/wildfires-zombie-fires-canada-bc-alberta-1.7119851>, last access: 9 July 2024, CBC News, 21st  
4768 February, 2024.
- 4769 Short, K. C.: A spatial database of wildfires in the United States, 1992-2011, *Earth System Science Data*, 6, 1–27,  
4770 <https://doi.org/10.5194/essd-6-1-2014>, 2014.
- 4771 Shuman, J. K., Balch, J. K., Barnes, R. T., Higuera, P. E., Roos, C. I., Schwiik, D. W., Stavros, E. N., Banerjee, T., Bela, M. M.,  
4772 Bendix, J., Bertolino, S., Billign, S., Bladon, K. D., Brando, P., Breidenthal, R. E., Buma, B., Calhoun, D., Carvalho, L. M. V.,  
4773 Cattau, M. E., Cawley, K. M., Chandra, S., Chipman, M. L., Cobian-Iñiguez, J., Conlisk, E., Coop, J. D., Cullen, A., Davis, K. T.,  
4774 Dayalu, A., De Sales, F., Dolman, M., Ellsworth, L. M., Franklin, S., Guiterman, C. H., Hamilton, M., Hanan, E. J., Hansen, W.  
4775 D., Hantson, S., Harvey, B. J., Holz, A., Huang, T., Hurteau, M. D., Ilangakoon, N. T., Jennings, M., Jones, C., Klimaszewski-  
4776 Patterson, A., Kobziar, L. N., Kominoski, J., Kosovic, B., Krawchuk, M. A., Laris, P., Leonard, J., Loria-Salazar, S. M., Lucash,  
4777 M., Mahmoud, H., Margolis, E., Maxwell, T., McCarty, J. L., McWethy, D. B., Meyer, R. S., Miesel, J. R., Moser, W. K., Nagy, R.

- 4778 C., Niyogi, D., Palmer, H. M., Pellegrini, A., Poulter, B., Robertson, K., Rocha, A. V., Sadegh, M., Santos, F., Scordo, F., Sexton,  
4779 J. O., Sharma, A. S., Smith, A. M. S., Soja, A. J., Still, C., Swetnam, T., Syphard, A. D., Tingley, M. W., Tohidi, A., Trugman, A.  
4780 T., Turetsky, M., Varner, J. M., Wang, Y., Whitman, T., Yelenik, S., and Zhang, X.: Reimagine fire science for the anthropocene,  
4781 PNAS Nexus, 1, pgac115, <https://doi.org/10.1093/pnasnexus/pgac115>, 2022.
- 4782 Siciliano, B., Dantas, G., Silva, C. M. da, and Arbilla, G.: The Updated Brazilian National Air Quality Standards: A Critical Review,  
4783 J. Braz. Chem. Soc., 31, 523–535, <https://doi.org/10.21577/0103-5053.20190212>, 2020.
- 4784 SIC Notícias: Incêndio em Odemira causou prejuízos de sete milhões de euros em habitações, available at:  
4785 [https://sicnoticias.pt/especiais/incendios-em-portugal/2023-09-08-Incendio-em-Odemira-causou-prejuizos-de-sete-milhoes-de-](https://sicnoticias.pt/especiais/incendios-em-portugal/2023-09-08-Incendio-em-Odemira-causou-prejuizos-de-sete-milhoes-de-euros-em-habitacoes-c3204bcb)  
4786 [euros-em-habitacoes-c3204bcb](https://sicnoticias.pt/especiais/incendios-em-portugal/2023-09-08-Incendio-em-Odemira-causou-prejuizos-de-sete-milhoes-de-euros-em-habitacoes-c3204bcb), last access: 9 July 2024, SIC Notícias, 2023.
- 4787 Silva, C. V. J., Aragão, L. E. O. C., Young, P. J., Espírito-Santo, F., Berenguer, E., Anderson, L. O., Brasil, I., Pontes-Lopes, A.,  
4788 Ferreira, J., Withey, K., França, F., Graça, P. M. L. A., Kirsten, L., Xaud, H., Salimon, C., Scaranello, M. A., Castro, B., Seixas,  
4789 M., Farias, R., and Barlow, J.: Estimating the multi-decadal carbon deficit of burned Amazonian forests, Environ. Res. Lett., 15,  
4790 114023, <https://doi.org/10.1088/1748-9326/abb62c>, 2020.
- 4791 Silva Junior, C. H. L., Pessôa, A. C. M., Carvalho, N. S., Reis, J. B. C., Anderson, L. O., and Aragão, L. E. O. C.: The Brazilian  
4792 Amazon deforestation rate in 2020 is the greatest of the decade, Nat Ecol Evol, 5, 144–145, [https://doi.org/10.1038/s41559-020-](https://doi.org/10.1038/s41559-020-01368-x)  
4793 [01368-x](https://doi.org/10.1038/s41559-020-01368-x), 2021.
- 4794 Silveira, M. V. F., Petri, C. A., Broggio, I. S., Chagas, G. O., Macul, M. S., Leite, C. C. S. S., Ferrari, E. M. M., Amim, C. G. V.,  
4795 Freitas, A. L. R., Motta, A. Z. V., Carvalho, L. M. E., Silva Junior, C. H. L., Anderson, L. O., and Aragão, L. E. O. C.: Drivers of  
4796 Fire Anomalies in the Brazilian Amazon: Lessons Learned from the 2019 Fire Crisis, Land, 9, 516,  
4797 <https://doi.org/10.3390/land9120516>, 2020.
- 4798 Skakun, R., Castilla, G., Metsaranta, J., Whitman, E., Rodrigue, S., Little, J., Groenewegen, K., and Coyle, M.: Extending the  
4799 National Burned Area Composite Time Series of Wildfires in Canada, Remote Sensing, 14, 3050,  
4800 <https://doi.org/10.3390/rs14133050>, 2022.
- 4801 Sloan, S., Locatelli, B., Andela, N., Cattau, M. E., Gaveau, D., and Tacconi, L.: Declining severe fire activity on managed lands  
4802 in Equatorial Asia, Commun Earth Environ, 3, 1–12, <https://doi.org/10.1038/s43247-022-00522-6>, 2022.
- 4803 Smith, H. G., Sheridan, G. J., Lane, P. N. J., Nyman, P., and Haydon, S.: Wildfire effects on water quality in forest catchments:  
4804 A review with implications for water supply, Journal of Hydrology, 396, 170–192, <https://doi.org/10.1016/j.jhydrol.2010.10.043>,  
4805 2011.
- 4806 Smith, S., Geden, O., Nemet, G., Gidden, M., Lamb, W., Powis, C., Bellamy, R., Callaghan, M., Cowie, A., Cox, E., Fuss, S.,  
4807 Gasser, T., Grassi, G., Greene, J., Lueck, S., Mohan, A., Müller-Hansen, F., Peters, G., Pratama, Y., Repke, T., Riahi, K.,  
4808 Schenuit, F., Steinhauser, J., Streffer, J., Valenzuela, J., and Minx, J.: State of Carbon Dioxide Removal - 1st Edition,  
4809 <https://doi.org/10.17605/OSF.IO/W3B4Z>, 2023.
- 4810 South African Broadcasting Corporation: 2023b Wildfire scorches 1140 hectares in Simon's Town, available at:  
4811 <https://www.sabcnews.com/sabcnews/wildfire-scorches-1140-hectares-in-simons-town/>, last access: 9 July 2024, 2023.
- 4812 South African Broadcasting Corporation News: 2023a Wildfires kill 34 in Algeria as heatwave sweeps north Africa - SABC News  
4813 - Breaking news, special reports, world, business, sport coverage of all South African current events. Africa's news leader,  
4814 available at: <https://www.sabcnews.com/sabcnews/wildfires-kill-34-in-algeria-as-heatwave-sweeps-north-africa/>, last access: 9  
4815 July 2024, 2023.
- 4816 Spessa, A. C., Field, R. D., Pappenberger, F., Langner, A., Englhart, S., Weber, U., Stockdale, T., Siegert, F., Kaiser, J. W., and  
4817 Moore, J.: Seasonal forecasting of fire over Kalimantan, Indonesia, Natural Hazards and Earth System Sciences, 15, 429–442,  
4818 <https://doi.org/10.5194/nhess-15-429-2015>, 2015.
- 4819 Spuler, F. and Wessel, J.: ibicus v1.0.1, , <https://doi.org/10.5281/ZENODO.8101898>, 2023.



- 4820 Spuler, F. R., Wessel, J. B., Comyn-Platt, E., Varndell, J., and Cagnazzo, C.: ibicus: a new open-source Python package and  
 4821 comprehensive interface for statistical bias adjustment and evaluation in climate modelling (v1.0.1), Geoscientific Model  
 4822 Development, 17, 1249–1269, <https://doi.org/10.5194/gmd-17-1249-2024>, 2024.
- 4823 Staver, A. C., Archibald, S., and Levin, S. A.: The Global Extent and Determinants of Savanna and Forest as Alternative Biome  
 4824 States, *Science*, 334, 230–232, <https://doi.org/10.1126/science.1210465>, 2011.
- 4825 Sellar, A. A., Jones, C. G., Mulcahy, J. P., Tang, Y., Yool, A., Wiltshire, A., O'Connor, F. M., Stringer, M., Hill, R., Palmieri, J.,  
 4826 Woodward, S., de Mora, L., Kuhlbrodt, T., Rumbold, S. T., Kelley, D. I., Ellis, R., Johnson, C. E., Walton, J., Abraham, N. L.,  
 4827 Andrews, M. B., Andrews, T., Archibald, A. T., Berthou, S., Burke, E., Blockley, E., Carslaw, K., Dalvi, M., Edwards, J., Folberth,  
 4828 G. A., Gedney, N., Griffiths, P. T., Harper, A. B., Hendry, M. A., Hewitt, A. J., Johnson, B., Jones, A., Jones, C. D., Keeble, J.,  
 4829 Liddicoat, S., Morgenstern, O., Parker, R. J., Predoi, V., Robertson, E., Siahhan, A., Smith, R. S., Swaminathan, R., Woodhouse,  
 4830 M. T., Zeng, G., and Zerroukat, M.: UKESM1: Description and Evaluation of the U.K. Earth System Model, *Journal of Advances  
 4831 in Modeling Earth Systems*, 11, 4513–4558, <https://doi.org/10.1029/2019MS001739>, 2019.
- 4832 Stephens, S. L., Mclver, J. D., Boerner, R. E. J., Fettig, C. J., Fontaine, J. B., Hartsough, B. R., Kennedy, P. L., and Schwilk, D.  
 4833 W.: The Effects of Forest Fuel-Reduction Treatments in the United States, *BioScience*, 62, 549–560,  
 4834 <https://doi.org/10.1525/bio.2012.62.6.6>, 2012.
- 4835 Stephens, S. L., Bernal, A. A., Collins, B. M., Finney, M. A., Lautenberger, C., and Saah, D.: Mass fire behavior created by  
 4836 extensive tree mortality and high tree density not predicted by operational fire behavior models in the southern Sierra Nevada,  
 4837 *Forest Ecology and Management*, 518, 120258, <https://doi.org/10.1016/j.foreco.2022.120258>, 2022.
- 4838 Stocks, B. J., Lawson, B. D., Alexander, M. E., Wagner, C. E. V., McAlpine, R. S., Lynham, T. J., and Dubé, D. E.: The Canadian  
 4839 Forest Fire Danger Rating System: An Overview, *The Forestry Chronicle*, 65, 450–457, <https://doi.org/10.5558/tfc65450-6>, 1989.
- 4840 Stott, P. A., Stone, D. A., and Allen, M. R.: Human contribution to the European heatwave of 2003, *Nature*, 432, 610–614,  
 4841 <https://doi.org/10.1038/nature03089>, 2004.
- 4842 Sullivan, H. and Tondo, L.: 'Like a blowtorch': Mediterranean on fire as blazes spread across nine countries, available at:  
 4843 <https://www.theguardian.com/environment/2023/jul/26/northern-hemisphere-heatwaves-mediterranean-fires-croatia-portugal>,  
 4844 last access: 9 July 2024, *The Guardian*, 26th July, 2023.
- 4845 Swain, D. L., Langenbrunner, B., Neelin, J. D., and Hall, A.: Increasing precipitation volatility in twenty-first-century California,  
 4846 *Nature Clim Change*, 8, 427–433, <https://doi.org/10.1038/s41558-018-0140-y>, 2018.
- 4847 Synolakis, C. E. and Karagiannis, G. M.: Wildfire risk management in the era of climate change, *PNAS Nexus*, 3, pgae151,  
 4848 <https://doi.org/10.1093/pnasnexus/pgae151>, 2024.
- 4849 Syphard, A. and Keeley, J.: Factors Associated with Structure Loss in the 2013–2018 California Wildfires, *Fire*, 2, 49,  
 4850 <https://doi.org/10.3390/fire2030049>, 2019.
- 4851 Tang, W., Llorca, J., Weis, J., Perron, M. M. G., Basart, S., Li, Z., Sathyendranath, S., Jackson, T., Sanz Rodriguez, E., Proemse,  
 4852 B. C., Bowie, A. R., Schallenberg, C., Strutton, P. G., Matear, R., and Cassar, N.: Widespread phytoplankton blooms triggered  
 4853 by 2019–2020 Australian wildfires, *Nature*, 597, 370–375, <https://doi.org/10.1038/s41586-021-03805-8>, 2021.
- 4854 Tang, W., He, C., Emmons, L., and Zhang, J.: Global expansion of wildland-urban interface (WUI) and WUI fires: insights from a  
 4855 multiyear worldwide unified database (WUWUI), *Environ. Res. Lett.*, 19, 044028, <https://doi.org/10.1088/1748-9326/ad31da>,  
 4856 2024.
- 4857 Tang, Y., Rumbold, S., Ellis, R., Kelley, D., Mulcahy, J., Sellar, A., Walton, J., and Jones, C.: MOHC UKESM1.0-LL model output  
 4858 prepared for CMIP6 CMIP, 2019.
- 4859 Tiempo: Venezuela se llena de nubes de humos por incendios forestales y una estación muy seca, available at:  
 4860 <https://www.tiempo.com/ram/venezuela-humos-incendios-forestales.html>, last access: 9 July 2024, *Tiempo.com | Meteored*,  
 4861 2024.

- 4862 Turco, M., Jerez, S., Doblas-Reyes, F. J., AghaKouchak, A., Llasat, M. C., and Provenzale, A.: Skilful forecasting of global fire  
4863 activity using seasonal climate predictions, *Nat Commun*, 9, 2718, <https://doi.org/10.1038/s41467-018-05250-0>, 2018.
- 4864 UC Davis: Global Administrative Regions Data, available at: [https://gadm.org/download\\_world.html](https://gadm.org/download_world.html), last access: 9 July 2024,  
4865 2022.
- 4866 UN Resident Coordinator in Chile: Chile: Incendios forestales, 2024 Sistema de Naciones Unidas, Reporte de Situación No. 3 -  
4867 Chile, available at: <https://reliefweb.int/report/chile/chile-incendios-forestales-2024-sistema-de-naciones-unidas-report-de-situacion-no-3>, last access: 9 July 2024, 2024.  
4868
- 4869 UNESCO World Heritage Centre: Landscapes of Dauria, available at: <https://whc.unesco.org/en/list/1448/>, last access: 9 July  
4870 2024, UNESCO World Heritage Centre, 2017.
- 4871 United Nations Environment Programme: Spreading like Wildfire – The Rising Threat of Extraordinary Landscape Fires. A UNEP  
4872 Rapid Response Assessment, available at: [https://www.unep.org/resources/report/spreading-wildfire-rising-threat-extraordinary-](https://www.unep.org/resources/report/spreading-wildfire-rising-threat-extraordinary-landscape-fires)  
4873 [landscape-fires](https://www.unep.org/resources/report/spreading-wildfire-rising-threat-extraordinary-landscape-fires), last access: 9 July 2024, Nairobi, Kenya, 2022a.
- 4874 United Nations Environment Programme: Global Peatlands Assessment: The State of the World's Peatlands, Nairobi, Kenya,  
4875 2022b.
- 4876 United Nations Population Division: World Population Prospects 2022, available at: <https://population.un.org/wpp/>, last access: 9  
4877 July 2024, 2022.
- 4878 Van Wagner, C. E.: Development and structure of the Canadian Forest Fire Weather Index System, Forestry Technical Report  
4879 35, Canadian Forestry Service, Ottawa, 1987.
- 4880 Van Wagtendonk, J. W.: Fire as a Physical Process, in: *Fire in California's Ecosystems*, edited by: Sugihara, N., University of  
4881 California Press, 38–57, <https://doi.org/10.1525/california/9780520246058.003.0003>, 2006.
- 4882 Wang, D., Guan, D., Zhu, S., Kinnon, M. M., Geng, G., Zhang, Q., Zheng, H., Lei, T., Shao, S., Gong, P., and Davis, S. J.:  
4883 Economic footprint of California wildfires in 2018, *Nat Sustain*, 4, 252–260, <https://doi.org/10.1038/s41893-020-00646-7>, 2021.
- 4884 Wang, Y., Chen, H.-H., Tang, R., He, D., Lee, Z., Xue, H., Wells, M., Boss, E., and Chai, F.: Australian fire nourishes ocean  
4885 phytoplankton bloom, *Science of The Total Environment*, 807, 150775, <https://doi.org/10.1016/j.scitotenv.2021.150775>, 2022.
- 4886 Wang, Z., Wang, Z., Zou, Z., Chen, X., Wu, H., Wang, W., Su, H., Li, F., Xu, W., Liu, Z., and Zhu, J.: Severe Global Environmental  
4887 Issues Caused by Canada's Record-Breaking Wildfires in 2023, *Adv. Atmos. Sci.*, 41, 565–571, [https://doi.org/10.1007/s00376-](https://doi.org/10.1007/s00376-023-3241-0)  
4888 [023-3241-0](https://doi.org/10.1007/s00376-023-3241-0), 2024.
- 4889 Ward, M., Tulloch, A. I. T., Radford, J. Q., Williams, B. A., Reside, A. E., Macdonald, S. L., Mayfield, H. J., Maron, M., Possingham,  
4890 H. P., Vine, S. J., O'Connor, J. L., Massingham, E. J., Greenville, A. C., Woinarski, J. C. Z., Garnett, S. T., Lintermans, M.,  
4891 Scheele, B. C., Carwardine, J., Nimmo, D. G., Lindenmayer, D. B., Kooyman, R. M., Simmonds, J. S., Sonter, L. J., and Watson,  
4892 J. E. M.: Impact of 2019–2020 mega-fires on Australian fauna habitat, *Nat Ecol Evol*, 4, 1321–1326,  
4893 <https://doi.org/10.1038/s41559-020-1251-1>, 2020.
- 4894 van der Werf, G. R., Randerson, J. T., Giglio, L., Collatz, G. J., Kasibhatla, P. S., and Arellano, A. F.: Interannual variability in  
4895 global biomass burning emissions from 1997 to 2004, *Atmos. Chem. Phys.*, 6, 3423–3441, [https://doi.org/10.5194/acp-6-3423-](https://doi.org/10.5194/acp-6-3423-2006)  
4896 [2006](https://doi.org/10.5194/acp-6-3423-2006), 2006.
- 4897 van der Werf, G. R., Randerson, J. T., Giglio, L., Collatz, G. J., Mu, M., Kasibhatla, P. S., Morton, D. C., DeFries, R. S., Jin, Y.,  
4898 and van Leeuwen, T. T.: Global fire emissions and the contribution of deforestation, savanna, forest, agricultural, and peat fires  
4899 (1997–2009), *Atmospheric Chemistry and Physics*, 10, 11707–11735, <https://doi.org/10.5194/acp-10-11707-2010>, 2010.
- 4900 van der Werf, G. R., Randerson, J. T., Giglio, L., van Leeuwen, T. T., Chen, Y., Rogers, B. M., Mu, M., van Marle, M. J. E.,  
4901 Morton, D. C., Collatz, G. J., Yokelson, R. J., and Kasibhatla, P. S.: Global fire emissions estimates during 1997–2016, *Earth*  
4902 *Syst. Sci. Data*, 9, 697–720, <https://doi.org/10.5194/essd-9-697-2017>, 2017.

- 4903 Vitolo, C., Di Giuseppe, F., Barnard, C., Coughlan, R., San-Miguel-Ayanz, J., Libertá, G., and Krzeminski, B.: ERA5-based global  
4904 meteorological wildfire danger maps, *Sci Data*, 7, 216, <https://doi.org/10.1038/s41597-020-0554-z>, 2020.
- 4905 Wetterhall, F. and Di Giuseppe, F.: The benefit of seamless forecasts for hydrological predictions over Europe, *Hydrology and*  
4906 *Earth System Sciences*, 22, 3409–3420, <https://doi.org/10.5194/hess-22-3409-2018>, 2018.
- 4907 Wiedinmyer, C., Kimura, Y., McDonald-Buller, E. C., Emmons, L. K., Buchholz, R. R., Tang, W., Seto, K., Joseph, M. B., Barsanti,  
4908 K. C., Carlton, A. G., and Yokelson, R.: The Fire Inventory from NCAR version 2.5: an updated global fire emissions model for  
4909 climate and chemistry applications, *Geosci. Model Dev.*, 16, 3873–3891, <https://doi.org/10.5194/gmd-16-3873-2023>, 2023
- 4910 Wigneron, J.-P., Li, X., Frappart, F., Fan, L., Al-Yaari, A., De Lannoy, G., Liu, X., Wang, M., Le Masson, E., and Moisy, C.: SMOS-  
4911 IC data record of soil moisture and L-VOD: Historical development, applications and perspectives, *Remote Sensing of*  
4912 *Environment*, 254, 112238, <https://doi.org/10.1016/j.rse.2020.112238>, 2021.
- 4913 Wittwer, G. and Waschik, R.: Estimating the economic impacts of the 2017–2019 drought and 2019–2020 bushfires on regional  
4914 NSW and the rest of Australia, *Aus J Agri & Res Econ*, 65, 918–936, <https://doi.org/10.1111/1467-8489.12441>, 2021.
- 4915 World Bank: World Bank Policy Note: Managing Wildfires in a Changing Climate, Washington DC, 2020.
- 4916 World Bank: Financially Prepared: The Case for Pre-positioned Finance in European Union Member States and Countries under  
4917 EU Civil Protection Mechanism, Washington DC, 2024.
- 4918 World Weather Attribution: Extreme humid heat in South Asia in April 2023, largely driven by climate change, detrimental to  
4919 vulnerable and disadvantaged communities – World Weather Attribution, available at:  
4920 [https://www.worldweatherattribution.org/extreme-humid-heat-in-south-asia-in-april-2023-largely-driven-by-climate-change-](https://www.worldweatherattribution.org/extreme-humid-heat-in-south-asia-in-april-2023-largely-driven-by-climate-change-detrimental-to-vulnerable-and-disadvantaged-communities/)  
4921 [detrimental-to-vulnerable-and-disadvantaged-communities/](https://www.worldweatherattribution.org/extreme-humid-heat-in-south-asia-in-april-2023-largely-driven-by-climate-change-detrimental-to-vulnerable-and-disadvantaged-communities/), last access: 9 July 2024, 2023.
- 4922 World Weather Attribution: Climate change, not El Niño, main driver of exceptional drought in highly vulnerable Amazon River  
4923 Basin – World Weather Attribution, available at: [https://www.worldweatherattribution.org/climate-change-not-el-nino-main-driver-](https://www.worldweatherattribution.org/climate-change-not-el-nino-main-driver-of-exceptional-drought-in-highly-vulnerable-amazon-river-basin/)  
4924 [of-exceptional-drought-in-highly-vulnerable-amazon-river-basin/](https://www.worldweatherattribution.org/climate-change-not-el-nino-main-driver-of-exceptional-drought-in-highly-vulnerable-amazon-river-basin/), last access: 9 July 2024, 2024.
- 4925 Xanthopoulos, G., Zevgoli, E., Kaoukis, K., and Athanasiou, M.: Greece - Lessons not learned, available at:  
4926 [https://issuu.com/wildfiremagazine-iawf/docs/wildfire\\_magazine\\_q4\\_2023\\_-\\_web](https://issuu.com/wildfiremagazine-iawf/docs/wildfire_magazine_q4_2023_-_web), last access: 9 July 2024, *Wildfire*, 2023, 2024.
- 4927 Yebra, M., Dennison, P. E., Chuvieco, E., Riaño, D., Zylstra, P., Hunt, E. R., Danson, F. M., Qi, Y., and Jurdao, S.: A global  
4928 review of remote sensing of live fuel moisture content for fire danger assessment: Moving towards operational products, *Remote*  
4929 *Sensing of Environment*, 136, 455–468, <https://doi.org/10.1016/j.rse.2013.05.029>, 2013.
- 4930 Yebra, M., Quan, X., Riaño, D., Rozas Larraondo, P., van Dijk, A. I. J. M., and Cary, G. J.: A fuel moisture content and flammability  
4931 monitoring methodology for continental Australia based on optical remote sensing, *Remote Sensing of Environment*, 212, 260–  
4932 272, <https://doi.org/10.1016/j.rse.2018.04.053>, 2018.
- 4933 Yin, H., Khamzina, A., Pflugmacher, D., and Martius, C.: Forest cover mapping in post-Soviet Central Asia using multi-resolution  
4934 remote sensing imagery, *Sci Rep*, 7, 1375, <https://doi.org/10.1038/s41598-017-01582-x>, 2017.
- 4935 Yu, M., Zhang, S., Ning, H., Li, Z., and Zhang, K.: Assessing the 2023 Canadian wildfire smoke impact in Northeastern US: Air  
4936 quality, exposure and environmental justice, *Science of The Total Environment*, 926, 171853,  
4937 <https://doi.org/10.1016/j.scitotenv.2024.171853>, 2024.
- 4938 Yukimoto, S., Kawai, H., Koshiro, T., Oshima, N., Yoshida, K., Urakawa, S., Tsujino, H., Deushi, M., Tanaka, T., Hosaka, M.,  
4939 Yabu, S., Yoshimura, H., Shindo, E., Mizuta, R., Obata, A., Adachi, Y., and Ishii, M.: The Meteorological Research Institute Earth  
4940 System Model Version 2.0, MRI-ESM2.0: Description and Basic Evaluation of the Physical Component, *Journal of the*  
4941 *Meteorological Society of Japan. Ser. II*, 97, 931–965, <https://doi.org/10.2151/jmsj.2019-051>, 2019.
- 4942 Zachariah, M., Vautard, R., Chandrasekaran, R., Chaithra, S., Kimutai, J., Arulalan, T., AchutaRao, K., Barnes, C., Singh, R.,  
4943 Vahlberg, M., Arrgihi, J., Raju, E., Sharma, U., Ogra, A., Vaddhanaphuti, C., Bahinipati, C., Tschakert, P., Pereira Marghidan, C.,  
4944 Mondal, A., Schwingshackl, C., Philip, S., and Otto, F.: Extreme humid heat in South Asia in April 2023, largely driven by climate



4945 change, detrimental to vulnerable and disadvantaged communities, Imperial College London, <https://doi.org/10.25561/104092>,  
4946 2023.

4947 Zheng, B., Ciais, P., Chevallier, F., Chuvieco, E., Chen, Y., and Yang, H.: Increasing forest fire emissions despite the decline in  
4948 global burned area, *Science Advances*, 7, eabh2646, <https://doi.org/10.1126/sciadv.abh2646>, 2021.

4949 Zheng, B., Ciais, P., Chevallier, F., Yang, H., Canadell, J. G., Chen, Y., Van Der Velde, I. R., Aben, I., Chuvieco, E., Davis, S. J.,  
4950 Deeter, M., Hong, C., Kong, Y., Li, H., Li, H., Lin, X., He, K., and Zhang, Q.: Record-high CO<sub>2</sub> emissions from boreal fires in  
4951 2021, *Science*, 379, 912–917, <https://doi.org/10.1126/science.ade0805>, 2023.  
4952  
4953